Fabrication of perfusion microbioreactor for culturing engineered heart tissue with electrical stimulation



Xin Liu

Hertford College

University of Oxford

A thesis submitted for the degree of

Doctor of Philosophy

Trinity 2019

Abstract

This thesis focuses on fabricating a perfused microbioreactor platform to generate functional human engineered heart tissue to be used for drug testing. To evaluate the feasibility of this system and make the conditions optimized for culturing cardiomyocytes in 3D constructs, rats' heart tissue models were firstly set up to test the efficacy for long-term culture. Myocytes from embryonic rats were cultured in 200mg/ml fibrinogen gel with 5 million/ml cell densities. The tissues were formed in 24-well culture dish and then transferred into the micro-bioreactors with carbon electrodes to provide electrical stimulations. Culture medium was perfused to maintain chemostat environment. To measure contractile force, the key function of cardiomyocytes *in vivo*, rod-shaped tissue constructs were generated and attached onto two flexible PDMS pillars (1mm diameter and 12mm length). They worked as a force transducer and their deformation was measured to estimate cellular contractile force with accurate mechanical model.

The dynamic perfusion system was stimulated to determine optimal design and operation of microbioreactor. By comparing the functions of the cells cultured in static and perfused environment, it was concluded that the perfused system would be necessary to generate more representative 3D *in vitro* models

Electrical stimulation is an important tool to induce functions of cardiomyocytes cultured *in vitro*. To investigate the electrophysiological activities of engineered heart tissue, different levels of electrical stimulations were applied onto the engineered heart tissue to mimic those in native heart. All the tissues were cultured 5 days before

electrical stimulations were initialled to ensure tissues are sufficiently stable. This can avoid the influence onto protein assembly due to early electrical stimulation.

In the experiments, monophasic electrical signals were applied onto the samples with amplitudes ranging from 1V/cm to 5V/cm and frequencies varying between 1Hz and 5Hz. While comparing the stimulated and non-stimulated samples, the optimal electrical stimulation condition is 3V/cm, 2Hz on the basis of performance of rEHT in terms of contractile force, beating rate and microstructures. It is then used to induce higher maturation of iPSC-CMs for human EHT generation.

After 20 days of long-term culture, the human engineered heart tissues are mature and functional and can be used for testing the effect of drugs. Five drugs, including Ouabain, Bay k8644, Milrinone, Amlodipine and Ryanodine, all clinically approved to treat various cardiovascular diseases, were used for the evaluation tests. The tested drugs at different dosages were added into the culture medium and the latter was perfused into the microbioreactor hosting the human engineered heart tissues. The dynamic responses of the hEHTs were recorded over 24 hours experiments. The responses were shown to be clinically relevant. Although further tests are required to validate the efficiency and efficacy of the developed microbioreactor platform, it showed potentials for high throughput testing and refining, reducing and replacing the use of animal tests.

Abstract ..... **ii**

List of Figure ..... **viii**

List of Table ..... **xvii**

Acknowledgement ..... **xviii**

Abbreviations ..... **xx**

Chapter 1 Introduction **1**

1.1. Background *1*

1.2. Aims of This Thesis *3*

1.3. Scope and Structure of Thesis *5*

Chapter 2 Literature Review **7**

2.1. Heart and Cardiovascular Diseases *7*

2.1.1. Introduction of Cardiac Muscle 7

2.1.2. Cardiovascular Disease 11

2.2. Tissue Engineering and Regeneration Medicine *14*

2.2.1. Tissue Engineering Development 14

2.2.2. Stem Cell Technology 17

2.2.3. Scaffold Design 21

2.2.4. 2D and 3D Cell Culture 22

2.2.5. Engineered Cardiac Tissue Generation 26

2.3. Dynamic Perfused Cell Culture and Drug Testing *29*

2.3.1. Cellular Force and Its Measurement Techniques 29

2.3.2. Introduction of PDMS 31

2.3.3. Mechanical and Electrical Stimulation for EHT 33

2.3.4. Three-dimensional Perfused Cell Culture and Perfusion System for Culturing EHT 37

2.3.5. EHT Application for Drug Development and Disease Modelling 40

Chapter 3 Microbioreactors for EHTs Development **42**

3.1. Introduction *42*

3.2. Materials and Methods *45*

3.2.1. Generation of Engineered Heart Tissue 45

3.2.2. PDMS Platform Design and Mechanical Modelling 49
3.2.3. Cell Sources 54
3.2.4. Isolation of Cardiomyocytes From Neonatal Rats 57
3.2.5. iPSc Derived Cardimyocytes and Splitting Cardiomyocytes from Coating 58
3.3. Results and Discussion 59
3.3.1. Design of EHT Microbioreactor 59
3.3.2. Scaffold Matrix for Cells Seeding 64
3.3.3. System Feasibility Study with Cardiomyocytes Isolated from Neonatal Rats 65
3.4. Summary 68
Chapter 4 Design of Dynamic Cellular Force Transducers 70
4.1. Introduction 70
4.1.1. Tension and Compression Tests 70
4.1.2. Nanoindentation 73
4.2. Materials and Methods 77
4.2.1. Mechanical Modelling Design and Samples Preparations 77
4.2.2. PDMS Mechanical Property Characterization with Compression and Tensile Test 80
4.2.3. Nanoindentation of PDMS Characterization 83
4.2.4. Bending Silicon Posts Force Measurements 85
4.3. Results and Discussion 86
4.3.1. Macroscopic Compression and Tensile Test Results 86
4.3.2. Nanoindentation Results 94
4.3.3. Bending Silicon Posts Force Measurements 98
4.4. Summary 100
Chapter 5 Microbioreactors with Optimal Perfusion System 102
5.1. Introduction 102
5.1.1. Bioreactor for Tissue Engineering 103
5.1.2. Perfusion System Application in Tissue Engineering 105
5.1.3. Shear Stress and Turbulence 107

5.2. Microfluidic Model and Numerical Simulation 109
5.2.1. Bioreactor Geometry Design and Perfusion System Set Up 109
5.2.2. Turbulence Kinetic Energy 114
5.3. Results and Discussion 116
5.3.1. Design of Bioreactor with Dynamic Media Flow Simulation 116
5.3.2. Velocity Analysis and Turbulence Kinect Energy 121
5.3.3. Effects of Dynamic Perfusion System for REHTs 126
5.4. Summary 127

Chapter 6 Microbioreactors with Optimal Electrical ..... Stimulations 129

6.1. Introduction 129
6.1.1. Cardiac Conducting System 129
6.1.2. Application of Electrical Stimulation into Cell Culture 132
6.1.3. Electrical Stimulation into Engineered Heart Tissue 133
6.2. Materials and Methods 135
6.2.1. Simulation of Embedded Electrical Stimulation 135
6.2.2. Raspberry Pi Control and Electrical Circuit Set Up 137
6.2.3. Continuous Electrical Stimulation and Contractile Force Analysis ... 143
6.3. Results and Discussion 145
6.3.1. Electrical Stimulation System Simulation and Optimization 145
6.3.2. Optimization of Electrical Stimulation Based on Neonatal Rats Engineered Heart Tissue 153
6.4. Summary 159

Chapter 7 Development of HEHT Models and Applications 161

7.1. Introduction 161
7.2. Materials and Methods 162
7.2.1. Cell Viability Test 162
7.2.2. Light Microscopy and Three-dimensional Microscopy 165
7.2.3. Pharmacological Force Regulation 167
7.3. Results and Discussion 169
7.3.1. Feasibility and Optimization Evaluation of the System with REHTs 169

7.3.2. Development of Human Engineered Heart Tissues with Electrical Stimulations 182
7.3.3. Drug Testing with Human Engineered Heart Tissue 194
7.4. Summary 201

Chapter 8 Conclusion and Future Work 203
8.1. Conclusion of Findings 205
8.1.1. PDMS Material Characterization 205
8.1.2. Bioreactor Configuration Design and Optimization 206
8.1.3. Electrical Stimulation System Design and Optimization 206
8.1.4. Culture of Engineered Cardiac tissue and Application into Drug Test Platform 207
8.2. Future Work 208
8.2.1. Study of PDMS Mechanical Properties Under Dynamic Condition in Different Frequency Domain 208
8.2.2. Integrated Temperature and Gas Monitoring Control System for This Micro-bioreactor 209
8.2.3. Further Optimization of Electrical Stimulation 209
8.2.4. Automatic Image Processing and Data Acquisition System 210
8.2.5. Other Disease Modelling and Drug Testing Work 210
8.2.6. Future application of the system 210

References 212

List of Figure

Figure 2- 1: Heart Anatomy: A cross-section of the heart showing the heart chambers and valves.[18] 8
Figure 2- 2: Model of filament actions while muscle contraction. (a) Relaxed muscle; (b) Contracted muscle.[23] 9
Figure 2- 3: Patterns of cardiac remodelling in HCM and DCM. (a) The anatomy of a healthy human heart. (b) Cardiac remodelling occurring in asymmetric HCM is characterised by hypertrophy (thickening) of the Left ventricular wall. (c) DCM is characterised by left ventricular enlargement associated with thinning of the left ventricular wall.[30] 12
Figure 2- 4: A sketch diagram shows a normal artery with normal blood flow and an artery with plaque build-up.[34] 13
Figure 2- 5: Tissue Engineering paradigm: From cells isolation to tissue generation and implantation.[41] 16
Figure 2- 6: Human stem cell applications: stem cell can multiply and differentiate into different types of cells within the human body.[45] 18
Figure 2- 7: The stem cells generation processes: (a) embryonic stem cells are derived from the inner mass of the blastocysts; (b) induced pluripotent stem cells are reprogrammed from fibroblasts with four genes overexpressing; (c) adult stem cells are obtained from adult human tissues and organs.[53] 20
Figure 2- 8: The schematic diagram of 2D and 3D cell culture[68] 24
Figure 2- 9: Spheroid fabrication method for generating 3D cell culture system[73] 25
Figure 2- 10: Chemical formula and chemical structure of PDMS [111] 32
Figure 2- 11: PDMS in random coil form [113] 33
Figure 3- 1: Illustration of the experimental procedure for generating and culturing engineered heart tissue; the orange parts are the PDMS platforms, the blue parts are the culture dishes and wells; the grey parts are the agarose molds and the light blue parts are the culture media. (a) Placing of the silicon platforms after the agarose slots are casted with the Teflon spacer; (b) Prepared reconstitution mixture is pipetted into the culture dish so that the gel can be formed and attached onto the top of the PDMS posts; (c) The engineered heart tissue are polymerized two hours later and media is

added into each well to ease the connection between tissue and agarose. (d)The generated tissues are transferred into bioreactor and cultured further for a couple more days. 47
Figure 3- 2: Geometric display of experimental instruments, both measured to millimeter scale. (a)The platform design with AutoCAD; (b) The platform with two silicon pillars made from PDMS; (c) Generated engineered heart tissue (pink one) attach onto the end of the two pillars; (d) Teflon spacer designed for creating agarose casting slots with four wells turned upside down. 49
Figure 3- 3: The beam deflection model. Force is applied along vertical direction. .. 51
Figure 3- 4: 3D Engineered Cardiac tissue generation process and further applied into clinical transplantation.[148] 56
Figure 3- 5: Illustration of micro-bioreactor design with electrical stimulations (Yellow arrows mean media flow direction, red rods are two carbon electrodes, red arrows mean electrical field direction, and blue rod represents tissue) 60
Figure 3- 6: Schematic diagram of the perfusion bioreactor set up (a) The systems can be controlled by the computer and Raspberry Pi programming; (b) The top view of the chamber design. (c) The set-up of perfusion system. 61
Figure 3- 7: The set-up of perfusion bioreactor with electrical stimulations (a) Pump used for establishing media flow (b) The electrical connection of bioreactor (c) The electrical stimulation established by programming of Raspberry Pi and various voltage levels can be achieved by this system. 63
Figure 3- 8: Typical force generation of rat engineered heart tissue (blue one represents to stimulated samples and red one represents non-stimulated samples) 67
Figure 4- 1: Stress-strain diagram for mild steel[150] 71
Figure 4- 2: Deben tension microtest stage & tensile testing schematic diagram[151] ... 72
Figure 4- 3: Typical compression test strain and stain curve and equipment for compression testing[153] 73
Figure 4- 4: Schematic representation of a loading-unloading curve for a nanoindentation measurement; P_{max} is the load at maximum indentation, h_{max} is the indenter displacement at peak load, h_f is the final depth.[159] 74
Figure 4- 5: Component of a nanoindentation system[161] 76

Figure 4- 6: Illustration of manufacturing PDMS platform. Blue parts represent culture dish as manufacture mould, grey parts represent PDMS. (a) PDMS cylinder sample: a standard cell culture dish is prepared as mould. (b)Silicon posts: a cubic slot is prepared by a standard cell culture dish with PDMS. Place half of the posts mould as the basement and pour the PDMS onto the mould. The other half of the mould is placed from the top. Bubbles are removed and curing in the baker. Remove the specimen from mould. 79
Figure 4- 7: The instrument setup of compression test of PDMS mechanical property characterization. 81
Figure 4- 8: A cross-section of the PDMS tensile specimen 82
Figure 4- 9: Veeco Dimension 3100 Atomic force microscope with TriboScope nanoindentation 84
Figure 4- 10: Tension test on deben tensile stage. One end of the PDMS post is clamped and a high-precision force sensor is connected. The other end of the post is fixed and connected to the movable stage. 86
Figure 4- 11: Typical compression test of PDMS network 5:1 88
Figure 4- 12: Averaging tensile engineering stress/strain curves for PDMS samples curing with different curing mixing ratio 92
Figure 4- 13: Relationship between mixing ratio of Sylgard 184 and the resultant Young's modulus. 93
Figure 4- 14: Typical AFM nanoindentation force reaction (nN) curves against separation (nm) for different curing times. The blue lines represent the compression force reaction and the red lines are the relaxation force reaction. 95
Figure 4- 15: AFM nanoindentation force reaction (nN) curves against separation (nm) for different mixing ratio of PDMS base and curing agent. The blue lines represent compression force reaction and the red lines are the relaxation force reaction. 97
Figure 4- 16: Deben tensile tests. Tension changes against displacement of the PDMS posts free end. 99
Figure 5- 1: Different cell culture systems in three-dimensional conditions: (a) Spheroids (b) Cells are seeded onto various types of scaffolds (c) Cells and tissue are cultured under static conditions and dynamic conditions. 104

Figure 5- 2: Schematic diagram of laminar flow and turbulent flow[185]. Laminar flow means the fluid travels in regular way without any disruption and turbulent flow is a less orderly flow with irregular fluctuations 108
Figure 5- 3: Model and measures of the perfusion bioreactor. (a) The microbioreactor design of chamber with quadrilateral shape channel (QSC). (b) The microbioreactor design of chamber with narrow towards wall channels (NTWC). (c) The microbioreactor design of chamber with narrow space channel (NSC). 111
Figure 5- 4: Dynamic fluid simulation with ANSYS Fluent of flow through a bioreactor with chamber of quadrilateral shape channel (QSC) with single inlet (a) initial time, (b) stable flow over 20 minutes and 3 inlets (c)initial time, (d) stale flow after 20 minutes and 5 inlets (e) initial time, (f) stale flow after 20 minutes..... 117
Figure 5- 5: Dynamic fluid simulation with ANSYS Fluent of flow through the bioreactor of chamber with narrow towards wall channels (NTWC). with single inlet. (a) Initial time (b) stable flow over 5minutes (c) stable flow over 10 minutes (d) stable flow over 20 minutes 118
Figure 5- 6: Dynamic fluid simulation with ANSYS Fluent of flow through the bioreactor of chamber with narrow space channel (NSC). (a) Initial time (b) stable flow over 5minutes (c) stable flow over 10 minutes (d) stable flow over 20 minutes 119
Figure 5- 7: Velocity results for all the bioreactors types under the condition of 0.01rmp inlet velocity 121
Figure 5- 8: V1 velocity streamline results for narrow towards wall channel (NTWC) 122
Figure 5- 9: V1 velocity streamline results for narrow space channel (NSC) 123
Figure 5- 10: Maximum velocity comparison between the different configurations. 123
Figure 5- 11: Turbulence results for different bioreactor configurations with various velocities..... 124
Figure 5- 12: Illustration of the micro-bioreactor with perfusion system and electrical stimulation..... 125
Figure 5- 13：Cardiomyocytes viability in rEHTs of static and dynamic culture (indicated by metabolism of alamarBlue). 126

Figure 6- 1: Heart chambers and natural cardiac pacemakers..... 130
Figure 6- 2: Action potential in cardiac muscle cells. Phases 0 to 4 represent different stages of membrane potentials of cardiomyocytes.[198]..... 131
Figure 6- 3: (a) The Raspberry Pi Model B; (b) Block diagram of Raspberry Pi hardware operation process.[213] 137
Figure 6- 4: The components of Raspberry Pi used for setting up..... 138
Figure 6- 5: The GPIO map of Raspberry Pi. There are 40 pins in total of Raspberry Pi Model 2/3 [214] 139
Figure 6- 6: The schematic diagram of converting digital voltages to analog values with application of PWM 140
Figure 6- 7: The schematic diagram of OP AMP and further voltage gain 141
Figure 6- 8: The schematic diagram of DAC connections..... 142
Figure 6- 9: Experimental set up: Sample attachés onto the platform and inserted into the micro-bioreactor. Electrical pulses are generated with Raspberry Pi and transmitted to the electrodes within chamber..... 143
Figure 6- 10: Optical video analysis system. Length measurement system according to the recorded video from microscope..... 145
Figure 6- 11: The equivalent circuit of a simple electrochemical “Randles” cell, where Rs represents the solution’s resistance, $C_{double\text{-}layer}$ is the double layer capacitance, and Rp is the polarization resistance. 146
Figure 6- 12: Practical and theoretical values for solution resistance of various electrode configurations. 147
Figure 6- 13: Measured solution resistor and measured capacitor against input voltage. 150
Figure 6- 14: Simulated modelling of electrical activity with a 5V pulse in the bioreactor. (a) Top view of the bioreactor’s electrical stimulation. (b) Cross-sectional view of the bioreactor with the electrical field..... 151
Figure 6- 15： Excitation threshold of the samples applied with different stimulation amplitudes and the data are acquired at day 11 (it means electrical filed required for synchronous beating of engineered cardiac tissue). Data are represented as mean +- standard. The analysis statistic is processed with one-way ANOVA test ($p < 0.05$) n =3 each group. 154

Figure 6- 16: Maximum capture rate and contraction force of the samples applied with different stimulation amplitudes and the data are acquired at day 11. Data are represented as mean +-standard. The analysis statistic is processed with one-way ANOVA test ($p < 0.05$) n =3 each group. 156
Figure 6- 17: Excitation threshold of the samples applied with different stimulation frequencies and the data are acquired at day 10. Data are represented as mean +-standard. The analysis statistic is processed with one-way ANOVA test ($p < 0.05$) n =3 each group. 157
Figure 6- 18: Maximum capture rate and contraction force of the samples applied with different stimulation frequencies and the data are acquired at day 10. Data are represented as mean +-standard. The analysis statistic is processed with one-way ANOVA test ($p < 0.05$) n =3 each group. 158
Figure 7- 1: REDOX of Resazurin become resorun cells metabolic activities. [215] .. 162
Figure 7- 2: alamarBlue fluorescence and absorption spectra.[216] 164
Figure 7- 3: Typical contractile force amplitude of neonatal rats EHT increasing against time while electrical stimulation applied (data acquired from Day 14)..... 170
Figure 7- 4: Maximum amplitude of contractile force variation under different electrical stimulation conditions. Data are represented as mean +-standard. The analysis statistic is processed with one-way ANOVA test ($p < 0.05$) n =3 each group. 172
Figure 7- 5: Excitation thresholds of rEHTs from day 8 to day 20. It decreases against culture time. Data are represented as mean +-standard. The analysis statistic is processed with one-way ANOVA test ($p < 0.05$) n =3 each group. 173
Figure 7- 6: Maximum capture rates of rEHT from day 8 to day 20. It shows an increase trend against culture time. Data are represented as mean +-standard. The analysis statistic is processed with one-way ANOVA test ($p < 0.05$) n =3 each group. 174
Figure 7- 7: The percentage reduction of AlamarBlue against time for rEHT treated with different electrical stimulations. 176
Figure 7- 8: Live/dead staining image shows the cell viability; Green indicators indicate live cells and red dots correspond to dead cells. (Scale bar represents to 100um). 177

Figure 7- 9: Quantitative analysis of the number of live/ dead cells for rEHTs with non-stimulation, 2V/cm and 3V/cm stimulations. Data are represented as mean +- standard. The analysis statistic is processed with one-way ANOVA test ($p < 0.05$) n =3 each group. 178
Figure 7- 10: The images show size variation of the neonatal rats engineered heart tissues stimulated with 3V/cm against time. (Day 1, day 3, day 6, day 9, day 12, day 15)..... 179
Figure 7- 11: The changes of cross-section radius normalized to Day 1 against culture time. (Day 3, day 6, day 9, day 12 and day 15)..... 180
Figure 7- 12: H&E staining images of rEHT with non-stimulation, stimulation of 2V/cm and stimulation of 3V/cm. (scale bar represents to 50um)..... 180
Figure 7- 13: Typical images of confocal microscopy of rEHTs (without and with 3V/cm electrical stimulation) to identify myocytes, gap junction and nuclei..... 181
Figure 7- 14: Contractile force amplitude of human EHT increasing against time while electrical stimulation applied (data acquired from Day 14). 183
Figure 7- 15: Maximum amplitude of hEHT contractile force variation under different electrical stimulation condition. Data are represented as mean +-standard. The analysis statistic is processed with one-way ANOVA test ($p < 0.05$) n =3 each group..... 184
Figure 7- 16: Excitation thresholds of hEHTs from day 8 to day 20. They all decrease against culture time. Data are represented as mean +-standard. The analysis statistic is processed with one-way ANOVA test ($p < 0.05$) n =3 each group..... 186
Figure 7- 17: Maximum capture rates of hEHT from day 8 to day 20. They all show an increase trend against culture time. Data are represented as mean +-standard. The analysis statistic is processed with one-way ANOVA test ($p < 0.05$) n =3 each group. 187
Figure 7- 18: The percentage reduction of AlamarBlue against time for hEHT treated with different electrical stimulations. 188
Figure 7- 19: (a) Live/dead staining image shows the cell viability, Green indicators indicate live cells and red dots correspond to dead cells. (Scale bar represents to 100um). (b) Quantitative analysis of the number of live/ dead cells for rEHTs with non-stimulation, 2V/cm and 3V/cm stimulations. Data are represented as mean +-

standard. The analysis statistic is processed with one-way ANOVA test ($p < 0.05$) n =3 each group. 189
Figure 7- 20: The images show size variation of the human iPSCs engineered heart tissues stimulated with 3V/cm against time. (Day 1, day 3, day 6, day 9, day 12 and day 15). 190
Figure 7- 21: The changes of cross-section radius normalized to Day 1 against culture time. (Day 3, day 6, day 9, day 12 and day 15). 191
Figure 7- 22: H&E staining images of stimulated and non-stimulated hEHT at day 20. (Scale bar represents to 50um) 192
Figure 7- 23: Typical images of confocal microscopy of rEHTs (without and with 3V/cm electrical stimulation) to identify myocytes, gap junction and nuclei. 193
Figure 7- 24: Histological construct of sarcomeres within pacing and non-pacing engineered cardiac tissues. 193
Figure 7- 25: hEHT contraction response curves before and after application of 0.5uM Ouabain. 195
Figure 7- 26: The relationship of average maximum contractile forces, contraction time and relaxation time against increasing concentrations of Ouabain. Data are represented as mean +-standard. The analysis statistic is processed with one-way ANOVA test ($p < 0.05$) n =2 each group. 196
Figure 7- 27: Test of Bay K-8644 onto hEHT. (a) Contraction response curves before and after application of 0.5uM Bay K-8644. (b) The relationship of average maximum contractile forces and various concentration of Bay -8644. (c) Contraction time and relaxation time against increasing concentrations of Bay K-8644. Data are represented as mean +-standard. The analysis statistic is processed with one-way ANOVA test ($p < 0.05$) n =2 each group. 197
Figure 7- 28: Test of Milrinone onto hEHT. (a) Contraction response curves before and after application of 5uM Bay K-8644. (b) The relationship of average maximum contractile forces and various concentration of Milrinone. (c) Contraction time and relaxation time against increasing concentrations of Milrinon. Data are represented as mean +-standard. The analysis statistic is processed with one-way ANOVA test ($p < 0.05$) n =2each group. 198

Figure 7- 29: Test of Amlodipine onto hEHT. (a) Contraction response curves before and after application of 5uM Amlodipine. (b) The relationship of average maximum contractile forces and various concentration of Amlodipine. (c) Contraction time and relaxation time against increasing concentrations of Amlodipine. Data are represented as mean +-standard. The analysis statistic is processed with one-way ANOVA test ($p < 0.05$) n =2 each group. 199
Figure 7- 30: Test of Ryanodine onto hEHT. (a) Contraction response curves before and after application of 5uM Ryanodine. (b) The relationship of average maximum contractile forces and various concentration of Ryanodine. (c) Contraction time and relaxation time against increasing concentrations of Ryanodine. Data are represented as mean +-standard. The analysis statistic is processed with one-way ANOVA test ($p < 0.05$) n =2 each group. 200

List of Table

Table 4- 1: The parameters of 5:1 PDMS samples used in compression test 87

Table 4- 2: The parameters of 9:1 PDMS samples used in compression test and obtained elastic modulus 89

Table 4- 4: The parameters of 10:1 PDMS samples used in compression test and obtained elastic modulus 89

Table 4- 5: Macroscopic compression test for PDMS network 15:1. 90

Table 4- 6: Macroscopic compression test for PDMS network of different mixing ratio..... 91

Table 4- 7: Variation of tensile test data with curing mixing ratio 93

Table 4- 8: The PDMS Young's modulus changes against curing time 96

Table 4- 9: The PDMS Young's modulus changes against mixing ratio..... 98

Table 4- 10: Platform design mechanical optimization 101

Table 5- 1: Mesh parameters of Computational Fluid Dynamics (CFD) Analysis.. 113

Table 5- 2: Fluid characteristics & chamber properties used in the CFD analysis ... 113

Acknowledgement

First of all, I would like to express my special thanks to my primary supervisor, Professor Zhanfeng Cui (FREng) for proposing such a great and challenging work as my DPhil project. Without his constructive feedback, patient guidance and full support, I cannot make it through to current stage so far. Also, I am grateful to my supervisor Professor Cathy Ye. She gave me a lot of valuable advices in experiment design and provided me with enormous support to guarantee my project progressing smoothly.

I would also like to thank Dr Julian George, who taught me many lab techniques, like cell culture and processing of all the facilities in Tissue Engineering group. Also, Dr Shaoyang Yeh introduced me to microscopy technology in biological field, especially taught me how to process the multi-photon microscope and confocal microscope. The knowledge and techniques I learned from them have great impacts on my DPhil project.

This DPhil work is the result of collaborations with other Institutions and research groups. The neonatal rats' cardiomyocytes was provided by Dr Angela Lee from Bhattacarya Group of Henry Wellcome Trust of Genomic Medicine. And I feel grateful to Ms Meng Yuan from Professor Lei's group to supply me with her precious iPSC-derived cardiomyocytes for further experiment and test. Without the help from Dr Siqi Ying on training me of using tension and compression platform, I am not able to complete the experiments in mechanical properties characterization of PDMS. Also, thanks to Dr Zhixin Zeng who provides me with the nanoindentation equipment and gives me the guidance of this test.

Thank you all to the students of the Tissue Engineering Group for your support, friendship, and help in particular to Di Shen, Thomas Chui, Fabio Bianchi, Erfan Soliman, Sharlayne Waller, Siqi Dai, YejiongYu, Shichen Zhu, Haoyu Wu, Mookie Phurit, Bo Zhang, Catriona Inverarity, Meghan Lim, Robin Nylandand and Ching Lam. Also I am grateful to the members from our group who gave me a lot help of training, knowledge and skills, including Dr Julian Dye, Dr Hui Wang, Dr Huidong Jia, Dr Zhaohui Li, Dr Naresh Kasoju, Dr Linh.

I would like specially thanks to Dr Andy Walker, who helps me with my writing and shape my thesis in proper state. His careful proofreading makes it into a readable form and it cannot be fully completed without his assistance. I also want to express my thanks to Johnson due to his kindly suggestions on my thesis and proofreading for my Chapter 1 to 3.

Thank you to my friends in Oxford and UK. I am so grateful I am a member of Oxford Chinese Basketball Team and all my teammates are all very nice and enrich my life in UK.

It is hard to find exact words to express my thanks to my thoughtful parents. Thank you for your patience, support and kindness. Your suggestions and encouragement are quite valuable for me.

It would be impossible for me to complete my project without the financial support from China Scholar Council. Thank you for funding my whole DPhil study.

Abbreviations

2D:	**Two-dimensional**
3D:	**Three-dimensional**
ADC：	**Analog to Digital Convertor**
AFM:	**Atomic force microscope**
ANOVA:	**Analysis of variance**
APC:	**Antigen presenting cells**
ARVC:	**Arrhythmogenic right ventricular cardiomyopathy**
BCA:	**Bicinchoninic acid assay**
BHF:	**British Heart Foundation**
BSA:	**Bovine serum albumin**
CaCl:	**Calcium chloride**
CFD:	**Computational fluid dynamics**
CHD:	**Coronary heart disease**
CM:	**Confocal Microscopy**
CMM:	**Cardiac maintenance medium**
CVD:	**Cardiovascular disease**
DAC:	**Digital to analog convertor**
DCM:	**Dilated cardiomyopathy**
DMEM:	**Dulbecco's modified Eagle's medium**
DO:	**Dissolved oxygen**
EDTA:	**Ethylenediaminetetraacetic acid**
EIS:	**Electrochemical impedance spectroscopy**

EHT:	**Engineered Heart Tissue**
EM:	**Electron Microscopy**
ESC:	**Embryonic stem cells**
ET:	**Excitation threshold**
FBS:	**Fetal bovine serum**
FDA:	**Food and Drug Administration**
FTIR:	**Fourier Transform Infrared Spectroscopy**
H_2O_2:	**Hydrogen peroxide**
HBSS:	**Hank's Balanced Salts Solution**
HCM:	**Hypertrophic cardiomyopathy**
H&E:	**Haematoxylin and eosin**
IgG:	**Immunoglobulin G**
iPSC:	**Induced pluripotent stem cells**
IR:	**Infrared**
Kg:	**kilo gram**
KV:	**kilo voltage**
MCR:	**Maximum capture rate**
MEMs:	**Micro-electromechanical system**
MPM:	**Multi-photon microscopy**
MSC:	**Mesenchymal stem cell**
NA:	**Numerical aperture**
NaCl:	**Sodium chloride**
NIR:	**Near Infrared**

NSC:	**Narrow space channel**
NWTC:	**Narrow towards wall channels**
OCT:	**Optical coherence tomography**
OD:	**Optical density**
PBS:	**Phosphate buffer saline**
PDMS:	**Polydimethylsiloxane**
PFA:	**Paraformaldehyde**
PWM:	**Pulse Width Modulation**
QSC:	**Quadrilateral shape channel**
RT:	**Room Temperature**
RNA:	**Ribonucleic acid**
SD:	**Standard derivation**
SEM:	**Scanning electron microscopy**
SVT:	**Supraventricular tachycardia**
TBS:	**Tris buffered saline**
TKE:	**Turbulence Kinetic Energy**

Chapter 1 Introduction

1.1. Background

In modern society, human is facing to the problems of fighting with various diseases. Over the past decades, cardiovascular disease (CVD) is still one of the leading causes of mortality all over the world.[1] This situation will become even more serious as the aging of population in the future. According to the statistical data from British Heart Foundation (BHF), there were over 0.6 million people died in 2017 and more than 1/4 of these deaths result from the cardiovascular diseases.[2] The other leading cause of death is cancer and its death toll is 0.16 million in total. Over half of deaths in UK were due to these two causes. It is reported that cardiovascular diseases affect 1.7 million British people and the annual related cost from cardiovascular is about £30 billion. The annual cost for research in treatment of this disease is a big number and this value keeps on increasing.[3] Thus, treatment of heart diseases has drawn worldwide attention particular in the field of tissue engineering.

The cardiovascular disease (CVD) is a set of diseases that affect the heart and circulating system. There are many reasons leading to higher possibilities of getting a cardiovascular disease, such as smoking, high blood pressure, diabetes, overweight and family history of CVD etc. What is more serious is that there is not any radical cure for cardiovascular diseases except heart transplantation. However, the lack of donors and rejection reaction are major problems. Two normal treatments for cardiovascular disease patients are taking cardiac drugs and surgical operation. Compared with the former treatment, surgery is relatively high-cost, high-risk and

irreversible. Hence, a majority of patients with such disease highly rely on taking drugs in the long term. Yet, it is expensive and inefficient to develop a new drug and the clinical approve is complicated and time-consuming. Currently, drugs toxicity and efficient study are conducted with non-human animal models at the beginning stage. And withdrawal of cardiovascular drugs from the market mainly results from unobserved toxicity in animal models. There is an urgent requirement to set up physiological human model to replace the animal model.

With the advance of biotechnology, biomaterials and regenerative medicine, now researchers are capable to develop organ models to accurately mimic their key functions and structures in the lab.[4] The set-up of those myocardial models provides new solutions to achieve clinical purposes of drug testing[5], physiological study of cardiac tissue[6] and *in vitro* disease remodelling[7]. This work also helps lower risk of misdiagnosis for patients with cardiovascular disease and estimates the therapeutic effects of various treatments.

It has been proved that human induced pluripotent stem cell derived cardiomyocytes (iPSC-CMs) hold a potential promise for establishing *in vitro* model for cardiac drug testing and for myocardium regenerative medicine for repairing damaged tissue.[5] However, application of iPSC-derived cardiomyocytes is limited by cellular maturation. 3D engineered *in vitro* culture of iPSC-CMs can enhance their degree of maturation towards closer to the performance of the cardiomyocytes within native human heart. There are enormous factors that can probably affect the cellular maturation, including scaffold materials, extracellular matrix structures, mechanical stimulations and electrical stimulations.

Development in bioengineering, material science and *in vitro* culture technologies has led to a rapid advance in cardiac tissue engineering from a perspective of dynamic culture. It has been proved that engineered tissue generated and cultured in bioreactor can better restore its natural microenvironments to some extent.[8] Perfused micro-bioreactors enable cardiomyocytes to be cultured three-dimensionally with functional stimulation responses and physical measurements with technical advantages for high throughput and parallel testing. Compared with conventional macro-scale *in vitro* cell culture system, personally designed micro-bioreactor platforms offer a great number of obvious advantages. It offers improved functions of cells, lower volume of reagents and ease integration and fabrication.

To develop sufficiently mature human engineered heart tissue and apply it into drug testing, we would like to develop a micro-bioreactor for generating and culturing it three-dimensionally.

1.2. Aims of This Thesis

The purpose of the project is designing a functional human engineered cardiac tissue that can be used as a model for drug testing and disease modelling. According to previous research work, in this project a platform is to be made from PDMS for single engineered cardiac tissue generation and long-term culture. Tissues are generated within 24-well culture dish and they can be easily transferred into our perfusion system for further *in vitro* culture. The requirements of such platform should be small, easy-transferred and based on single well of culture dish. It is not just a support for tissue attachment, and the platform also works as a force

transducer. The accuracy of this force transducer highly relies on mechanical translation modelling of force and pillars' deformation and the properties of material (PDMS) used for platform construction. Thus, it is reasonable to have an overall mechanical properties characterization of PDMS to improve accuracy of contractile force measurement.

With an aim of setting up a dynamic media flow environment for 3D-cultured cardiomyocytes, a number of design configurations for microbioreactor will be made to determine the optimal dynamic flow. We aim to limit the presence of disturbance flow and provide an even distributed and smooth flow of medium through the tissues. This will allow a better control of medium flow within the chamber. Besides configuration determination, the parameters like media flow rate and initial time of media flow will also be investigated.

Considering the application of electrical stimulation onto engineered cardiac tissue, we aim to study the best conditions of electrical signals to induce the engineered heart tissue models in our system. We would like to provide the samples with compatible electrical field for cells and tissues. And within the range of safe electrical signals, the effects of different electrical stimulation conditions will be studied to achieve the purpose of improving cellular maturation and well-developed tissue construction.

While the whole system parameters were confirmed, the cardiomyocytes isolated from neonatal rats were seeded in to scaffold to form 3D construction. They will be cultured in perfusion microbioreactor to evaluate the feasibility of the system. Different electrical fields will be used to find the best conditions for enhancing the

performance of rat engineered heart tissue (rEHT). And then the findings will be applied to develop human engineered heart tissue with iPSC-derived cardiomyocytes with same protocol.

After developing a functional human-based engineered cardiac tissue with key features, our aim is to apply the tissue samples cultured in our *in vitro* system into drug testing. To validate the system's feasibility, the performance of drugs with known action on changing cardiac contractile activities will be studied and compared with their functions in clinical trials.

1.3. Scope and Structure of Thesis

In my DPhil project, with the aim of developing a functional *in vitro* model of human cardiac tissue, a microbioreactor was fabricated for culturing cardiomyocytes in three-dimensional condition.

This thesis consists of eight chapters in total where the chapter 1 has already given a brief introduction of the research background and the purpose I would like to achieve in my DPhil project. Chapter 2 will describe state of the art of engineered heart tissue development and the urgent needs in this field. In chapter 3, it will describe the motivation of building up a perfusion microbioreactor for culturing engineered heart tissue. The basic design of the system is stated there as well. In the next chapter, the principle and process of fabricating PDMS platform to generate and support the tissue will be described. We especially focus on material's mechanical properties characterization, as the platform also plays a role in force measurement. In chapter 5, the dynamic perfused flow is optimized via designing

different configurations of bioreactor to ensure the cells can be cultured for long term under controllable media flow. The electrical stimulation system is integrated into the cell culture chamber and used for studying the effects of electrical environment on engineered cardiac tissue. Thus, chapter 6 describes the generation and optimization procedure of electrical system from electrode configurations, signal amplifier and controlling methods of electricity source. In chapter 7, the neonatal rats' cardiomyocytes engineered cardiac tissue are cultured and analysed for evaluating the feasibility of the system. After inspecting different conditions of dynamic culture environment, mechanical and electrical stimulations, the culture pattern is determined and used for developing human engineered heart tissue. With these effects, their degree of maturation and tissue functions are enhanced. To assess the practicability of using this model for screening the efficiency and toxicity of cardiovascular drugs, the generation of hEHTs are used for initial drug testing after three-week culture. In the last chapter, the conclusion from the project will be discussed with a perspective future plan.

Chapter 2 Literature Review

2.1. Heart and Cardiovascular Diseases

2.1.1. Introduction of Cardiac Muscle

Heart is a muscular organ locating in the centre of the chest.[9] Working as the central part of the circulatory, it pumps blood to the whole body. The blood flow through the blood vessels network including arteries, veins and capillaries.[10] Via these vessels, the oxygen-rich blood can be transferred to the whole body from the heart. The blood supplies oxygen and nutrients to keep all the organs working properly.[11] Then, deoxygenation blood carries waste and carbon dioxide back to lung to form the whole circulatory system.[12] A healthy heart supplies the body with correct amount of blood with right beating rate under control of the autonomic nerve system. Otherwise, the organs will not receive enough blood with oxygen and nutrient. There is approximately 7000L of blood pumped by the heart with a healthy adult every day.[13] The heart will do about 2.5 billion times contraction in total during a human averaging life.[14]

The human heart contains four chambers and two of them locate at the left and the other ones are on the right.[15] The lower chambers are ventricles receiving blood from the upper chambers called atria (shown in figure 2-1). It is a muscular organ and the size of heart is approximately a man's closed fist. It locates inside the thoracic cavity and wrapped by a wall called pericardium.[16]

There are totally three layers forming the cardiac wall. Epicardium is the outer one to give protection of heart by reducing friction and endocardium is the inner layer.

Between these two layers, myocardium locating at the middle. Myocardium is the thickest layer and is made up of cardiac muscle tissue. As the engine, it provides main power for pumping blood out of the chambers.[17] These layers and tissues are the main parts I will look into in my project.

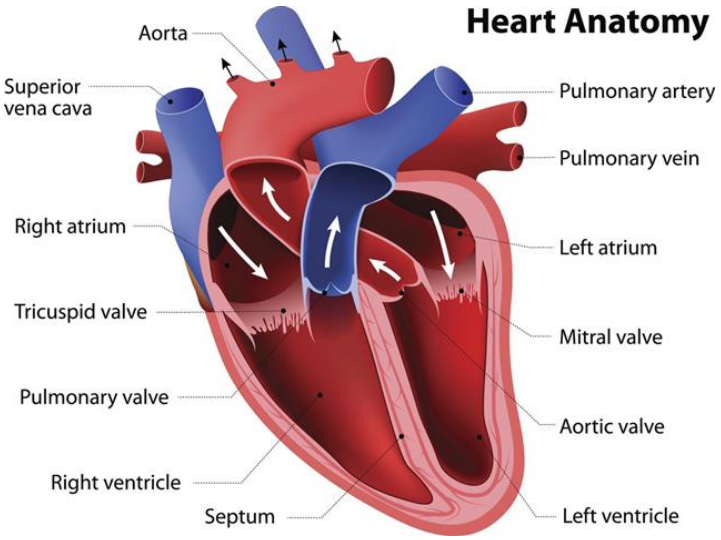


Figure 2- 1: Heart Anatomy: A cross-section of the heart showing the heart chambers and valves.[18]

Like skeletal muscle, the tissue within the cardiac muscle shows striated organization due to the presence of sarcomeres.[19] Yet the cardiac muscles are networks of interconnections between cardiomyocytes (also known as cardiac muscle cells). The myofibrils are the basic component of cardiomyocytes and they are the repeating parts within the sarcomeres.[20] Each sarcomere is made up of two filaments with different proteins. As you can see from figure 2-2, myosin forms the thick and flexible filament and actin forms the relatively thin and rigid filament. The myosin is protein with globular head and fibrous tail. Its head is connected with

actin and ATP that provides energy for muscle action.[21] The z-disc is the end of each sarcomere. Two filaments connect with each other here and it is also the joint of sarcomeres. The calcium flux and electrical impulses regulating the muscle contraction are transmitted via these intercalated disks.[22]

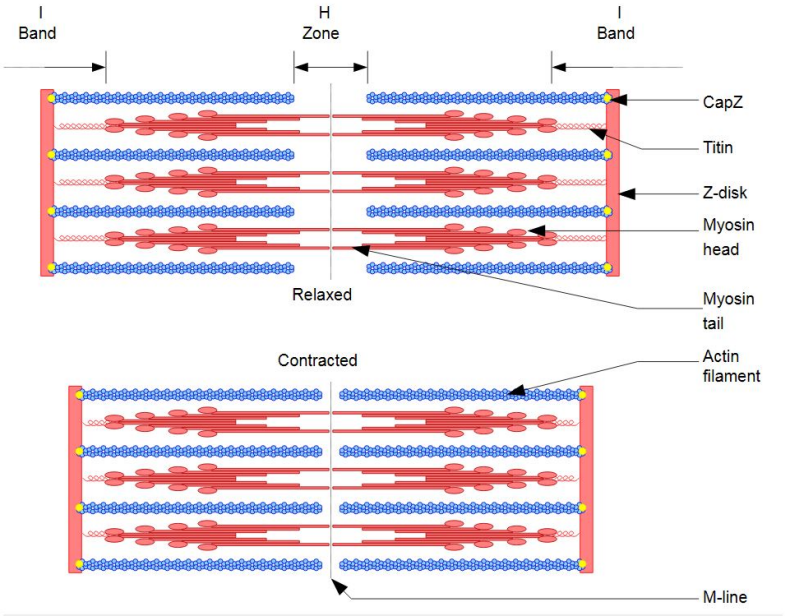


Figure 2- 2: Model of filament actions while muscle contraction. (a) Relaxed muscle; (b) Contracted muscle.[23]

As it is stated above, the z-discs are the gap junctions connect those cardiomyocytes together and the action potentials and calcium pass through these channels between cells during muscle contraction. These discs can be observed under microscope showing as thin lines separating adjacent cardiomyocytes. It is also in perpendicular to the direction of muscle fibres, so it is regarded as the boundary of different cardiomyocytes. Hence, observing z-discs is one method of determining the cardiomyocytes numbers.

The contraction is the most important function of cardiac muscle. It is known that the coordinated contraction of cardiomyocytes is the basic component of cardiac muscle. Such contraction is adjusted by the action potentials passing through the gap junctions of z-discs. Action potentials are the electrical signals stimulating the mechanical response of cells. This depends on the influx of calcium ions into cells and release of these ions.[24] The electrical resistance through intercalated discs is very low and this allows free diffusion of ions between cells.

From figure 2-2, it can be better understood the mechanical contraction of cardiac muscle. In the filament model, there are three zones- H zone is between two I band. The action potential is induced by the pacemaker cells within the sinoatrial and atrioventricular nodes while receiving stimulation from nervous system. The calcium channels are activated by such action potentials transmitting through sarcomeres and this resulting in calcium ions flowing into cardiomyocytes. Increasing of calcium ions level within the cytoplasm releases actin from link of myosin. The actin filaments are shortened and pulled towards the sarcomere, resulting in cardiac muscle tissue contraction. Afterwards, the calcium concentration drops down and the actin filaments return to their original position relaxing cardiac muscle.

The continuously beating of heart supplies oxygenated blood with nutrient to the tissues within the human body to keep them survives. Hence, it is deserved to understand the mechanical model of cardiac muscle and its electrophysiology.

2.1.2. Cardiovascular Disease

The Cardiovascular disease (CVD) is a set of diseases that affect the heart and circulating system. There are many different types of cardiovascular diseases. They can be divided into three main classes of diseases, including cardiomyopathy, vascular diseases and abnormal cardiopalmus.[25]

Cardiomyopathy is a disease of the cardiac muscle. This disease affects the size, shape and function of heart muscle of patients with such disease.[26] Most of cardiomyopathies are inherited disease. They are hypertrophic cardiomyopathy (HCM), dilated cardiomyopathy (DCM), and arrhythmogenic right ventricular cardiomyopathy (ARVC). Hypertrophic cardiomyopathy (HCM) means cardiac muscle wall of patients becomes thicken as it can be seen from figure 2-3. Thickened myocardium makes the heart muscle stiff. By contrast, dilated cardiomyopathy (DCM) is a disease of the heart muscle being stretched and thin.[27] With such disease, the heart loses the ability to pump blood over the whole body efficiently. Arrhythmogenic right ventricular cardiomyopathy (ARVC) is another inherited disease. The proteins that hold heart muscle cells together cannot be developed properly under this condition. It makes the walls of ventricle become thin and stretched.[28] Different from above three diseases, arrhythmogenic right ventricular cardiomyopathy (ARVC) is caused by extreme stress rather than passing on through families. This disease is temporary and results in patients' cardiac muscle being weak.

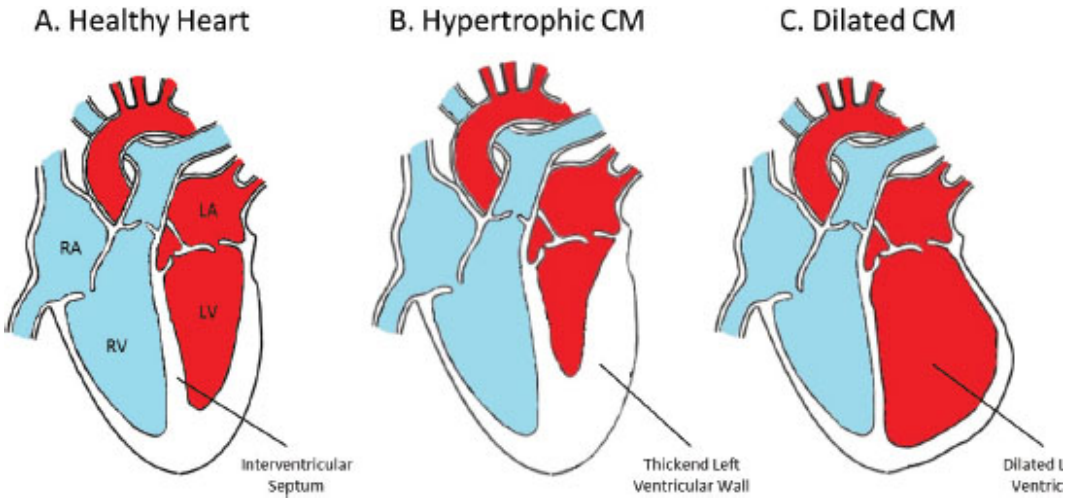


Figure 2- 3: Patterns of cardiac remodelling in HCM and DCM. (a) The anatomy of a healthy human heart. (b) Cardiac remodelling occurring in asymmetric HCM is characterised by hypertrophy (thickening) of the Left ventricular wall. (c) DCM is characterised by left ventricular enlargement associated with thinning of the left ventricular wall.[30]

In terms of vascular disease, there are many different types. The most well-known one is coronary heart disease (CHD). The coronary arteries become narrow under such condition.[31] As it can be seen from figure 2-4, the arteries are blocked by fatty material called atheroma formed gradually within the cardiac muscle walls and this is called atherosclerosis. This will result in the cut-off of oxygen and nutrient supply for the whole body. Oxygen-rich blood cannot be delivered to heart muscle and patients with this disease have larger strain on the heart.[32] This can lead to different symptoms like angina and can potentially results in permanently damage of heart. The most serious result will be heart attack and heart failure. Besides these, another

type of vascular diseases is the blood cut-off between the brain and heart. This disease is called stroke and can cause brain damage.[33]

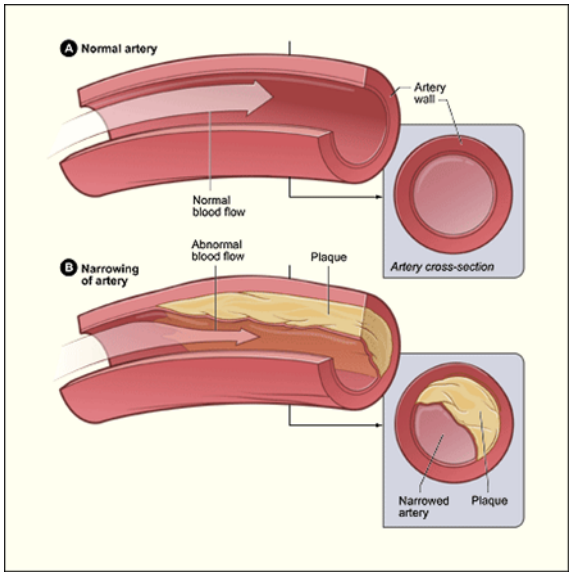


Figure 2- 4: A sketch diagram shows a normal artery with normal blood flow and an artery with plaque build-up.[34]

The other important type of cardiovascular disease is arrhythmia or heart rhythm problem. The heart has a properly working electrical system. It helps adjust the rhythm and control the heart pump blood around the whole body. Once this system has problem, people will experience the abnormal heart rhythm. There are more than 2 million patients in UK being affected by these cardiovascular diseases. Compared with other types of CVDs, patients with such diseases seldom lead to directly death if diagnosed properly. The most common abnormal heart rhythm is atrial fibrillation. The pacemakers normally send out regular electrical impulses, but the impulses can be disorganised at different places within the atria that lead to AF happening. In such condition, the heartbeats are irregular and faster beating. Like atrial fibrillation,

some other fast heart rhythms also happen including supraventricular tachycardia (SVT), inappropriate sinus tachycardia, atrial flutter, ventricular tachycardia and ventricular fibrillation. These abnormal heart rhythms are collectively known as tachycardia. By contrast, there is also disease of slow heart rhythms and they are called bradycardia.[35]

2.2. Tissue Engineering and Regeneration Medicine

2.2.1. Tissue Engineering Development

Although the origin of tissue engineering definition is not clear, it is generally accepted that the term of tissue engineering was firstly put forward by Y.C. Fung over 30 years ago.[36] In 1985, he submitted a proposal to the National Science of Living Tissue. And three years later, the term "tissue engineering" was defined as the application of principles and methods of engineering and life sciences toward to the fundamental understanding of structure-function relationships in normal and pathological mammalian tissues and the development of biological substitutes to restore, maintain or improve tissue function at a National Science Foundation Workshop.[37] The field of tissue engineering is the comprehensive applications of clinical medicine, engineering, physical and material science to resolve the problems in the life sciences. Specifically, the engineering methods and biotechnologies were used to fabricate artificial tissues and organs with culturing cells on porous scaffolds three-dimensionally.[38]

There are thousands of patients receiving surgical operations every day to repair or replace injured tissues due to disease, injury or trauma. One of the most significant

aims of tissue engineering is thus regenerating damaged tissues for organ regeneration. The first organ implantation surgery was successfully made by Joseph in 1954 and he transplanted a healthy kidney for a patient and the donor is the twin brother of the receiver.[39] Hence, the adverse immune response of the organ against the receiver was avoided as the identical gene sequence. Five years later, Murray performed genetically nonidentical organ transplantation.[40] Such operation saved a lot of people's lives by now. Yet, there are some actual issues for this operation must be faced. The waiting list of organ transplantation surgery is far longer than the donors that can provide enough number of organs or tissue. Even the receivers who accepted the operation and implanted the organs from donors, they still need to face the problem of adverse immune response. The appearance of tissue engineering is thus playing an important in migrating the shortage of tissues from organ donors by *in vitro* generation of functional tissues.

Another purpose of tissue engineering is developing and mimicking tissue *in vitro* for disease modelling and drug screening application. Animal model is currently the methods for drug discovery and toxicity test. The drawbacks of animal model on this application are obvious. Such model requires high cost, low efficiency and ethical problems and low physiological similarity to humans. The last one result in many medications recalls each year and this lead to a lot of social problems. Bioengineered tissue models have been regarded as the alternative manner in drug screening, test and disease modelling. Last 5-10 years has witnessed great progress in generating cellular 3D environments that form tissues to mimic specific organ functions. These tissues make it possible to model *in vitro* injury or disease. Recent

years, the emerging of micro-tissue and on-chip size platforms enables the drug testing and delivery in laboratory. This small size of tissue makes it easier to maintain cell viability and restore tissue functions. By comparing with conventional tissue culture, this drug testing and disease-modelling platform requires shorter experimental time and lower cost.

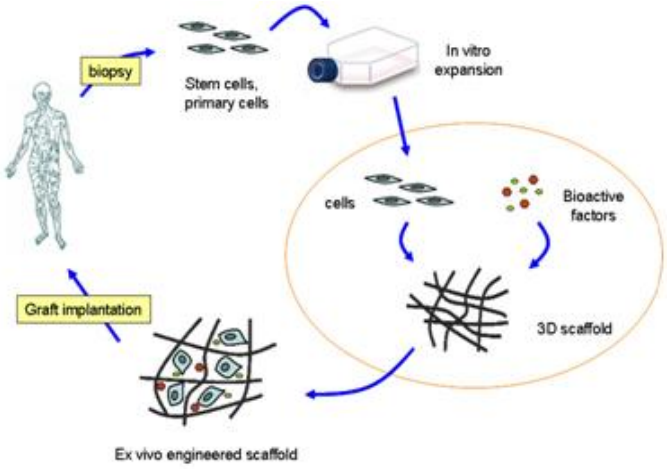


Figure 2- 5: Tissue Engineering paradigm: From cells isolation to tissue generation and implantation.[41]

Enormous progress has been achieved over the past decades in the field of tissue engineering. As it is stated above, this research field combines the techniques of scaffold development, cell culture and bioreactor design which can be seen from figure 2-5. The cells are isolated from the cell source and they will be seeded onto a scaffold. Tissue engineering heavily relies on the use of porous 3D scaffolds that cells can attach and grow.[42] They provide the appropriate cellular environment for the generation of tissues and organs. The tissue formed by cell-seeded scaffold is normally cultured within a device or system called bioreactor with growth factors

applied and mechanical and chemical stimuli onto tissues. The developed tissues are observed and detected within this bioreactor. Tissues with successfully restoring functions are cultured *in vitro* and can be directly implanted into an injured site of human body.[43]

2.2.2. Stem Cell Technology

The design approaches of tissue engineering include just cell structures, cells and scaffolds, and scaffolds only. The cell source is an important factor in successfully generating engineered tissue. In mid-19th century, it is found that cells are the fundamental components of life and some cells are potentially able to produce other types of cells. This cell was firstly discovered in human cord blood in 1978 called stem cell.[44] Researchers paid attention on use of stem cells including embryonic stem cells (ESCs), mesenchymal stem cells (MSCs) and induced pluripotent stem cells (iPSCs) in bioengineered tissue regeneration.[45] All stem cells are capable of dividing and replicating themselves for long time periods. And they are also unspecialized and can generate specialized cell types. Stem cells can be divided into two classifications as embryonic stem cells and adult stem cells. A new type was then identified after induced pluripotent stem cells being discovered in 2006.[46]

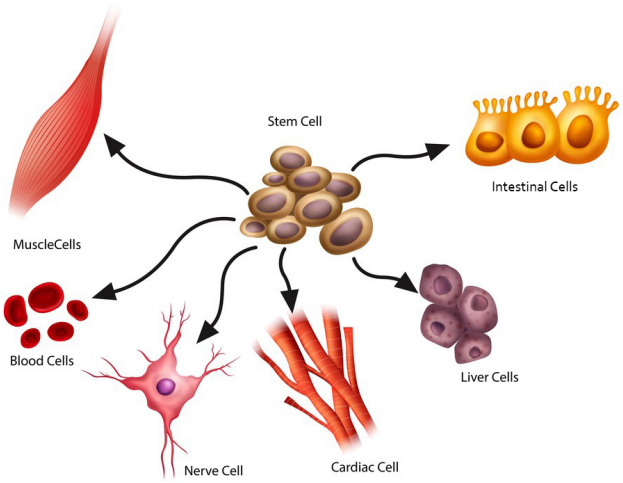


Figure 2- 6: Human stem cell applications: stem cell can multiply and differentiate into different types of cells within the human body.[45]

Embryonic stem cells (ESCs) are stem cells derived from the undifferentiated inner mass cells of the 3- to 5- day-old human embryos (or called blastocysts).[47] The cells are pluripotent and propagating. They can give rise to many specialized cell types and organs of human, such as heart, lungs, skin and other tissues. Therefore, they can be a useful tool for understanding the specialized cell mechanisms and organ structure establishment. Embryonic cell can be kept for long time culture, and thus potentially generating a great number of cells from the cell source. The first obtain of stable mouse embryonic stem cell lines was realized by Martin from mouse in 1981[44,48] and Thomson firstly reported the discovery of human embryonic stem cells (hESC) from human embryos 17 years later.[49] Thousands of hESC lines are generated from embryos to this day each year. According to the characterization of this cell, its greatest promise is to generate special cells for regenerated tissue to

replace patients' damaged parts of tissue due to degenerative diseases and injuries. Yet, there still are many challengers to apply the embryonic stem cells onto clinical application. The most significant problem is the possible rejection reaction from the receivers' immune systems. As most ES cells are derived from *in vitro* fertilization, they are allografts for the patients of implantation.[50] This problem is really hard to be overcome for human embryonic stem cells and the only possible method is nuclear transfer. Currently, just few researchers in some labs can realize this method. This is due to great difficulty, low efficiency, large number of cells requirement and thus the differentiation of ES cells cannot be produced in large-scale. Besides this, another problem is the related social ethics.

The adult stem cells are undifferentiated cells from the human body and they can self-renew to regenerate damaged cells and tissues. They are found in the living organism to maintain and repair the tissue of the human body. The adult stem cells were identified from the bone marrow in the 1950s. Researchers found the two kinds of stem cells there and they are hematopoietic stem cells and mesenchymal stem cells.[51] Afterwards more adult stem cells have been discovered from many tissues and organs, such as brain, blood, skeletal muscle, skin and etc. Compared with the embryonic stem cells, adult stem cells have limited capability of proliferation once they are removed from the body. It is difficult for them to have large number of cells regeneration.[52] This limits the development of the research field of adult stem cells application onto tissue repair for tissue injury or degeneration diseases. The current potential treatments are including bone tissue repair with cells derived from bone marrow and for diabetes with regeneration of insulin-producing cells. There still

cannot be found the trans-differentiation ability of adult stem cells and whether the control of the differentiate process exists.

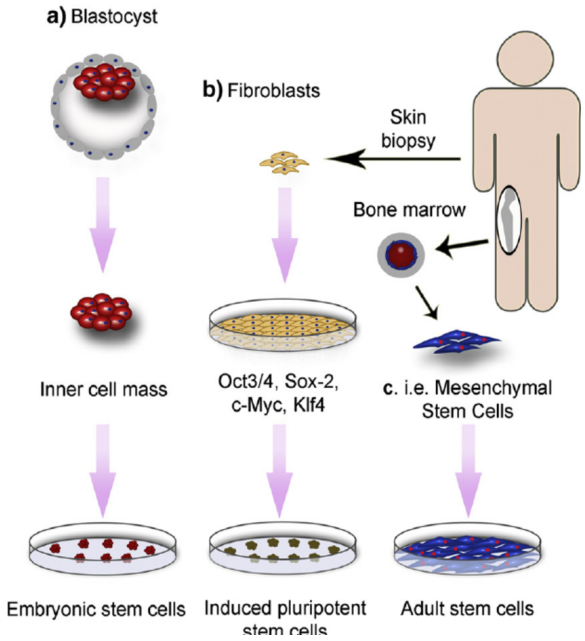


Figure 2- 7: The stem cells generation processes: (a) embryonic stem cells are derived from the inner mass of the blastocysts; (b) induced pluripotent stem cells are reprogrammed from fibroblasts with four genes overexpressing; (c) adult stem cells are obtained from adult human tissues and organs.[53]

The limitations of these two stem cells are quite apparent. In 2006, a new type of stem cell was discovered from mouse and named as induced pluripotent stem cells (iPSCs) and human iPSCs were produced one year later.[46] The induced pluripotent stem cells (iPSCs) were generated with genetically conversion from adult cells with four specific genes encoding (shown in figure 2-7). This type of cell perfectly resolves the issues of embryonic stem cells clinical application as the cell source is from adult cells and there is not any ethical issue. Although current study of iPSCs is proceeding and some problems are not solved, this cell holds potential for tissue

regeneration. Researchers and scientists hope to use the tissue in drug test, disease modelling and further tissue implantation.

2.2.3. Scaffold Design

The scaffold fabrication is another significant step within the research field of engineering tissue. To successfully regenerate tissues and organs in the human bodies, many special requirements should be satisfied. Scaffolds provide an environments or matrixes that cells can be seeded and attached *in vitro*. Numerous scaffold structures and materials have been discovered and detected for different applications in generating engineered tissue. Some considerations are significant while designing those scaffolds, including biocompatibility, biodegradability, mechanical properties of the material, construction structure and manufacturing technology etc.[38]

As scaffold is the place where cells lay down, the most essential feature of scaffold for tissue engineering is biocompatibility. To prevent the rejection from the body, normally the materials shall be inert property to immune reaction. As the implantation part and rather a permanent implant, the bioengineered tissue is designed to be replaced by the bodies' own cells over a long-time period. The scaffold should be biodegradable to allow cells attached to generate their own extracellular matrix. The mechanical properties of scaffolds should also be carefully considered. In some engineered tissue, like cardiac tissue, bone tissue, producing scaffolds with appropriate mechanical properties is a great challenger. Sufficient mechanical strengths of scaffolds in these tissues will not just help restore cellular

functions, and they also prevent the possibility of damage by surgical handling during implantation. Besides the material, the technology of manufacturing scaffolds is the most significant factor that affect whether the designed scaffold can be applied in successfully producing desired bioengineered tissue. To ensure diffusion of nutrients between cells within tissues, permeability of the scaffold should be carefully designed with high porosity properties. The proper porous interconnected construct also need to allow the waste production flow out of the scaffold and the degradation parts of the tissue exit the body.[54] Thus, the pores have a critical range of size while manufacturing the scaffold. That heavily depends on the cell types used for engineered tissue. It cannot be too small to block the cells migration within the structure. To establish the surface for cells attaching, the pore size should be small enough to make a critical number of cells be able to attach.[54] The advances of engineering and 3D printing provide more methods of manufacturing scaffolds to lower cost and easily design specific products.

2.2.4. 2D and 3D Cell Culture

Cell culture is an important tool for studying the fundamental mechanism of formation and function of tissues *in vitro.* This method can be further used for physiology study of cell behaviour or investigate how the function is affected under different conditions of diseases.[55,56] Cell behaviours, like differentiation, migration, growth are impacted by microenvironment that they are placed.[57,58] Thus, it is deserved to understand the morphology and functions of tissues and organs via cell culture. Currently, it has been widely used in understanding of tissue formation,

diseases modelling, drug delivery, protein production and regenerative medicine.[59,60,61]

It has been over 100 hundreds year since the first cell culture was achieved by Harrison with culturing nerve fibres *in vitro*.[62] The conventional cell cultures are most conducted under two-dimensional cell culture condition. In 2D cell culture conditions, the cells are cultured within a glass or plastic culture dish with coating surfaces as a monolayer or kept as a suspension form.[63] There are more than two adhesions. The first one takes place at the point of contact between cells and the bottom of container called focal adhension. Then, the fibrilar adhesion occurs while fibre like actin is secreted.[64] This will provide the energy for cells to be firmly attached at the surface of culture flask. After such process, the migration of cells can be accelerated and start to accumulate to form aggregation. It is obvious that 2D cultures has its advantages such as simple, high efficiency and enable us to improve the understanding of cellular behaviours via restoring part of functions of cells and tissues. On the other hand, it is also known that there are numerous limitations of 2D cell culture *in vitro*. Firstly, in 2D cell culture, the interactions between cells or cell and extracellular matrix cannot be fully restored. The interactions are related to the differentiation, proliferation, growth and other cellular functions of cells within the tissues. Furthermore, one of the most important differences is the cellular morphology, as cells trend to be flat while cultured in two-dimensional rather than presenting their normal forms *in vivo*.[65] These will result in inaccurate modes for mimicking cells and tissues functions in the body. This will also have negative impacts on the functions, structural organization and signals of cells. To overcome

such problems, some creative methods have been applied to customise the cellular morphology in 2D culture like micro-pillars, and micro-wells. There is one further disadvantage of cells cultured in two-dimensional condition that access to the constitution of medium is homogeneous without any gradient an cannot be controlled, including nutrient, gas exchange and metabolites.[66]

Due to such many shortcomings of 2D cell culture systems, the demand of three-dimensional culture for cells to better mimic natural tissues or organs is urgent and compulsory. In the human body, cells perform in 3D environment and the interactions between cells and cell-extracellular matrix have great impacts on basic behaviours and fundamental functions of cells and organs[67]. 3D form cell culture system provides cells with gradient access of nutrients, oxygen and dispose of waste. A well-established 3D microenvironment can advance the cell proliferation, migration and protein formation.[56]

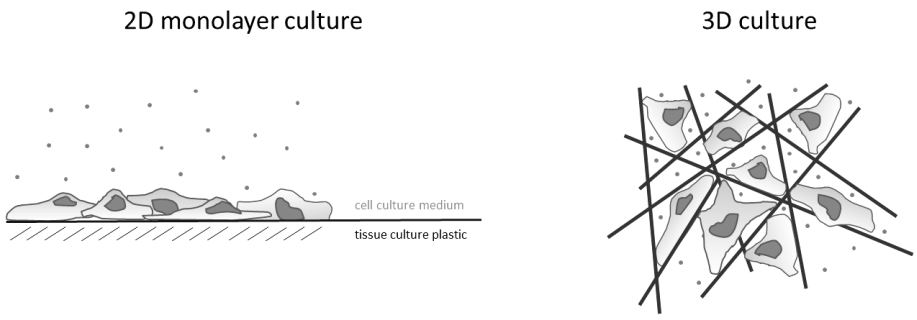


Figure 2- 8: The schematic diagram of 2D and 3D cell culture[68]

The first 3D cell culture system appeared in the 1970s and was realized by Hamburg and Salmon. They used soft agar solution as the matrix to culture human melanoma

cells.[69] According to the method of setting up model, 3D cell culture can be classified into 4 types. They are sphered culture[70], stack of cell sheets[71], cell culture in gel-like substances[72] and cells seeded into various scaffold.

In terms of the approach of cell sheet for generating engineered tissue, a micro-patterned thermo-responsive surface can be used for cells being attached. While the temperature drops to $20°C$, a single cell sheet will fall off from the surface. By stacking multiple cell sheets together, a 3D construct can be formed. Compared with other technology for 3D culture system formation, stacking of cell sheets provide cells with better influx of cellular migration. In clinical, there are many fields have applied this technology for human use, including heart, cornea, ear, knee cartilage and lung.

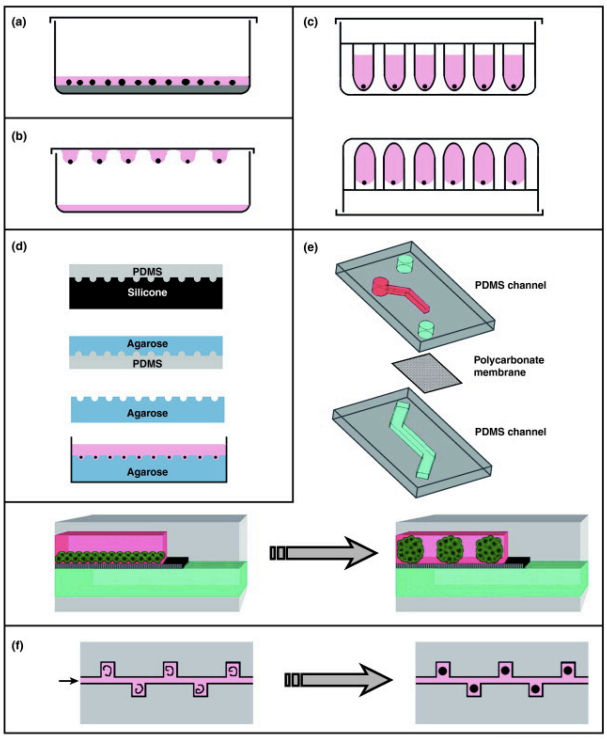


Figure 2- 9: Spheroid fabrication method for generating 3D cell culture system[73]

Last decade witnessed great advance of scaffold developing technique for encapsulating cells into such structure. Various scaffolds with cells attached gave us opportunities to establish *in vitro* 3D tissue model and study the interactions between cells and ECM. Biopolymers isolated from animal tissues are one kind of the most often used materials for generating scaffolds. It has been proved that they can mimic the biochemical environment that cells experience in the native tissue and make tissue to better restore their functions. Hyaluronic acid[74], gelatine[75] and collagen[76] are all normally used natural polymers for creating scaffold, while alginate and chitosan are two materials from non-mammal tissue[72]. Apart from biopolymer scaffold, prefabricated scaffolds and block-based scaffolds are new methods to provide better porous and control of the environment. Many applications have been made into generation of cancer model, stem cells and organs culture, liking liver, heart and etc.[77]

2.2.5. Engineered Cardiac Tissue Generation

Last decade has witnessed great progress in tissue engineering and it holds great potential applications on solving many tough clinical problems. Such research gives patients with cardiovascular diseases a great hope after the first cardiac tissue was generated with the cardiomyocytes isolated from embryonic chicken over 20 years ago.[78] Since that, the development of bioengineered cardiac tissue became an emerging and rapidly growing research field.

Burrows cultured some explanted hearts from embryonic chick in 1912 and the individual cardiac cells were observed migrated away from the tissue. But this was

not drawn too much attention from the researchers as they cannot isolate the cells from heart until Cavanough found a method in 1955.[79] He dissociated cardiomyocytes from neonatal chick and maintained them as single cells. Five years later, the isolation and culture of mammalian cardiomyocytes were firstly realized by Harary and Farley (1960).[80] Most long-term culture and studies of cultured myocytes were performed on cardiomyocytes from neonatal animals, as it is much more difficult to isolate adult cardiac myocyte which was not resolved until 1977.[81] Another difficulty is the further extremer conditions in culture adult myocytes and this still limits the development of adult cardiomyocytes research nowadays.

Like other artificial tissues, isolated cardiomyocytes were originally cultured onto the surfaces of multi-well plates, culture flasks and petri dishes referred as monolayers with cells attached. These can be easily realized and help understand basic functions of cardiomyocytes *in vitro*. However, it is known that tissues in the body are three-dimensional structures and thus two-dimensional culture cannot represent all the properties of cardiomyocytes properly. 3D *in vitro* engineered heart tissue can be achieved by assembling cellular monolayers onto each other. Shimizu et al devised a special method to generate 3D engineering heart tissue by stacking 2D cell sheets together.[82] A temperature-responsive polymer was used so that the cell layers can detach from the culture surface without any damage when the temperature drop down to 32°C from 37°C. Four cell sheets were layered together to obtain a thick cardiac patch. The stacking of cell sheets can beat continuously.

Compared with other techniques to form *in vitro* 3D engineered heart tissue, this scaffold-free method is quite suitable for transplantation due to simplicity and the

lack of extracellular matrix. After several tests of implantations onto animals over past years, the first patient who has dilated cardiomyopathy was treated with the stacked myoblast sheets in 2012.[83] After transplantation, his clinical condition improved drastically. The thickness and requirements of force transducer for functional analysis limited its application in drug testing and disease modelling.

Another attractive approach for generating cardiac tissue is reseeding cells onto decellularized animal hearts. The technology for decellularization has already been well developed, but the difficulty of seeding back cells at enough efficiency is still a problem. Guyette developed a bioengineered cardiac tissue based on native extracellular matrix with 500 million hiPSC-derived cardiomyocytes.[84] Similarly, this method is also not a good way for drug testing but hold a great potential application for cardiac regeneration.

As the basic units of cardiac tissue, beating and the generation of contractile force are the key functions of cardiomyocytes and thereby providing energy for pumping the blood to the whole body. The main feature to be investigated is their ability to contract and Moscona developed some beating spheroids with myocytes from embryonic chicken according to this.[85] This is regarded as the first 3D construct of heart tissue *in vitro*. Compared with cardiomyocytes cultured in monolayers, this construct shows more similar functions to intact heart even though they were still not able to fully remodel natural heart tissue.

Currently, most engineered cardiac tissues are developed with hydrogel scaffold. The first successful engineered heart tissue was made by Eschenhagen T with the cardiomyocyte from embryonic chicken in 1997.[78] To make this engineered cardiac

tissue, the embryonic chicken myocytes were cultured onto scaffold made from collagen I. The two ends of the tissue attached to two separate Velcro-coated glass tubes, so the force generated can be measured.

With fibrin, Brian fabricated three-dimensional cardiac muscle tissue. Cardiac muscle fibres were observed with uniform cellular alignment. The cells cultured in such model could be cultured for about 2 weeks.[86] Two years later, Brian introduced a method of generating functional engineered cardiac tissue with pluripotent stem cells.[87] A fibrin-based hydrogel matrix and embryonic mouse stem cell derived cardiomyocytes were applied for such purpose. The structure was kept for more than 21 days (3 weeks) and showed some similar functions of native heart tissue. The cells distribute evenly and aligned along the force line. The culture periods for these models cannot be more than 3 weeks, but such time is not sufficient for further analysis especially for drug testing. Also the maturation of cells is another problem, and this could be potentially resolved via various stimulations like mechanical and electrical stimulations.

2.3. Dynamic Perfused Cell Culture and Drug Testing

2.3.1. Cellular Force and Its Measurement Techniques

It is known that forces generated by cells play an important role in regulating cells adhesions, proliferations and functions.[88] To accurately characterize cellular forces, a great number of work have been made over the past decades.[89,90,91] Mechanical forces from the cells are the engine of the bending, deformation and alignment for tissue development and wound healing.[92,93] Compared with the molecular genetic

tools to investigate the expression, distribution and activities of specific proteins, the study of cellular mechanical forces is still largely insufficient. This study could be especially important for those cells with intense mechanical activities like smooth muscle cells and cardiac muscle cells.[94,95] Thus, the measurements of the interactions between cells, cells and extracellular matrix are critical. This research field has a great application and influence in biological, physiological and medical area.[96]

To detect the forces generated from cells, accurate measurements heavily rely on suitable engineering device and techniques. It can help to provide a similar micro-environment and a real-time detection of cellular forces. Conventional methods for measuring cellular forces include cell poking (a method to determine mechanical properties of single cells with measuring forces of indenting cells attached to a glass coverslip),[97] optical tweezers (a highly focused single-beam gradient laser beam force to trap and manipulate small particles),[98] atomic force microscopy (a high resolution type of scanning probe microscopy that can be used to measure the forces from the probe and the sample),[99] micro-plate manipulator (using microplate to pull the cells from rectangular glass bars and manipulation and mechanical perturbation of individual cells can be observed with microscopes),[100] micropipette aspiration (with micropipette, the surfaces of individual cells can be aspirated into a glass tube. The leading edges of the surfaces of these cells can be tracked with optical microscopes).[101] All these methods rely on specific designed equipment and complicated sample preparation, yet these are quite hard to be used for measurement of cardiomyocytes contractile forces. As a biocompatible viscoelastic material,

enormous applications of PDMS in cellular forces measurement in various methods have been made.[102,103,104] Different designs of platform have been put forward to quantify forces generated by various cells or tissues. To accurately measure cellular forces, the force sensors need to be carefully calibrated before using as the force transducers to obtain cellular forces.

For cardiac muscle cells cultured within cardiac tissue, the force is generated via the protein myosin being activated by inducing pacemaker cells pulling actin filaments to realize interactions between cells through gap junctions.[105] As the cardiomyocyte is a single nuclei cell, the contraction of the tissue is totally due to interaction between cardiac muscle cells.[106] Thus, the measurement of cellular force can be transformed to measurement of the contraction of cardiac muscle tissue.

2.3.2. Introduction of PDMS

With the development of micro-electromechanical system (MEMS), increasing numbers of such technologies have been applied into biomedical research area.[107] In this project, we aim to develop a method to three-dimensionally culture cardiomyocytes *in vitro* and do real-time monitor of cellular activities. To generate an engineered cardiac tissue, a platform needs to be set up for tissue attachment. With such platform and specific mechanical modelling, we developed a method to measure cellular interactions and monitor their variations under different conditions.

The material that we used to generate the platform for engineered heart tissue is Polydimethylsiloxane (PDMS). It is a silicone-based organic polymer and known for its unusual rheological properties. It has been widely used in manufacturing

biosensors, medical devices and elastomers.[108,109,110] This material is optically clear, and it is considered to be transparent, non-toxic and biocompatible with tissues and cells. [111]

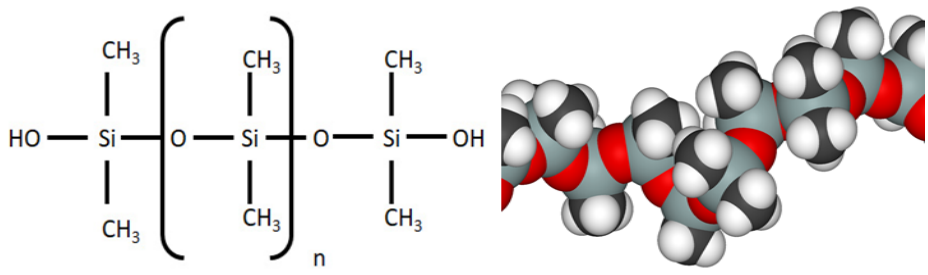


Figure 2- 10: Chemical formula and chemical structure of PDMS [111]

The chemical formula for PDMS is $(H_3C)_3SiO[-Si(CH_3)_2O-]_nSi(CH_3)_3$, where n is the number of repeating monomer $[SiO(CH_3)]_2$ units and its basic chemical formula is shown in figure 2-10. The low n corresponds to liquid PDMS and larger n results in a flexible polymer chain with a high level of viscoelasticity. That means the viscoelastic property of PDMS can be controlled to get the desirable conditions with different manufacture process.

It is known that PDMS construct is a crosslinking network of polymer chains. The diameter of these polymer chains ($SiO(CH3)_2$) is about 0.7nm.[112] Once they connect with each other, they are in a random coil form with a thickness of 10nm (shown in figure 2-11). To fabricate desirable PDMS stuff, liquid PDMS is mixed with a cross-linking agent. After bubbles are removed from the mixture, it is poured into specific designed moulds and heated for a period to obtain an elastomeric replication of the moulds.

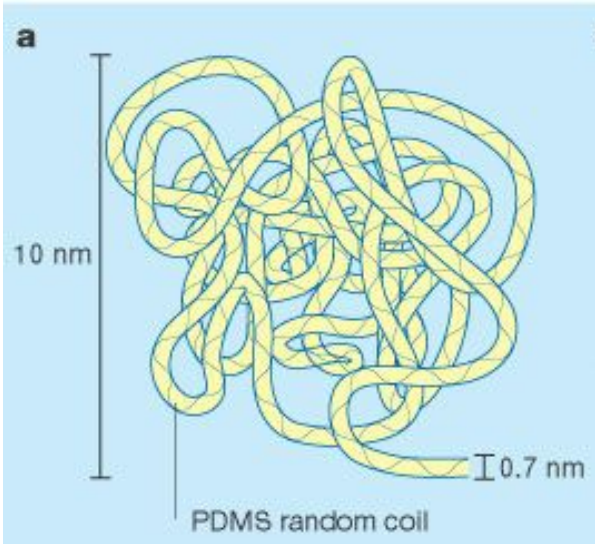


Figure 2- 11: PDMS in random coil form [113]

PDMS has a wide range of applications in industry. Here we used this material to fabricate the culture platform to support the tissues and it also works as a cellular force transducer with the pillars made from PDMS. This kind of force transducer has many advantages over other materials including its biocompatibility, low cost, greater mechanical strain, easy fabrication, and chemical inertness.

2.3.3. Mechanical and Electrical Stimulation for EHT

Tissue engineering has a great advance in the last decade. It has been proved that different types of stimuluses can improve the construct and functions of cells cultured *in vitro*, like growth factors, drugs, special microenvironments and different scaffold materials. In particular, mechanical and electrical stimulation holds great potential application in regulating cells and tissue culture in laboratory.

Introducing of mechanical stimulation helps enhance contraction of cardiomyocytes cultured in 2D. For 3D engineered cardiac tissue, the presence of mechanical stimulation improves the performance of EHT in terms of cellular alignment[114], gene and protein expression[115], and tissue function[116].

For hydrogel-based engineered heart tissue, a mechanical support is required to driving EHTs development and maturation. Static supports were utilized in the early works and these just allow limited deflections of tissue, like Velcro-coated glass tubes[117], metal braces[118] and Velcro-frames[119]. New systems with elastic anchors allow the tissues to contract with each beat and improve the physiological functions of cardiomyocytes[120]. With these stimulations, the cells cultured in EHTs show better organization, larger cell size, myofilament length and higher cellular density. It can be concluded that mechanical stretch is significant to the 3D maintenance and cellular maturation in three-dimensional condition.

Various electrical activities within the human body guide the development and maintenance of tissues. In central nervous system, neurons develop special capabilities for sending electrical signals along axons so that fast communications between cells can be achieved in long distance. The ions moving across membranes form electrical signals called action potentials.[121] With action potential, central nervous system receives and coordinates information thereby controlling the activities of the whole bodies. The continuous pumping of ion channels across the cells established voltage gradients named membrane potentials. Unlike other organs, there are some special cells within healthy hearts called sinoatrial node. They are found in the right atrium and regulate the cardiac activities by producing action

potentials. All the cardiomyocytes are connected by gap junctions to interconnect with each other resulting in tissue contraction.

Endogenous electrical system plays a significant role in all the living organs. To mimic the electrical signals *in vivo*, researchers tried to use external electrical stimulations onto bioengineered tissue. The first application of electrical stimulation is in 1942 and Gutmann used ES to mimic the nervous system in denervated muscles to keep their functions.[122] In the following years, the electrical signals have been shown that they are able to control cellular growth, maturation and orientation.

Bioelectrical system plays an important role in cardiac development and functionality. In the human body, electrical signals passing through cells make the cells contract at the same pace throughout the whole heart and pump blood to the whole body via heartbeat. With the electrical stimulation, cells *in vitro* cultured in 3D construct can be induced to pace synchronously. It can change the contractile activities of EHT from beat rate[123], duration[124], and contractile force generation[105]. Most electrical stimulations are constructed with carbon electrodes, and all the set-ups are simple and rough. Thus, the electrical filed for stimulation requires an optimization process to provide best bioelectrical environment for cells. Then, the cardiomyocytes cultured in EHT can be studied in terms of growth and cellular maturation while different stimulations are applied.

Bioelectrical system plays an important role in cardiac development and functionality. In the human body, electrical signals passing through cells make the cells contract at the same pace throughout the whole heart and pump blood to the whole body via heartbeat. With the electrical stimulation, cells *in vitro* cultured in

3D construct can be induced to pace synchronously. It can change the contractile activities of EHT from beat rate[123], duration[124], and contractile force generation[105]. Most electrical stimulations are constructed with carbon electrodes, and all the set-ups are simple and rough. Thus, the electrical filed for stimulation requires an optimization process to provide best bioelectrical environment for cells. Then, the cardiomyocytes cultured in EHT can be studied in terms of growth and cellular maturation while different stimulations are applied.

This is especially true for engineered heart tissue. Bioelectrical system plays an important role in cardiac development and functionality. In the human body, electrical signals passing through cells make the cells contract at the same pace throughout the whole heart and pump blood to the whole body via heartbeat. Contraction is one of the most important features of cardiomyocytes and it is regulated by excitation-contraction coupling process in cellular level. The specialized external electrical stimulation can affect various behaviours of engineered heart tissue, like beat rate[123], duration[124], and contractile force generation[105]. With the electrical stimulation, cells *in vitro* cultured in 3D construct can be induced to pace synchronously.

The design and use of electrical stimulation has drawn great attention in cardiac research field and many applications have achieved. It is proved that electrical stimulation helps overcome challenges of insufficient cellular alignment, differentiation and metabolic activities.[125, 124, 126] They are quite significant in restoring the features and functions of engineered heart tissue *in vitro.*

Although many trials of electrical stimulations have been made in recent years, there are still some improvements to be achieved. Most electrical stimulations are constructed with carbon electrodes, and all the set-ups are simple and rough. Thus, the electrical filed for stimulation requires an optimization process to provide best bioelectrical environment for cells.

In this thesis, I introduced a personal designed microbioreactor integrated with electrical simulation system to introduce electrical field onto engineered heart tissue. Deeper understanding of electrical filed effects was investigated under perfused culture condition. To obtain best stimulation results, the system was simulated and optimized with different parameters applied. With such system, the parameters of electrical stimulation can be controlled and adjusted to achieve better growth and cellular maturation while different stimulations are applied.

2.3.4. Three-dimensional Perfused Cell Culture and Perfusion System for Culturing EHT

Currently, the cell culture is largely based on static culture within multi-well plates, cell culture flask and petri dish in laboratory. In these conventional 2D cell culture methods, the medium supply and waste removal are all relied on manually change. This can potentially result in large fluctuations during the process of medium change. Furthermore, occasional shortage of nutrients or oxygen may lead to organelle dysfunction and lowering cellular viability for the cells with high metabolic activities.

The emergence of bioreactor can resolve such problems by providing a stable microenvironment for cell culture, as they are maintained *in vivo*. In the body, the nutrients delivery and the removal of metabolic waster via blood flow through capillaries with regulation of central nervous system. This guarantees the cells being maintained relatively steady. Perfused bioreactor is designed for mimicking such microenvironment and interstitial fluid flow in the human body. The medium can be delivered and removed by continuous control thereby maintaining cells a desirable and necessary condition. Compared with traditional static culture, perfusion helps improve cellular viability and maintain metabolic functions. It has been proved that the fluid flow over tissue ECM has great effects on the morphology and migration of different cells.[127,128] This is mainly due to a better control of diffusion. With such control, the gas exchange between cells and tissues can be optimized. It also provides a higher mass transfer and more physiological solute concentrations.

To generate perfused culture, personal designed device, known as bioreactor, is required to provide a place for biological and chemical processing. The environment within it can be carefully controlled and monitored. There are many different types of bioreactors designed for various purposes. The fluid flow has been special controlled to optimize the mass transport over tissue surface or through tissue construct. For example, they are stirred suspension culture bioreactor, rotating wall vessel bioreactor, hollow fibre bioreactor and direct perfusion bioreactor.[129, 130]

These bioreactors are designed for generating desirable tissue with large number of cells. Yet these products are not suitable for drug testing or parallel experiments, as they are high cost in setting up and running. Thus, it is meaningful to scale down

such systems to lower related cost. In such background, the design of chip-sized micro-bioreactor makes the experiments can be operated at the same time and lowers the cost with less consumption. With mature 3D cell culture technology, microfluidic devices have great applications for small-sized tissue generation *in vitro.* They give a well-controlled environment for complex structure of tissue small scale. The cells number and culture medium are lowly required. The size of these devices makes it possible to portable and convenient move.

It is therefore significant to design three-dimensional culture within suitable micro-bioreactor for generating engineered heart tissue for drug testing. Perfusion culture has special importance for drug test application. The drugs and process of applying drugs can be easily operated out of the bioreactor thereby avoiding distribution of cell culture environments. The concentrations of drugs are well controlled to give a high-quality result of relationship between drug application and cells response. It is also easy to realize research cells reaction under different concentrations. This is hard to be made with static culture, as the level of metabolic consumption of drugs cannot be measured in real-time. The drug delivered in the body is also perfused with blood flow that can be mimicked by perfused culture.

To improve nutrient delivery and gas exchange, there are many bioreactors have been designed for culturing engineered cardiac tissue. With different bioreactors, such as, rotating[131], dynamic flexure[132], cyclic stretch[133] and pulsatile bioreactors[134], engineered cardiac tissue has been widely studied.

As described before, mechanical and electrical stimulation can both have great effects on cellular activities and functions of cardiomyocytes cultured in 3D EHT

construct. Thus, it is valuable to determine the effects of coupling of electrical and mechanical stimulation for proper functions of cardiac tissue. Yet, in previous study, there are limited number of work have been done to design a bioreactor for culturing 3D engineered cardiac constructs with media perfusion and electrical stimulation. There ever a perfusion and electrical stimulation system for culturing a recellularized decellularized heart. A continuous electrical system (1Hz, 5V) is applied to promote intercellular connection. This work shows the feasibility of using decellularized whole heart for *in vitro* models of a functional heart[135].

Another system is bio-wire platform, which allows both electrical stimulation and perfusion of wire-based engineered cardiac tissue. Neonatal rats cardiomyocytes are used for generation of EHT and it is found that presence of electrical signals makes it have better cellular alignment and mechanical performance. However, it is essential to develop a perfusion system for a hydrogel-based engineered cardiac tissue. With suitable electrical stimulation and mechanical stimulation, a perfusion bioreactor could play a key role in the application of using such EHT platform for drug development and drug testing.

2.3.5. EHT Application for Drug Development and Disease Modelling

Although the application of engineered heart tissue onto cardiac repair is still in experimental test phase and does not enter clinical arena, a great number of progresses have been made over the last decades. Besides cardiac tissue transplantation, engineered heart tissue has various use in *in vitro* physiological and disease modelling.[136] Another important application is drug screening. Normally,

new drugs cannot be directly tested on human cardiac cells, as there is not human heart cell line. The conventional methods on new cardiac drugs tests are relying on animal models. However, exist of species-specific differences between human and animal in terms of heart makes the estimation inaccurate. Some toxic properties to the human heart of drugs cannot be detected by these models. This leads to withdraw of drugs has entered clinical trials and even occasionally results in serious problems like death. Due to this, the creation of engineered heart tissue shows extreme value in identifying such drugs before the process of clinical trials. The drug discovery process can be accelerated thereby lowering research cost and make it safer and more effective in treatments.[137]

Compared with using EHT for mimicking native heart tissue, it is more important to have an engineered construct with simple, robust, and low cost features aiming for drug testing. It provides a better physiological environment and cellular maturation. In previous study, there are only few works have been conducted for testing different drugs with various concentrations. Thus, it is required to develop a system that can realize the purpose of drug testing, especially for different kinds of drugs with various concentrations.

Chapter 3 Microbioreactors for EHTs Development

3.1. Introduction

There is an urgent need for generating functional human engineered cardiac tissue for physiological study and transplantation. As the advance of induced pluripotent stem cell (iPSC) technology, personal specific stem cells can be obtained and expanded into various types of cells. Enormous methods have been developed to efficiently induced iPSC into human cardiomyocytes. It provides potentially limitless quantities of cardiomyocytes. This will enable the achievement of generating human cardiac model for physiological study and drug screening. However, the quality of cardiomyocytes derived from iPSCs in terms of their functional and structural maturation is different from that of native human cardiomyocytes. iPSC-CMs are small in size and in round shape. Their sarcomeres are unorganized and T-tubules are missed. They have relatively low response to stimulations and slower contraction compared with native cardiac muscle cells.

It is know that there are many factors could potentially enhance cells functionality and degree of maturation, including three-dimensional cell culture, perfused media flow, and various stimulations. Therefore, the purpose of my DPhil is to develop a functional human cardiac model with improved physiological functions and evaluate its performances for drug testing. To achieve this purpose, a perfusion microbioreactor is designed with electrical stimulation system embedded.

Measurement of cellular forces is always a critical field of research.[138] The mechanical interaction between cells and extracellular matrix is a great factor that affects the cells migration, division, functions, and tissue formation.[139,140] This is

especially significant for cardiomyocytes within cardiac tissue, as they are the basic contractile units of cardiac muscle.[38] As one of the most significant features of this cell, contractile forces generated by cardiomyocytes can be used to evaluate the function of cells and tissues. Thus, designing specific mechanical system for providing mechanical stimulation onto cells and accurately measuring cellular forces is quite important. The contractile forces generation from cardiomyocytes in the tissue have been studied for a couple of years.

Thus, the first task of my project is developing a platform for cardiomyocytes being *in vitro* cultured three-dimensionally. To generate engineered cardiac tissue, a polymer material called polydimethylsiloxane (PDMS) was used to fabricate the platform to provide a culture surface for engineered heart tissue in 3D and it also works as an accurate cellular force transducer to acquire the contractile force generated from cardiomyocytes network.

As a silicon material, the force can be tracked by material deformation with specially design. Hence, the configuration of the platform should be carefully designed and a precision mechanical modelling needs to be set up. The mechanical property of PDMS was studied to ensure the system designed here is reliable and accurate as it highly depends on different factors during manufacture process of the platform.

The purpose of tissue engineering is generating functional tissues that can re-establish the structure and functions of damaged parts within the human body. To mimic natural extracellular matrix, cells are seeded onto special designed biological substitutes. According to previous studies and researches, it has been proved that

scaffold plays a significant role in providing the support for cells so that they can restore their three-dimensional form and natural functions.

To further accurately monitor and adjust the conditions of cell culture, the scaffold with cells can be cultured within a perfusion microbioreactor. In such equipment, the cell culture status can be monitored and adjusted via dynamic medium flow control.

Moreover, it has been widely accepted that electrical stimulation has great effects on the functionalities of engineered cardiac tissue.[141] It is meaningful to integrate an electrical stimulation system into the microbioreactor for improving cellular performance via providing bioelectrical environment. To generate the electrical field with low side effects onto cells viability and activities, carbon is selected as the electrode material as its high capacitance and resistance to chemical environment.[142] Compared with other materials like steel and ceramic, its characteristics of charge transfer is especially significant.[143]

To evaluate the feasibility of the system, cardiomyocytes isolated from neonatal rats were cultured within the microbioreactor. After determine the optimal conditions and parameters of setting up the system, it can be used in developing engineered heart tissue with iPSC-derived cardiomocytes as human cardiac model for drug testing.

3.2. Materials and Methods

3.2.1. Generation of Engineered Heart Tissue

Here we want to generate the *in vitro* three-dimensional engineered heart tissue to mimic the microenvironment of cardiomyocytes within native heart. As stated before, the heart is a muscular organ that pumps the blood to the whole body. Thus, the contractile forces generated by cardiac muscle cells and cardiac tissues are the key factors to determine the functionality of the cells and tissues. To accurately measure and real-time monitor the contractile force generated by engineered heart tissue, a platform made with PDMS was designed and manufactured. Following the approved protocol designed by Arne[105], the engineered heart can be generated and attached onto the platform made from PDMS.

In this experiment, cells used were the cardiomyocytes isolated from embryonic rats and human iPSC-derived cardiomyocytes. To generate bioengineered cardiac tissue, rectangular agarose casting moulds were made with Teflon spacers. As shown in Figure 3-1, 1.5mL 2% agarose (in PBS, Sigma Aldrich A9539, UK) was added into each well with Teflon spacer inserted. After around half an hour, agarose was solidified, and the spacer was removed. An agarose slot 12mm in length, 3mm in width and 4mm in depth was formed in each well. The stock solution was prepared with 50mg/mL bovine fibrinogen (Sigma-Aldrich, UK, F8630) with 0.5mg /mL aprotinin (Sigma-Aldrich, USA, A1153) in 0.9% saline solution. To make a reconstitution solution, 5 million cells/mL was mixed with 100uL/mL Matrigel (Sigma-Aldrich, USA, 126) and 5mg/mL bovine fibrinogen with corresponding volume DMEM. 120mL prepared reconstitution mix was then added into the

agarose slot in each well with 2.5uL thrombin (3U/ml, Sigma-Aldrich, UK, T4648). To make the construct of hydrogel with polymerized fibrinogen, the whole 24-well plate was put into the standard cell culture incubator at 37°C with 5% CO2 for 2 hours. Afterwards, 300mL of cell culture medium was pipetted into the wells to erase the connection between the engineered heart tissue and the agarose so that the platform could be easily taken out. All the constructs are placed into a new 24-well culture dish with EHT medium for culturing 3 days.

The medium was made up of 10% horse serum (Thermo Fisher Technologies, USA, 26050), 1% penicillin/streptomycin with 10µg/mL insulin (Sigma-Aldrich, USA, I9278), 400µmol/L tranexamic acid (Sigma-Aldrich, USA, 857653) and 33µg/mL aprotinin in Cardiomyocyte Maintenance Medium (AXOL, UK, ax2530-500). The bioengineered cardiac tissues were then cultured in the 24 well culture dish for 3 days within the incubator and the media was changed every 48 hours. They were then transferred into the autoclaved micro-bioreactors individually and kept in the incubator box with media flow through the tissues.

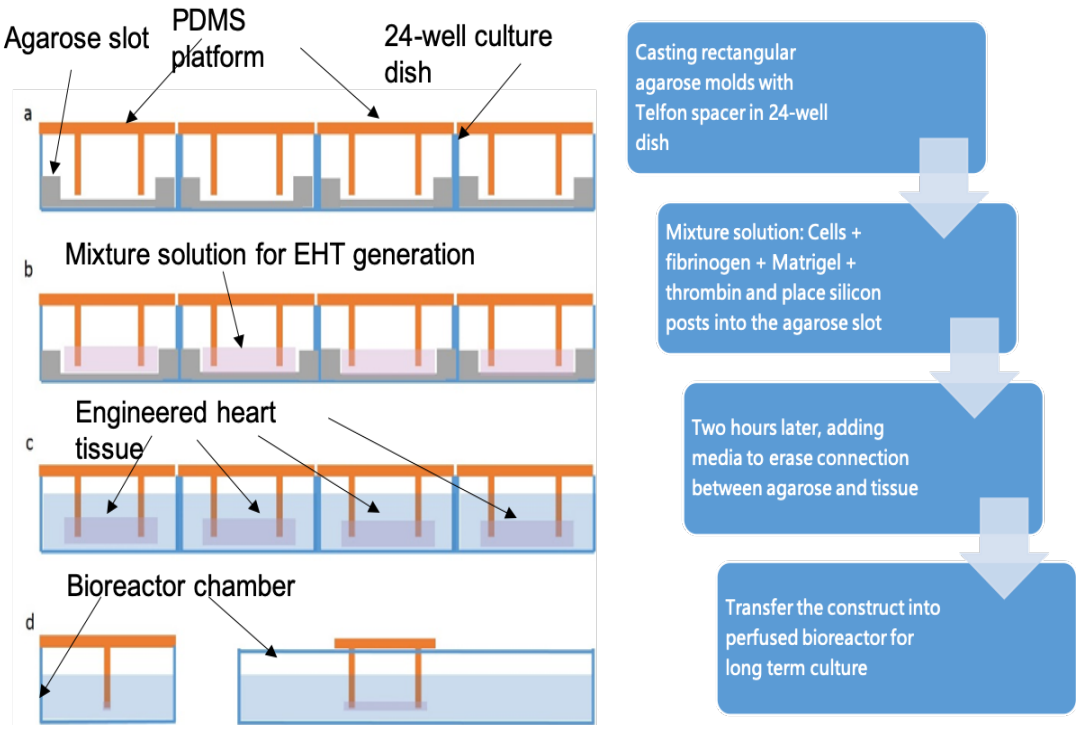


Figure 3- 1: Illustration of the experimental procedure for generating and culturing engineered heart tissue; the orange parts are the PDMS platforms, the blue parts are the culture dishes and wells; the grey parts are the agarose moulds and the light blue parts are the culture media. (a) Casting agarose (2% gel) slots with the Teflon spacer in each well of 24-well culture dish; (b) Prepared reconstitution mixture (cells, fibrinogen, Matrigel, thrombin) is pipetted into the culture dish so that the gel can be formed and attached onto the top of the PDMS posts; (c) The engineered heart tissue are polymerized two hours later and media is added into each well to ease the connection between tissue and agarose. (d)The generated tissues are transferred into bioreactor and cultured further for a couple more days. Cross and longitudinal section of bioreactor is displayed.

To make the generated tissue samples more flexible and easier to be transferred into microbioreactor, the configuration is modified to single-well design of 24-well culture dishes as shown in figure 3-2 (a) & (b). From figure 3-2 (c), it can be seen that the engineered tissue attached onto the ends of two silicon posts. To generate the mini-sized engineered heart tissue *in vitro* based in 24-well culture dish, the first step is creating rectangular agarose slots within each well. The Teflon spacer that we designed here is for one row (4 wells) of the 24-well culture dish as shown in figure 3-1 (d). After fully dissolving 2% agarose powder (Sigma, USA, A9539) in PBS with hot plate, 1.5ml of the solution is added into each well with Teflon spacer being inserted to form the casting moulds. It took about half an hour for agarose solidification before the spacer being removed. The agarose slots formed in each well are 12mm in length, 3mm in width and 4mm in depth. A stock solution is prepared for generating the scaffold gel to form three-dimensional constructs for cardiomyocytes attaching. The stock solution is made up of 200mg/ml bovine fibrinogen (Sigma-Aldrich, USA, F4753) with 0.5µg /mL aprotinin (Sigma-Aldrich, USA, A1153) in 0.9% NaCl solution.

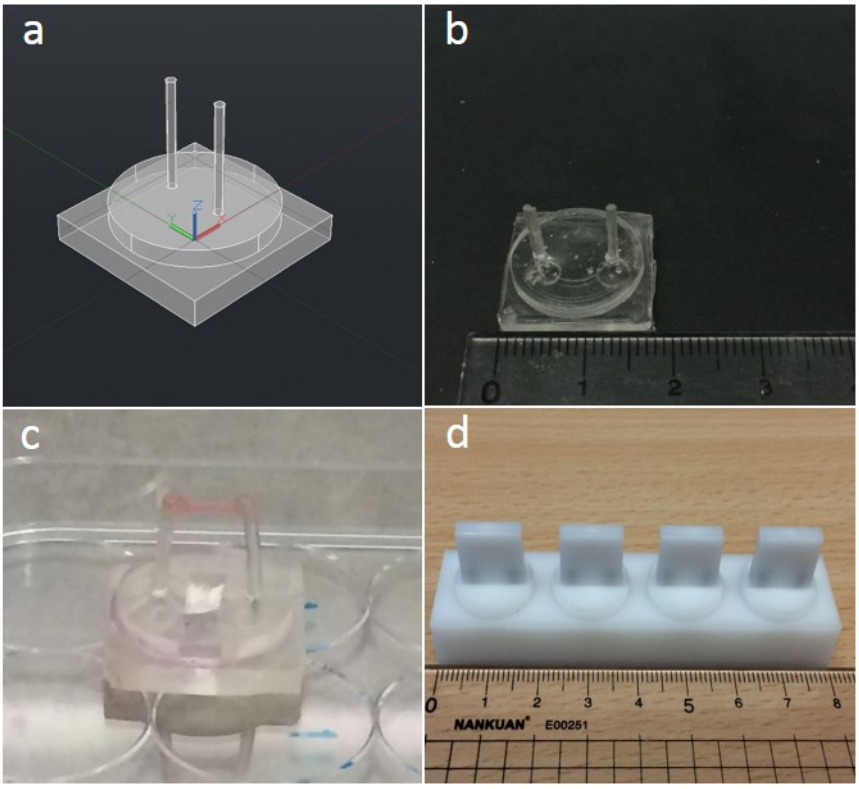


Figure 3- 2: Geometric display of experimental instruments, both measured to millimeter scale. (a)The platform design with AutoCAD; (b) The platform with two silicon pillars made from PDMS; (c) Generated engineered heart tissue (pink one) attach onto the end of the two pillars; (d) Teflon spacer designed for creating agarose casting slots with four wells turned upside down.

3.2.2. PDMS Platform Design and Mechanical Modelling

As the platform has direct contact with cells and tissues, it should suitable for using in cell culture environment and have great biological compatibility. Also, to accurately measure contraction force generated by engineered cardiac tissue, it has to be low stiff. PDMS is the perfect material meets all the requirements.

To convert the PDMS pillars deformation to force, accurate characterization of PDMS mechanical properties is demanded. As a viscoelastic material, the mechanical properties of PDMS highly rely on many factors during manufacture process. Thus, it is important to study the unique properties of the soft materials in detail so that most suitable design can be made and characterized.

As shown in figure 3-2 (c), the generated tissue attached onto the silicon posts. To determine the relationship between force and displacement of silicon pillars ends, the platform can be simply described as a cantilever beams model and the posts were bent upon the contraction of cardiomyocytes. The magnitude of force can be calculated from the displacement at the top of the two silicon posts, which can be seen from the figure 3-3.

The standard cantilever beam deflection follows the Euler beam theory. Let the length of the post to be L and a concentrated force F is subjected to the free end of the post. Within the elastic range, the curvature of the silicon posts can be described as,

$$E = \frac{1}{\rho} = \frac{M}{EI} \tag{3.1}$$

Where ρ is the curvature, M is the bending moment E is the elastic modulus, I is the cross section moment of inertia.

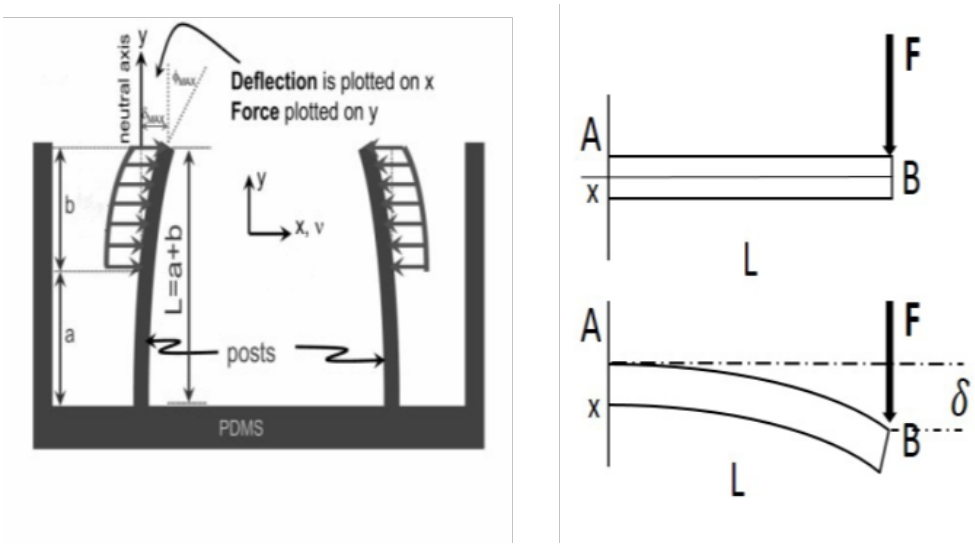


Figure 3- 3: The beam deflection model. Force is applied along the vertical direction.

When the force is applied, both the bending moment and the curvature vary with the distance from the fixed end of the post. Hence, the moment can be expressed as M (x). The equation (3.1) can be written as,

$$E = \frac{1}{\rho} = \frac{M(x)}{EI} \tag{3.2}$$

The curvature M (x) is related to the force F and distance x, which is defined as zero at B.

$$\frac{1}{\rho} = \frac{-Fx}{EI} \tag{3.3}$$

Assume a point Q (x, y) in the post; the curvature of this point can be described as,

$$\frac{1}{\rho} = \frac{-\frac{d^2\delta}{dx^2}}{[1 + \left(\frac{d\delta}{dx}\right)^2]^{\frac{3}{2}}} \tag{3.4}$$

Where y represents the curve in vertical direction and $\left(\frac{d\delta}{dx}\right)^2$ can be negligible compared with 1. So, the curvature is written as,

$$\frac{1}{\rho} = \frac{d^2\delta}{dx^2} \tag{3.5}$$

After substituting equation (5) into equation (2), it can be obtained that,

$$\frac{d^2\delta}{dx^2} = \frac{M(x)}{EI} \tag{3.6}$$

To solve this equation, integrating x makes this equation to,

$$EI\frac{d^2\delta}{dx^2} = -Fx \tag{3.7}$$

or

$$EI\frac{d^2\delta}{dx^2} = -\frac{1}{2}Fx^2 + C_1 \tag{3.8}$$

At the fixed end, x=L and $\frac{d\delta}{dx} = 0$. So $C_1 = \frac{1}{2}FL^2$ and equation (8) can be expressed as:

$$EI\delta = -\frac{1}{2}Fx^2 + \frac{1}{2}FL^2 \tag{3.9}$$

Then, further integrating it to

$$EI\delta = -\frac{1}{2}Fx^2 + \frac{1}{2}FLx + C_2 \tag{3.10}$$

Similarly, x=L and δ=0 at B. So C_2 =-1/3FL^3. Displacement of post end can be expressed as,

$$\delta = \frac{F}{6EI}(-x^3 + 3L^2x - 2L^3) \tag{3.11}$$

As the force is applied at the free end (x=0), the displacement of the free end is,

$$\delta = -\frac{FL^3}{3EL} \tag{3.12}$$

From this equation, it can be seen that the force has positive correlation to the free end displacement. I represents as a real moment of inertia, which is just related to form of the platform. In terms of cylinder, I is equal to 1/4πR4. Hence, the force can be described as,

$$F = -\frac{3EI\delta}{L^3} = -\frac{3E\pi R^4}{4L^3}\delta \tag{3.13}$$

where minus means direction, E is the elastic modulus of PDMS, R and L are the radius and length of the post. Mechanical model of the contraction force and relative degree of silicon posts deformation is confirmed. Contractile Forces (F) are applied at the top of the sticks and the displacement of free end is represented as δ (mm).

From this equation, to determine the transfer modelling between the movement of the free ends of the PDMS posts (can be measured with camera and video), the

geometry of the silicon posts is to be determined and the PDMS mechanical properties are to be measured.

3.2.3. Cell Sources

Currently, experiments carried out in the lab can be realized with primary cells isolated from the donors or with prepared cell lines from cell bank. Those primary cells normally contain various cell types from natural tissue. Thus, it is necessary to collect the right cell type wanted for the experiment. There are two problems related to the primary cell's application. The harvest process of primary cells is extremely difficult, especially for different cell types. The other problem is that they have to be used after isolation directly, as storage of such cells is very hard, and their life span is short. Yet, its advantage is also obvious that they have better results of restoring morphology and functions while these cells seeded into 3D constructs.

In this project, we aim to culture cardiomyocytes in 3D condition for engineered heart tissue generation. Determination of cell types for culture is especially important for cardiomyocytes, as this kind of cell has very limited ability of proliferation.

Nowadays, neonatal rat cardiomyocyte is normally used as the cell type for regeneration of cardiac tissue due to its simple isolation and culture. It has been over half century since the first neonatal rat cardiomyocytes isolated by Harary and Farley.[80] They obtained the cells from Wistar rats and cultured them showing beating activities for more than one month. Afterwards, researchers made many modifications based on their protocol of isolation and culture of cardiomyocytes.

There are two significant steps of the process cannot be altered. They are enzyme digestion step and purification step for removing non-cardiomyocytes[144]. Culturing neonatal rat cardiomyocytes for setting up 3D cardiac tissue model has one advantage is avoiding the impacts of hemodynamic factors like that *in vivo.* Besides this, it is easy for us to control other concomitant factors. However, the limitations of using neonatal rat cardiomyocytes are apparent. The isolation process has to be done while the cells required every time. And these cells show limited proliferation results with long isolation time. Normally the time required for this process range from 12 hours to 48 hours. As the cells are isolated from neonatal rats, the ages of rats are 1 to 2 days, which is not predictable. Also waste and inefficient problem cannot be avoided if very small amount of cells are acquired.[145]

Compared with neonatal rat cardiomyocytes, cardiac muscle cells from adult rats are fully differentiated and do not grow by cell division. Although adult cardiomyocytes are more mature, these adult ventricular cardiomyocytes connect with each tightly with intercalated discs and ECM network. Therefore, it is hard to breaking these connections without damaging cells.[146] Even though the cells are harvested successfully, there is another problem cannot be resolved as it is very hard for adult cardiomyocytes to attach onto scaffolds and ECM made *in vitro*.[147]

Different from the cells from rats, using human stem cell derived cardiomyocytes for setting up *in vitro* model is able to provide a human based platform for drug test and toxicity screening. It is better to model human diseases or investigate the side effects of those cardiovascular drugs. Stem cell that can differentiate into various

cell types is a valuable tool for tissue regeneration and potentially play a significant role in replacement of damage tissue in clinical.

People nowadays have successfully derived beating cardiomyocytes *in vitro* with human embryonic stem cells (ESCs) and induced pluripotent stem cells (hiPScs). They give people more opportunities to set up new model for *in vitro* cardiac tissue model. As shown in figure 3-4, the ESCs and iPSCs are used to fabricate the 3D tissue with biodegradable scaffold or stacking cell sheets. They aim to develop transplantable tissue for repair damaged cardiac tissue in patient's body.

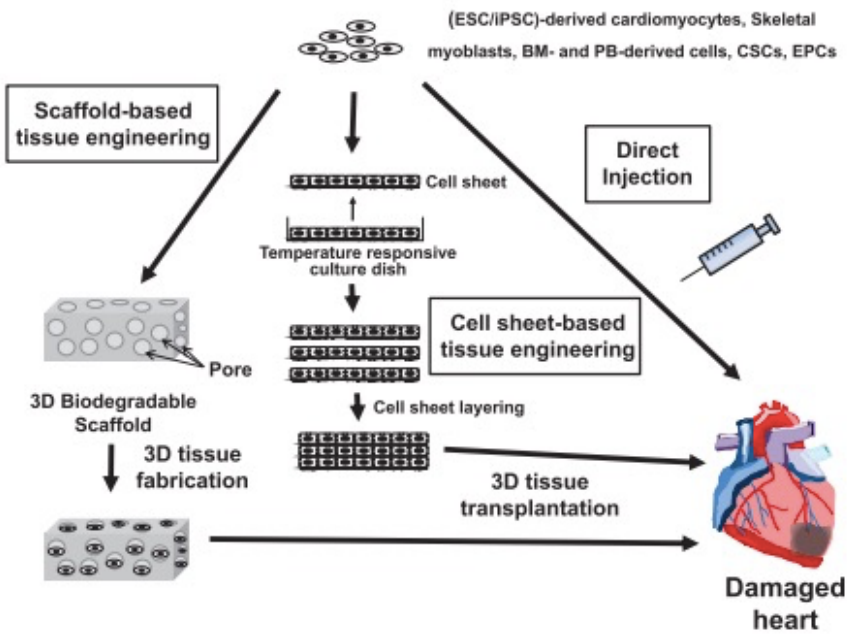


Figure 3- 4: 3D Engineered Cardiac tissue generation process and further applied into clinical transplantation.[148]

The key issue of using human stem cells for creating engineered cardiac tissue is purification of cardiomyocytes after differentiation. Too much immature

cardiomyocytes may lead to inaccurate results of functions of tissue model generated.[7] It is especially true while applying them into transplantation and clinical use, as contamination will result in production of teratoma. Thus, it is deserved to enhance the maturation of cardiomyocytes and further increase that in those generated tissue.

3.2.4. Isolation of Cardiomyocytes From Neonatal Rats

As we stated before, the cell sources can be used for setting up engineered cardiac tissue are cardiomyocytes isolated from neonatal and adult rats, and stem cell derived cardiomyocytes. Considering the cardiac muscle cells from adult rats is hard to attach onto scaffold and be cultured in 3D model. We used cardiomyocytes from neonatal rats to build our engineered cardiac tissues. The first step is isolating cells from neonatal rats with high quality. We made this isolation with a litter of neonatal rats. They are around 12 pups with aging of 48 hours.

One day before process of isolation, autoclaving the necessary tools including scissors and forceps with 121°C heating cycle for one hour and drying for half an hour. Trypsin solution and Hank's Balanced Salts Solution (HBSS) are thawed in refrigerator. To prepare 20% fetal bovine serum (FBS) stock solution, FBS, L-glutamine, gentamicin and 2-mercaptoethanol are added into cardiac maintenance medium (CMM).

During the day of isolation, all the works are conducted within a culture hood. Firstly, the rat pups are collected from their mother and kept in warm environment. Then we use gauze to blot the blood of the pups and slit their chests to make the

heart visible. After taking the heart with scissors, they are left in the culture dish with HBSS on ice. The next step is quite important to extract cardiac tissue and wipe off any non-heart tissue. The purified heart tissues are cut into small pieces (around 2-3mm^3) and then placed within trypsin solution under 4 °C.

Preparing 1mg/ml collagenase solution with adding HBSS into collagenase. 10% 10% FBS with CMM are added into tube containing tissue pieces with HBSS solution. After being kept in water bath for 1 min, the tissues are float in the solution. Then 10ml collagenase is added to break the connection between cells and extracellular matrix. The tubes are the centrifuged at 410 rcf for 8 min and cold HBSS is added into tubes and re-suspend. Tissues were removed with cell strainer before centrifuging those cells at 410 rcf for 10min. We aspirate supernatant and re-suspend the cells pellets in 10% FBS CMM. The cells are then kept in an incubator with 37 °C and 5% CO_2 for 1 hour. The cells suspension is finally ready for further next culture step.

3.2.5. iPSc Derived Cardimyocytes and Splitting Cardiomyocytes from Coating

To produce human engineered cardiac tissue, the cell source we used is human induced pluripotent stem cells (hiPSC). The commercial cardimyocyte cell lines are purchased from AXOL and they were reprogramed from neonatal male donor cord blood CD34+ cells with episomal method. Upon received, cardiomyocytes maintenance medium and plating medium are prepared. Maintenance medium is made with basal medium and supplement and stored at -80 °C. Once thawing at 4°C

overnight, 10% fetal bovin serum (FBS) and y-27632 dihydrochloride rock inhibitor (10uM) is added into cardiomyocytes maintenance medium for producing plating medium. After medium is made, we thaw the cells and make them ready for being cultured. The cells are transferred from LN storage by carrying cells within dry ice and put it into a water bath immediately for 1-2 minutes. The vial is taken to a hood after 70% ethanol spray and wiped. Once thawed, the cells are transferred drop-wise into a 15mL sterile conical tube with 10mL plating medium and wash the vial with 1mL then transferred to the conical tube for centrifugation at 200g for 5 minutes. Aspirate the supernatant and re-suspend the cell pellet in 100uL of medium. The viability of these cells is around 70%. Hence, it is necessary to do cell count before cell seeding. 0.5million cells are used to generate each single engineered cardiac tissue.

3.3. Results and Discussion

3.3.1. Design of EHT Microbioreactor

As it has been stated before, a micro-bioreactor will be designed to provide perfusion system for culturing engineered heart tissue. Such system is used for delivering media to the generated engineered cardiac tissues according to the protocol described above. As the platform and the generation of EHT are based on 24-well culture dish, it is thus required to design the chamber matching the platform. To realize standard design and parallel testing, the micro-bioreactor is designed with a glass slide as a basement. This will make it possible that the tissue can be observed by an inverted microscope or camera from the bottom of the microbioreactor.

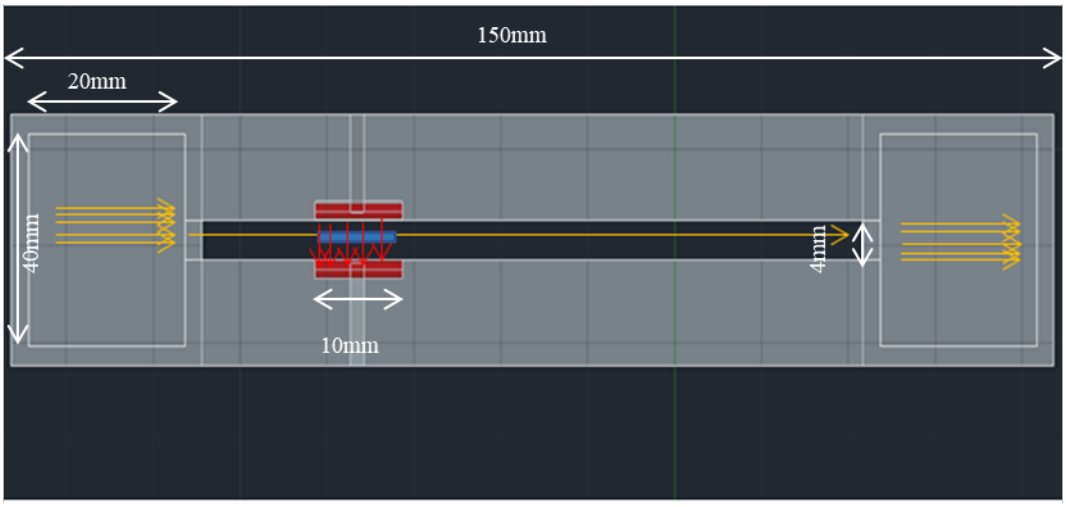


Figure 3- 5: Illustration of micro-bioreactor design with electrical stimulations (Yellow arrows mean media flow direction, red rods are two carbon electrodes, red arrows mean electrical field direction, and blue rod represents tissue)

The chamber of the perfusion system was manufactured by 3D printer according to design diagram drawn with AutoCAD. The perfusion micro-bioreactor should be flexible and portable. The chamber is in a chip-sized as it is based on a glass slide. Its low cost and easy fabrication make it capable to be used for parallel testing. A number of chambers can be manufactured and multi-evaluations can be achieved at the same time. Also it should be reusable after being autoclaved with high temperature. Media is introduced from the end of left-hand side. After flow through the tissue, it is pumped out from the other side. The media flow is controllable by an external pump. To keep the samples being cultured at stable cell culture environment, the microbioreactor is placed in an incubator to guarantee the temperature and oxygen level. Two carbon electrodes are used to provide electrical field for engineered heart tissue. Each carbon electrode is connected with one end of

platinum cable and the other end of the cable is Raspberry Pi. As the electricity source, the integrated circuit board is capable to control the input of the electrical field via programming with Python.

The perfusion system for 3D engineered heart tissue culture consists of 4 parts. The first one is inlet and outlet pumps shown in figure 3-6 and it provides the engine to maintain the media flow through the microbioreactor. Two adapted Winged Needle Infusion Set (BD Valu-set, UK) were used to connect the pump with the micro-bioreactor via inlet and outlet. To avoid any leakage from the holes of inlet and outlet, two thin silicon sheets are attached onto inside walls of the inlet and outlet. In this situation, the needles can be inserted and pulled out easily without any media getting out from the chamber.

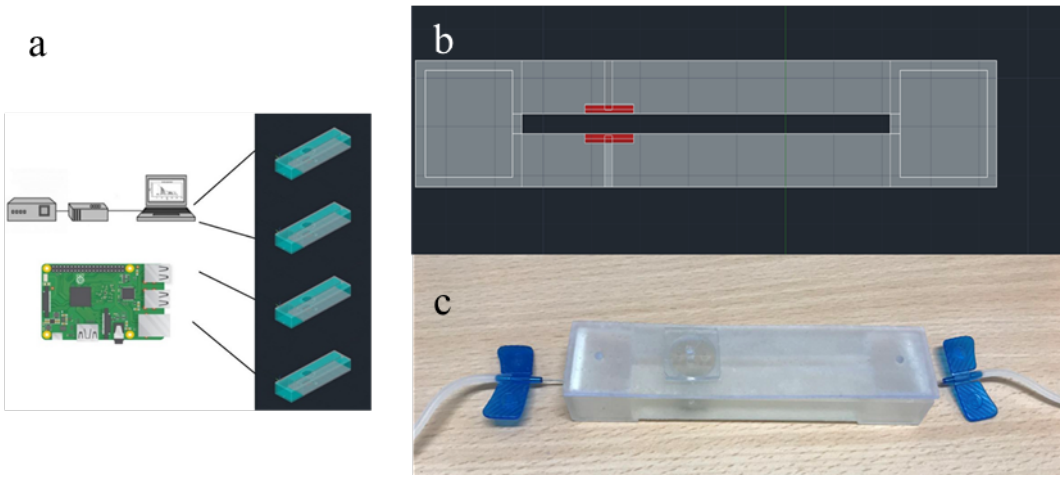


Figure 3- 6: Schematic diagram of the perfusion bioreactor set up (a) The systems can be controlled by the computer and Raspberry Pi programming; (b) The top view of the chamber design. (c) The set-up of perfusion system.

The second part is the bioreactor chamber. The chamber and its cover are designed by AutoCAD (Autodesk, UK) and manufactured by commercial 3D printer – Form 2 3D printer from Formlabs. After being printed out and left for drying up, the supports of the samples are removed with forceps and scissors. A normal glass slide is placed at the bottom and regarded as the basement of the bioreactor. This enables the observation of tissue culture with inverse microscope. The third part consists of those two carbon electrodes. They are 12mm in length and 2mm in diameter. Platinum cables are used to connect the rods by PDMS gel and the other ends of the platinum cables are connected with Raspberry Pi. The last one is a commercial individually closed incubator to maintain temperature and gas exchange for all the microbioreactors.

After all the equipment is set up, the system is ready for use. The casted-engineered heart tissues constructed with neonatal rats were cultured under different conditions. The rat models are used to evaluate the feasibility of the system and determine the optimal conditions of electrical stimulations.

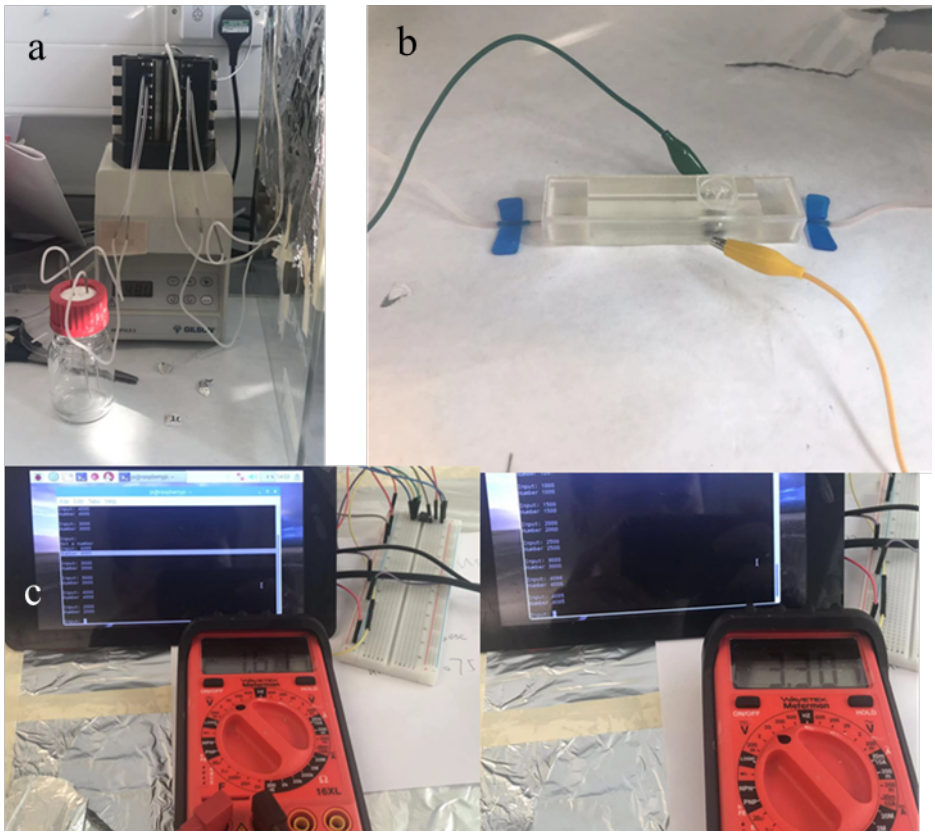


Figure 3- 7: The set-up of perfusion bioreactor with electrical stimulations (a) Pump used for establishing media flow (b) The electrical connection of bioreactor (c) The electrical stimulation established by programming of Raspberry Pi and various voltage levels can be achieved by this system.

For the samples with electrical stimulation, the electrical signals were introduced onto the samples after day 5. Different levels of amplitude, frequency and period of these electrical signals were applied onto the samples. The effects of those factors for the cardiomyocytes and engineered heart tissues are investigated in terms of capture rate, contractile force, excitation threshold, cell viability and morphology etc.

Some further optimization of these configurations should be processed and these will be discussed in the following chapters. Once the confirmation of the system is made, the human cardiac tissue model will be generated and culture in our

microbioreactor. After long-term culture, the human engineered heart tissue is used as a human drug-testing platform for cardiac disease drugs.

3.3.2. Scaffold Matrix for Cells Seeding

The natural hydrogel products are used to mimic *in vivo* environment so that intercellular connections can be formed, and cells can lay down there. Water content within the construct is reduced as the cells keep on compressing the tissue, which makes the construct smaller over time. Although the mechanical stability is not high enough like natural tissue, it satisfies the condition of integrating with force analysis. As this is the main characterisation of cardiomyocytes, it is quite suitable for setting up the model for conducting *in vitro* drug testing. The most commonly used hydrogels nowadays are protein collagen I, mixture of collagen I and Matrigel and fibrin. Compared with collagen, fibrin can provide quicker polymerization process. This prevents the cells gathering at the bottom of the construct due to gravity thereby providing an even distribution of cells within the tissue.[149] That are why we chose fibrin material as the constitution of scaffold used in our project.

After obtaining spontaneously beating cardiomyocytes (both from neonatal rats and induced from pluripotent stem cell), the dissociated cells were washed twice with PBS and then DMEM with DNase. After centrifuging at 100g for 10mins, the cells are re-suspended in basic medium containing 1% penicillin/streptomycin. The cell number is determined by cell count with CASY and the final concentration of cells is adjusted to 5 million cells/ml.

As described before, to generate fibrin-based engineered cardiac tissue, mixing isolated cardiomyocytes into 5mg/ml bovine fibrinogen (200 mg/ml in NaCl 0.9% with 0.5 mg/mg aprotinin), 100 ml/ml Matrigel, 3U/ml thrombin and DMEM and quickly casting the reconstitution into agarose slots (2% in PBS) within each well of 24-well culture dish. Then the PDMS platforms with two silicon posts are inserted immediately into the well. After waiting 2 hours for the solution polymerised, the scaffold to build ECM for the cells is formed. By adding medium to break the connection between tissues and agarose casting moulds, each single tissue can be easily taken from the well for further culture and analysis. The culture medium for neonatal rats EHT is made up of DMEM, 10% horse serum, 2% chick embryo extract, 1%PS, 10ug/ml insulin and 33ug/ml aprotinin. The culture medium used for human iPSC derived cardiomyocytes EHT is similar as that for rEHT, but the only difference is replacing DMEM with plating medium.

3.3.3. System Feasibility Study with Cardiomyocytes Isolated from Neonatal Rats

By now, a platform made from PDMS for culturing minimized fibrin-based EHTs has been designed and fabricated. The preliminary design of micro-bioreactor is made with electrical stimulation can be initialled. To approve the feasibility of the system before applying it into developing human engineered cardiac tissue, engineered heart tissue with neonatal rat cardiomyocytes were generated and cultured in the system for long term.

The cardiomyocytes isolated from neonatal rats were cultured in 3D structure within hydrogel. This strip tissue makes the single cells suspend within fibrinogen and Matrigel. Compared with the collagen based engineered heart tissue, the use of fibrinogen to replace collagen makes the hydrogel polymerized faster. With the thrombin, the 3D *in vitro* model can form quickly and fixed onto the tops of two PDMS posts. After the tissues are polymerized, the platforms with tissues are transferred into perfusion microbioreactors. The cells spread within the tissue after a period culture time. The contacts between cells were generated, which leaded to the reduction of the muscle strip length. The gel of the tissue was remodelled to about 6.8mm. Contractile forces produced by the cardiac muscle cells bend two silicon posts towards the centre along the straight line.

According to observation, there was no contraction at day 1 while neonatal rat engineered cardiac tissues were generated. Spontaneous beating was observed around day 3 and this contraction frequency kept decreasing after several-day culture. Chronic constant pacing is initialled at day 5 and rhythmical beating was found one day later (day 6). Electrical stimulation induces markedly higher contractile force generated from the tissues and the force increases against culture time until day 14 and stays at a constant level afterwards.

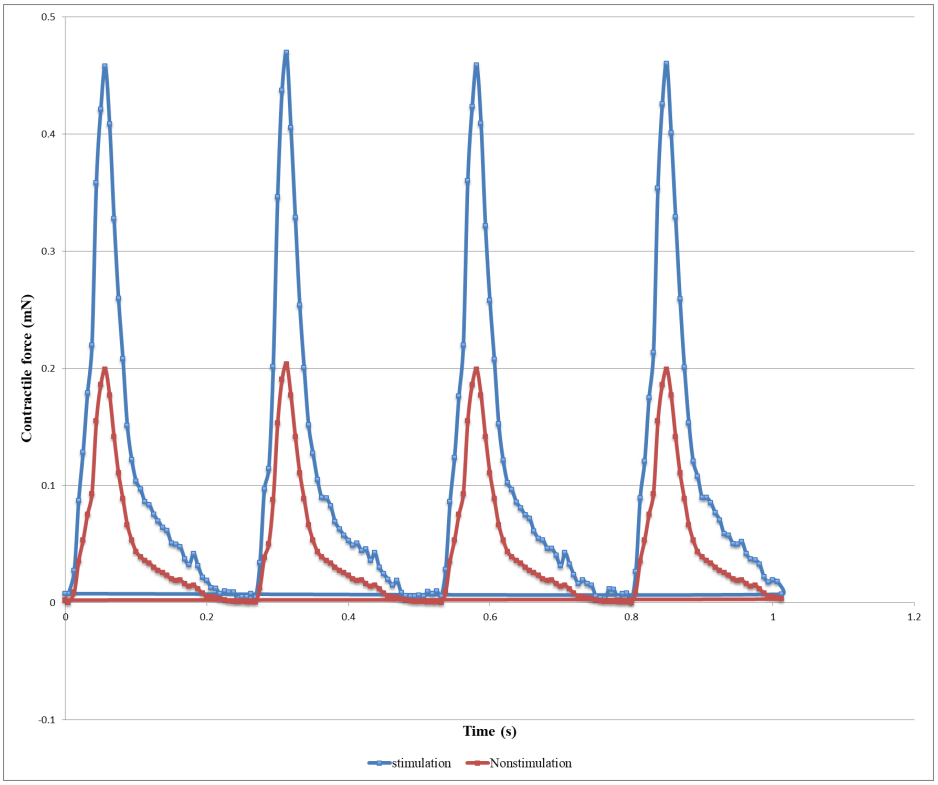


Figure 3- 8: Typical force generation of rat engineered heart tissue cultured for 14 days (blue one represents to samples stimulated with electrical signals (3V/cm, 2Hz and 100ms duration) and red one represents non-stimulated samples)

Structurally the cells initially show as round in shape and even distribution of cells network were observed within the tissue. In day 2 and 3, the cells elongated and interconnections between each cell were formed. The cardiomyocytes started to beat as single cells at day 3. After 5 days, the cells gathered together to coherent beat and deflect the posts rhythmically.

From the general observation of engineered heart tissue generated and culture in our microbioreactor. This system is workable for generating rat engineered cardiac tissue. Yet, to make most use of this system and determine the optimal stimulation

conditions. Further simulation and system optimization will be operated and discussed in the following chapters.

3.4. Summary

In this project, we aim to fabricate a perfused microbioreactor for developing a human engineered heart tissue model for drug testing. Yet, it is hard to generate a functional human engineered heart tissue and even further culture them with 3D construct for long term. There are enormous difficulties to be solved, including cell sources, suitable scaffold matrix and immature function and structure of tissue. The advance of iPSC could potentially supply enough cardiomyocytes for generating engineered heart tissues. There have been many high efficiency methods for deriving iPSC to human cardiomyocytes. However, long-term culturing iPSC-CMs is another problem and it requires higher degree of maturation for practical applications. It is known 3D cell culture with various stimulations is able to enhance cells function and maturity. Therefore, a microbioreactor was developed based on a glass slide in size and fabricated with 3D printer. A PDMS platform is used for supporting EHT attachment and works as a force transducer. The integrated electrodes can create a uniform electrical field for tissues. After initial evaluation with culturing neonatal rats' cardiomyocytes in this system for tissue engineering cardiac muscle generation, such tissue show critical contractile functions and survive for long term. By comparing the performances between stimulated and non-stimulated groups, it can be found that the presence of electrical field improves cellular contractions and changes cell shape with cellular distribution and alignment

of cells network. Due to these findings, we would like to apply this system onto generating and culturing 3D human cardiac tissue *in vitro*. Before that, some further optimization should be processed in terms of platform design, perfusion system and electrical stimulation conditions.

Chapter 4 Design of Dynamic Cellular Force Transducers

4.1. Introduction

A platform made from PDMS was used for engineered heart tissue attaching. The contraction of cardiomyocytes is able to bend the silicon posts. Thus, it also works as a force transducer to transfer the deformation of pillars into contractile force generated from the tissue. We have described the mechanical modelling of the action follows in chapter 3. According to that model, the accuracy of the force measurement heavily relies on mechanical properties of PDMS and the pillars geometry including diameter and length.

Hence, the mechanical property of PDMS was studied to ensure the system designed here is reliable and accurate as it highly depends on different factors during manufacture process of the platform. Various mechanical characterization methods were applied to determine optimal fabricating process and evaluate their performance.

4.1.1. Tension and Compression Tests

The first technique used here to measure mechanical properties of PDMS is macro-scale tension and compression tests. While a load is applied onto a material, the load will result in deformation of the material. The relationship between the load and material deformation is expressed by a stress-strain diagram as shown in figure 4-1. This relationship diagram of stress and strain is obtained from the tensile tests with tensile test machines. The stress σ is the average force per unit area of the sample. δ

is the change of the length on sample while tension occurs. There are different stages of tensile test before rupture happening.

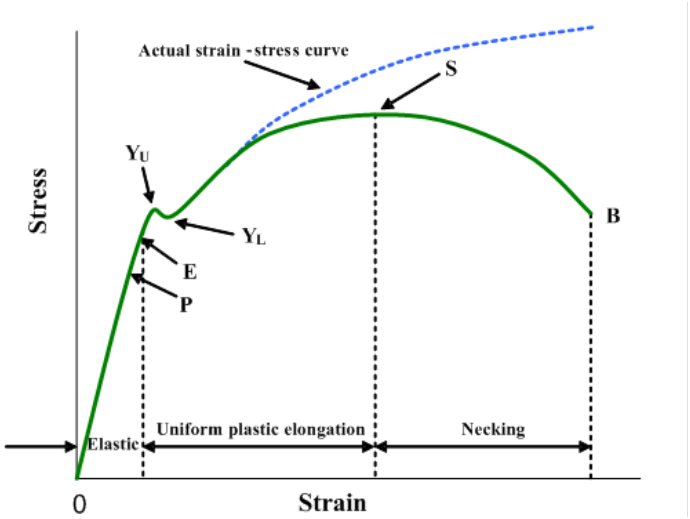


Figure 4- 1: Stress-strain diagram for mild steel[150]

The first period is elastic area and the range is varied for each material to have the linear relationship. After the threshold, increasing strain leads to plastic deformation. The strain drops a bit and goes up again, but not linear any more. There is another point (S) after which the stress starts to decrease with the larger strain. This is called necking period. At the end of the curve or it stops at point B that means the sample breaks there and the corresponding stress is called fracture stress.

In this project, the tensile test was conducted with Deben tension micro-test stages. Deben tension micro-test stages is specifically designed to allow real-time observation of the high stress region of a sample. The sample can be mounted at the centre of the stage with one end fixed and a dual threaded lead-screw drives the

other end of the sample under control of a motor. Load cells range from 2N to 5000N cover most applications. The extension rates of the stage can range from 0.1mm/min to 15mm/min. All stages have linear scales for elongation measurement and accurate speed control. The machine used in this project is the 200N tensile stage. It uses the miniature load cells in the range of 2N to 200N.

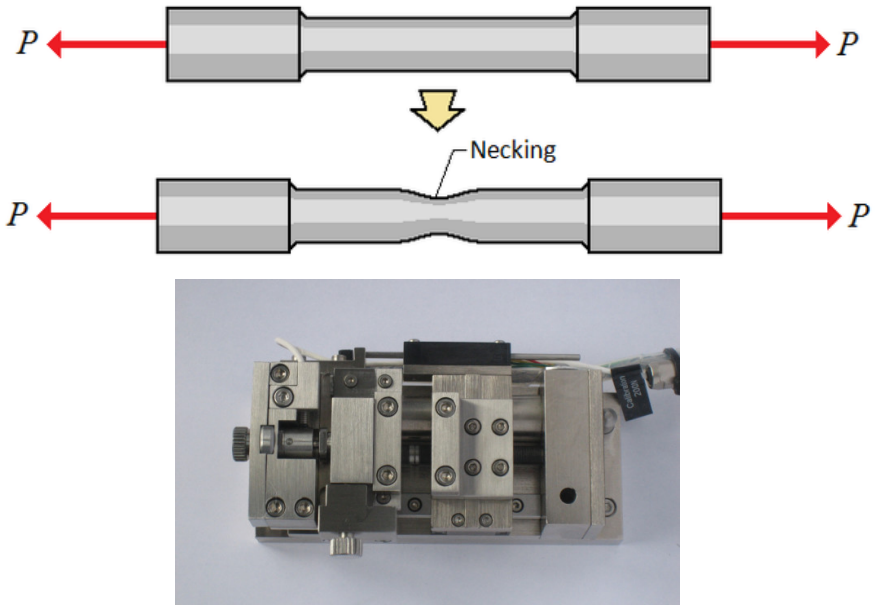


Figure 4- 2: Deben tension micro-test stage and tensile testing schematic diagram[151]

The compression test of a material is the opposite action of tensile test and it also reflects the property of the material with stress-strain curve. The machine used for compression test is applying force onto samples with displacement gauge measuring deformation of PDMS sample.

As it is stated before, a specimen is stretched with the mechanical load and necking will occur at the end of that stage. Similarly, while compressing a specimen with increasing load as shown above, there is a range of elastic deformation of the

material and then it gets into plastic deformation stage. In this period, the sample becomes barrel shaped to increased resistance to further shortening.[152]

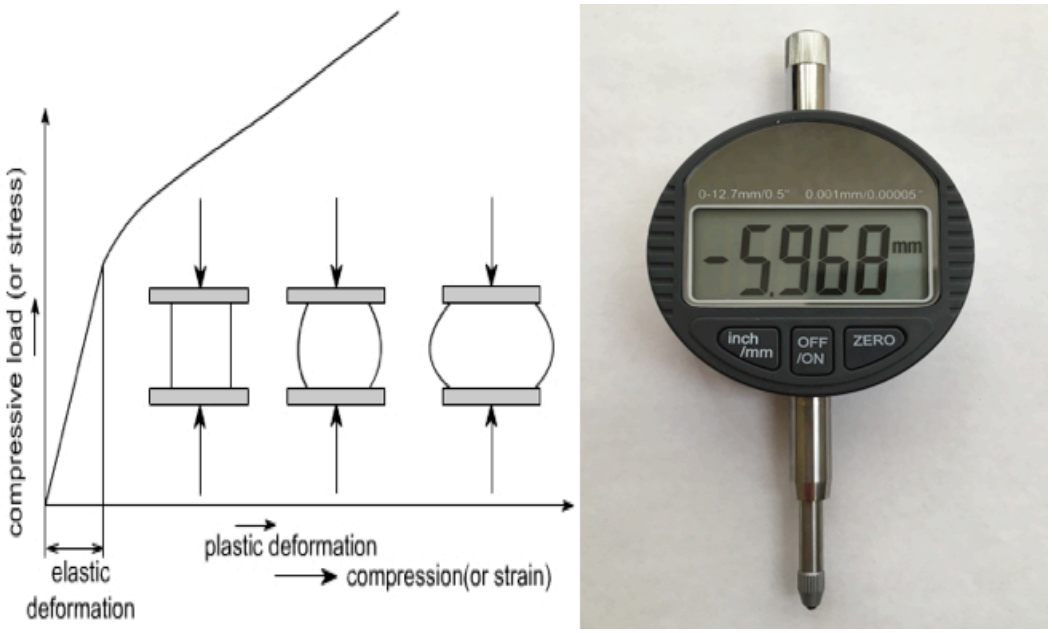


Figure 4- 3: Typical compression test strain and stain curve and equipment for compression testing[153]

4.1.2. Nanoindentation

Nanoindentation has been proved to be an effective technology to measure the mechanical properties of materials at the Nano- and micro-scales.[154] The nanoindentation technique was developed in the mid-1970s to measure the hardness of small volumes of material.[155] Last four decades have witnessed great advances in applying nanoindentation onto measuring mechanical properties (like Young's modulus) of different materials and many achievements have been made.[156,157,158]

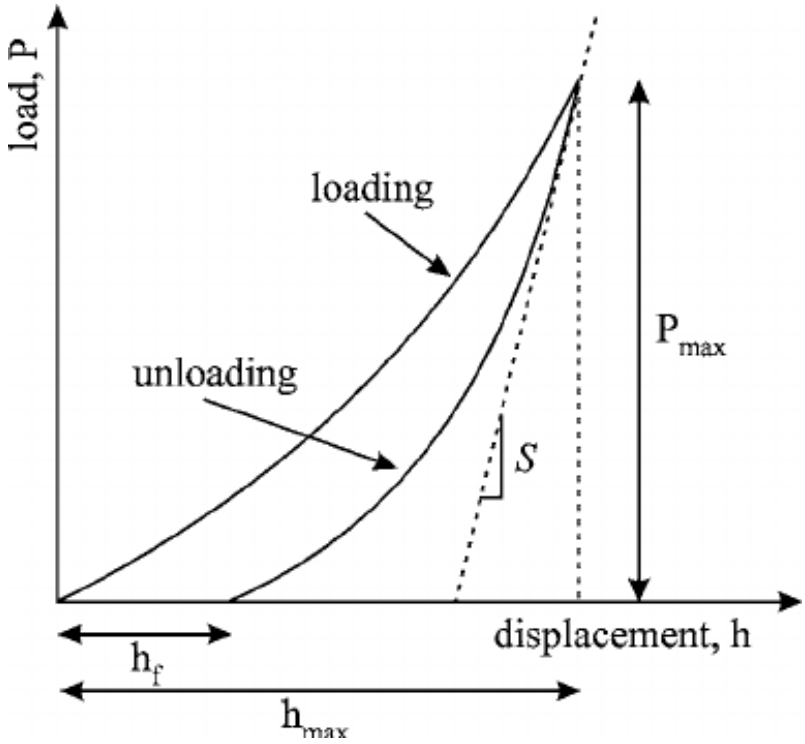


Figure 4- 4: Schematic representation of a loading-unloading curve for a nanoindentation measurement; P_{max} is the load at maximum indentation, h_{max} is the indenter displacement at peak load, h_f is the final depth.[159]

Nanoindentation systems use a hard tip (normally a diamond tip with known mechanical properties) to press into the sample with a known increasing load and the depth or the displacement made from that can be detected as a function of time. According to the relationship between load and depth, the mechanical properties can be obtained through data analysis.[160]

Figure 4-4 shows the curve of determining the Young's modulus of samples tested with nanoindentation. The values of peak load (P_{max}), maximum depth (h_{max}) and depth after unloading (h_f) are those key values to be used.

Hardness is a measure of the resistance to localized plastic deformation induced by mechanical indentation. Thus, hardness H can be calculated as:

$$H = \frac{P}{A} \tag{4.1}$$

where P is the load and A is the contact area at the peak load. The reduced modulus E_r can be calculated as:

$$E_r = \frac{s\sqrt{\pi}}{2\beta\sqrt{A}} \tag{4.2}$$

The Young's modulus of the material can be obtained with the reduced modulus via:

$$\frac{1}{E_r} = \frac{1 - v^2}{E} + \frac{1 - v_i^2}{E_i} \tag{4.3}$$

Where v is the possion's ratio of the material; E_i and v_i are the young's modulus and possion's ratio of the indenter tip (diamond).

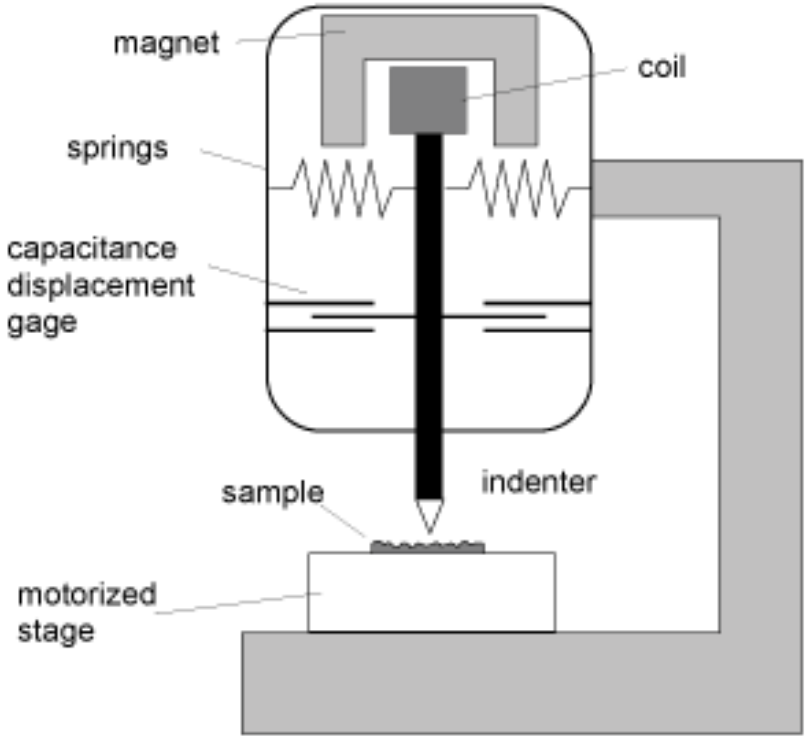


Figure 4- 5: Component of a nanoindentation system[161]

As shown in Figure 4-5, in the Nanoindentation test, an indenter is penetrated the sample by moving the motorized stage. The load-depth curve is thus recorded. To evaluate the accurate value of elastic modulus of PDMS, some mechanical models need to be confirmed, as this material is viscoelastic rather than simple rigid or elastic.

4.2. Materials and Methods

4.2.1. Mechanical Modelling Design and Samples Preparations

As described in former chapter, following the cantilever beam deflection, the relationship between force and posts deformation is shown in the following equation.

$$F = -\frac{3EI\delta}{L^3} = -\frac{3E\pi R^4}{4L^3}\delta \qquad (4.4)$$

where minus means direction, E is the elastic modulus of PDMS, R and L are the radius and length of the post. Mechanical model of the contraction force and relative degree of silicon posts deformation is confirmed. Contractile Forces (F) are applied at the top of the sticks and the displacement of free end is represented as δ (mm).

From this equation, to determine the transfer modelling between the movement of the free ends of the PDMS posts (can be measured with camera and video), the geometry of the silicon posts is to be determined and the PDMS mechanical properties are to be measured.

Yet, PDMS is not as stiff as metals, but not as soft as liquids. Such polymer shows a viscoelastic behaviour which is an intermediate between viscous and elastic behaviour. Hence, it is necessary to characterize the mechanical properties of PDMS and a better force convention model for the platform is required.

In this experiment, three methods were used to do the related mechanical test for this platform. To characterize the mechanical property of PDMS, I firstly used conventional compression and tensile test on the macro-scale PDMS bulks manufactured under different conditions. To determine the working principle of the

compression test, a FEA model simulation is conducted. Also, nanoindentation technology was applied onto the PDMS samples to acquire micro-scale viscoelastic characterization with more accurate results. Finally, a direct measurement was made with Deben tensile test stage to compare the modelling results and practical values.

Before conducting the characterization, the first step was fabrication of the specimens used for investigation. PDMS bulks and posts were made following the process that is shown in the figure 4-6. To make the PDMS platform, Sylgard 184 silicon elastomer base and Sylgard 184 silicone elastomer curing agent are used. According to conventional method of curing PDMS network, the PDMS platform is made as following.

1) Placing the plastic weight boat onto the scale and tare.
2) Pour the Sylgard 184 silicon elastomer base into the weight boat and tare.
3) Pour corresponding value of the Sylgard 184 silicon elastomer curing agent into the weight boat.
4) Mix them with spoon for about 100 times until totally mixed.
5) Put the weight boat with mixture into a desiccator and vacuumize it with pump to remove all the bubbles during mixing process. It needs to be avoided that the PDMS mixture does not foam out of the weight boat. Once large bubbles foam out, we vent the vacuum box to remove large bubbles.
6) As shown in figure 4-6, carefully pour the PDMS mixture into the designed moulds for acquiring PDMS samples.
7) Put the moulds into a hot oven with 65°C and wait for PDMS network curing for certain period.

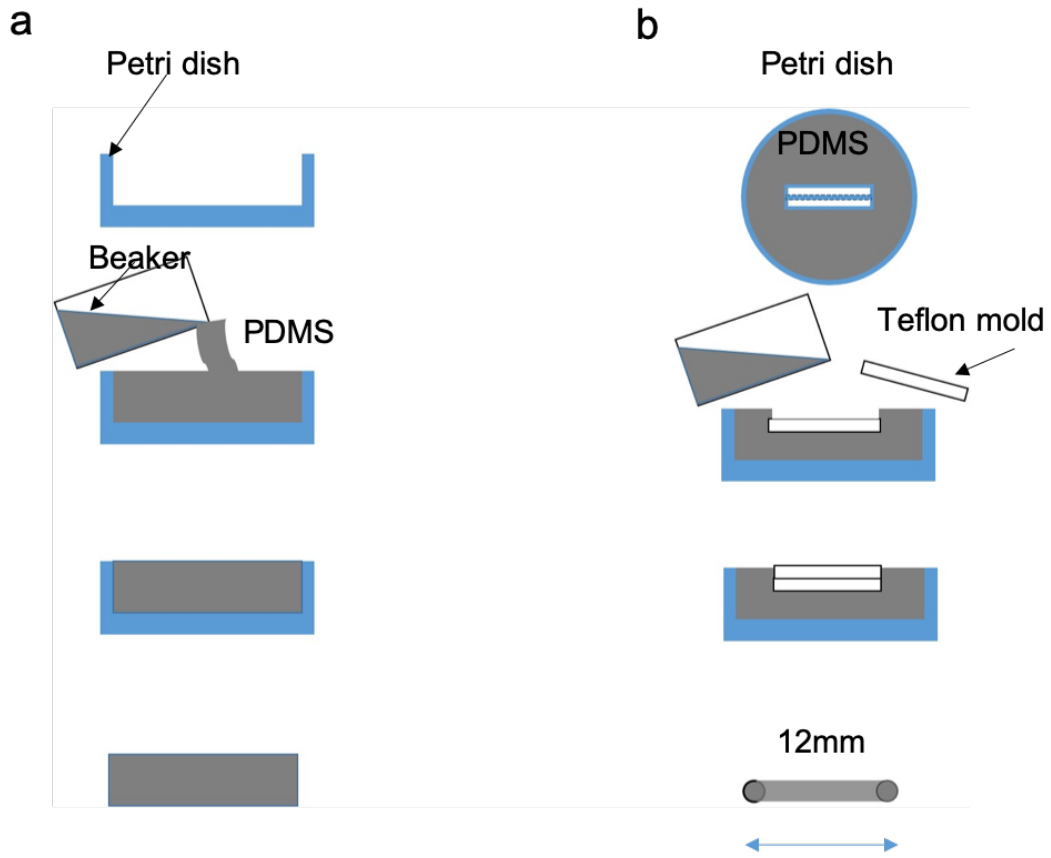


Figure 4- 6: Illustration of manufacturing PDMS platform. Blue parts represent culture dish as manufacture mould, grey parts represent PDMS. (a) PDMS cylinder sample: a standard cell culture petri dish is prepared as mould. (b)Silicon posts: a cubic slot is prepared by a standard cell culture dish with PDMS. Place half of the posts mould as the basement and pour the PDMS onto the mould. The other half of the mould is placed from the top. The specimen is located in the centre of mould as a cylinder form. Bubbles are removed and curing in the baker. Remove the specimen from the mould.

The silicon posts were manufactured for tensile stage test. A PDMS mould with a cuboid slot was made beforehand as shown in the figure 4-6 (first line at the right

side). The mixture was added into the slots and the whole mould was left in the incubator for 3 hours. The silicon posts can be obtained by removing the mould with knife. The silicon posts were used to perform the bending force characterization experiment.

The bulks (on the right row of the figure) were made for doing macro-scale viscoelastic characterization of PDMS. The effects of curing time and volume ratio of polymer and agent were measured in this part. The polymer Sylgard 184 silicon base was firstly mixed with the curing agent at a volume ratio of 10:1. After fully stirring and removing bubbles in vacuum, the mixture was poured into five petri dishes as moulds. To investigate how the curing time affects the PDMS mechanical properties, these five samples were cured in a 65 °C oven for 2 hours, 3 hours, 4 hours, 6 hours, 12 hours and 24 hours respectively. Another eight samples were prepared with different volume ratio of polymer and a curing agent, which were two sets of 5:1, 9:1, 10:1 and 15:1. One set was used for compression test and the other one was used for nanoindentation test. The PDMS samples used in this experiment were left in air for at least 24 hours before doing the mechanical properties test. All the measurements were performed at room temperature (23℃).

4.2.2. PDMS Mechanical Property Characterization with Compression and Tensile Test

There are many different types of compression testing machines to measure the materials' mechanical properties, like SANS range of compression testing machines

(Australia), Universal Compression Testing Machine (SYE-2000) (China), etc. However, these machines are used for hard material like metals as they provide heavy load. It is not suitable to use them onto PDMS samples. Therefore, a more suitable instrument was used for PDMS network compression testing with the scale and displacement gauge.

As shown in figure 4-7, a weight stage is placed onto the top of the gauge to apply force to the samples with measuring displacement of the during compression testing. The prepared samples are contacted with the metal tip (diameter 3mm). Yet, there is a problem that it is hard to make the full contact between the gauge and sample. The testing force starting from 50g can help resolve this problem.



Figure 4- 7: The instrument setup of compression test of PDMS mechanical property characterization.

With such designed instrument setup, the stress and strain of the sample can be calculated with the following equations:

$$\text{Stress } \sigma = F/\pi \times (\tfrac{d}{2})^2) \tag{4.5}$$

$$\text{Strain } \varepsilon = \mathrm{dL}/\mathrm{L}_0 \tag{4.6}$$

Where F is the force from the weight applied onto the sample. D is the diameter of the contact area. dL is the displacement of the tip under compressive force. From the first equation above, it is easy to see the slope of stress-strain curve is the elastic modulus of the sample.

Deben tensile test stage is used for tension testing of PDMS sample. The sample used for tensile test is made as shown in figure 4-8. The fabrication process of the PDMS sample also follows the procedure described above.

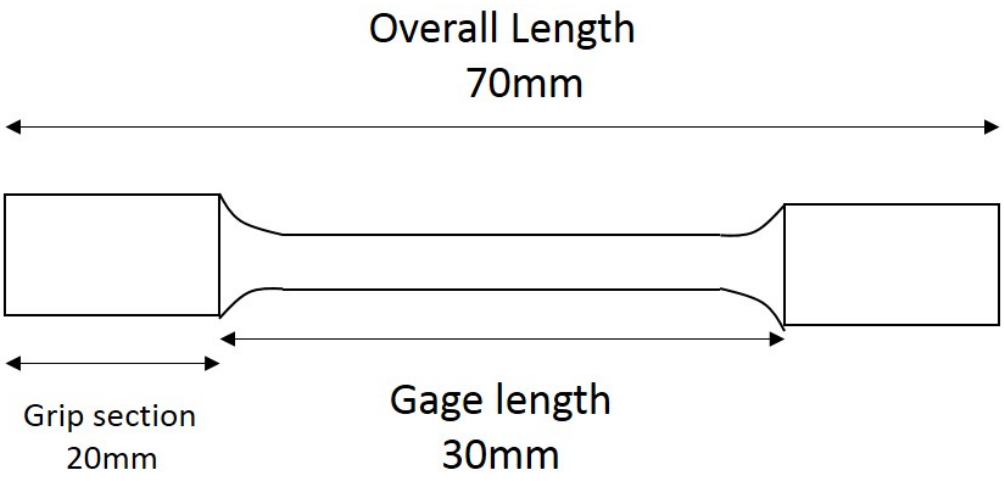


Figure 4- 8: A cross-section of the PDMS tensile specimen

Here is the cross-section of the PDMS tensile specimen. Follow the ASTM D412 test standard; the sample was made as two wide grips at sides with a narrow section in the middle. A casting mould was printed with 3D printer and PDMS mixing solution was filled in to make the samples. The thickness of the sample is 3mm with 10mm in width. Two grips are 20mm in length and they are clamped by the jaws of the tensile stage. The length of the gage section is 30mm. Experiment was carried out at room temperature. Load cell we used is 1kN and the moving jaw ran with 5mm/min. The PDMS samples were held and extended until breaking. The obtained data are moving distance against force sensed by the load cell. Then, those values are converted to stain and stress relationship. Different curing time and curing ratios of the samples were prepared and tested. For each group, five specimens with same manufacture conditions were investigated to avoid any accidental errors. Young's modulus (E) can be calculated by the slope of the linear parts of stress-strain curves.

In macroscopic compression test and tensile test, the PDMS samples with different mixing network ratio were used for experiment test. They are samples with 5:1, 7:1, 9:1, 10:1 and 15:1. All the samples were made according to the same protocol as described above.

4.2.3. Nanoindentation of PDMS Characterization

As stated before, another method used to characterize the mechanical properties of the material is nanoindentation test. Nanoindentation technology has been widely used in mechanical properties detection of metals, ceramics and polymers after it was firstly developed. The machine we used here is the Dimension 3100, a multi-

function atomic force microscope (AFM). It can be operated under atmospheric pressure at room temperature. An optical microscope is equipped with this AFM. A TriboScope is attached for this AFM as an upgrade made by Hysitron. It is a depth-sensing nanoindentation system, which makes it be able to do the quantitative characterization of mechanical properties on the nanometre length scale.



Figure 4- 9: Veeco Dimension 3100 Atomic force microscope with TriboScope nanoindentation

As PDMS has the property of viscoelastic and its mechanical condition heavily depends on its manufacture process. We aim to investigate the effects of the manufacturing conditions onto the mechanical properties of PDMS, samples made with different curing time and various volume ratios of polymer and agent were tested with nanoindentation experiment. The manufacture process is same as that

used for macro scale compression and tensile test. To determine how the curing time affects the PDMS mechanical properties, six groups samples were cured in a 65 °C oven for 2 hours, 3 hours, 4 hours, 6 hours, 12 hours and 24 hours respectively. Each group have three samples made under same conditions. In terms of the effects of mix volume ratio of polymer and the curing agent, four groups of PDMS samples were prepared for test. They are 5:1, 9:1, 10:1 and 15;1 respectively. Three samples in each group as well. All the samples prepared here were left in air for at least 24 hours and measurements were conducted at room temperature.

4.2.4. Bending Silicon Posts Force Measurements

A direct measurement was conducted by deben tensile stage to imitate the bending silicon posts. Tensile stage is specifically designed to do micro-test. To reduce the effects from noise, 2N load cell was used here. It has linear scales for elongation measurement and speed control.

The pre-manufactured PDMS sample was clamped to a pair of jaws as shown in the figure 4-10. One end of the silicon post was clamped at one stage. At the moving stage, a personalized clamp was made and applied at the other end of the silicon posts. The free end of the PDMS stick moved with the moving stage at 0.5mm/min. A curve that displays the real-time change of force against extension distance can be recorded by the micro-test software.

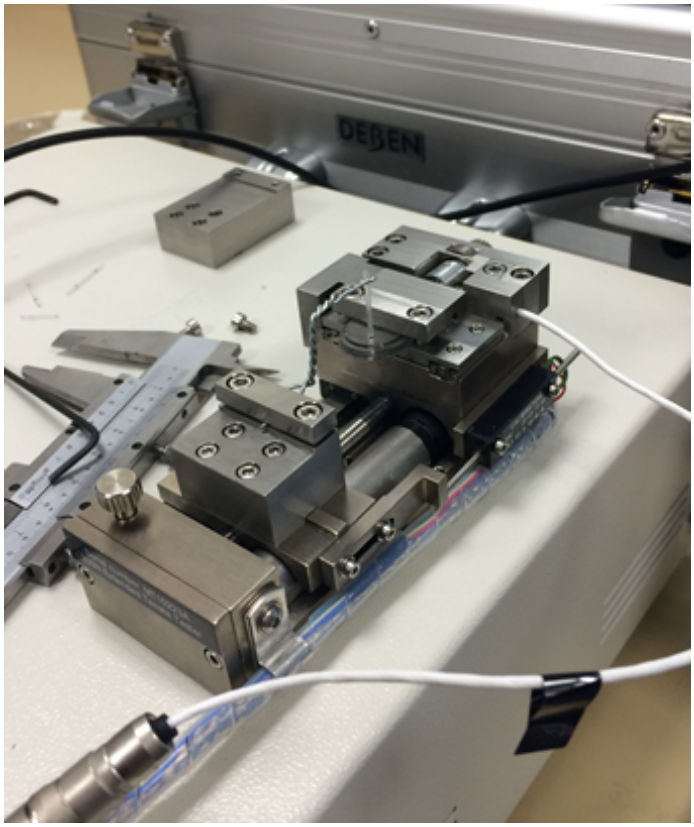


Figure 4- 10: Tension test on deben tensile stage. One end of the PDMS post is clamped and a high-precision force sensor is connected. The other end of the post is fixed and connected to the movable stage.

4.3. Results and Discussion

4.3.1. Macroscopic Compression and Tensile Test Results

As it is stated in the experimental method part, the compression test was performed with the designed instrument. After the system was setup and cylindrical PDMS network samples were prepared, compression tests were conducted on different groups of PDMS network samples.

The first PDMS network sample tested is the sample with 5:1 volume mixing ratio. After the sample was cured within the oven for three hours, it was removed from the petri dish and cut into 3mm and 4mm in diameter. Four most suitable samples were selected for compression test.

Table 4- 1: The parameters of 5:1 PDMS samples used in compression test

	Sample 1	Sample 2	Sample 3	Sample 4
Thickness, mm	2.534	2.512	2.503	2.525
Diameter, mm	4.052	3.921	2.848	2.828
Thickness/ Diameter Radio	0.625	0.641	0.879	0.893

In Table 4-1, the shapes of four samples tested are recorded. Two samples with 3mm diameter and another two samples with 4mm diameter were used respectively. With the application of method described above, one typical compression testing curve for PDMS sample with 5:1 network is shown in figure 4-11.

In figure 4-11, after linearly fitting the data, a trend line is calculated. The slope of the linear line is $3.642*10^6$ Pa, which means the elastic modulus of that sample (PDMS network 5:1) is 3.642 MPa.

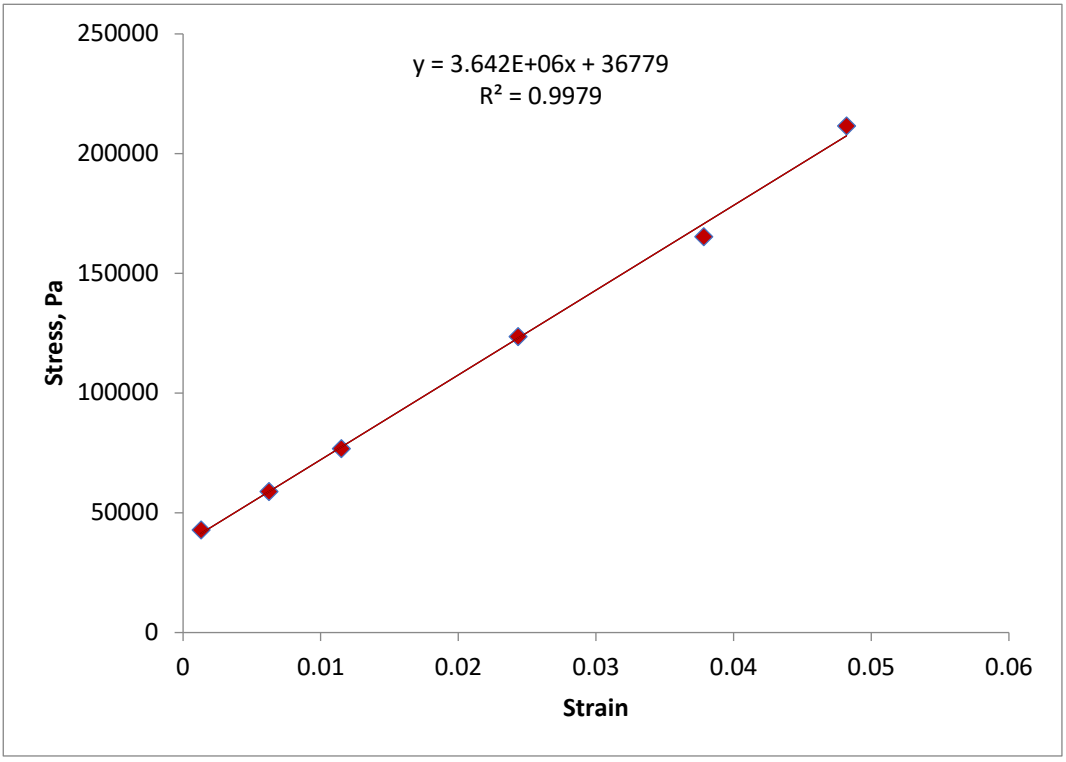


Figure 4- 11: Typical compression test of PDMS network 5:1

With the same calculation method, the young's modulus of the other three samples (sample 2, 3, 4) was obtained as: 3.628 MPa, 3.714 MPa and 3.742 MPa. Thus, we can conclude that the average elastic modulus of PDMS sample with 5:1 network obtained by compression test is 3.6815MPa with 0.0465MPa standard deviation.

In the same way, the samples of 9:1 network PDMS were cut into 3mm and 4mm in diameter respectively. The detailed information of the samples was listed in the Table 4-2.

Table 4- 2: The parameters of 9:1 PDMS samples used in compression test and obtained elastic modulus

	Sample 1	Sample 2	Sample 3	Sample 4
Thickness, mm	2.578	2.502	2.489	2.513
Diameter, mm	4.012	3.978	2.899	3.029
Thickness/ Diameter Radio	0.643	0.629	0.858	0.830
Elastic modulus, MPa	2.737	2.689	2.712	2.698

It can be seen from table 4-2, the average elastic modulus of PDMS sample with 9:1 network obtained by compression test is 2.709MPa with 0.0155MPa standard deviation.

Table 4-3 shows the detailed information of samples and experimental results from samples with 10:1 PDMS network.

Table 4- 3: The parameters of 10:1 PDMS samples used in compression test and obtained elastic modulus

	Sample 1	Sample 2	Sample 3	Sample 4
Thickness, mm	2.525	2.472	2.559	2.501
Diameter, mm	3.927	4.266	2.976	2.921
Dimeter / Thickness Ratio	0.661	0.656	0.939	0.929
Elastic modulus, MPa	2.418	2.468	2.530	2.454

The elastic modulus of PDMS network 10:1 is 2.466 and the standard deviation is 0.0158.

The parameters of the samples and experimental results from 15:1 samples are shown in table 4-4. After calculating with the results, we can conclude the young's modulus of PDMS 15:1 network is 1.106 MPa and the standard deviation is 0.0343

Table 4- 4: Macroscopic compression test for PDMS network 15:1.

	Sample 1	Sample 2	Sample 3	Sample 4
Thickness, mm	2.565	2.453	2.512	2.577
Diameter, mm	3.923	3.888	2.961	3.017
Diameter / Thickness Ratio	0.661	0.656	0.939	0.854
Elastic modulus, MPa	1.079	1.154	1.065	1.127

As it can be seen from the results above, the mechanical properties of PDMS samples obtained and calculated with the macroscopic compression tests show that their elastic modulus is affected by the manufacture process. Different mixing ratios of base and agent result in various degrees of crosslinking and make the samples have different modulus. To investigate the relationship between mixing ratio of base and agent and the elastic modulus of PDMS, the results are described there in Table 4-5. At the same time, the geometry of the tested samples is also studied to determine their effects on the mechanical properties of PDMS.

These are the results obtained from the macroscopic compression tests. From this table, we can see that the Young's modulus of the PDMS is affected by the mixing ratio of base and agent. But this property does not have too much relation with the geometry of the PDMS sample. Hence, the samples' ratio of thickness and diameter is not a great variation to determine the mechanical properties of PDMS.

Table 4- 5: Macroscopic compression test for PDMS network of different mixing ratio

	E1	E2	E3	E4	$E_{avg,}$
	Diameter 4mm		Diameter 3mm		
Network 5:1	3.642	3.628	3.714	3.742	3.6815
Network 9:1	2.737	2.689	2.712	2.698	2.91
Network 10:1	2.418	2.468	2.530	2.454	2.466
Network 15:1	1.079	1.154	1.065	1.127	1.106

To further investigate the mechanical properties of this material, macroscopic tension test was conducted, and the experimental results were shown below. The influence of curing mixing ratio on the tensile strength of PDMS was determined by averaging the data from 3 test samples. The stress/strain curve of the PDMS tensile test was shown in figure 4-12. It displayed a linear elastic region and followed by a nonlinear region before failure happened. The Young's modulus of the PDMS samples for different curing mixing ratio was calculated according to the linear elastic region with Hooke's law. The results were shown in table 4-5.

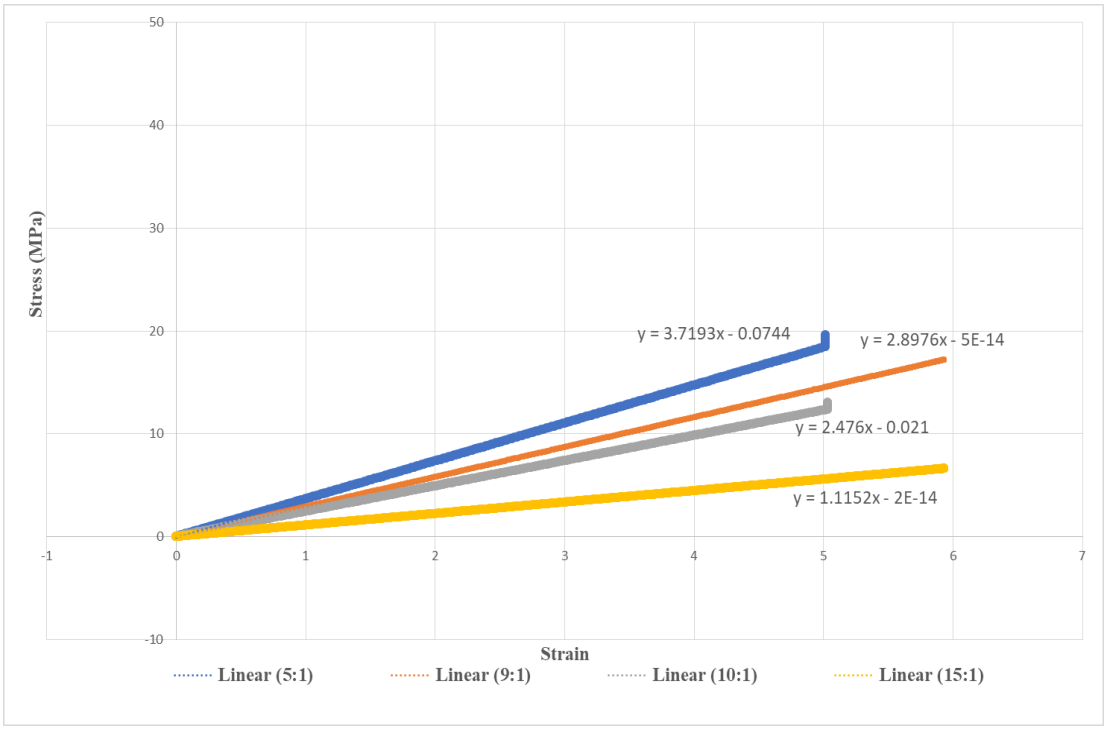


Figure 4- 12: Averaging tensile engineering stress/strain curves for PDMS samples curing with different curing mixing ratio

The elastic modulus of the PDMS samples for different mixing ratios was calculated using Hooke's law within the linear region of the tensile test strain/stress curve. The results after data processing were presented in table 4-6.

In this table, the elongation at failure, failure load and ultimate tensile strength were also displayed as the reference. It can be seen from the figure 4-13 that both Young's modulus and ultimate tensile strength of the PDMS sample are negatively correlated to the mixing ratio. That means the higher mixing ratio make the material softer and vice versa. However, the relation is linear or exponential or logarithmic is not determined as lack of data. This can be investigated in the future study.

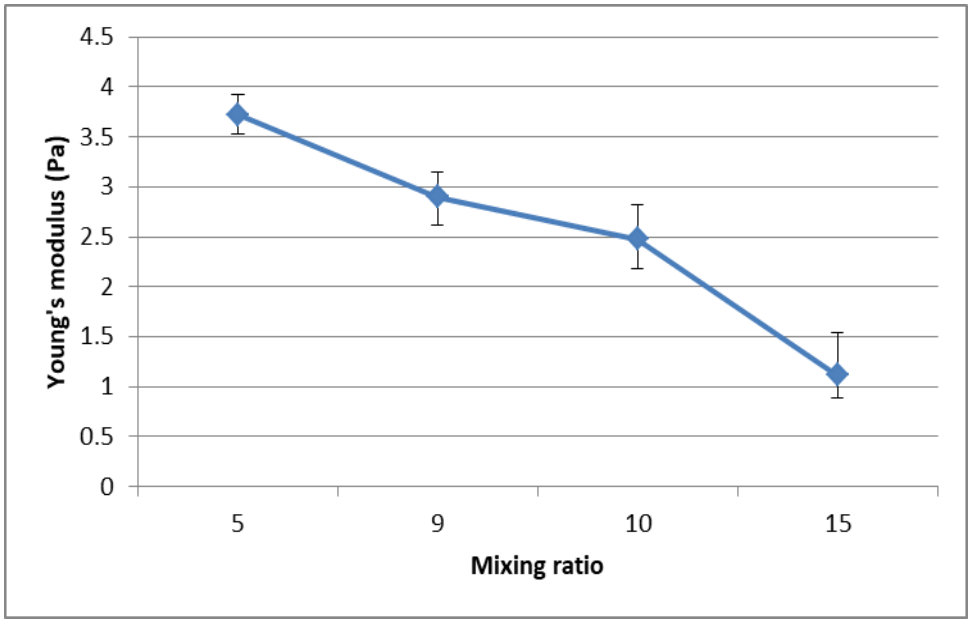


Figure 4- 13: Relationship between mixing ratio of Sylgard 184 and the resultant Young's modulus. Data are represented as mean±SE. The analysis statistic is processed with one-way ANOVA test ($p < 0.05$) N =3 each group

Table 4- 6: Variation of tensile test data with curing mixing ratio

Mixing ratio	Averaging elongation (mm)	Averaging failure load (kN)	Young's modulus (MPa)	Ultimate tensile strength (MPa)
Network 5:1	95.1	95.4	3.7193	5.272
Network 9:1	74.2	113.4	2.8976	4.984
Network 10:1	62.1	98.6	2.476	4.178
Network 15:1	44.7	88.7	1.1152	2.947

4.3.2. Nanoindentation Results

After doing the macroscale compression and tensile test to determine the mechanical properties of PDMS, a practical experiment was designed and conducted to measure the PDMS mechanical properties. We investigated the macroscale viscoelastic characterization of PDMS via doing a Nano-indentation test on the PDMS bulk samples with an atomic force microscope (AFM). It is known that the properties of PDMS are affected by a couple of different factors. We mainly studied the effects of curing time and volume ratio of polymer and agent. The samples were prepared according to the manufacturer's instruction. To investigate how curing time affected the PDMS mechanical properties, five groups were cured in a 65°C oven for 2 hours, 3 hours, 4 hours, 6 hours, 12 hours and 24 hours respectively (all other conditions remained the same). Each group has three samples made with same conditions and tests were conducted to ensure the results are robust.

Another four groups were then prepared with different volume ratios of polymer and curing agent, which were 5:1, 9:1, 10:1 and 15:1 (the curing time was set at 3 hours for all the samples). The PDMS moulds used in this experiment were left in air for at least 24 hours before doing the mechanical properties test. All the measurements were performed at room temperature. Each group also has three samples with same conditions and further experiments were repeated onto every sample to ensure the results are reliable.

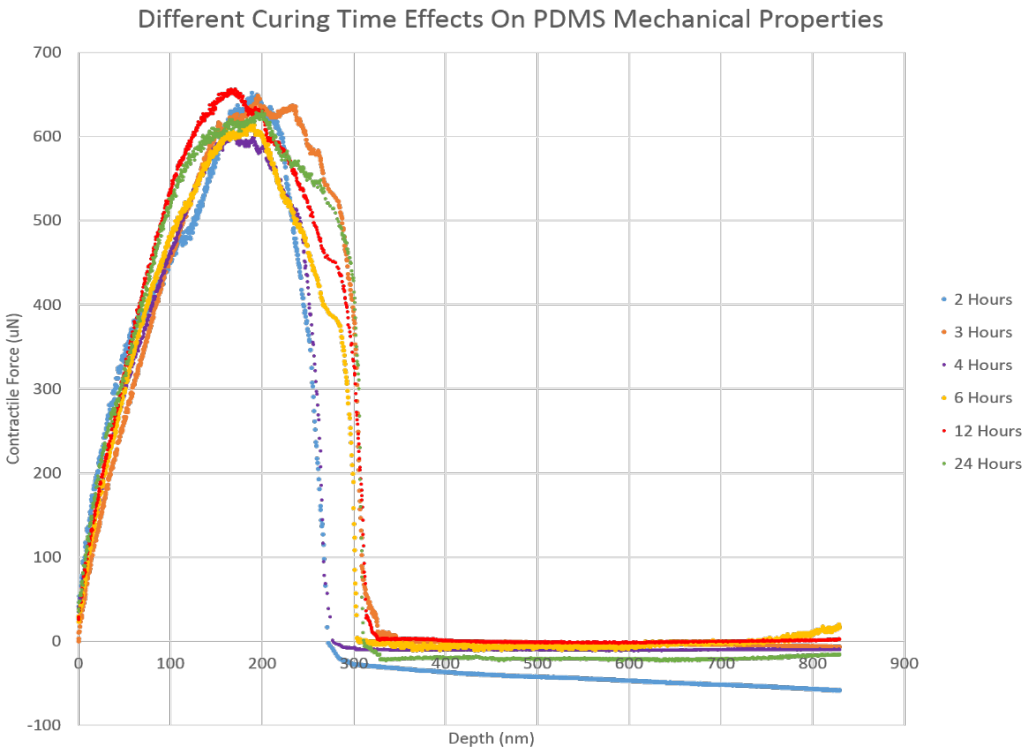


Figure 4- 14: Typical AFM nanoindentation force reaction (nN) curves against separation (nm) for different curing times. The blue lines represent the compression force reaction and the red lines are the relaxation force reaction.

Data were recorded using the AFM micro-test software and processed with NanoScope Analysis (Bruker Ltd.). After the baselines of these curves were corrected, the adjusted force-compression lines corresponding to different curing time were shown. According to the Hooke's law, the elastic modulus, E, could be calculated. Each sample was repeated and measured three times to avoid accidental errors. The average values adopted are shown in figure 4-14. In terms of the mixing rate of silicon base and curing agent, typical data were calculated in a similar way.

Table 4- 7: The PDMS Young's modulus changes against curing time

Curing time	Young's modulus (MPa)
2 hours	2.59±0.23
3 hours	2.65±0.37
4 hours	2.75±0.14
6 hours	2.41±0.28
12 hours	2.78±0.17
24 hours	2.88±0.23

From table 4-7, the average value of six curing time elastic modulus was 2.68 with a standard deviation of 0.37. This indicated that the stiffness of PDMS was not sensitive to the curing time. In contrast, it was easy to conclude that the mixing rate of Sylgard 184 base and curing agent had a great impact on the mechanical properties of PDMS (from table 4-8). The Young's modulus was in inverse proportion to the ratio.

As it can be seen from figure 4-14, the mixing ratio of PDMS base and curing agent had great effects on the mechanical properties of such material. According to these results, we can conclude that the low mixing ratio made the PDMS sample hard. In this application, the PDMS was used to support the tissue and worked as the force transducer. Thus, the material could not be too soft or too high. Small Young's modulus may lead to too large deflection of the pillars and it won't follow the mechanical model above if their deformations are too large. Large one makes the

deflection inconspicuous and hard to be measured or more experimental errors. Thus, a ratio of 10:1 was considered to be the most suitable condition in such condition and chosen as the manufacture standard for making the platform used in this experiment. Although the curing time did not enormously affect the mechanical properties of PDMS, the unified curing standard was kept for each manufacture of the platform. The Sylgard 184 base and curing agent ratio was kept at 10:1 with the curing time being 3 hours, thereby ensuring the elastic modulus was 2.63MPa±0.5MPa.

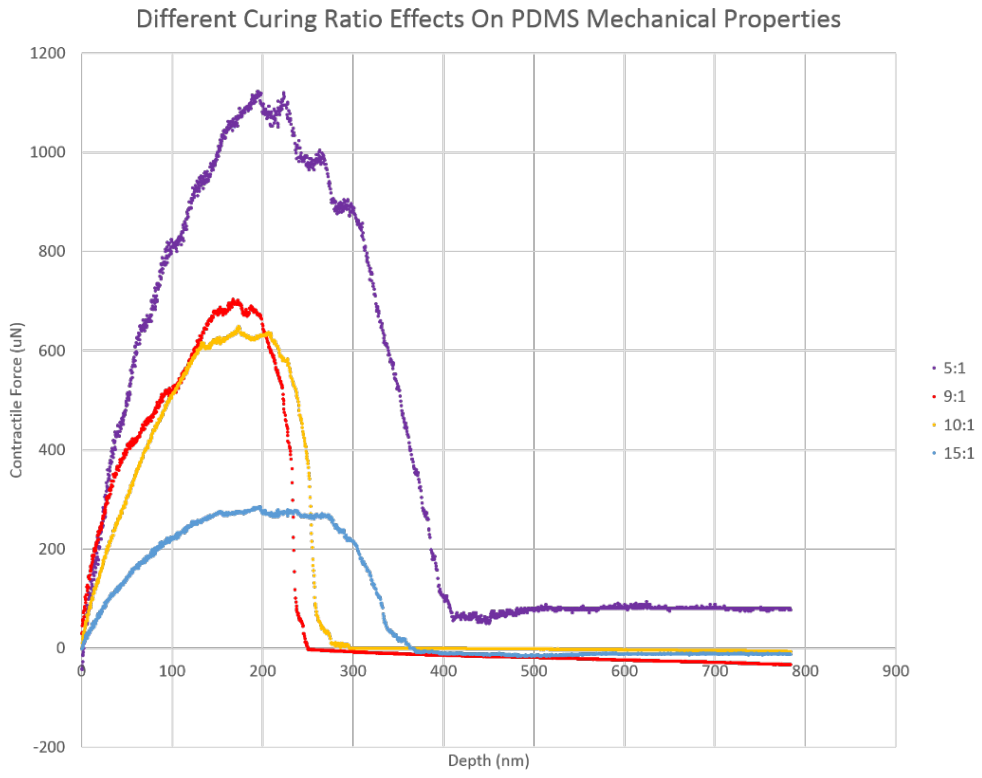


Figure 4- 15: AFM nanoindentation force reaction (nN) curves against separation (nm) for different mixing ratio of PDMS base and curing agent. The blue lines represent compression force reaction and the red lines are the relaxation force reaction.

Table 4- 8: The PDMS Young's modulus changes against mixing ratio

Sylgard 184 base and curing agent ratio	Young's modulus (MPa)
5:1	4.83+-0.43
9:1	2.78+-0.16
10:1	2.62+-0.28
15:1	1.13+-0.22

4.3.3. Bending Silicon Posts Force Measurements

In previous studies, different tests have been applied to measure the elastic properties of PDMS[162], which found the mixing ratio greatly affected on the mechanical properties of PDMS. Even with the same mixing ratio, the young's modulus measured still varied from each other, ranging from 1.5 MPa to 3.2 MPa with a mixing ratio of 1:10.[163 164]

As the force transducer accuracy is highly reliant on this value, it was desirable to test this practically. Our measuring mean value was about 2.63MPa, which was within the reasonable range according to a review of the literature. Hence, this value was applied in all further simulations and experiments.

As stated previously, the mechanical model of the platform needed to follow cantilever beam deflection. A deben tensile stage test was conducted to further prove this. As a direct measurement of the bending measurement and test, 2N load cell was used to reduce the effects from noise. It totally mimicked the actual motion of the platform by connecting the silicon post's free end with the moving stage

(1.5mm/min). The force sensor measured the force reaction from the deformation every 500ms. In terms of the silicon post's geometry, they were 10mm in length and 1mm in diameter.

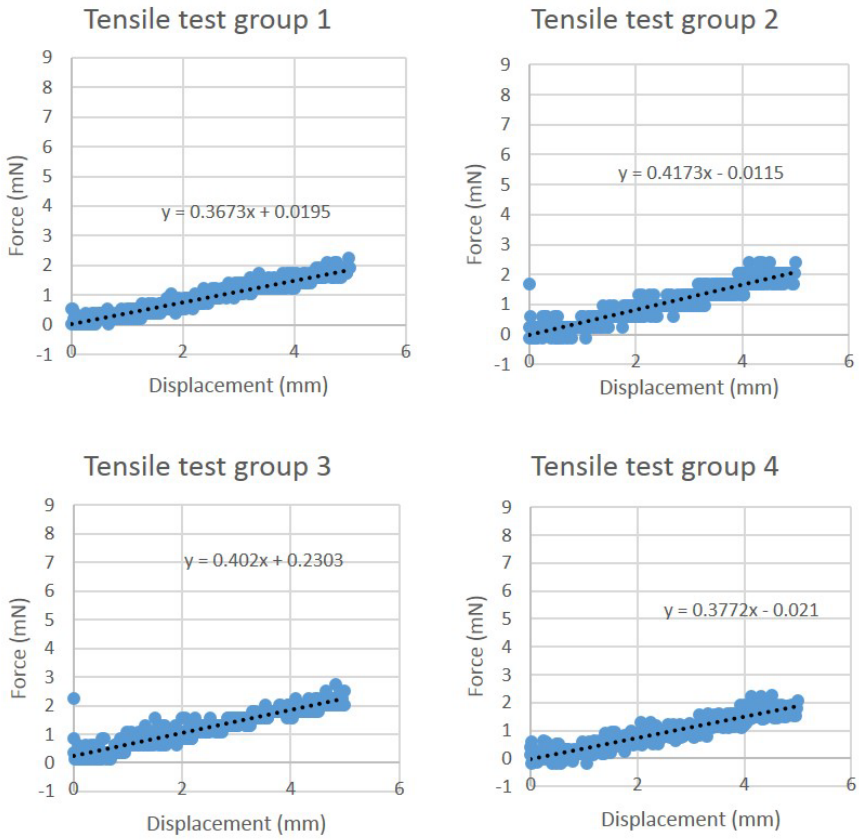


Figure 4- 16: Deben tensile tests. Tension changes against displacement of the PDMS posts free ends.

The data shown in figure 4-16 were measured from four different silicon pillars. All the tests were repeated three times on each sample under the same condition to avoid experimental errors. It could be concluded that the tensile force was linear with increasing displacement of PDMS pillars. It meant that the beam deflection model is workable for cellular force measurement in this project. The averaging

proportionality coefficient was 0.39095 from the data. The standard deviation was 0.04 (a relatively small value), which showed that value was not casual and could, therefore, be used. From the cantilever beam deflection, the theoretical force-displacement relationship was calculated as $F \approx 0.39\sigma$. This value was extremely close to the experimental result (0.39095). Thus, we conclude that the cantilever beam deflection model was quite reliable in this system and we can use this model to determine the cellular forces.

4.4. Summary

The platform is not just to be utilised for supporting the tissue, but also to work as a force transducer. Its geometry plays a key role in this system, so it was meaningful to carry out the mechanical model optimization studies. According to the literature, the contraction force from such a number of cells varies from 0.1mN to 0.5mN. Apart from the geometry (diameter and length), other conditions have been confirmed (PDMS mechanical properties). Following the beam deflection model, it was desirable to make the posts deformation within an easy-measure range. It was thus found that the diameter could not exceed 1mm and that the length needed to be from 10mm to 15mm. Hence, we decided to use 12mm length with 1mm diameter as the final design.

Table 4- 9: Platform design mechanical optimization

Diameter/ Length	6mm	8mm	10mm	12mm	15mm
1mm	0.11mm	0.26mm	0.51mm	0.89mm	1.73mm
2mm	7um	16.4um	32um	55.3um	0.11mm
4mm	0.4um	1.02um	2um	3.46um	6.76um

It is concluded that the micro-bioreactor with a silicon platform is effective for qualifying the contractile force of 3D cultured cardiomyocytes. Theoretical analysis on the displacement and force relationship proved to be correct as it was calibrated by the experimental data. To optimize the force transducer function, different geometries of the PDMS platform were investigated and the best design was silicon post 1mm in diameter and 12mm in length. Using a controlled camera or microscope, the cellular force could be measured via an optical method with such a transfer model as has been proven correct before.

Chapter 5 Microbioreactors with Optimal Perfusion System

5.1. Introduction

We aim to generate functional engineered heart tissue and establishment of tissue structure *in vitro* can be used to mimic the construct in the human body. In the human body, the nutrients exchange, gas delivery and waste removal are made by blood flow. To provide and maintain a stable microenvironment like this for cell culture, special designed perfused bioreactor is applied to guarantees the cells and tissues being cultured in steady and controllable conditions. The medium can be transferred by external control to achieve suitable conditions for cells. It has been proved that perfusion system shows great advantages in enhancing cells viability and functionalities.

In this project, by using 3D printing and external pump, continuously perfused system is fabricated based on glass slide. In such equipment, the cell culture situation is monitored and adjusted via dynamic fluid control. Some parameters of media flow need to be carefully determined to get optimized environment for cells, such as wall shear stress, flow velocity and media flow pathway. After simulation and practical test, the configuration of the bioreactor chamber is designed thereby achieving the best perfusion situation for the engineered heart tissue cultured in this equipment.

5.1.1. Bioreactor for Tissue Engineering

Tissue engineering is a research field that requires several disciplinary areas like biology, material, biochemical and engineering and etc. It aims to mimic the natureal tissue *in vitro* by seeding cells onto scaffolds to generate functional three-dimensional tissues, which can be cultured for long term. During cell culture process, one of the most significant process of tissue culture is evenly distribution of cells throughout the scaffold.[165] The scaffolds need to mimic the functions of the extracellular matrix and provide a support for cells attached. They must have enough porosity to allow transports of nutrients and waste, and other characteristics like biodegradable and biocompatible. Currently, tissue culture is mostly done under the static conditions within the culture flasks or dishes and kept in the incubator. In such culture situation, the mass transport is made by media diffusion. Yet, it has been proved by Novosel that the flow diffusion distance in the tissue is less than 200um.[166] Static culture leads to insufficient nutrient and metabolic waste exchange efficiency within large 3D tissue constructs and it is also easy to introduce containments as the media change is heavily relied on lab work. This will result in cells death and poor extracellular matrix production. The problem of limited quantities of nutrients and waste transportation can be relieved by the application of dynamic culture conditions, such as different perfused bioreactors, which helps improve mass transport through the scaffold. These perfusion systems can also be used to apply mechanical stimulations to the cells via the medial flow to enhance cells viability and assist extracellular matrix formation.

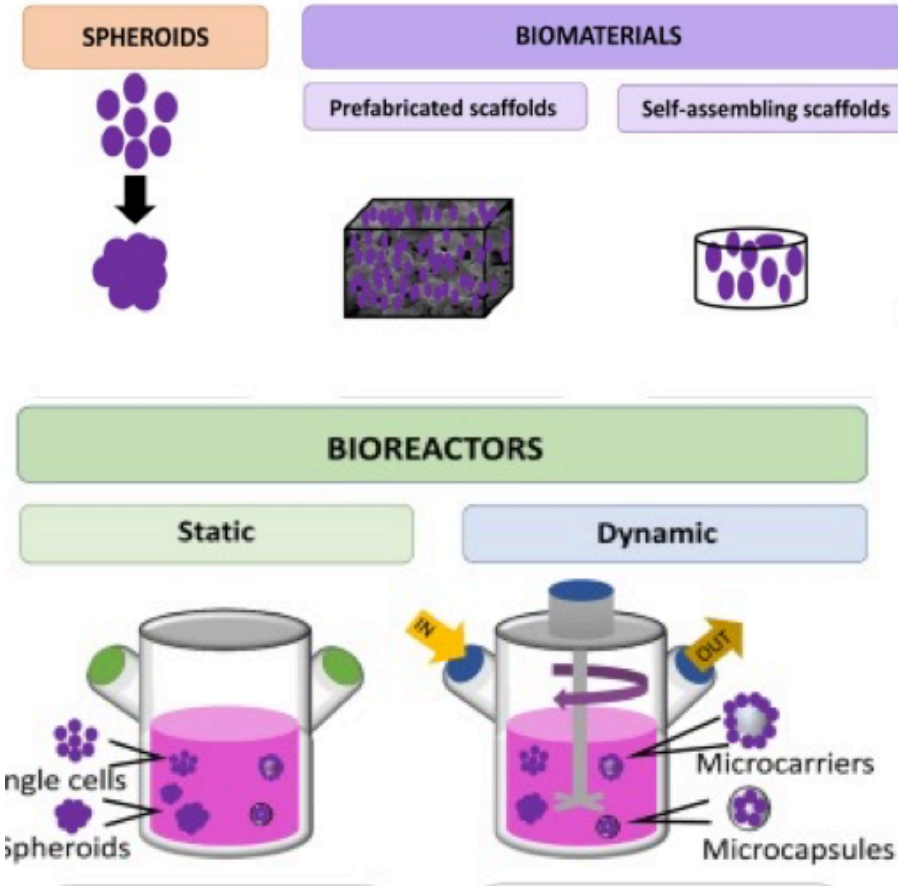


Figure 5- 1: Different cell culture systems in three-dimensional conditions: (a) Spheroids (b) Cells are seeded onto various types of scaffolds (c) Cells and tissue are cultured under static conditions and dynamic conditions.[166]

Thus, in previous study, several bioreactors, like stirred tank bioreactors, rotating wall bioreactors, and perfusion bioreactors have been developed and applied to control cell culture conditions and provide relevant stimulus for cells.[167,168,169,170] The purpose of applying these bioreactors for tissue culture is to develop new tissue *in vitro* by supplying chemical and physical regulator signals onto cells to guide their proliferate or to produce functional extracellular matrix.

5.1.2. Perfusion System Application in Tissue Engineering

The unified and stable environmental is compulsory condition for culturing cells. Special designed microfluidic bioreactor can provide an even and controlled environment when culturing tissues *in vitro*. Effective control of temperature, pH, dissolved oxygen levels, and media perfusion is valuable and can enhance cells viability and maturation. Compared with conventional cell culture, the application of microfluidic devices not only provides a stable mimetic *in vivo* environment, but also lowers the consumption and cost of the experiment. The manufacture of relatively miniaturized devices also accelerates the realization of Lab-on-chip.[171] They provide a highly sensitive and reliable condition and smaller size means multiple sequential experiments can be conducted at the same time.[172] Normally, the size of micro-bioreactor ranges from 0.01 to 1000 μm^3.[173]

As the extension of micro-electromechanical-system technology, microfluidic devices were firstly developed in the 1980s.[174] For different application purposes, the micro-bioreactor can be fabricated with different materials to fulfil specific requirements, such as metal, glass and polymers. Over the past decades, the development and application of various micro-bioreactor has increased dramatically.[175,176,177] In the book of Encylopedia of medical devices and instrumentations, Zhu et al described the progress in micro-bioreactor research area before 2005.[178] Many aspects related to microfluidic devices have been referred in this book, such as the designs, operation and applications. More than 10 years ago, Zanzotto developed a micro-bioreactor made by PDMS to observe the behaviour of bacteria.[179] In his system, the microfluidic device was fabricated and its functions

were verified. Three parameters were measured and controlled by the optical sensors. They are optical density (OD), dissolved oxygen (DO) and pH. It is found that the bacterial fermentation is similar to that carried out within the control samples that were left in the incubator. Hence, it firstly showed it is effective and can be further applied into some other bioprocess experiments. In 2009, an imaging platform was developed by Taylor et al. to dynamically analyse the single cells response when they were combined together with stimulations applied.[180] It was the first application of microbioreactor for specific cellular research. In the following year, some microfluidic devices were designed and put into use for culturing stem cells.[181,182] Besides these, the micro-bioreactors also have great applications in doing drug screening test. In Laposa's work, toxicity and effects of cardiac drugs were tested with cardiomyocytes derived from human embryonic stem cells in 2011.[183] The microbioreactors were utilized to keep the cells cultured in same conditions as *in vivo* environment. Furthermore, these systems also enable the realization of in-parallel experiments to be conducted at the same time.

As it has been described before, various approaches have been achieved to develop engineered heart tissue with different cell sources, scaffolds materials, and structures. The generated different types engineered heart tissue can be formed and cultured *in vitro* for long-time period (more than 2 weeks). Hence, it is meaningful to apply microfluidic technology onto culturing engineered cardiac tissue. The controlled dynamic media flow and temperature make the cells within the engineered heart tissue could be alive for longer time and express better functions. Compared with conventional static culture condition, it is also able to provide a convenient

observation condition for samples. The solution concentration can be controlled as well, such as media and drug concentration so that drug tests can be conducted under a uniform condition.[184] Although this is especially important for engineered heart tissue aiming to do drug delivery and screening, the micro-bioreactor technology has seldom been applied in this research area. It potentially has great help on tissue culture and accuracy control of results.

5.1.3. Shear Stress and Turbulence

As described before, the dynamic culture environment provided by the bioreactor can enhance the performance of cells cultured *in vitro* in the long term. The better exchange of oxygen and nutrients across the cells throughout the scaffolds helps improve the viability of cells and restore their functions.[54] However, the perfused media flow in the micro-bioreactor will introduce shear stress and it is different from that in native heart. If the shear stress is too high, it will be harmful to the cellular viability and functions. For the perfusion micro-bioreactor, the aim is to develop a dynamic fluid environment for tissue culture. To have uniform flow distribution and lower the shear stress with enough mass transport efficiency, the laminar flow is demanded. The shear stress distribution within the bioreactor was affected by many factors like the geometry of bioreactor chamber, scaffold location, and inlet velocities etc.

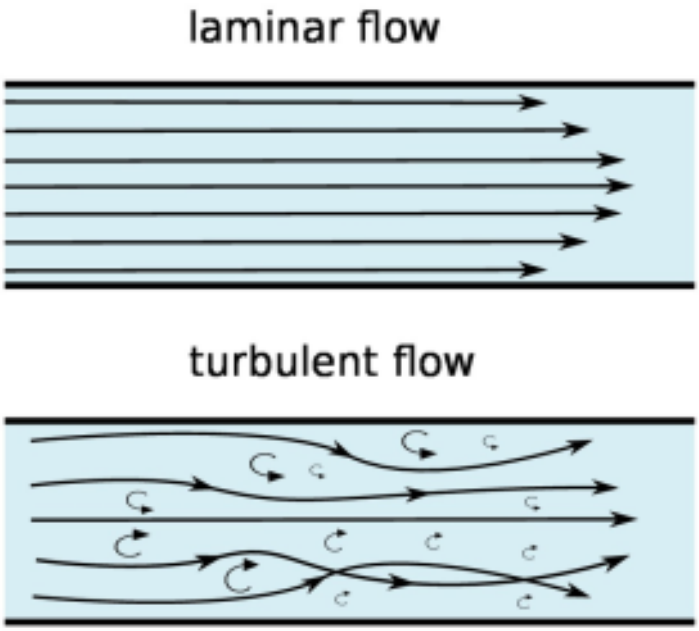


Figure 5- 2: Schematic diagram of laminar flow and turbulent flow[185]*. Laminar flow means the fluid travels in regular way without any disruption and turbulent flow is a less orderly flow with irregular fluctuations*

Laminar flow is a kind of fluid flows in which the fluid travels in regular way without any disruption.[186] By contrast, turbulent flow is a less orderly flow and occurs while the fluid undertaking irregular fluctuations and mixing.[187] As it can be seen from the figure 5-2, the fluidic properties including flow speed and pressure at any point keep same. On the other hand, the velocity and pressure of the fluid at one point keeps change in both amplitude and direction for turbulent flow. To keep the mass diffusion within the culture chamber and tissues, the laminar flow is demanded for uniform oxygen and nutrient distribution like that in native vessel system.

Laminar flow normally occurs at low flow speed and turbulence happens over a threshold. To determine a flow is laminar or turbulent, the Reynolds number is used. The Reynolds number is calculated by the ratio of the inertial force to the shearing force of the fluid.[187] This value depends on the geometry of chamber and flow pattern. Take a common example of a pipe, the Reynolds number can be calculated as:

$$R_e = \frac{\rho u D_H}{\mu} = \frac{u D_H}{v} = \frac{Q D_H}{vA} \qquad (5.1)$$

Where D_H is the diameter, Q is the flow rate, A is the area of the cross-section, u is the fluid velocity, μ and v are the dynamic and kinematic viscosity and ρ is the fluid density.

5.2. Microfluidic Model and Numerical Simulation

5.2.1. Bioreactor Geometry Design and Perfusion System Set Up

To mimic the biological environment of natural tissue or cells, a perfused platform offers suitable *in vitro* conditions. Compared with a static culture system, a continuously perfused bioreactor makes it easier for media to get through the scaffold enabling the cells at the centre of tissue to access enough nutrient and oxygen. In this research, the generated bioengineered cardiac tissue was to be used for drug tests or physiological mimicking of the native human cardiac tissue. Single well cell culture always requires lots of time and high expense. It is, therefore,

desirable to apply perfusion system to provide uniform media flow and supply enough nutrients and oxygen throughout the cells seeded within the scaffolds in three-dimensional construct. In terms of drug testing, it would involve a great number of tests of identical cell culture. The application of perfused bioreactor provides an easy way to introduce different formations and concentrations of drugs. Yet, the dynamic fluid should be carefully characterized to provide a uniform and optimized.

In this bioreactor, the media, which flows within the chamber and through the tissue, is viscous-dominated slow flow. This could be modelled by the Stokes-Equation:

$$H\nabla p=\mu\nabla^2 u \qquad (5.2)$$

Where p is the fluid pressure, u is the velocity, and μ is the fluid viscosity.

Many factors have effects on the efficiency of the perfusion system. For example, the geometry of the bioreactor determined the flow path. In the bioreactor chamber, a stagnant zone was created in the peripheral region when the media flowed through the tissue centre. To optimize media flow and mass transport environment for the cells, uniform flow and low shear stress within the chamber are required.

The fluid shear stresses acting on the tissues and cells also depended on many factors, including the internal structural shape and position of the scaffolds, the culture chamber design, and the perfusion mode. Hence, to confirm the parameters of the bioreactor, it is necessary to simulate and monitor the fluid flow inside the perfusion chamber.

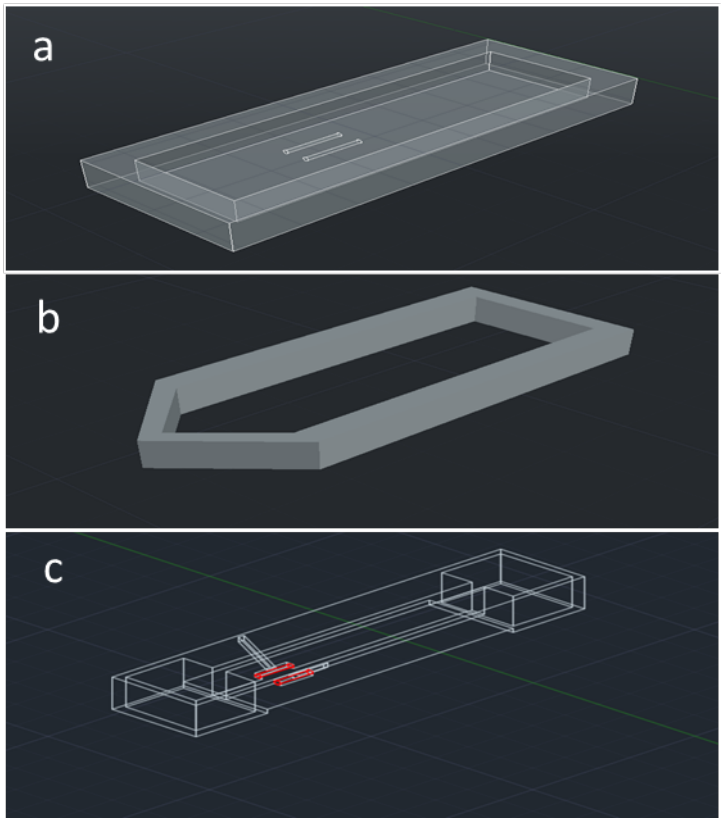


Figure 5- 3: Model and measures of the perfusion bioreactor. (a) The microbioreactor design of chamber with quadrilateral shape channel (QSC). (b) The microbioreactor design of chamber with narrow towards wall channels (NTWC). (c) The microbioreactor design of chamber with narrow space channel (NSC).

To find the conditions most suitable for a perfused platform, computational fluid dynamics (CFD) was used to provide a method to model the system. With the aid of commercial computer-aided design software, AutoCAD (Autodesk, USA), the perfusion bioreactor chamber designs were modelled. There are three bioreactors with different shapes shown in figure 5-3.

Three different chambers are designed and analysed. The first one is the chamber with quadrilateral shape channel (QSC) (figure 5-3 (a)). The length of the chamber is 150mm and the width is 50mm with 5mm thickness boundaries around. Two electrodes are placed 20mm from the inlets. For this design, single inlet and multi-inlets were simulated and analysed. The second design is the bioreactor with narrow towards wall channels (NTWC) (Figure 5-3 (b)). In this design, two attempts were made with square channel and narrow towards wall channel. The length of channel is 150mm in total with 50mm in width and the thickness boundaries is still 5mm. The range of narrow towards wall channels is 10mm in length. The last design is narrow space channel (NSC) (Figure 5-3 (c)). The electrodes were placed into two premade grooves with same geometry of electrodes to avoid the turbulent flow due to present of electrodes.

Commonly in all the perfusion bioreactors the fluid flows directly to the scaffold in a linear way, originating most of the times a uniform distribution of the fluid in the scaffold surface, but sometimes the fluid also reaches high values of shear stress due to the high impact of the fluid right into the scaffold resulting in cellular necrosis. In this particular perfusion bioreactor, besides the straightforward fluid, the aim is also to have, in a controlled way, different tensions, and different velocities, forcing the scaffold to proliferate the cells with different stimulus to create a heterogeneous tissue. In order to accomplish these differences and to better understand the correlation between the changes of the fluid velocity on the surface of the scaffold, three designs of bioreactors were stimulated with the Computational Fluid Dynamics (CFD) simulation. The parameters of different bioreactor configurations and

velocities were considered. To conduct the dynamic fluid flow simulation, the mesh parameters for these models are displayed in Table 5-1.

Table 5- 1: Mesh parameters of the Computational Fluid Dynamics (CFD) Analysis

Bioreactor chamber design	Total elements	Elements type	Average elements size (mm)
Quadrilateral shape channel (QSC)	475400	Quadrilateral	0.05
Narrow towards wall channels (NTWC)	878480 &1245000	Quadrilateral and triangle	0.1
Narrow space channel (NSC)	429600	Quadrilateral	0.1

The CFD simulations were carried out taking into account the properties of the fluid, different velocities and the properties of perfusion chamber is listed in the Table 5-2.

Table 5- 2: Fluid characteristics and chamber properties used in the CDF analysis

Parameters	Value
Media density	998.2 kg/m^3
Fluid Viscosity	0.0019 Pa/s
Flow rate	0.1rmp, 0.02rmp, 0.03rmp, 0.04rmp, 0.05 rmp
Pressure	1 atm
Fluidic model	Laminar flow

Bioreactor inlet and outlet diameter	0.5mm
Bioreactor volume	3.5ml

5.2.2. Turbulence Kinetic Energy

One of the fundamental problems of Fluid Dynamics has been, and still is, the Turbulence. Taking that into account, there are several theoretical analysis and prediction models that are carried out in CFD simulations.

The description of turbulent flow is so complex, and for that reason, the existing formulations may go from just simple definitions of skin friction or heat transfer coefficients, going up to a more specific energy spectra's and turbulence fluctuation magnitudes and scales.[188]

Fluid can be characterised by several models: there are the zero-equation models, one-equation models, two-equation models and there are more advanced models.[187] To carry out the study of the turbulence within the chamber of this perfusion bioreactor, the Turbulence Kinetic Model was used and it is a one-equation model. It's an alternative to the algebraic model and it predicts, by solving one additional transport equation, the turbulent flow.

In fluid dynamics, turbulence kinetic energy (TKE) is the mean kinetic energy per unit mass associated with eddies in turbulent flow.[189] Despite the fact that common turbulent scales are often used as the variable in the transport equation, one of the most used methods is the calculation of the characteristic turbulent velocity scale proportional to the square root of the specific kinetic energy of turbulent fluctuations

that is usually referred as turbulence kinetic energy, denoted by k.[190] The variable k can be obtained by the mean of the turbulence normal stresses:

$$k = \frac{1}{2}(\overline{(u')^2} + \overline{(v')} + \overline{(w')} \tag{5.3}$$

where k is the turbulence kinetic energy; u', v' and w' are the three fluctuating components of velocity. The full form of the TKE equation can be observed in the following equation:

$$\frac{\partial k}{\partial t} = \bar{u}_j \frac{\partial k}{\partial x_j} = -\frac{1}{\rho_0}\overline{\frac{\partial u_\iota' p'}{\partial x_i}} - \frac{1}{2}\overline{\frac{\partial u_j' u_j' u_\iota'}{\partial x_i}} + \nu \frac{\partial^2 k}{\partial x_i^2} - \overline{u_\iota' u_j'}\frac{\partial \bar{u}_\iota}{\partial x} - \nu \overline{\frac{\partial u_\iota'}{\partial x_i}}\overline{\frac{\partial u_\iota'}{\partial x_j}} - \frac{g}{\rho_0}\overline{\rho' u_\iota' \delta_{\iota 3}} \tag{5.4}$$

Where $\frac{\partial k}{\partial t}$ is the local derivative, $\bar{u}_j \frac{\partial k}{\partial x_j}$ is the advection, $\frac{1}{\rho_0}\overline{\frac{\partial u_\iota' p'}{\partial x_i}}$ is pressure diffusion, $\frac{1}{2}\overline{\frac{\partial u_j' u_j' u_\iota'}{\partial x_i}}$ is turbulent transport, $\nu \frac{\partial^2 k}{\partial x_i^2}$ is molecular viscous transport, $\overline{u_\iota' u_j'}\frac{\partial \bar{u}_\iota}{\partial x}$ is production, $\nu \overline{\frac{\partial u_\iota'}{\partial x_i}}\overline{\frac{\partial u_\iota'}{\partial x_j}}$ is dissipation, $\frac{g}{\rho_0}\overline{\rho' u_\iota' \delta_{\iota 3}}$ is Buoyancy flux.

5.3. Results and Discussion

5.3.1. Design of Bioreactor with Dynamic Media Flow Simulation

The micro-bioreactor described here comprised four main parts: (i) the culture chamber, (ii) the cell culture platform, (iii) carbon electrodes, and (iv) an inlet pump. The culture chamber was manufactured by 3D printing with polymer material. As the core part of the bioreactor, the cell culture platform is made of polymerdumethylsiloxane (PDMS), a kind of biocompatible material to support the tissue. To understand how the media flow and thus make the cells within the 3D scaffold gain the optimized contact with the media with best nutrients and oxygen transient, the fluidic situation within the chamber was simulated with the commercially available software Ansys Fluent (version 17.2). We aimed to make the media (or mixing with drug) stably flow through the tissue culture zone. To achieve these purposes, different geometries and sizes of the bioreactors were simulated to find the optimized conditions.

The initial design was a square chamber. Flow dispersion within this chamber depended on different factors, such as the number of the inlets, the inlet velocity, and the geometry of the bioreactor.

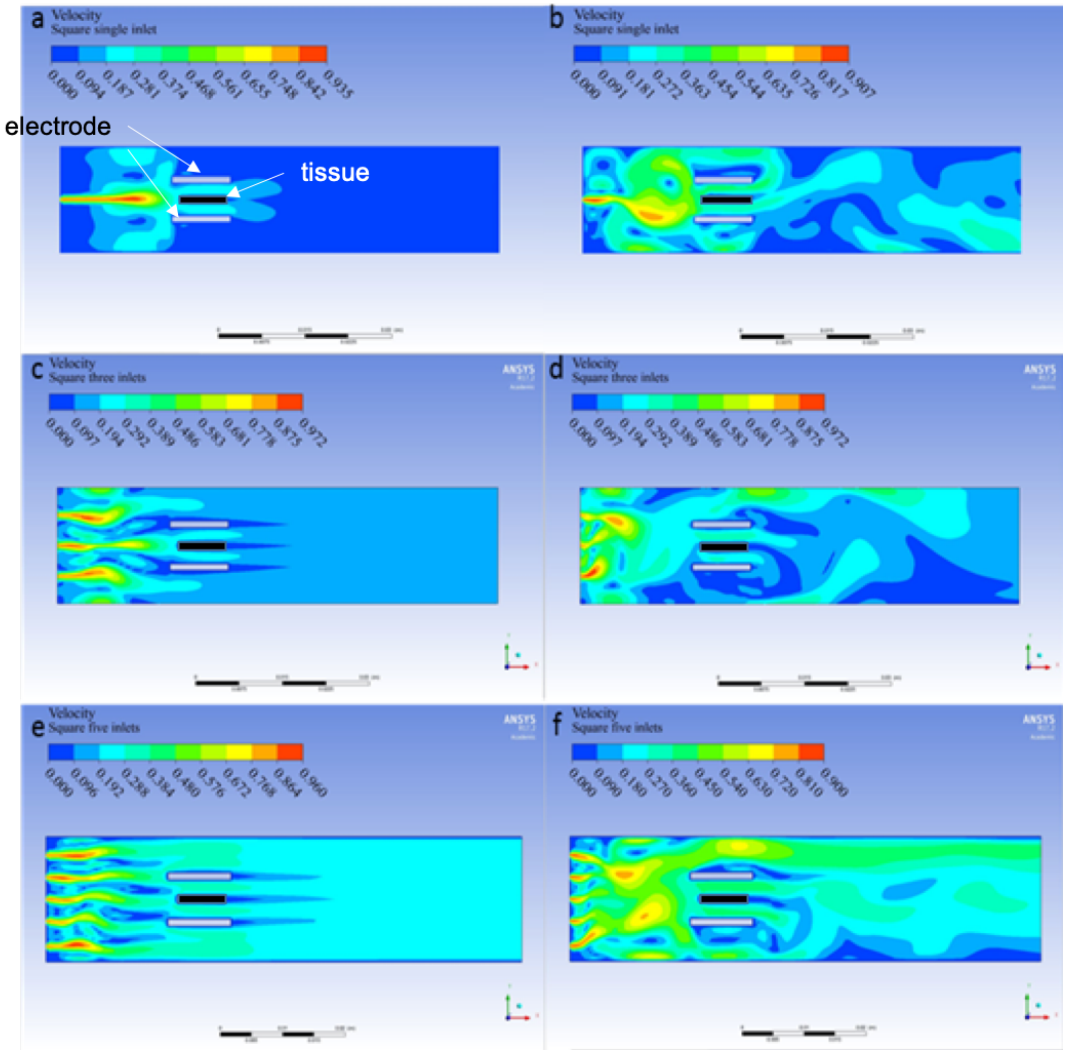


Figure 5- 4: Dynamic fluid simulation with ANSYS Fluent of flow through a bioreactor with chamber of quadrilateral shape channel (QSC) with single inlet (a) initial time, (b) stable flow over 20 minutes and 3 inlets (c)initial time, (d) stale flow after 20 minutes and 5 inlets (e) initial time, (f) stale flow after 20 minutes. (The unit of velocity is mm/min). Black squares mean tissue sample and grey squares mean electrodes.

Simulated results using bioreactors with single and multiple inlets are represented here. At the inlet ends (from left-hand side), the flow was uniformly distributed over

the bioreactor. But after flowing through the tissue (the one locates at the centre of two carbon electrodes), the flow cannot be controlled any more. Single inlet flow was found to be more stable and controllable compared with others. By adjusting the flow velocity, a relatively stable flow condition could be achieved.

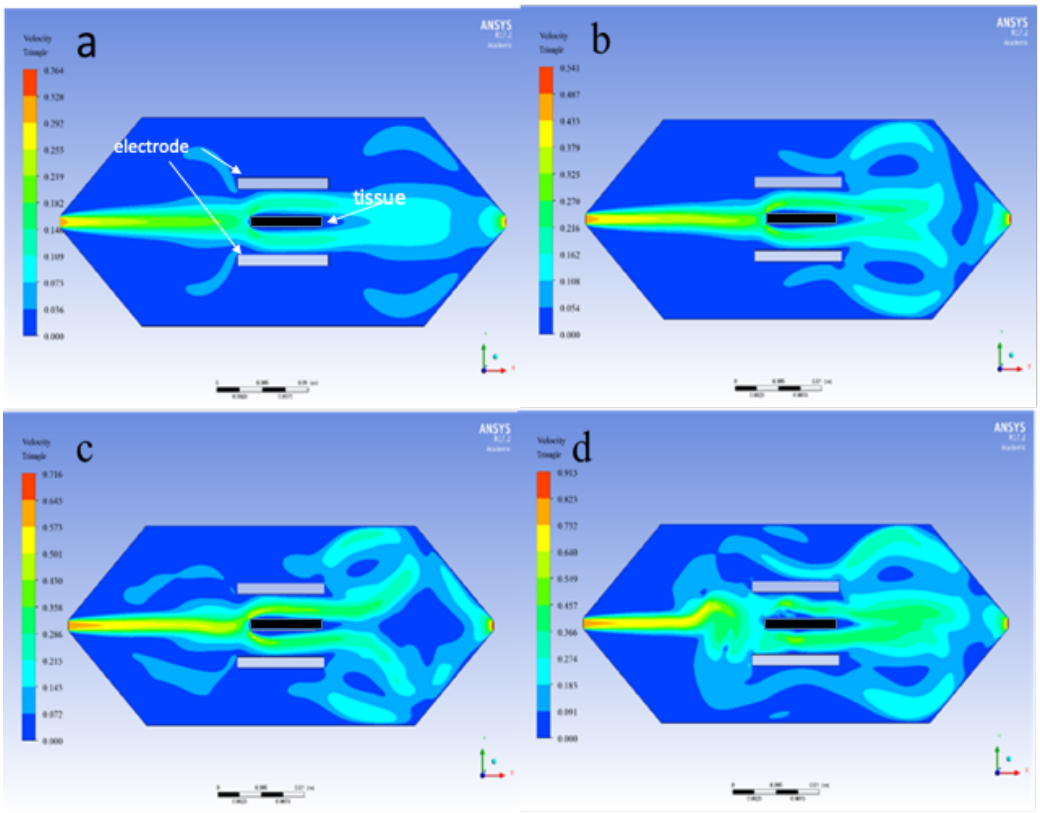


Figure 5- 5: Dynamic fluid simulation with ANSYS Fluent of flow through the bioreactor of chamber with narrow towards wall channels (NTWC). with single inlet. (a) Initial time (b) stable flow over 5minutes (c) stable flow over 10 minutes (d) stable flow over 20 minutes. (The unit of velocity is mm/min). Black squares mean tissue and grey squares mean electrodes.

In the square chamber, flow is hard to be controlled and the fluid situation within the chamber is quite random except in the area close to the near-inlets while the flow

was introduced. To better control the flow, a triangular region was set to make the media flow more smoothly over the tissue. In this form of the bioreactor, the stability of the media flow highly relied on the flow rate. By changing the inlet flow velocity, we can get the fluidic situation that we want (as shown in Figure 5-5).

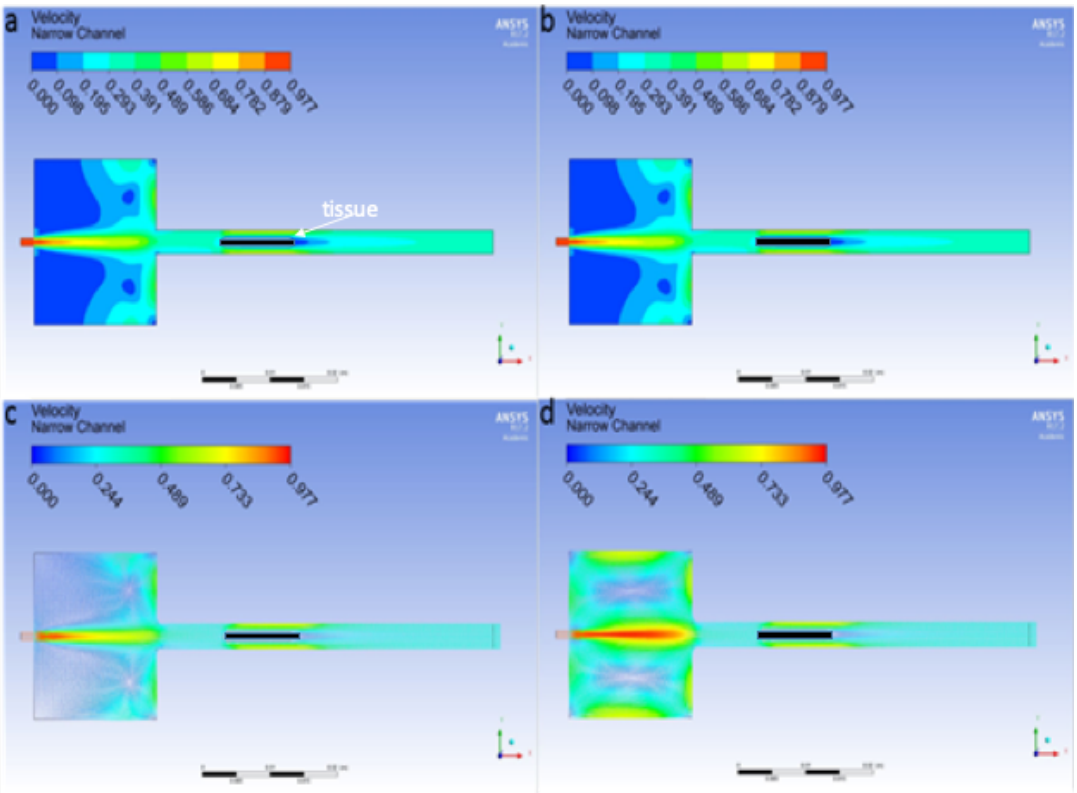


Figure 5- 6: Dynamic fluid simulation with ANSYS Fluent of flow through the bioreactor of chamber with narrow space channel (NSC). (a) Initial time (b) stable flow over 5minutes (c) stable flow over 10 minutes (d) stable flow over 20 minutes. (The unit of velocity is mm/min). Black squares mean the tissue and electrodes are integrated within the chamber of the bioreactor so effects from them can be ignored.

In this form of micro-bioreactor, a flow rate higher than 0.9mm/min made the turbulent situation worse and the flow is hard to be controlled. The media flow was relatively stable when the inlet velocity was lower than 0.9mm/min. But we can still find that the flow become unpredictable after a long time of continuously pumping media in.

We can find these were still not the best conditions for the perfusion system. In those designs, the effects of carbon rods could not be ignored. Thus, a better design was made to avoid such effects. A new design was made and manufactured by using 3D printing. A chamber worked as the buffer zone and the following narrow path was used to cover the carbon rods and let the media flow through just the tissue. By simulating different inlet velocities flow through the channel; it was found that this form could effectively control the flow (this can be seen in Fig.5-6). We can therefore conclude that this geometric design of the bioreactor showed the best fluid results.

While comparing three different designs, it could be seen that the third one keeps the tissue experience smooth flow of media around its structure and the fluid is relatively controllable. This design did not rely on control of the flow rate. Adjustment of the flow rate was more flexible compared to other designs. This system aims to be used for drug testing and screening, so this is quite important. As we assume that cells are distributed within the scaffold evenly, they can access to homogeneous nutrient.

5.3.2. Velocity Analysis and Turbulence Kinect Energy

As mentioned before, the simulations were performed taking into account three different velocities, namely V1, V2, V3, V4, V5 with the corresponding velocities of 0.01rmp, 0.02rmp, 0.03rmp, 0.04rmp, 0.05rmp, respectively.

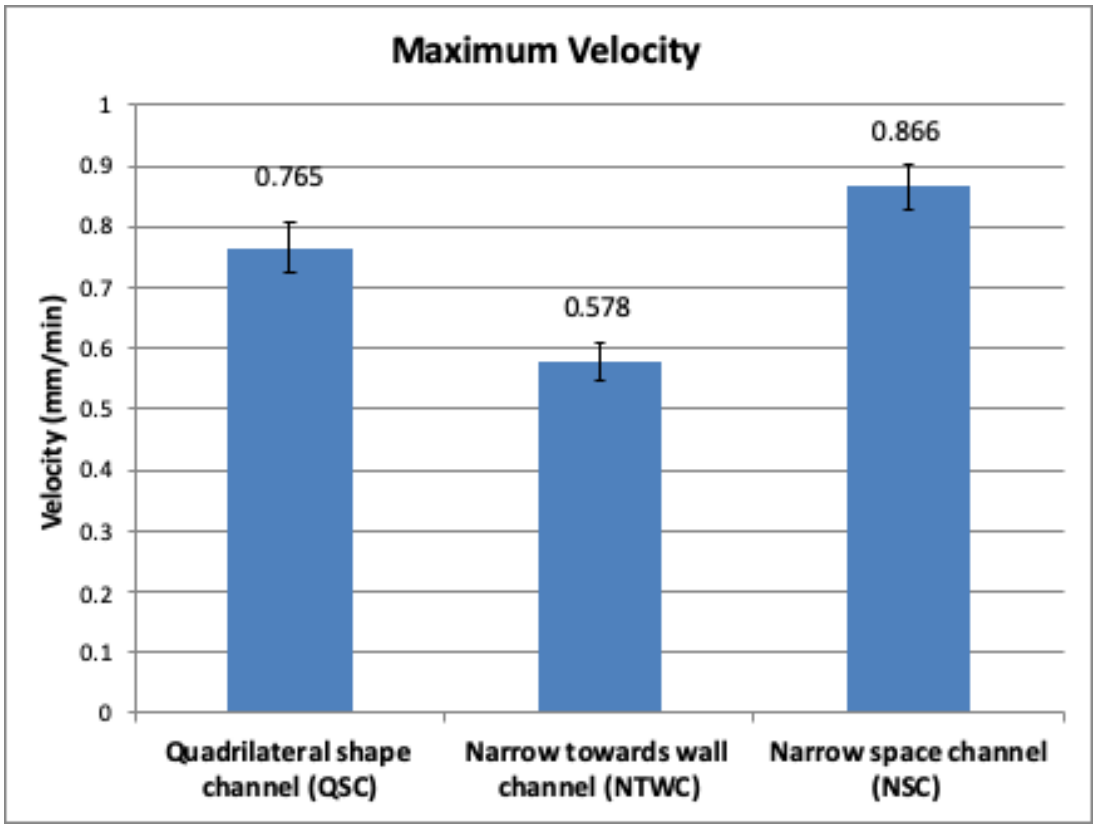


Figure 5- 7: Velocity results for all the bioreactors types under the condition of 0.01rmp inlet velocity. It represents the maximum velocities reach to the samples.

The simulations were carried out to better understand the behaviour of the fluid inside the chamber and the highest velocity of different bioreactor configuration of V1 (0.01rmp) is shown in Figure 5-7. The highest is that in NSC bioreactor (0.866mm/s) and the NTWC have the lowest velocity.

Observing the velocity streamlines, it's possible to analyse that both the highest values reached within the perfusion bioreactors were achieved in the inlet and outlet tubes. As it is described before, the media flow of rectangular shape channel bioreactor cannot be controlled properly. Thus, to determine the turbulent flow and shear stress, only micro-bioreactor of narrow towards wall channel (NTWC) and Narrow space channel (NSC) are analysed.

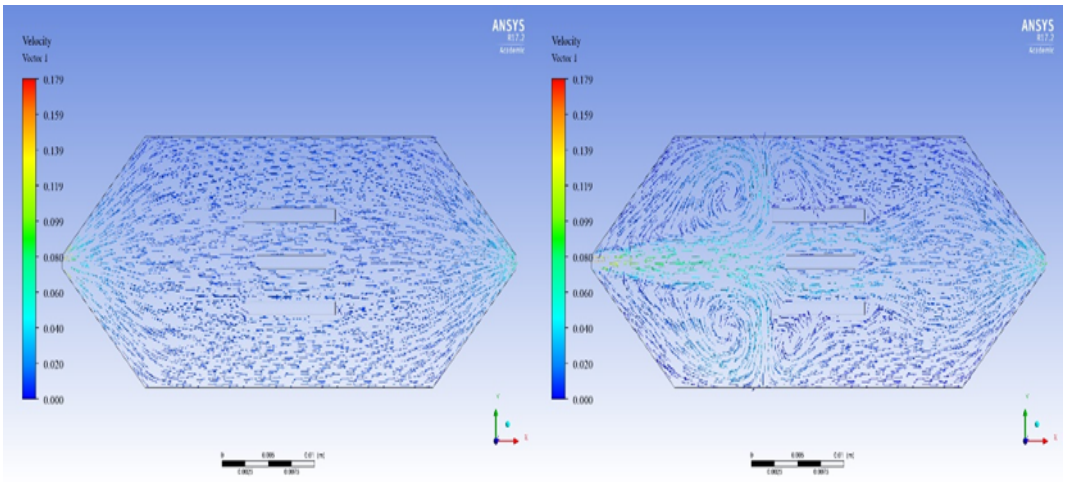


Figure 5- 8: V1 velocity streamline results for narrow towards wall channel (NTWC) (The unit of velocity is mm/min)

In the case of narrow towards wall channel (NTWC), the membrane forces the flow towards the walls and it creates vortexes increasing the velocity within the chamber, even if the velocity drops down severely when it exits the membrane due to the higher volume of fluid present in the chamber.

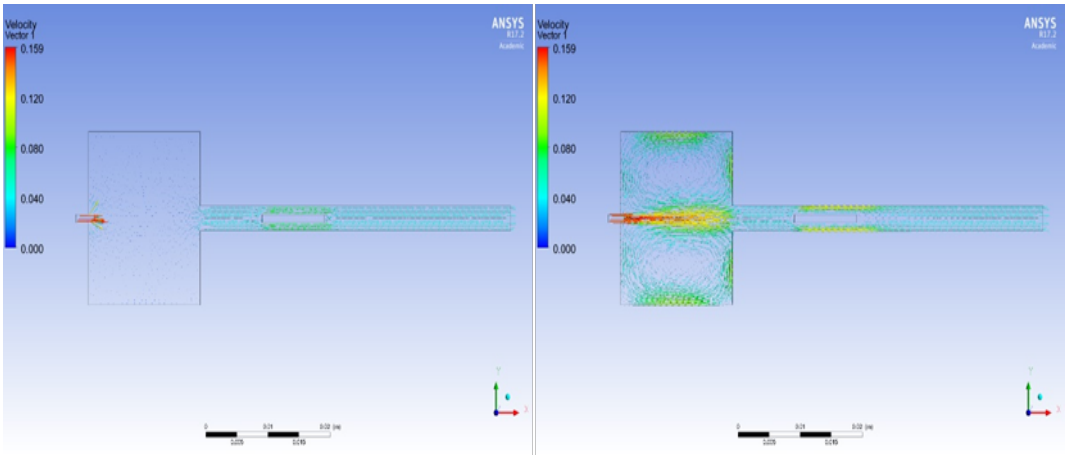


Figure 5- 9: V1 velocity streamline results for narrow space channel (NSC) (The unit of velocity is mm/min)

In the case of narrow space channel (NSC), the flow is in a straight line and the values within the chamber are very low.

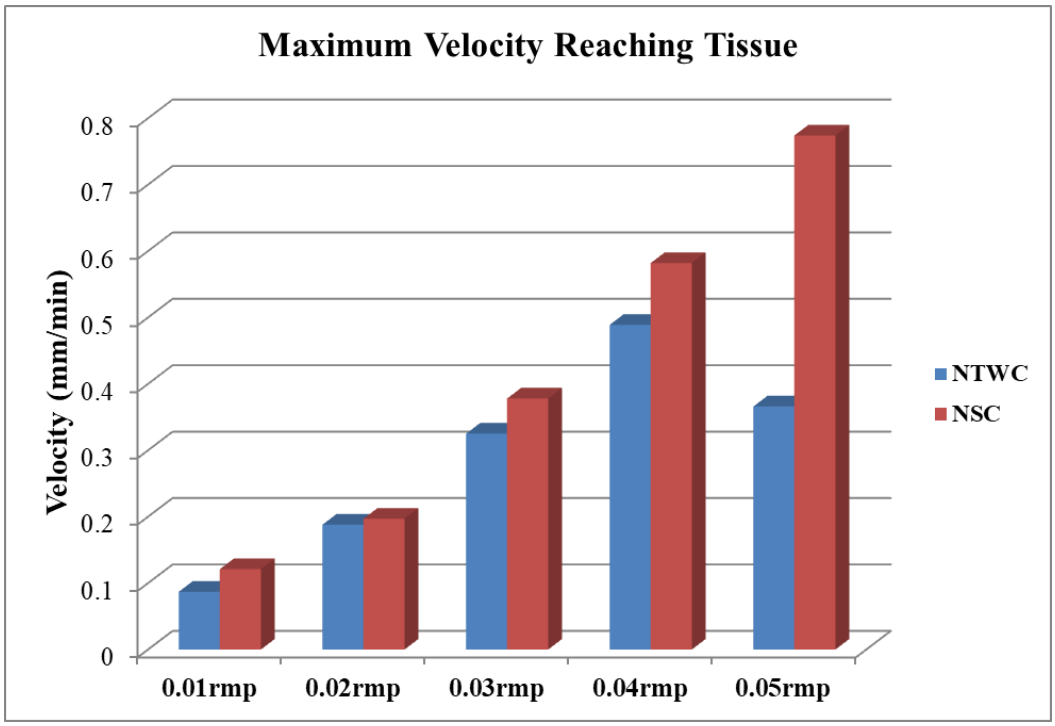


Figure 5- 10: Maximum velocity comparison between the different configurations.

The simulations for the other inlet velocities (V2, V3, V4, and V5) were conducted and the results are shown in Figure 5-10. It can be seen from the diagram that the velocity of NSC increases against linearly. But for NTWC bioreactor, the velocity proportionally increases against flow rate before 0.04 rmp and it drops afterward.

Using the TKE one-equation model, it was possible to observe the fluid turbulence behaviour within the chamber and in the scaffold. For the V1 velocity it's observable in the Figure 5-11. The turbulence behaviours of these two bioreactor configurations are compared here.

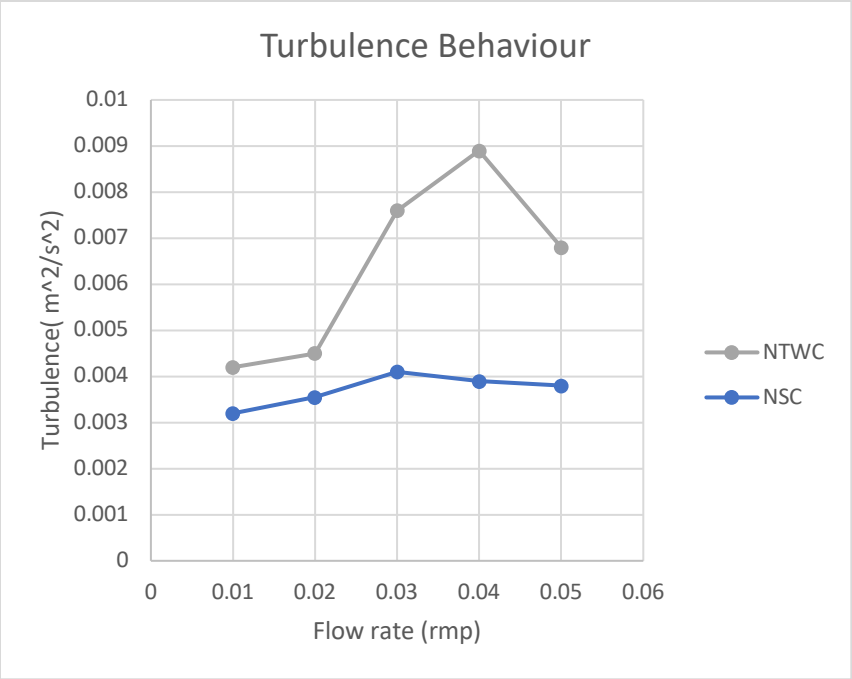


Figure 5- 11: Turbulence results for different bioreactor configurations with various velocities

It can be seen from the figure, the turbulence value of NSC bioreactor is relatively smaller than that of NTWC. In terms of NSC, the turbulence behaviour is relatively stable, and the effects of velocities are very small.

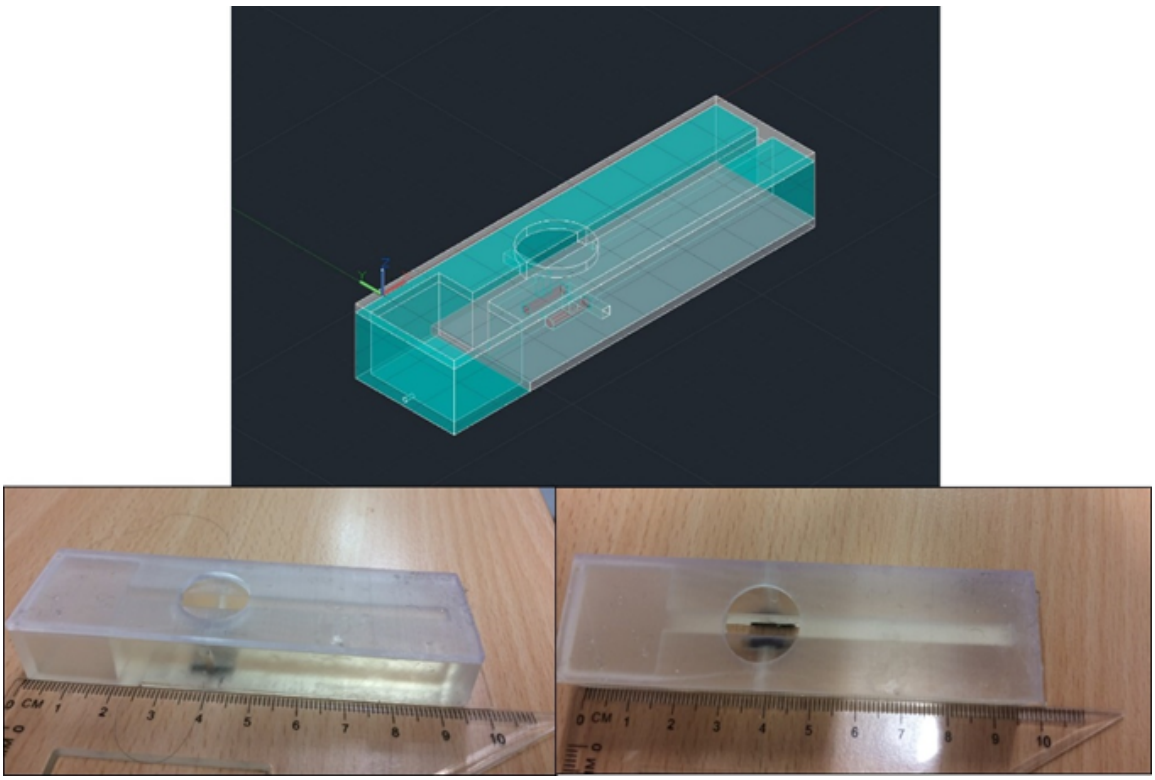


Figure 5- 12: Illustration of the micro-bioreactor with perfusion system and electrical stimulation

From the results, it's possible to conclude that the narrow space channel configuration is the one that allows having higher velocities within the chamber and in the scaffold area, due to the vortexes created by the fluid being forced towards narrow space of the chamber. In this case the vortexes located in inner centre of the chamber and with a clockwise rotation, giving the fluid more velocity direct towards to the scaffold and limits the turbulence effects raised by two electrodes. In this

situation, the effect of flow rate at the inlet end in this condition is relatively lower. Therefore, the micro-bioreactor with narrow space channel (NSC) is selected as the final design for culture 3D engineered heart tissue.

5.3.3. Effects of Dynamic Perfusion System for REHTs

The application of perfusion system has enormous advantages over static culture. It provides a more even distribution of nutrient for tissue and the media flow can be manually controlled.

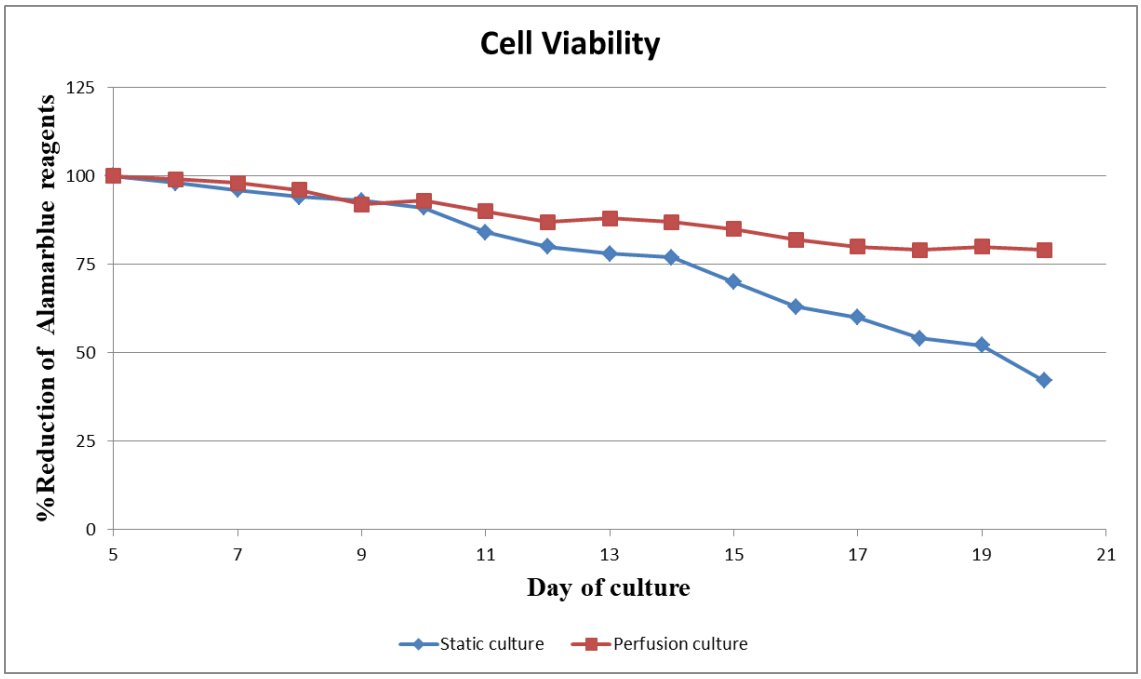


Figure 5- 13：Cardiomyocytes viability in rEHTs of static and dynamic culture (indicated by metabolism of alamarBlue).

By comparing the static culture and dynamic perfusion culture, the cells metabolic study is conducted with alamarBlue over period of culture. The cell viability test is

initialled from day 5. As shown in Figure 5-13, the cell viabilities show a dramatic decline in the first two weeks for both static and dynamic culture. After that, the cell numbers of static culture EHT started to drop sharply to 45% at day 20, while that value of tissue cultured in bioreactor still keep a stable level around 80%.

Hence, we can know that dynamic perfusion culture system provides the EHTs with a suitable environment for long-term culture. This is especially important for cardiomyocytes as such cells require long time culture for higher level of maturation. At the same time, the contraction activities of rEHTs were observed that cells cultured in 24-well culture dish can be held for about 15 days. The beating activities of the EHTs over that time start to weaken and cells stop contract at about 25 days. Apart from this, EHTs cultured in bioreactor can be further applied with mechanical and electrical stimulations.

5.4. Summary

In this chapter, the perfusion microbioreactor for 3D engineered heart tissue culture is discussed. To provide an even media distribution culture environment, the perfusion system is applied. The design of the micro-bioreactor has been simulated with commercial software and its geometry is determined to have the optimal dynamic fluidic situation within the chamber. The simulation aims to avoid introducing too much turbulent flow and make it easier to control the fluid flow situation within the chamber. After considering three different chamber configurations, the one with narrow shape channel (NSC) is chosen as the final design. And the flow rate from the inlet is limited by 0.05rmp to lower the shear

stress; otherwise it may lead to cells damage. In the experimental work, the inlet flow rate can range from 0.01rmp to 0.05rmp.

By comparing static and perfused cell culture, it can be found that perfusion system provides EHTs with even distribution of medium flow and this improves culture efficiency and cell viability. Engineered heart tissue cultured within micro-bioreactor maintains their functions and structures for longer period. This is especially important for EHTs, as it requires longer time for cardiomyocytes to be mature.

Chapter 6 Microbioreactors with Optimal Electrical Stimulations

6.1. Introduction

It is well known that application of electrical field has great impacts on generation and development of cardiomyocytes in engineered cardiac tissue. Thus, to evaluate the performance of our tissue model under electrical stimulations, an electrical field induced and controlled by Raspberry Pi via using two carbon electrodes was integrated into the microbioreactor. The electrical signals were stimulated with commercial software to locate the even distribution of electrical field so that tissue can be place at this area

To determine the safe and functional range of electrical field, system was simulated and designed. After giving an optimal condition for engineered heart tissue, the influence of electrical signals under various conditions can be further studied.

We used engineered cardiac tissue generated with rat cells to determine the optimal conditions of electrical stimulations that could be potentially applied into human tissue model. The performance of rat engineered cardiac tissue was characterized from excitation threshold, beat rate, amplitude of contraction, and contraction kinetic.

6.1.1. Cardiac Conducting System

The heart has an electrical system controlling the pace of human blood pumping by regulating the heart rate and rhythm.[191] For healthy adult, a steady heart rate ranges

from 60 to 100.[192] This electrical system will increase this value during physical activities and lower it while at rest. The heart is a muscular organ and the heart wall is made up of cardiac cells. This electrical process is realized by electrical signals passing through cellular membrane.[193] There is a conducting cell called cardiac pacemaker carries the electrical signals to induct other cardiomyocytes forming an electrical pathway.[194] This is able to trigger the heart chamber to contract and guarantee adjacent cells being activated at the same pace. The rapid transmission of the electrical signals keeps the cells within the heart contract in one coordinated motion, which forms the heartbeat.[195]

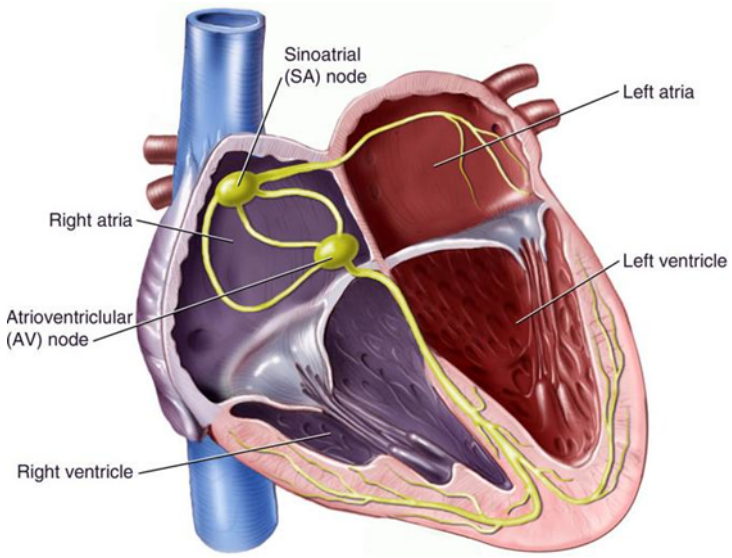


Figure 6- 1: Heart chambers and natural cardiac pacemakers

To better investigate and understand the mechanical principle of heartbeat, it is necessary to study the cardiac muscle electrophysiology. The cardiac action potential is the voltage change across the cell membranes of cardiomyocytes.[196] Compared with action potentials of other electrically excitable cells, the cardiac

action potential is induced by the special cells described above (the cardiac pacemakers) rather than by nervous activities. Sinoatrial node creates 60-100 action potentials, which transfer across cells via gap junctions. This leads to all cells contract together and they are all electrically connected.[197] Thus, we can see the heartbeat rate and strength are determined by the action potential.

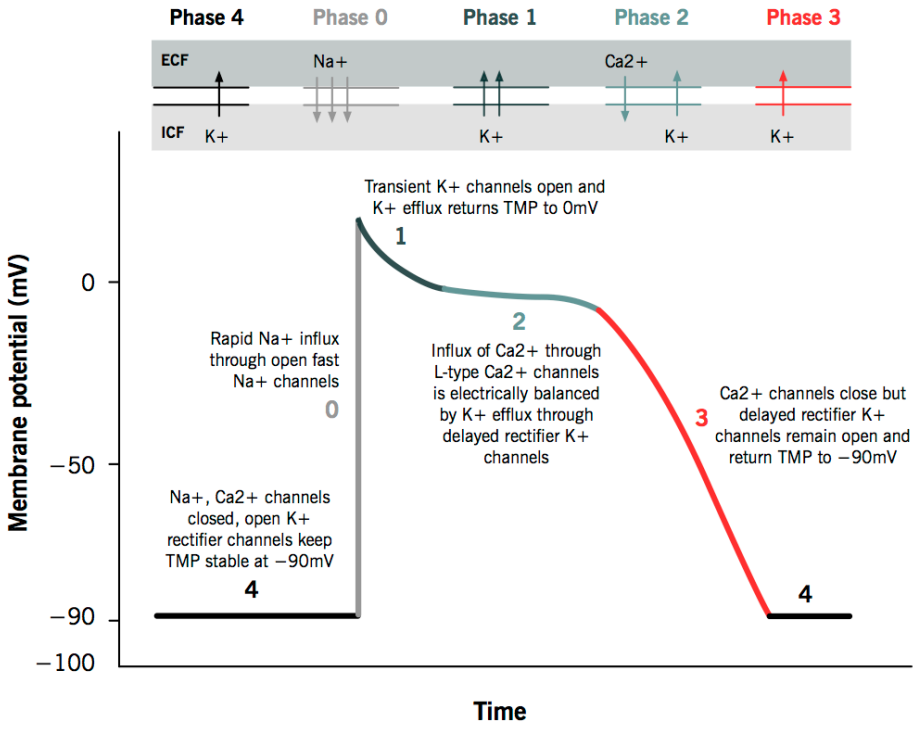


Figure 6- 2: Action potential in cardiac muscle cells. Phases 0 to 4 represent different stages of membrane potentials of cardiomyocytes.[198]

For cardiac action potential, there are five different phases as shown in Figure 6-1. In the phase 0, the action potential starts with the positive change of voltage, known as depolarization. This leads to sodium channels open thereby allowing influx of sodium ions into cells. After a short delay, the Na^+ channel is inactivated rapidly and

the movement of sodium ions is limited in phase 1. At the same time, the potassium channels are open for efflux of potassium ions. The next phase is also known as plateau and the membrane potential keeps at a constant level. The charge movement is near balance status in this period. In the Phase 3, rapid repolarization occurs due to movement of potassium ions from cells. This ensures a positive current flow outward from the cell, which results in a lower membrane potentials. Then, the action potential enter to phase 4 while cell at rest, known as diastole. In this situation, the membrane voltage is normally at a low level around -90mV[197]

6.1.2. Application of Electrical Stimulation into Cell Culture

There have been great progresses in application of electrical stimulation in cell culture and tissue engineering. The effects of electrical signals on migration, orientation, proliferation and differentiation of cells have been investigated.[116,199,200] It has been proved that stimulus of electricity is significant to the physiology and formation of all the tissues. The action potential is the most well-known electrical field in the body.[201] As a membrane potential, it is used to deliver signals and form the communication bridges between cells. This bioelectricity in the body can also adjust the cellular functions and growth.

The electrical signals delivering among cells control the development and regeneration of cells and tissues. Therefore, it is meaningful to design and apply electrical stimulation onto *in vitro* engineered tissue so that the cellular growth, migration and activities can be controlled via adjusting these electrical signals. Previous, a lot of works have been done to use the electrical stimulation in tissue

engineering, like enhancing the contraction force of muscle cells, control the proliferation and differentiation of stem cells and change the alignment of neuron networks.

6.1.3. Electrical Stimulation into Engineered Heart Tissue

As it is said before, in recent years, the development of engineered heart tissue is an emerging and rapidly growing research area and has drawn great attention from worldwide researchers. Although the application of cardiac implantation is still in the experimental test stage and has not yet entered clinical area, many progresses in this research have been made in the past years. The other main purpose of cardiac tissue engineering is to develop functional engineered heart tissue *in vitro* for physiological study of cardiac tissue, heart disease remodelling and drug test. Thus, the successful regeneration of cardiac tissue should keep as much as similar properties of native heart tissue. Apart from mimicking the functional 3D structure of seeding cells onto scaffold, contractile force and electrophysiology of the bioengineered cardiac tissue should be carefully investigated.

The heart is the organ responsible for pumping the blood and supplying oxygen to the whole body. Excitation-contraction coupling is the basic property of the cardiac tissue. The coordinated contraction of the cardiac muscle and the heart-beating rate is controlled and adjusted by the pacemaker cells. They generate the electrical impulses that transfer between adjacent cells via gap junctions. The heart is therefore regarded as the most actively bioelectrical organ in the body. Electrical signals applied onto tissue can influence the cardiac myocytes growth and

development. The application of electrical stimulation can adjust the contractile force of heart tissue from the beating rate, duration and magnitude. To fully restore the construct and function of cardiac tissue *in vitro*, it is necessary to mimic the electrical activities in the native heart and apply them onto the tissues.

There are several researchers have focused on the bioelectrical system study in the heart, like arrhythmia, defibrillation, pacing and cardiac development. Various designs of electrical stimulation system have been made to apply electricity onto cardiomyocytes cultured in 2D and 3D scaffolds. Proper electrical system makes the cells distribution more homogeneous and therefore results in better contractile force generated by the engineered heart tissue. It was 40 years ago while the electrical stimulation was firstly applied in improving the maturation of skeletal muscle cells cultured *in vitro.*[202] In the following several decades, the application of electrical stimulation onto tissue culture has made great progress. The effects of electrical stimulation onto cardiomyocytes cultured in engineered heart tissue have been investigated. It is important for maturation and alignment of cardiomyocytes in the tissue.[203,204] Over 20 years ago, continuous electrical stimulation was firstly applied onto adult heart muscle cells and a stable electromechanical function of adult cardiomyocytes is kept in primary culture.[205] In 2006, Bian applies rapid pacing onto monolayers of ventricular myocytes isolated from neonatal rat.[206] They used this system to remodel the arrhythmia and electrical signals were used to regulate the rate and duration of cardiac cells excitation. Afterwards, different trials have been made to control the growth and functions of cardiomyocytes and engineered heart tissue cultured *in vitro*. [114, 124, 207]

The design of applying electrical stimulation on cells within a culture system aims to restore the electrical signals of the native tissue physiologically. It has been proved that the electrical fields within the embryonic heart are mainly pulsating current.[208] The current guides cardiac myosin growth during the development of heart tissue. On the other hand pulsatile electrical currents present for adult cardiomyocytes to improve the cellular maturation.[209]

One of the most important aims of developing engineered heart tissue is mimicking functions of native heart and using it to testthe efficiency and toxicity of the cardiac drugs. Thus the application of miniaturized perfusion platform is meaningful, as cells number required will be low with small size construct. That is why we developed a micro-scale bioreactor to culture the mini engineered cardiac tissue *in vitro.* In such system, the electrical stimulation is applied and optimized. The mechanical response can be recorded and analysed with adding various drugs and different concentrations in the same conditions. This parallel platform allows several culture and analysis can be conducted at the same time.

6.2. Materials and Methods

6.2.1. Simulation of Embedded Electrical Stimulation

As it stated previously, the bioengineered cardiac tissues in 3D construct were transferred into the micro-bioreactor following pre-culture within 24 well culture dishes. Two rod-shaped electrodes with 10mm in length were fitted into the chamber and placed 6mm apart. Raspberry Pi, a card-sized circuit board, is utilized to control

the electrical signals adjustment via those two carbon electrodes. Platinum cables were used to connect the two electrodes with the GPIO pins on the Raspberry Pi. To make it simple and effective, we used monophasic pulses to avoid the undesirable effect from biphasic pulses inhibiting action potential. It has been proven that the secondary pulse is hyperpolarizing, which may disturb the initiation of the action potential.

In previous studies, some work has been done on optimizing electrode material for electrical stimulation.[210,211,143] Compared with other material, carbon has a number of advantages including higher capacitance and resistance to chemical corrosion. The most significant point is that carbon was found to have the best charge transfer characteristics. Therefore, we decided to use carbon electrodes set up the electrical system in the bioreactor here.

To model and optimize the electrical field within the micro-bioreactor, it is assumed that the condition is electroquasistatic. Commercial software was used to simulate the electrical field with its AC/DC electric module. In the electroquasistatic situation, it is considered to be homogeneous and isotropic. The electrical field could be calculated according to Maxwell's equations. The isotropic media was measured with conductivity of 1.5 S/m.

Conservation of charge $\nabla J=0$

Gauss's law: $\nabla E=\rho/\varepsilon$

Ohm's law for conductors: $J=\sigma E$

Electrical field: $E=-\nabla \emptyset$

Where E is the electrical field (V/m), φ is the scalar potential, J is the current density (A/m), σ is the conductivity (S/m), ρ is the charge density (C/m^3), and ε is the permittivity of the media (F/m).

6.2.2. Raspberry Pi Control and Electrical Circuit Set Up

The Raspberry Pi is a series of small single-board computers developed by the Raspberry Pi Foundation.[212] It is a low cost, credit-card sized computer that plugs into a computer monitor, and uses a standard keyboard and mouse. It is a little device that enables people to explore computing, and to program in languages like Scratch and Python. It's capable of doing everything like a desktop computer to do.

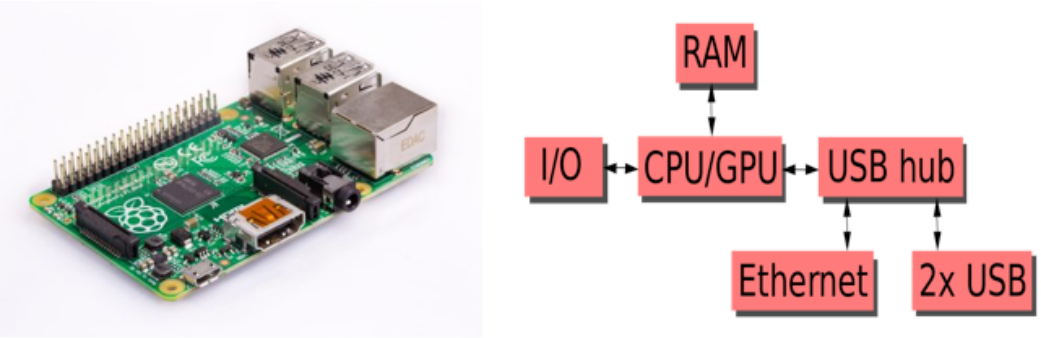


Figure 6- 3: (a) The Raspberry Pi Model B; (b) Block diagram of Raspberry Pi hardware operation process.[213]

Here we used Raspberry Pi, Model B to control the electrical signals applied onto the tissue within the perfusion bioreactor. A 5V power supply is used to power up

the electrical board, and external keyboard, mouse and a monitor are connected via the USB ports and HDMI cable.



Figure 6- 4: The components of Raspberry Pi used for setting up

To set up the Raspberry Pi, a micro-SD card with the downloaded operating system was inserted into the card slot on the underside of the Raspberry Pi. After all this hardware set-up, the power supply is applied to enable Raspberry Pi to work. The Raspbian operating system was used and the Raspberry Pi is configured. Once all these are done, the Raspberry Pi is ready to use.

A powerful feature of the Raspberry Pi is the row of GPIO (general-purpose input/output) pins along the top edge of the board. Any of the GPIO pins can be designated (in software) as an input or output pin and used for a wide range of purposes as shown in figure 6-5.

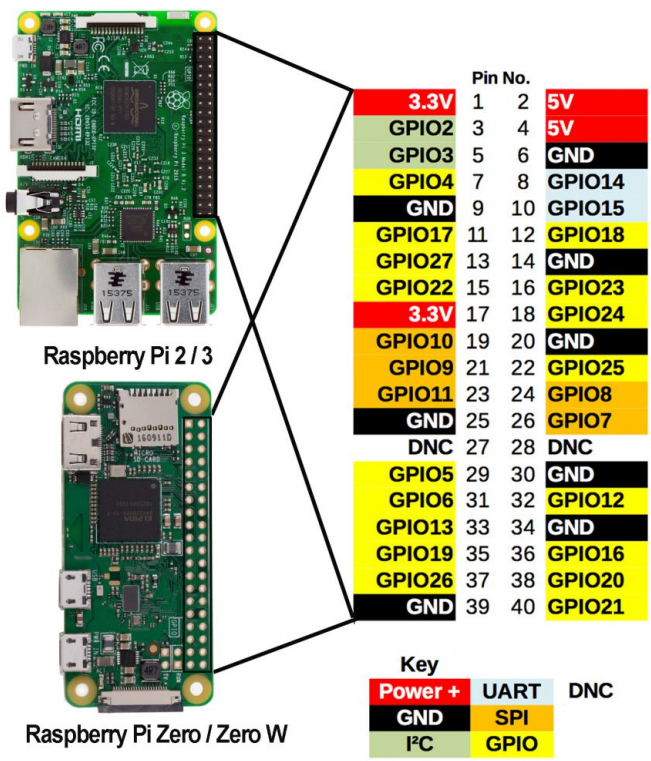


Figure 6- 5: The GPIO map of Raspberry Pi. There are 40 pins in total of Raspberry Pi Model 2/3 [214]

To apply electrical stimulation, two electrodes were connected with the Raspberry Pi via platinum cables. The power supply of the Raspberry Pi is 5V and thus the output voltage cannot exceed that value. And the output that Raspberry Pi supplies is digital value. The desirable voltage is analogue. So before supplying electrical signals for engineered heart tissue with Raspberry Pi, the first step is changing the voltage output format from digital to analog. There are two different methods to have analogy outputs from Raspberry Pi. The first method is use of the Pulse Width Modulation feature (PWM). The other method is using a real Digital to Analog Converter chip, or DAC.

For the first method, with the application of Pulse Width Modulation, a variable but steady voltage level can be created. By contrast, a more precise voltage levels or dynamic analog wave can be formed by using a Digital to Analog Converter chip.



Figure 6- 6: The schematic diagram of converting digital voltages to analog values with application of PWM

A principle frequency can be used to generate the pulse width modulation (PWM) by adjusting the on-off duration. The on-off duration ranges from 0% to 100%. Once keep it at on stage, a positive pulse is obtained and the varying voltage level can be realized by store the power within the capacitor. To further reduce the noise, a low-pass filter was applied to remove the principle frequency at output end. Then, a stable and variable voltage can be achieved across the capacitor as shown in figure 6-7.

The low-pass filter is made up of a resistor (R1 = 1k) and a capacitor (C1=4.7uF). It can reduce the principle frequency to some extent. However, in such condition, just a rather static output is generated.

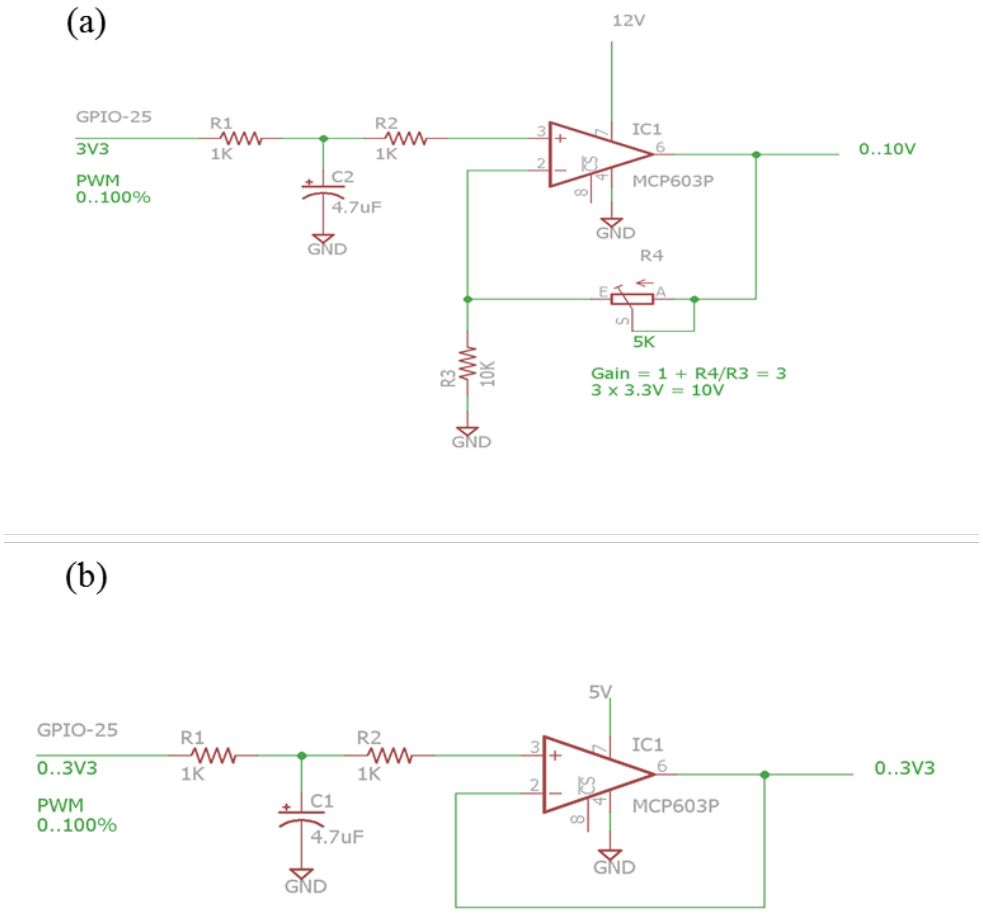


Figure 6- 7: The schematic diagram of OP AMP and further voltage gain

To further improve the accuracy, a following circuit is used with low input impedance. In that case, the capacitor is loaded and may not reach the full voltage at the 100% duty cycle setting. This problem can be resolved by using an Op Amp. The circuit then is shown in figure 6-7(a).

For the second method, a Digital-Analog-Convertor (DAC) chip is used to generate dynamic waveforms and obtain more accurate voltage levels. In my project, the

DAC selected is an MPC 4921. It has 12 bits resolution and an SPI interface as shown in figure 6-8.

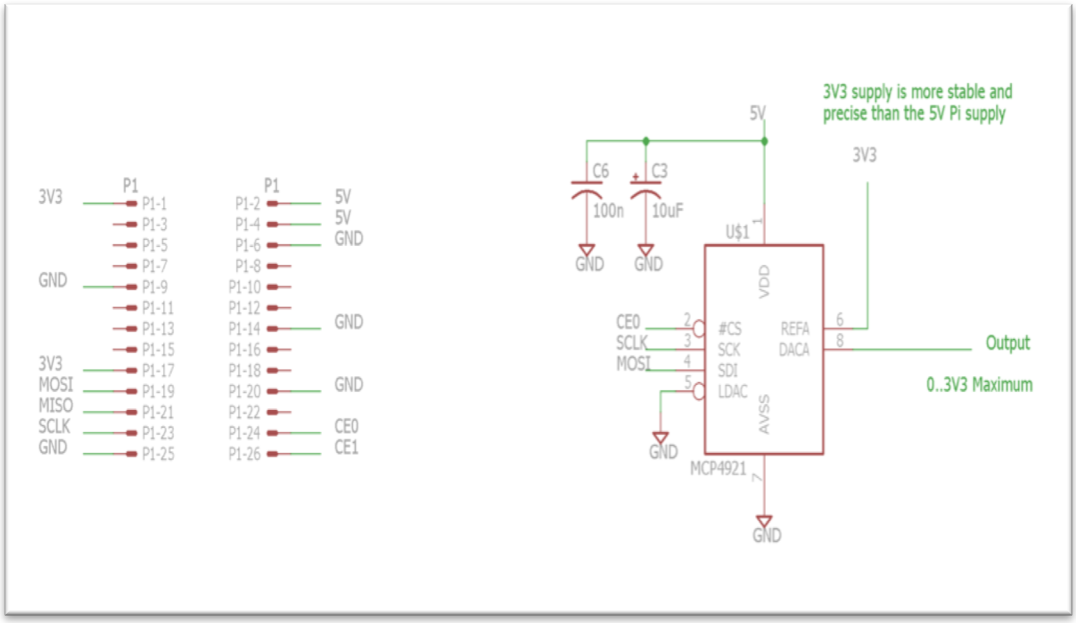


Figure 6- 8: The schematic diagram of DAC connections

DAC uses a reference voltage to convert the voltages from digital to analog. The reference voltage is set at 3.3V, which is the maximum output voltage of Raspberry Pi. This also means the highest output from the DAC we can get is 3.3V. In figure 6-8 we can see the connections between MCP 4921 and Raspberry Pi GPIO. To communicate the device through the SPI bus, the SCLK is connected with the clock; MOSI is used to deliver the information; and CE works as a device selector.

With the help of MCP4921, the analogy voltage can be represented by 10 bit steps digital numbers. That means the output voltage from Raspberry Pi (3.3V) can be converted into 1024 different values. The step of the voltage is 3300mV / 1024 =

3.22mV. A dynamic voltage ranging from 0 to 3.3V with a 3.22mV resolution can be achieved with programming by Python.

6.2.3. Continuous Electrical Stimulation and Contractile Force Analysis

As described before, the tissues are attached onto PDMS platform with two 12mm-length silicon posts with 1mm in diameter. After pre-culture within the 24-well culture dish, the construct is transferred into the micro-bioreactor we designed as shown in Figure 6-9.

The two electrodes are 12mm in length with 2mm in diameter and they are placed 4mm apart from each other to yield a homogenous electrical field. The fibrin-based EHTs locate at the centre position between these electrodes as discussed before for optimized electrical environment for the tissues.

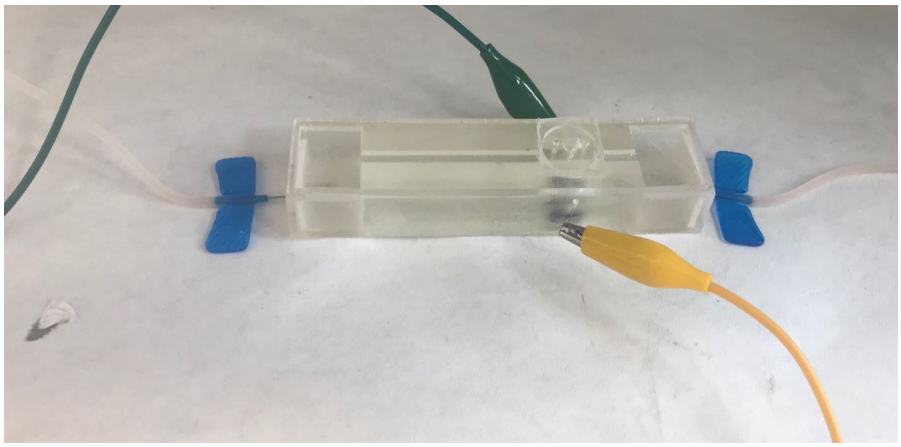


Figure 6- 9: Experimental set up: Sample attachés onto the platform and inserted into the micro-bioreactor. Electrical pulses are generated with Raspberry Pi and transmitted to the electrodes within chamber.

The continuous electrical stimulation was initialled from day 5 after EHTs were generated. Raspberry Pi works as the electrical source and the maximum output is 3.3V with 0.33mV steps used for control the electrical amplitudes. We used monophasic pulses as its simplilty and easy control to avoid any disturbance. As the maximum electrical field amplitude that will not have negative effects on those tissues is 6V/cm, the range of electrical amplitude is set as form 1V/cm to 5V/cm with 500mV increment. The frequency we used is 1, 2, 3, 4 and 5Hz. To assess the contractile performance of engineered cardiac tissue under different electrical fields, some factors are measured and evaluated. Excitation threshold (ET) is the minimum voltage required to make synchronous contractions in response to electrical signals over the whole tissue. Monophasic electrical pulses with 100ms duration are applied onto the samples and they start from 0V/cm to 5V/cm with 100mV increment. The maximum capture rate (MCR) is evaluated as well. By applying 1.5 ET of the voltage and keep on increasing the frequency until contraction becomes unstable. The threshold value is called MCR.

These values are recorded every three days from day 8. To determine the force generation of EHTs, the bright field microscope is used to record the contractile motion. The obtained video is analysed with motion track software as shown in figure 6-5. With the mechanical modelling stated above, the contractile force generated from each engineered cardiac tissue can be evaluated. All the measurements were processed and repeated three times independently and data were expressed as mean with standard deviation.

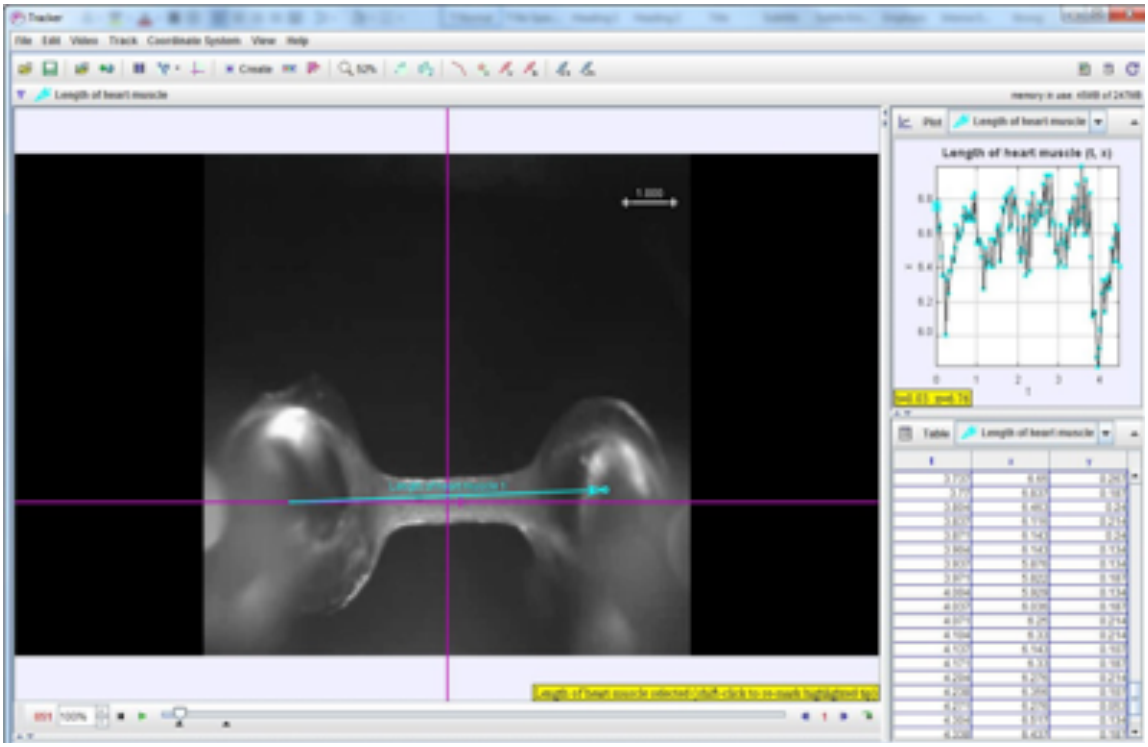


Figure 6- 10: Optical video analysis system. Length measurement system according to the recorded video from microscope

6.3. Results and Discussion

6.3.1. Electrical Stimulation System Simulation and Optimization

It has been proved that carbon has a number of advantages including higher capacitance and resistance to chemical corrosion to be used as the electrodes. Besides electrode material, there are many factors have effects on the results of electrical stimulation, such as electrode configurations, input voltages, induced duration and etc. To determine the optimized conditions, the factors are characterized before the set-up of electrical stimulation system.

The first thing to be confirmed is the electrode configuration. Method used here is the current measurements with electrochemical impedance spectroscopy (EIS). With an electrochemical interface and a frequency response analyser, the EIS values can be acquired.

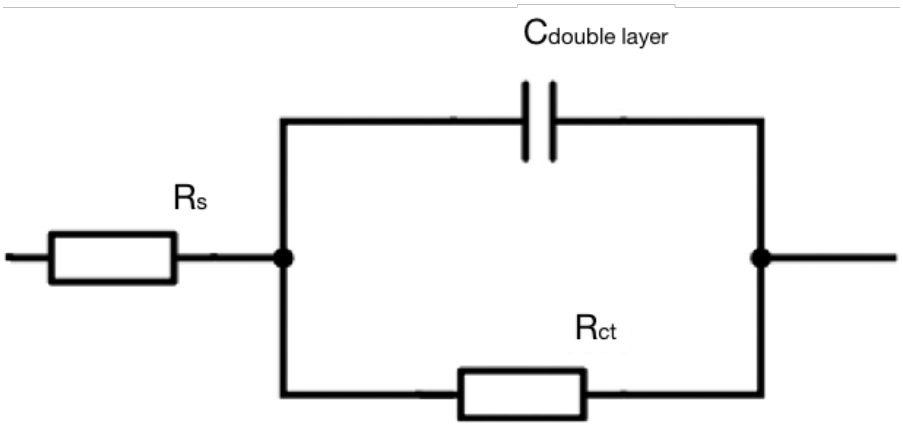


Figure 6- 11: The equivalent circuit of a simple electrochemical "Randles" cell, where Rs represents the solution's resistance, $C_{double\text{-}layer}$ is the double layer capacitance, and Rp is the polarization resistance.

Here the frequencies applied range from 0.01 to 10^6 Hz and the amplitude range of input voltage is from 0.03V to 5V. After the data were collected with ZView and fit to a Randles's cell equivalent circuit as shown in figure 6-11.

To determine electrical stimulation effects, the value of Rs is used as the reference factor. The resistor R_s is calculated with a parallel-plate linear model of Rs.

$$R = \frac{d}{\sigma A} \tag{6.1}$$

Where R is resistance, d is the distance between the electrodes, σ is the conductivity of the solution and A is the surface area exposed to the electrolyte.

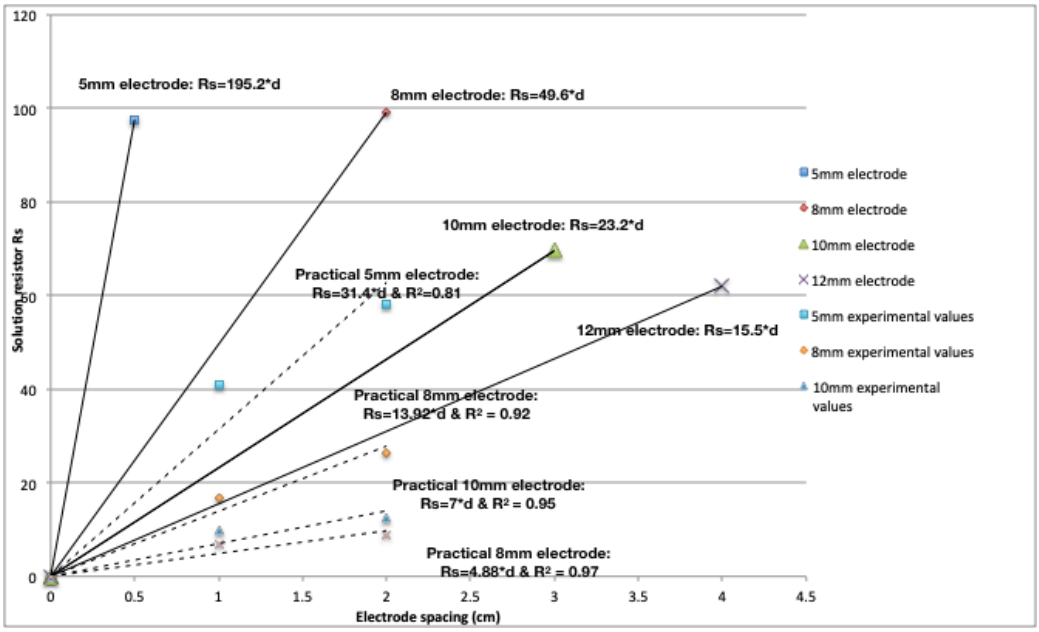


Figure 6- 12: Practical and theoretical values for solution resistance of various electrode configurations.

4 different samples were prepared with 5mm, 8mm, 10mm and 12mm in length. To evaluate the effects of the electrode length, we compare the feedback value of R^2. From figure 6-12, it can be seen that the length of electrode has great effects on the Rs value. By accessing the value of R^2, we can conclude that increasing electrode length results in more closely fitting in the theoretical model.

This also makes the experimental results of the slope (1/σA) more close to that of theoretical data. The experimental, theoretical and ratio between them are shown in Table 6-1.

Table 6- 1: The experimental, theoretical and ratio between them of Rs

	5mm electrode	8mm electrode	10mm electrode	12mm electrode
Rs (experimental)	195.2	49.6	23.2	15.5
Rs (theoretical)	31.4	13.92	7	4.88
Ratio	6.23	3.56	3.31	3.18
R^2	0.81	0.92	0.95	0.97

The values for the ratios of the slopes of the lines corresponding to 8mm, 10mm and 12mm length electrodes to that of their theoretical lines are close enough (3.56， 3.31 and 3.18, respectively). The difference can be within the reasonable range of experimental errors. Thus, it indicates that a factor of 3.2 can be used to adjust the experimental data with the actual values if we calculate it with parallel-plate model. On the second, we found that once in the ranges of configuration, those electrodes may result in relatively stable effects with each other. The reference of the range is determined by the ratio of length to spacing. If the ratio is larger enough (more than 2), it can be regarded to follow same model. Considering the engineered cardiac

tissue we generated here is 10mm in length and 1mm in diameter, we finally choose the size of the electrodes to be 12mm in length with 4mm spacing.

After confirming design of the electrode configuration, it is also important to determine electrode behaviours under different input voltage conditions with the geometry of electrode stated before. By applying 30mV, 0.5V, 1V, 3V and 5V input voltage; we can find the changing of resistor R_s and capacitor $C_{double\text{-}layer}$ (shown in figure 6-13).

We can find that there is a slight decrease for the Rs while increase the amplitude of input voltage. By contrast, the capacitor is in a verse way, larger input voltage corresponds to higher values of capacitor $C_{double\text{-}layer}$. Yet the changes of these values are in a relatively small range. That means varying input voltages do not have great effects on the electrode behaviours and the electrical stimulation is in a stable situation under such conditions. We examine the effects of input voltage frequency as well. It is also proved the frequency has few impacts on the electrical stimulation. These findings make it possible to apply different electrical stimulation conditions onto engineered heart tissue.

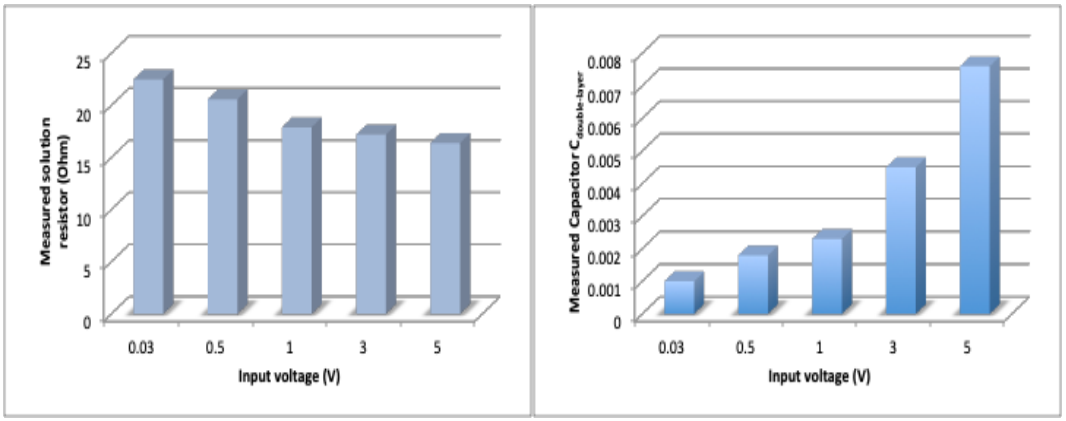


Figure 6- 13: Measured solution resistor and measured capacitor against input voltage.

According to the study above, it can be easily seen that electrode configuration has great effects on the electrical stimulation efficiency. We can conclude that longer electrodes in relative to their spacing are better design in terms of configuration. The ratio between them should be over 2 to offer suitable electrical signals. As the engineered tissue generated is 10mm in length and 1mm in diameter, the geometry of the carbon electrodes we chose is 12mm in length and 2mm in diameter with 4mm spacing. In such case, the tissue can therefore be induced with the electrical field created by the electrical stimulation system.

After determining the electrode configuration, it is necessary to make sure the location of tissues being placed in the micro-bioreactor so that they can suffer from even distribution of electrical field. To model the electrical signals across the tissue, a simulation was run with the commercialized software COMSOL. Two carbon electrodes were placed 4mm apart from each other (red ones). The glass surface was assumed to offer an electrical insulating boundary condition. The simulation results

from COMSOL are displayed in figure 6-14. Voltage amplitude varied from 1 to 5V and the frequencies simulated were 1, 3 and 5Hz. The aim of this simulation was to determine the electrical field distribution and ensure that the tissue was placed at the right place within homogeneous electrical field.

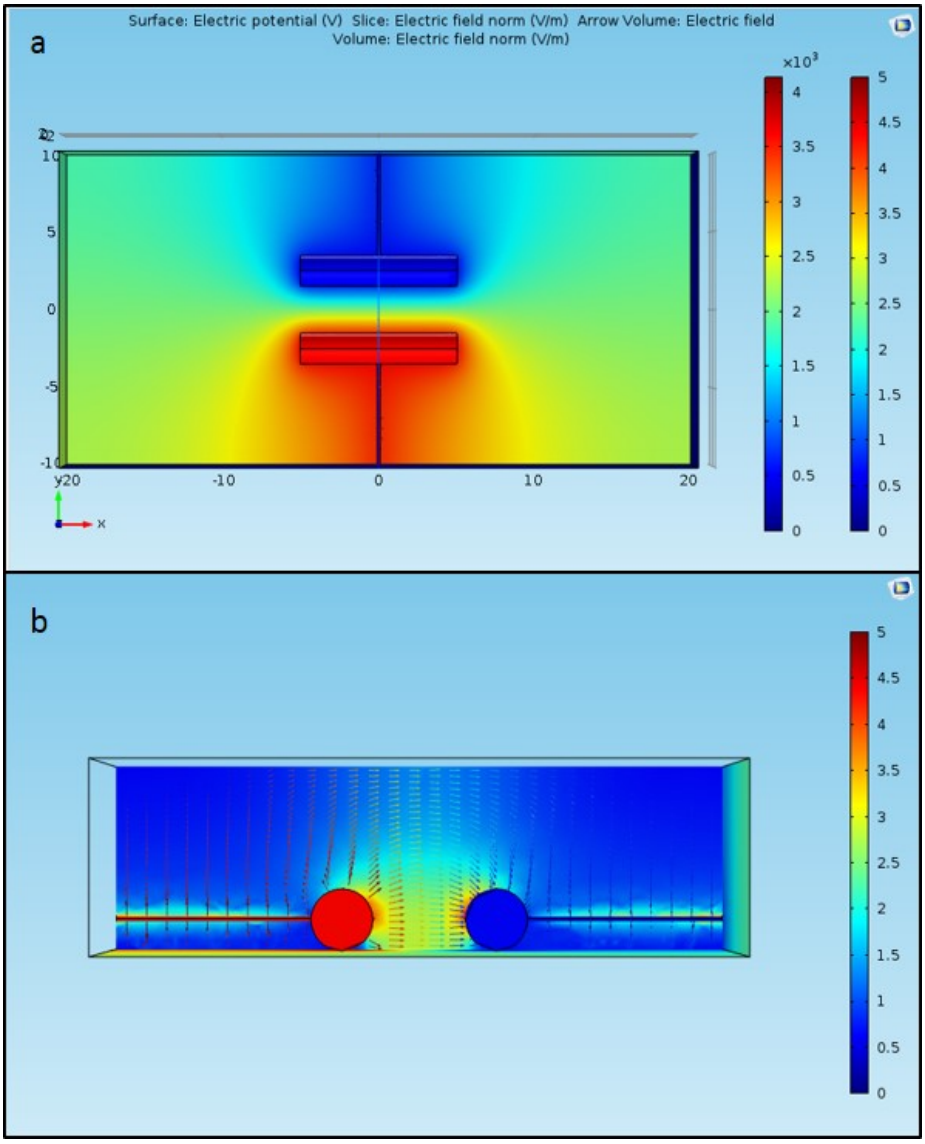


Figure 6- 14: Simulated modelling of electrical activity with a 5V pulse in the bioreactor. (a) Top view of the bioreactor's electrical stimulation. (b) Cross-sectional view of the bioreactor with the electrical field.

It was assumed that cells distribute evenly within the tissue. Hence, to give a uniform electrical stimulation onto all the cardiomyocytes, tissue should be placed at the region with uniform electrical signals. The tissue was placed at the centre of the channel. We needed to determine the vertical position of the tissue to ensure that it was located within the uniform area as shown above. In the centre position, the uniform electrical signals started from 0.2mm to 1.8mm in vertical height above the glass surface. Considering the diameters of the tissue were about 1mm, the gap between the tissue and the glass surface could range from 0.2mm to 0.8mm.

After all these conditions being confirmed, the preparation of electrical stimulation system is done, and they can be set up for further use. Before application of electrical signals onto tissue avoiding any harmful effects, electrical factors of system need to be further considered and studied. It is known that the electrical stimulation efficiency heavily relies on the system initiation. Early introduction of electrical signals influences the formation of protein within the cardiac tissue thereby inhibit the contractive functionality. On the other hand, the effects of electrical stimulation will not be enough for tissue generation if electrical system is applied too late. In terms of 2D cultured cardiomyocytes, the initial time of electrical stimulation should be after 24 hours seeded, and contractile force measurement starts from day 5. By contrast, for the cardiomyocytes casted with the Matrigel into fibrinogen scaffold, the best time to introduce electrical signals is 3 days after tissue formation. In this situation, the contractive activities can be observed and recorded from day 10.

The electrical stimulation designed here aims to mimic the bioelectrical signals within the native heart. The generated engineered heart tissue is cultured within the culture medium *in vitro*. Its conductivity is high enough (15 mS/cm) compared with that value of fluid in human body (3-12mS/cm). The electrical field in the native heart range from 0.01V/cm to 10V/cm. However, it is found that the contraction generated from engineered heart tissue becoming weak while the amplitude is over 8V/cm. For amplitude over 10V/cm, the sample will not beat any more. Thus, in my project, the maximum stimulus used is 5V/cm. The pulse duration here is 100ms and it is enough to excite the samples. As it is stated before, to make it simple and compatible, monophasic analog pulses is used as the source of the electrical stimulation.

6.3.2. Optimization of Electrical Stimulation Based on Neonatal Rats Engineered Heart Tissue

In native heart, electrical pulses induced by pacemaker cells pass through the whole heart. These electrical signals lead to the depolarization of cellular membranes thereby giving rise to synchronous contraction between cardiomyocytes. To mimic such electrical environment within the heart, electrical stimulation is applied onto tissues.

It has been proved that bioelectrical signals have numerous positive effects on cellular differentiation, migration and orientation. Here, we used monophasic electrical pulses to stimulate the rats' engineered cardiac tissue (rEHT). To determine the effects of bioelectrical environment under different conditions,

various signals with different parameters were applied via the integrated electrical system. The electrical-mechanical functional performances of those cardiac tissues are studied from perspective of excitation thresholds (ET), maximum capture rates (MCR) and amplitudes of contraction (AOC). It is known that optimized situation of electrical stimulation should make engineered cardiac tissue perform with low ET, high MCR and high AOC.

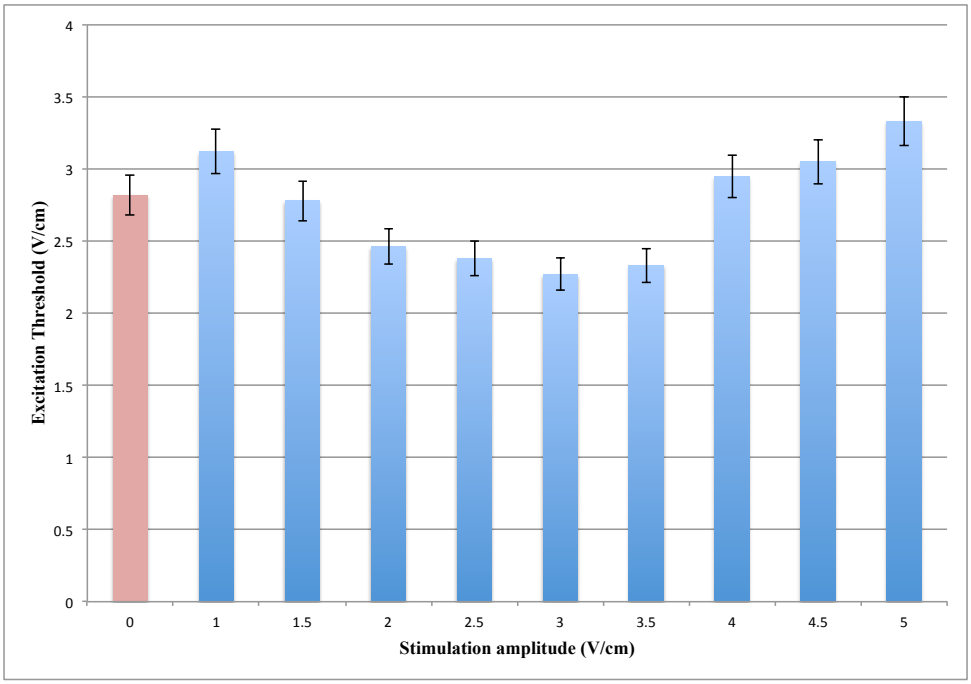


Figure 6- 15：Excitation threshold of the samples applied with different stimulation amplitudes and the data are acquired at day 11 (it means electrical filed required for synchronous beating of engineered cardiac tissue). Data are represented as mean ±SE. The analysis statistic is processed with one-way ANOVA test ($p < 0.05$) N =3 each group.

Excitation threshold indicates the electrical excitability of cardiomyocytes and heart tissue. In figure 6-15, the excitation thresholds of the engineered cardiac tissue

stimulated with different amplitudes of electrical signals is displayed. The pink one is the non-stimulated control group. Based on the results shown there, the excitation thresholds are higher on the two ends and show lower values in the middle within the range between 1V/cm to 5V/cm. According to this, it can be concluded that electrical signals with amplitudes of 2V/cm to 3V/cm have relatively better electrical excitability compared with other magnitudes.

The maximum capture rate and amplitude of contraction indicate cellular contractile behaviours. As shown in figure 6-16, the performance of cellular contraction of engineered cardiac tissue is determined in terms of maximum capture rate and maximum contraction force. The maximum capture rate shows an obvious decline while the stimulation amplitude is over 4V/cm and we already know that the tissue will stop beat while the stimulation amplitude is over 8V/cm. Although the difference between each group is not quite distinct within the range of 1V/cm to 4V/cm, it still can be concluded that around 3V/cm (2.5 to 3.5) electrical stimulation makes the constructs have higher beating rates. Looking into maximum contractile force variation, we can find that the values increase against the rise of amplitudes and this trend become verse while the amplitude is over 4V/cm. After comparing the results of different groups for various electrical signals applied, it can be easily found that the electrical signals have great effects on the functionality of engineered cardiac tissue and the constructs reached their most activated contraction while 2V/cm to 3V/cm electrical stimulations are applied onto the samples. Thus, we decide to use these parameters to provide a bioelectrical environment for the engineered heart tissues.

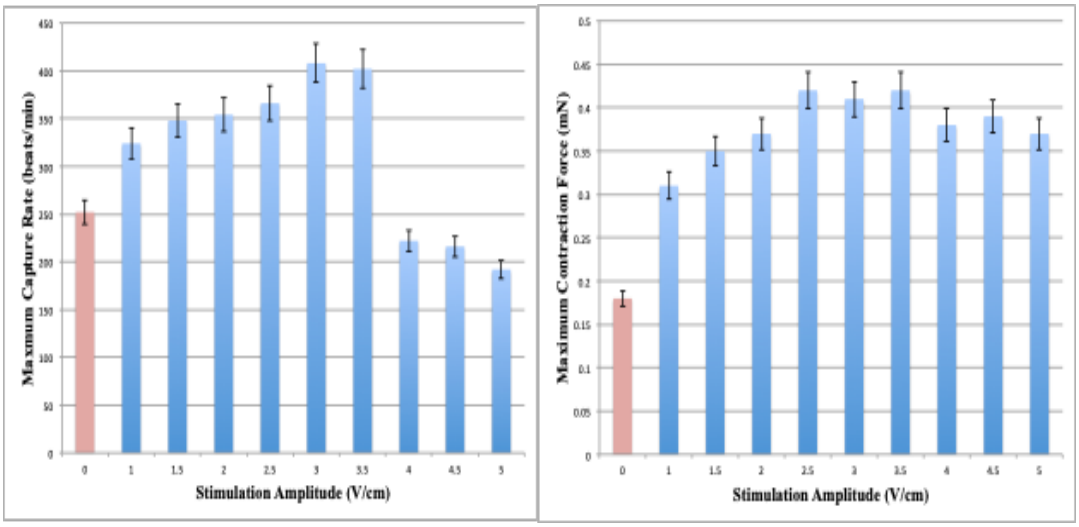


Figure 6- 16: Maximum capture rate and contraction force of the samples applied with different stimulation amplitudes and the data are acquired at day 11. Data are represented as mean ±SE. The analysis statistic is processed with one-way ANOVA test ($p < 0.05$) N =3 each group.

To optimize the effects of frequency, we adjusted the amplitude of electrical signals at 3V/cm to avoid any disturbance due to different magnitudes. The performances of the engineered cardiac tissues are evaluated with these references as well, including excitation thresholds, maximum capture rates and amplitude of contraction. While the electrical pulses were introduced, it is hard for us to justify the effects of frequency below 1Hz due to this frequency is close to spontaneous beating of cells. On the other hand, the beating activities of cardiomyocytes become poorer over time, if too high frequency (over 5Hz) of electrical stimulation is applied. Therefore, we only focus on investigating the results in the range of 1Hz and 5Hz and a non-stimulate group is used as control reference. The frequency does not show great effects on excitation threshold of the samples as shown in figure 6-17.

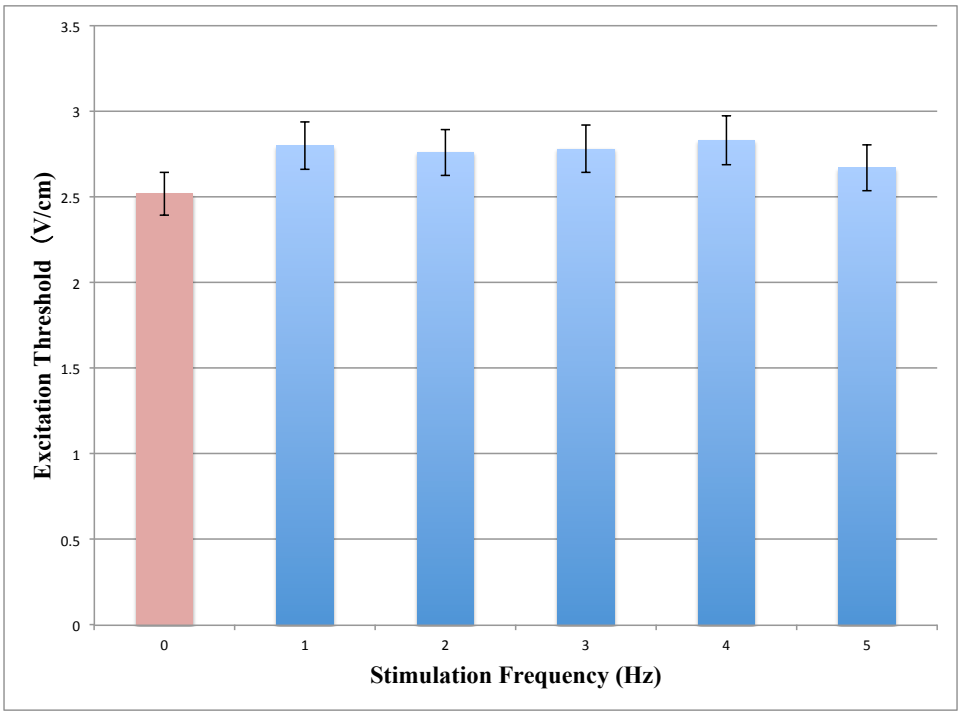


Figure 6- 17: Excitation threshold of the samples applied with different stimulation frequencies and the data are acquired at day 10. Data are represented as mean ± SE. The analysis statistic is processed with one-way ANOVA test ($p < 0.05$) N =3 each group.

By contrast, the variation of electrical frequency has much more effects on the contractile behaviour of the tissue. From the figure 6-18, the maximum capture rates of the samples show a decline trend while the amplitude of contraction has a slight increase. The contractile force increases from 0.44mN to 0.48mN from 1Hz to 4Hz and they are all larger than the sample without stimulation. But compared with the change due to stimulation amplitude variation, the contractile force is not very sensitive to stimulation frequency changing.

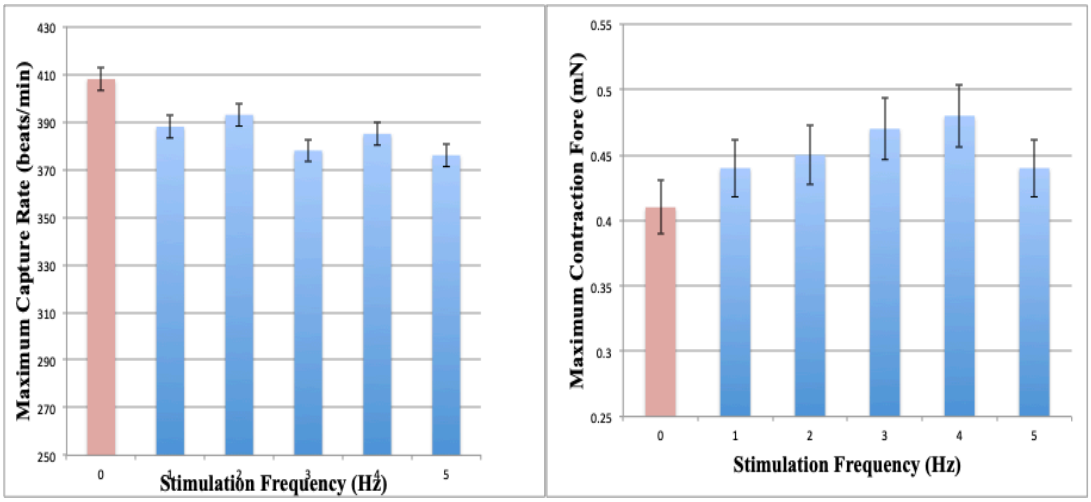


Figure 6- 18: Maximum capture rate and contraction force of the samples applied with different stimulation frequencies and the data are acquired at day 10. Data are represented as mean±SE. The analysis statistic is processed with one-way ANOVA test ($p < 0.05$) N =3 each group.

Observing the data from above figures, we can find that the cellular mechanical responses are more sensitive to the amplitude change of electrical stimulation comparing to that of excitation threshold. The MCR especially shows great sensitive to both frequency and magnitude variation of electrical signals. By contrast, both changes of frequency and amplitude do not have too much effect on excitation threshold. It just depends on the presence of electrical stimulation as we can see the obvious difference between results of all the groups and that of control. Hence, the parameters can be confirmed to provide electrical stimulation for those engineered cardiac tissue. Amplitudes we chose are 2V/cm and 3V/cm with 2Hz in frequency and 100ms duration.

6.4. Summary

In this charter, the system of electrical stimulation is designed and optimized to provide a suitable bioelectrical environment for the bioengineered cardiac tissue. The effects of electrical stimulation are widely known on cellular functions and maturation during their assembly process. Yet, most work is done by qualitative analysis rather than quantitative analysis of cellular activities under electrical signals application. Hence, we decided to develop such electrical stimulation system so that it can be realized to study the cardiomyocytes and engineered heart tissue under different electrical conditions. In this system, considering the properties of different materials, carbon electrode is selected as the best electrical source for introducing electrical signals from Raspberry Pi, a small sized computer. With a digital-analog-converter, the digital voltage is transferred into dynamic waveforms and an especial precise voltage level can be achieved. In this situation, the output voltage from Raspberry Pi can be controlled by programming to achieve different levels with 3.22mV as the step.

The initial time of electrical stimulation is set to day 5 to avoid any side effects on protein formation due to too early electrical signals applied or weak stimulation effects resulting from late application. For configuration of electrode, we finally chose the electrode with 12mm length and 2mm diameter with 4mm spacing. The tissue is located between these two electrodes with 0.2mm distance above the coverslip surface thereby suffering even distribution of electrical field within the chamber. Besides this, the electrical stimulation conditions were optimized as well.

The maximum amplitude of electrical signals cannot be over 5V/cm and monophasic pulses are selected as the electrical source with 100ms pulse duration.

To determine the optimized conditions of electrical fields, excitation threshold, maximum capture rate and amplitude of contraction are used as the evaluation references Parameters of electrical stimulation selected for further use in regulating functions of EHTs is set as monophasic electricity with 2V/cm to 3V/cm, 2Hz and 100ms duration.

After all these conditions being confirmed and set up, the electrical system can be further applied in investigating the effects of electrical stimulation on culture and formation of engineered heart tissue.

Chapter 7 Development of HEHT Models and Applications

7.1. Introduction

The configuration of microbioreactor for generating and culturing engineered heart tissue has been confirmed and optimized. The feasibility of that system has been evaluated by culturing neonatal rat cardiomyocytes. In this chapter, the effects of electrical stimulation system will be investigated and we will find a optimal condition to enhance the cells functions and structure.

Different parameters of electrical stimulations were tested and the responses of rEHTs were recorded and analysed. Optimal conditions of electrical fields were determined as 2-3 V/cm amplitudes, 2Hz frequency and 100ms duration. The presence of suitable electrical stimulations to mimic the electrophysiological microenvironments in native heart improves maturation of cardiomyocytes and control isotropy of rEHTs.

The findings of neonatal rats' cardiomyocytes resulting from field stimulations were applied into culturing human cardiomyocytes *in vitro*. After tests and observation, it can be found that degree of maturation of iPSC-CMs is improved and functions of the hEHTs were enhanced.

With the aim of verify its application in drug screening, several isotropic modulator drugs with known clinical effects were applied onto these long-term cultured tissues. The results closely met the drugs functions in clinical trials. The practicability of this system in generating higher maturation level of EHTs and its relative application in basic drug testing is proved.

7.2. Materials and Methods

7.2.1. Cell Viability Test

There are two different cell viability measurement methods were used throughout the project. AlamarBlue, as a cell viability assay reagent, provides a fast, sensitive and low cost method to quantitatively measure the proliferation and cytotoxicity of multiple cell lines. It contains a blue indicator dye called resazurin that has been proved to be permeable, non-toxic and weakly fluorescent. The amount of resazurin consumed by cell growth can be used as an oxidation-reduction (REDOX) indicator to reflect the colorimetric change resulting from cellular metabolic reduction. As it can be seen from figure 7-1, the product of resorufin is pink with high fluorescence. Through detecting the level of oxidation, alamarBlue is able to give a directly quantitative measurement of cell viability.

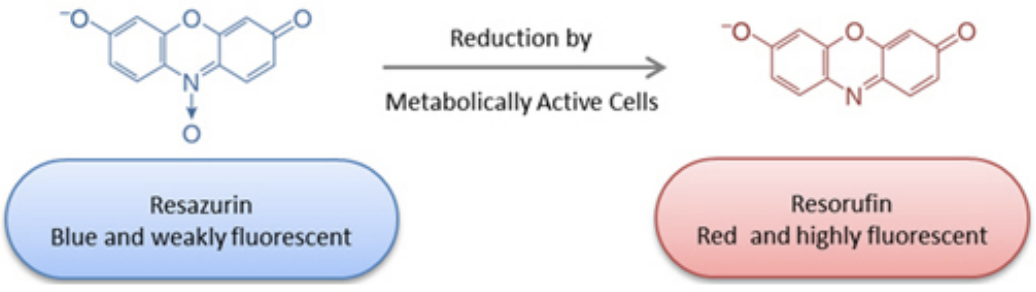


Figure 7- 1: REDOX of Resazurin to become resorun under cells metabolic activities. [215]

One of the distinct advantages of alamarBlue is its simple and easy workflow. According to the protocol and previous studies, 10% alamarBlue reagent (DAL1025,

Invitrogen) was added into the cell culture medium and incubated for 3 hours at 37 °C. A negative control sample of 5 µL alamarBlue reagent in 50 µL cell culture medium and a positive control of 100 % reduced alamarBlue reagent (5 µL sterile water in 50 µL cell culture medium) are prepared. 50 µL solutions was extracted from the samples, the data can be recorded by a micro-plate spectra fluorometer (WALLAC VICTOR2 1420 multi-label counter model, Perkin Elmer, UK) with fluorescence-based or absorbance-based models.

The excitation wavelength is 540nm for fluorescence mode, while the emission wavelength is 590nm. In terms of absorbance, the data are collected at 570nm and 600nm. Figure 7-2 shows the spectra of fluorescence and absorbance. From the Figure, the difference between oxidized and reduced is more distinct with fluorescence mode. Hence, the method mainly used in this project is fluorescence-based to determine the cells viability. The percentage reduction of AlamarBlue can be calculated as:

$$\%AlamarBlue\ consumption: \frac{Fl590\ test\ agent - Fl590\ untreated\ control}{Fl590\ of\ 100\%\ reduced\ control - Fl590\ untreated\ control} \times 10$$

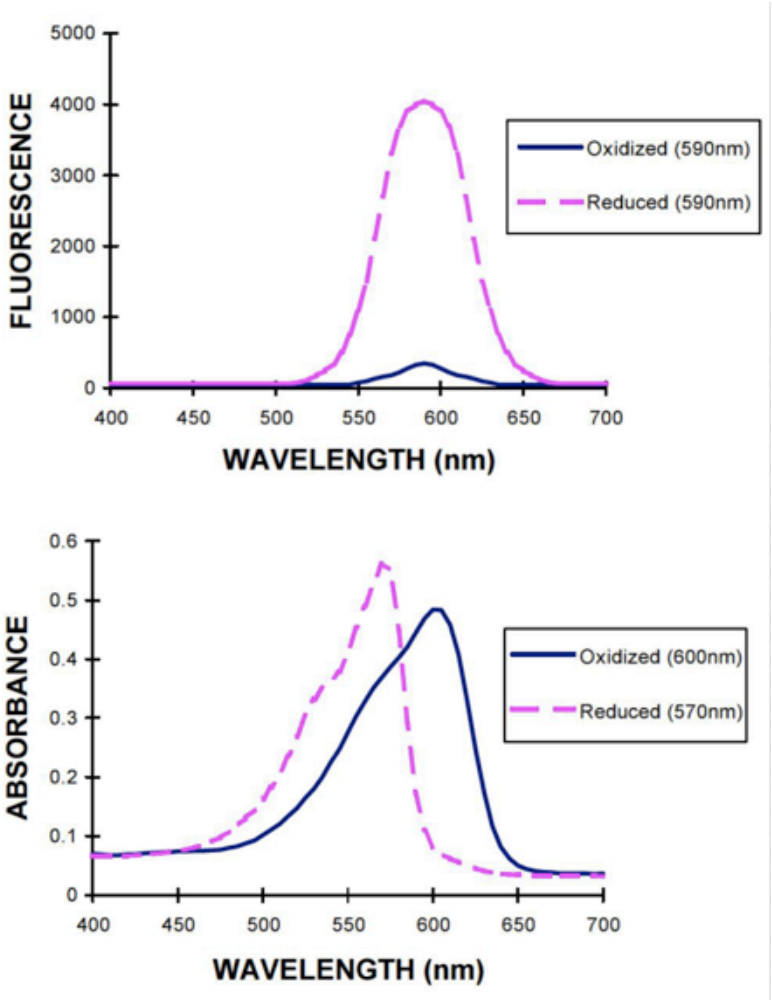


Figure 7- 2: alamarBlue fluorescence and absorption spectra.[216]

In addition to AlamarBlue, a live/dead viability assay (L3224, Invitrogen) is used to examine the live and dead cells labelled with two fluorescence colours. Live and dead cells are recognised by Calcein-AM (intense green fluorescence; excitation= 495 nm and emission= 515 nm) and ethidium homodimer-1 (it only enters dead cells with damaged membranes and shows intense red fluorescence, excitation= 495 nm, emission= 635 nm) respectively. This assay not only enables us to determine cell

viability, but also helps study the morphology within the tissue construct, including cells distribution and location.

According to the practical protocol, 2mM calcein-AM and 4mM ethidium homodimer-1 were fully mixed in PBS. After removing the tissues from the wells and washing them twice with sterile PBS, then 1ml prepared staining solution is added and incubated for 2 hours with foil paper covered for keeping darkness at 37°C. Prior to mounting on slips for observation with microscope, the samples were washed twice with PBS. Observation was conducted with an inverted fluorescent microscope, images were captured, and green dots indicated live cells while red dots corresponded to dead cells. After image processing, the cell viability and distribution can be evaluated.

7.2.2. Light Microscopy and Three-dimensional Microscopy

In our study, to observe the cellular and tissue morphology, the samples of engineered heart tissues are stained with traditional haematoxylin and eosin (H&E) and immunofluorescence staining.

To stain the samples with H&E, we follow the conventional protocol. Taking the samples from the culture dish and washing twice with pre-warmed PBS, the samples are fixed with 4% methanol-free formaldehyde solution in PBS at room temperature for 12 hours (normally overnight). Then, all the samples are embedded into paraffin blocks. By using microtome, the samples are sectioned to 4um thickness and the samples are kept in hot water bath before being placed on the slide. After being

labelled and left in a drying rack for air dry. The samples are ready for staining with H&E.

Prior to staining, the slides bound with samples are performed with de-paraffinsation in xylene solution and re-hydration in ethanol of decreasing concentration. Once these are completed, the samples are kept in haematoxylin solution for 2 minutes and washed with fresh water for twice. Then, they are stained with Eosin for half minutes. Finally, the samples are ready for observation after they are dehydrated with increasing concentration ethanol solution (60%, 70%, 80%, 90% and 100%).

For immunofluorescence staining, the engineered cardiac tissues were used as whole samples for processing. They were fixed with 4% paraformaldehyde (PFA) within 24-well culture dishes. It took half an hour to fix them at room temperature and then permeabilized in PBS with 10% fetal calf serum and 0.05% Triton X-100 at 4 °C for 3 hours. After rehydration, the samples were blocked with 1% bovine serum albumin (BSA) for 2 hours.

Then all the samples were incubated at 4 °C for overnight treated with primary antibody, mouse IgG1 anti- α-sarcomere actinin (1:100, ab9465, Abcam), to identify myosin After a 3-hour washing with PBS, the samples were incubated with goat anti-mouse IgG1-conjugated Alexa Fluor 633 (1:100, A21126, Invitrogen) at room temperature for 12 hours. It is followed by targeting CX34 with rabbit anti-connexin 43 / GJA1 antibody (1:200, ab11370, Abcam) for 24 hours and then treated with goat anti-rabbit IgG-conjugated Alexa Fluor 594 (1:100, A-11037, Invitrogen). Finally all the tissues are applied with DAPI mounting solution on top of them to

identify nuclei and waiting for 2 hours in dark condition. After washing with PBS twice, the samples are examined with confocal microscope.

Confocal microscopy was performed on a Nikon A1 HD25/A1R HD25 system combined with the Ti2-E inverted microscope, and the imaging area of this machine is nearly twice that of conventional system make us able to obtain more data.

7.2.3. Pharmacological Force Regulation

This platform aims to be used for drug testing and screening, so it is necessary to prove whether it is feasible or not to study the effects while drugs applied onto the human engineered cardiac tissue. The generation of contractile force is the key function of cardiac muscle cells. The main characterization of our platform is determining contractile force and heartbeat rate. Thus, it can be used for investigating the effects of positive and negative inotropic drugs. The contraction generated by each sample was measured with the mechanical modelling described before. The rate control is set as 2Hz. After the hEHTs were culture for 20 days, they were incubated with continuously adding amount of drug. The inotropic modulator drugs include Ouabain, Bay K8644, Milrinone, Amlodipine, Verapamil and Ryanodine. They are all clinical drugs with known pesticide effects. Stock solutions were prepared in distilled water. Before introducing drugs, contractile force of tissues cultured in normal medium were recorded and analysed as the baseline reference. Then, all the drugs were loaded into the bioreactor with increasing concentration every 2 hours. By using the recirculating perfused method, the concentrations of the drugs are kept at a constant level. The increasing

concentrations of drugs are $5*10^{-9}$M, $5*10^{-8}$M, $5*10^{-7}$M, $5*10^{-6}$M and $5*10^{-5}$M. After the drug tests, all the tissues were washed with free medium three times and put back into bioreactor for further culture. Fresh media is pumped back and perfused within the chamber. Compared with the static culture in 24 well culture dishes, this drug release process removes manual experimental process. Thus, it avoids risks of experimental errors and introducing contaminations. For each test, data were acquired with video record. The tissue responses in terms of beating rate and maximum contractile force are analysed as the reference for evaluation of drug treatments.

Ouabain is a cardiac glycoside. It acts by inhibiting the Na/K-ATPase membrane pump that results in increase of intercellular sodium and calcium concentrations. The effect of such drug is activating the contractile protein of cardiomyocytes and enhances the cellular contractile force. Normally, it can be used for treating congestive heart failure, hypotension and arrhythmias.

Although Bay K8644 is not clinically used in treatment, it still plays a great role in basic pharmacological research. As a positive inotropic agent, it increases influx of Ca^{2+} by increase the open time of the channels. In this situation, the contractile force is regulated to increase.

Milrinone is a drug for heart failure treatment. As a phosphodiesterase-3 inhibitor that can increase the heart's contractile ability, it prevents degradation of cAMP thereby increasing PKA activation.

Amlodipine is a CCB (Calcium channel blocker). It reduces the amount of calcium ions entering cardiomyocytes by blocking the calcium ion channels. It just affects

the contractile force not heart rate. Verapamil is a non-dihydropyridines CCB. It increases myocardium contractile force and helps regulate the heart rate.

Ryanodine is a biphasic inotropic modulator. It can block the phasic release of calcium, but at low concentration may not block the tonic cumulative calcium release. At low (<10 uM) concentrations, ryanodine binding locks the RyRs into a half-open state and eventually depletes the store, while higher (~100 uM) concentrations irreversibly inhibit channel opening. Thus, it has negative inotropic effect in low concentration and positive one in high concentration.

7.3. Results and Discussion

7.3.1. Feasibility and Optimization Evaluation of the System with REHTs

At day 5, we initialled the samples with 2V/cm and 3V/cm electrical stimulation respectively for engineered heart tissue generated with neonatal rat cardiomyocytes. The frequency and duration were set at 2Hz and 100ms. We found that the rat engineered cardiac tissues (rEHTs) started to beat immediately one day after electrical signals applied. Mechanical function analysis of rats engineered cardiac tissue started from days 8 (3 days after electrical activities) and data were recorded every three days until day 20 (days 11, days 14, days 17 and days 20). The displacements of silicon posts free ends are recorded by the microscope. With the mechanical modelling described before, the contractile forces variation of engineered cardiac tissue can be evaluated.

As shown in figure 7-3, the beating activities of rEHTs at day 14 are displaced there. We can find that presence of electrical stimulation has great effects on the amplitude of EHT contraction. For tissue stimulated with 3V/cm, the maximum contractile force is almost double that of samples without stimulation. While comparing samples with 3V/cm and 2V/cm, it can be easily observed that higher amplitude of electrical stimulation induces relatively larger contractile force.

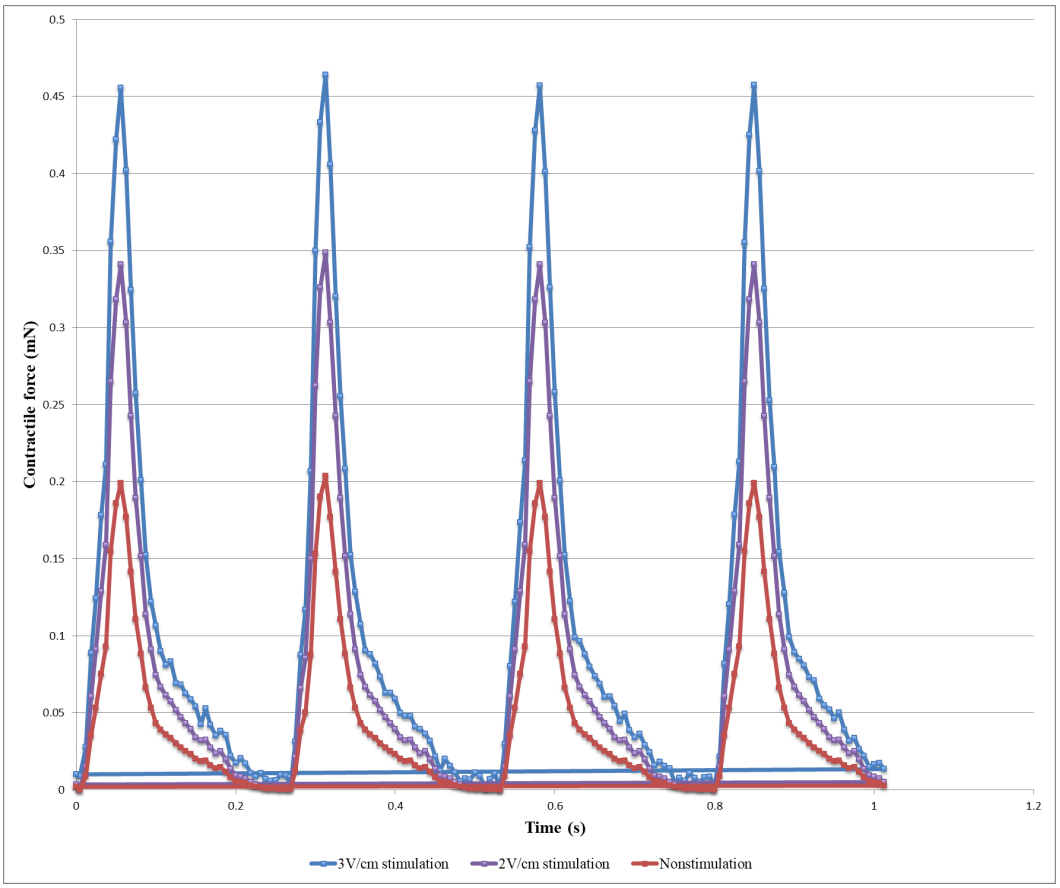


Figure 7- 3: Typical contractile force amplitude of neonatal rats EHT increasing against time while electrical stimulation applied (data acquired from Day 14).

To further study the pacing activities of rEHT, we kept on tracking the contractile force change of those samples. The maximum contraction force of samples in day 8, day 11, day 14, day 17 and day 20 are shown in Figure 7-4.

The figure shows the difference in cellular contractile behaviour between stimulated and non-stimulated samples of rEHT. From the figure, the engineered heart tissue without stimulation shows a relatively stable contraction over this period. The forces generated from those tissues keep at around 0.18mN. By contrast, it can be seen that the contractile forces increase as a function of time in culture for all the samples with stimulation. The contractile forces increase from day 8 (actually from day 6) to day 14 and afterwards the force generated from the tissue will not change anymore. Hence, a conclusion can be made is that it took two weeks for the neonatal rats' cardiomyocytes to settle down within the EHT and stay at a stable condition. For 3V/cm electrical stimulated samples, the contractile forces generated from the tissue reached at 0.48mN. That value of 2V/cm is just 0.35mN.

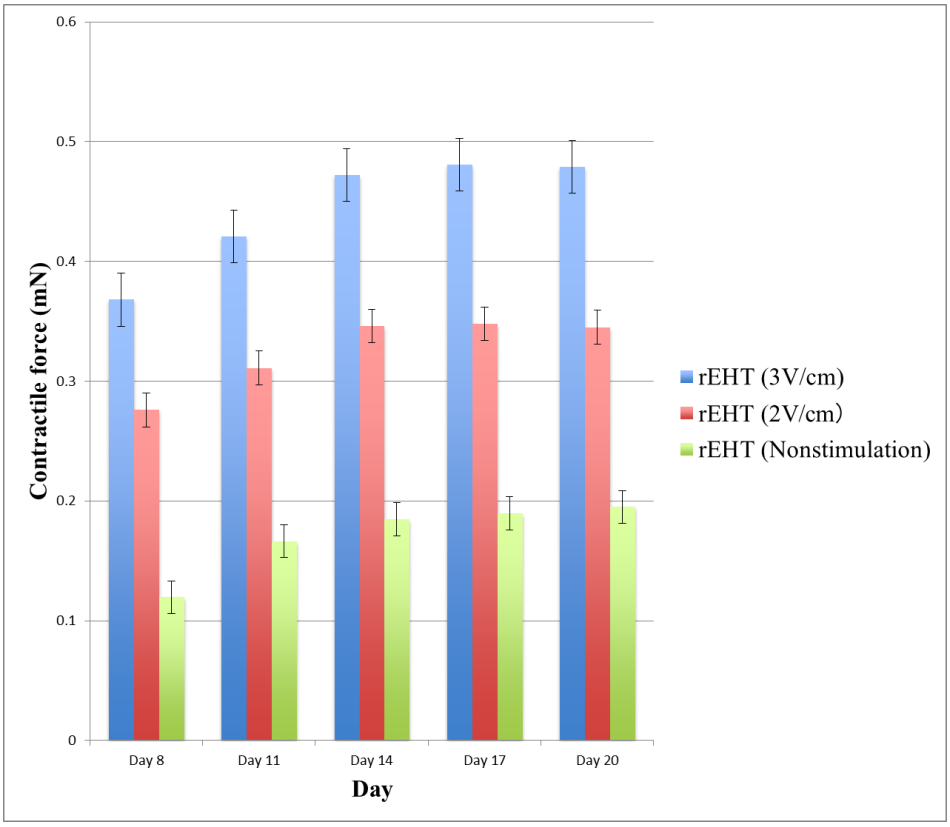


Figure 7- 4: Maximum amplitude of contractile force variation under different electrical stimulation conditions. Data are represented as mean±SE. The analysis statistic is processed with one-way ANOVA test ($p < 0.05$) $n = 3$ each group.

According to the imaging data captured by microscope, we also determine the change of ET and MCR to further study the contractile activities. Only samples applied with 3V/cm stimulation are studied. Figure 7-5 shows that excitation threshold and maximum capture rates at this period.

The ET shows a decline trend against culture time from day 8 to day 20 for both stimulation and non-stimulation EHTs. The stimulated samples have significantly lower ET compared to the samples without stimulation from day 8 to day 20. Yet the different becomes smaller over culture time.

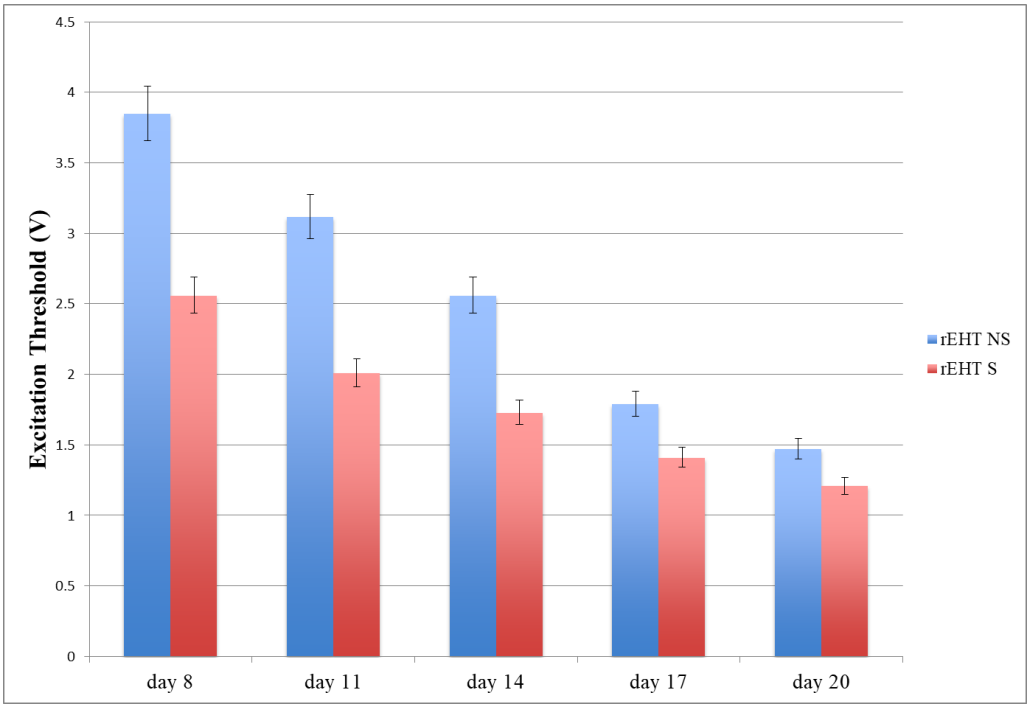


Figure 7- 5: Excitation thresholds of rEHTs from day 8 to day 20. It decreases against culture time. Data are represented as mean±SE. The analysis statistic is processed with one-way ANOVA test ($p < 0.05$) N=3 each group.

By comparing the maximum capture rate shown in figure 7-6, we can find the MCR rose as a function of culture time as a whole trend. Stimulated engineered cardiac tissues exhibit an increase in MCR from day 8 to day 20 and the values are higher than those of non-stimulated samples. However, the MCR of non-stimulated samples just rose from day 8 to day 14 and keep at a constant level (about 350bpm) after two-week culture.

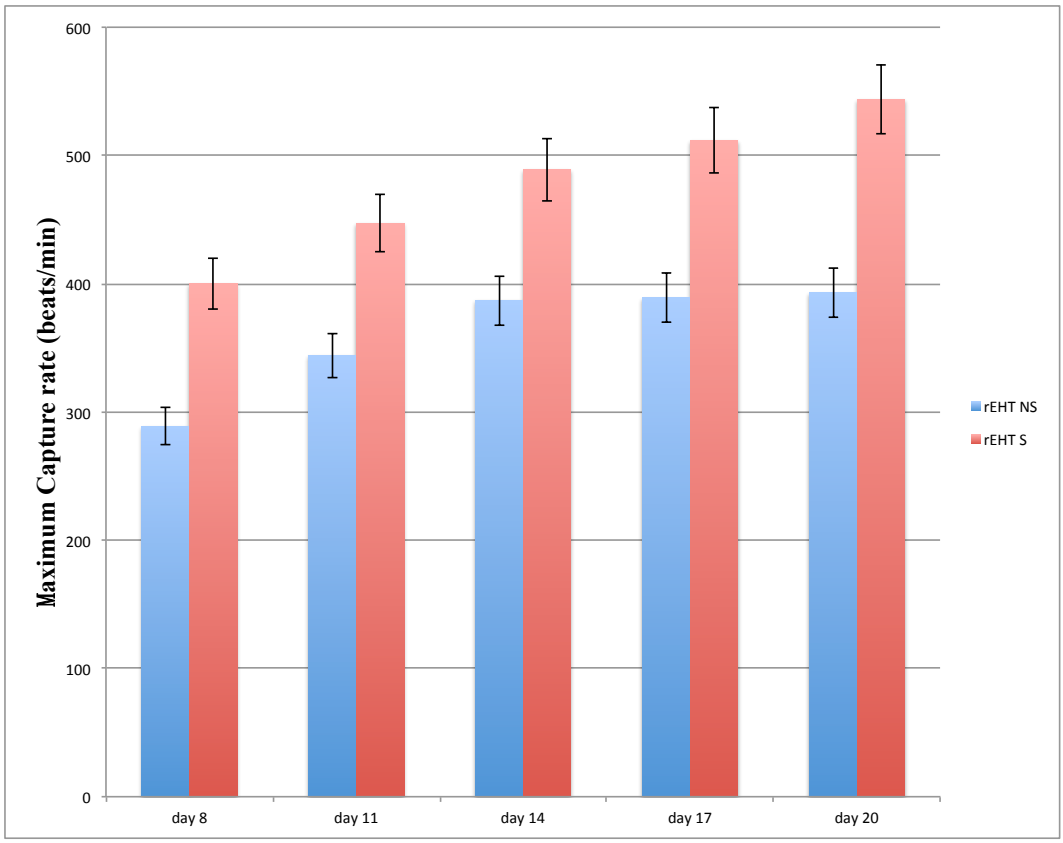


Figure 7- 6: Maximum capture rates of rEHT from day 8 to day 20. It shows an increase trend against culture time. Data are represented as mean±SE. The analysis statistic is processed with one-way ANOVA test ($p < 0.05$) N =3 each group.

In summary, there was no contraction observed at day 0 while neonatal rat engineered cardiac tissues were generated. Spontaneous beating was observed around day 3 and this contraction frequency kept decreasing after several-day culture. Chronic constant pacing is initialled at day 5 and rhythmical beating was observed one day later (day 6). Electrical stimulation induces markedly higher contractile force generated from the tissues and the forces increase against culture time until day 14 and stay at a constant level afterwards. After two-week culture, the

contractile force amplitudes of the paced rEHTs exhibit average twice as much as that of non-stimulated samples.

We have concluded the contractile functions can be enhanced with continuous electrical stimulation for engineered cardiac tissue. Qualitative test is able to provide more accurate and objective measurement in terms of cells viability. The metabolic activity or cell viability of each sample is measured by AlamarBlue assay.

For neonatal rats engineered heart tissues, there are three different groups to be evaluated, which are tissue without stimulation, with 2V/cm and 3V/cm stimulation. The rEHTs were originally seeded with 0.5 million neonatal rats' cardiomyocytes.

The data were acquired from day 1 and then from day 8 and acquired every three days until day 20 (day 8, day 11, day 14, day 17 and day 20). At each time, the perfusion motion is stop and 10% AlamarBlue reagent is added to each sample. After 3 hours incubation, 100ul of the solution was taken from the chamber and read with a fluorescent micro-plate reader. The percentage reduction of AlamarBlue is calculated as equation stated before and displayed in the figure 7-7.

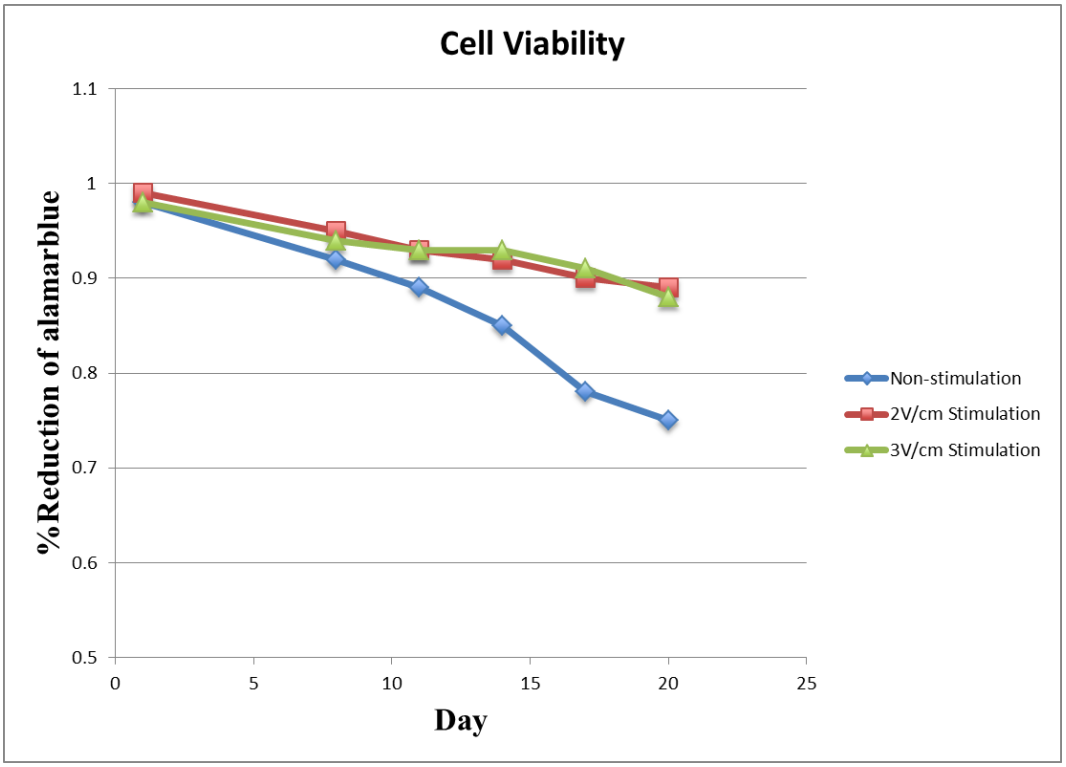


Figure 7- 7: The percentage reduction of AlamarBlue against time for rEHT treated with different electrical stimulations.

It is clear that samples without stimulation show faster decrease compared with those stimulated samples. Their cell viabilities drop to about 75% for non-stimulated engineered cardiac tissue after 20-day culture. By contrast, application of electrical stimulation increases this value to about 90% live cells are kept at day 20.

To further quantity study the samples and their morphology, live/dead imaging are processed. After cell staining, the samples were observed with microscope for determine the cell density. As live/dead staining is an end-point study, we acquired the samples at day 20 for rEHT. The cardiomyocytes encapsulated in the engineered cardiac tissues are viable. With Nikon fluorescent microscope, the indication for cell density of each sample is shown in figure 7-8.

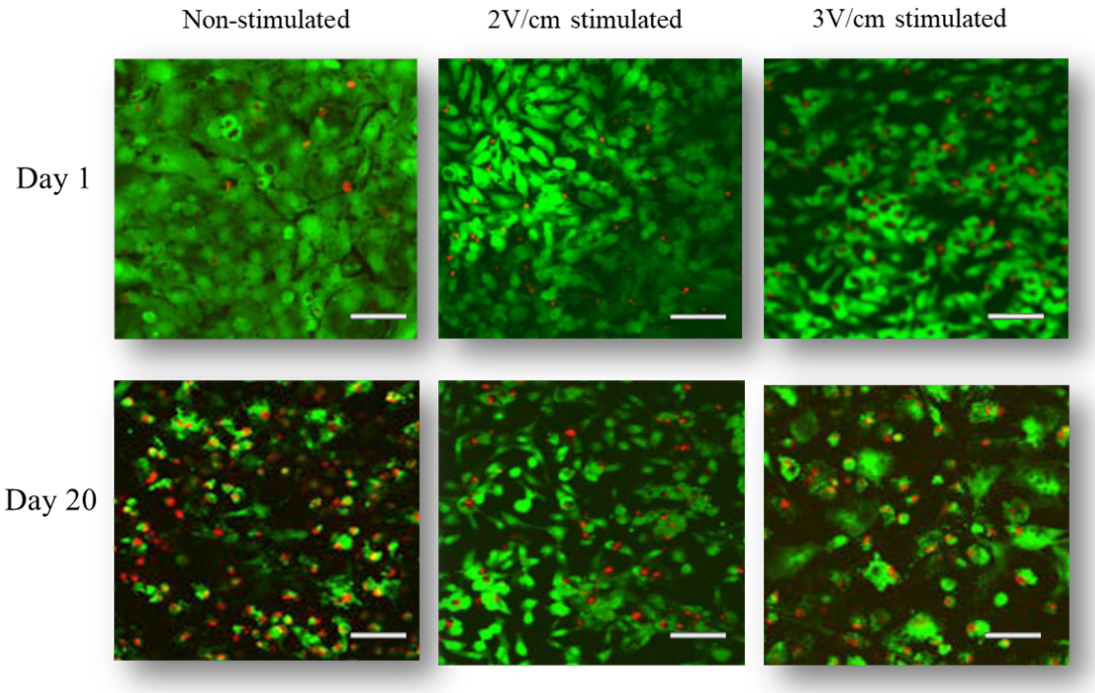


Figure 7- 8: Live/dead staining image shows the cell viability; Green indicators indicate live cells and red dots correspond to dead cells. (Scale bar represents to 100um).

From the figure, it can be observed that the electrical stimulation obviously enhances the cell viability in the engineered cardiac tissue. Cells were counted after imaging process and automatically calculated with ImageJ. Larger number of dead cells was observed from non-stimulated samples, while the cell viability in stimulated tissues is unchanged.

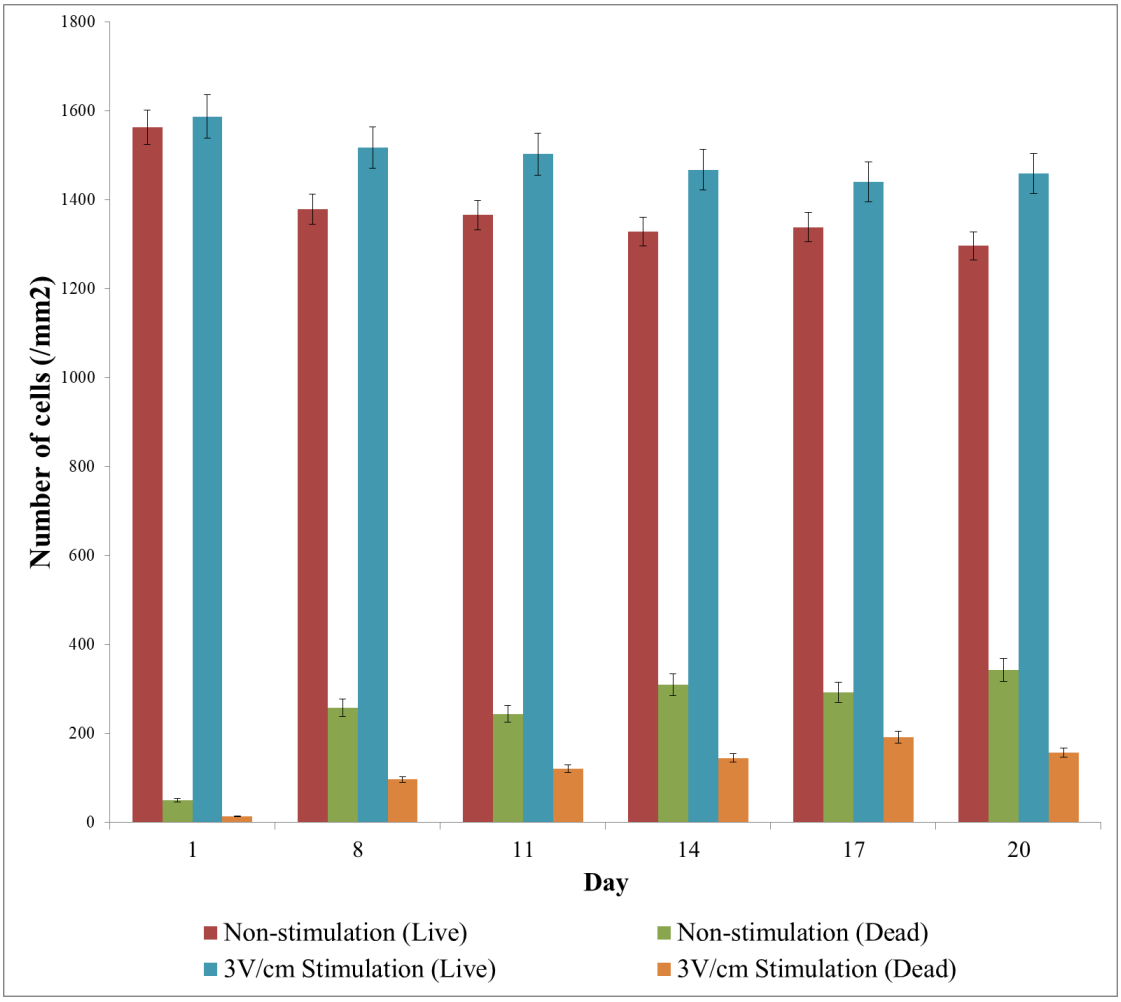


Figure 7- 9: Quantitative analysis of the number of live/ dead cells for rEHTs with non-stimulation, 2V/cm and 3V/cm stimulations. Data are represented as mean±SE. The analysis statistic is processed with one-way ANOVA test ($p < 0.05$) N=3 each group.

For the cardiomyocytes cultured in three-dimensional constructs, it started to evenly distribute within the scaffold after being seeded (day 1). And then cells took about 2-3 days to spread within the matrix and connect with each other. The interconnections between cardiomyocytes induce synchronous contraction of EHT and also result in the remodelling of hydrogel. The sizes of tissue are reduced due to

this remodelling. With the observation under the bright field microscope, we can find that the all the engineered samples are reduced in terms of tissue construct size against culture time.

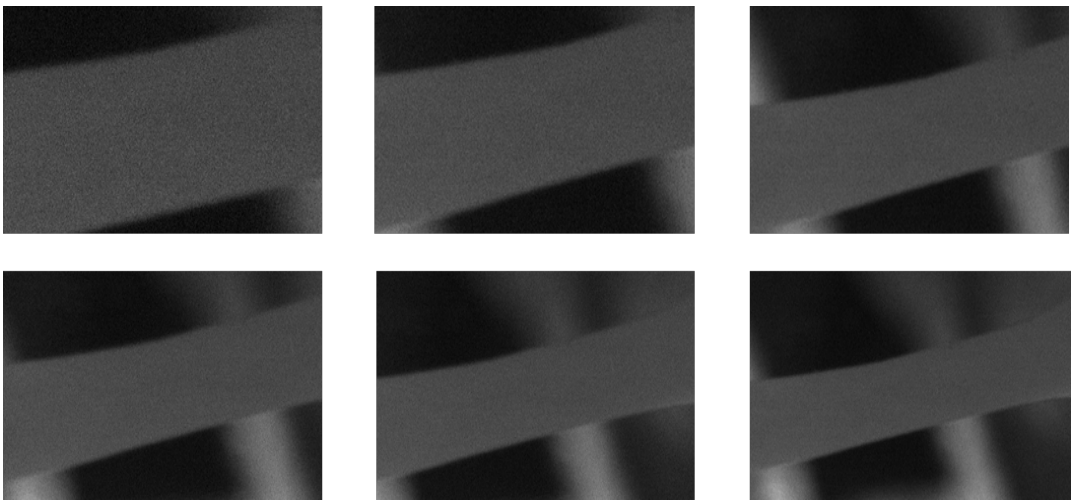


Figure 7- 10: The images show size variation of the neonatal rats engineered heart tissues stimulated with 3V/cm against time. (Day 1, day 3, day 6, day 9, day 12, day 15).

From the figure, we can see that the cross-sectional areas of rEHT decreased during culture and this decrease trend stop around day 9. Form figure 7-10, we can find that the rEHT show a 20 % reduce of radius at day 3 and finally reduce to only 24% of original size. The presence of electrical stimulation decreases the diameter of the samples. That means the contractile force against cross-section area is improved for the pacing samples.

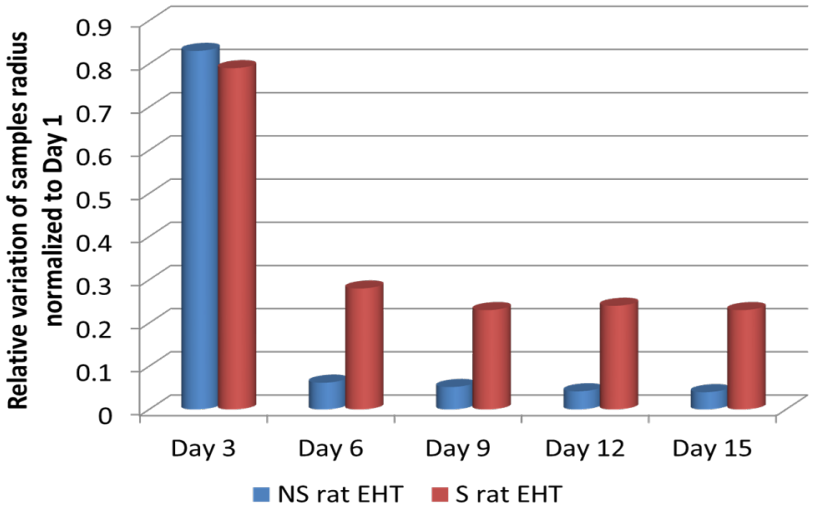


Figure 7- 11: The changes of cross-section radius normalized to Day 1 against culture time. (Day 3, day 6, day 9, day 12 and day 15).

To evaluate the difference between EHT with and without electrical stimulation in terms of function and structure, the fixed EHTs are stained with H&E staining after 20-days culture. Then, the samples are observed with light microscope to learn their performances.

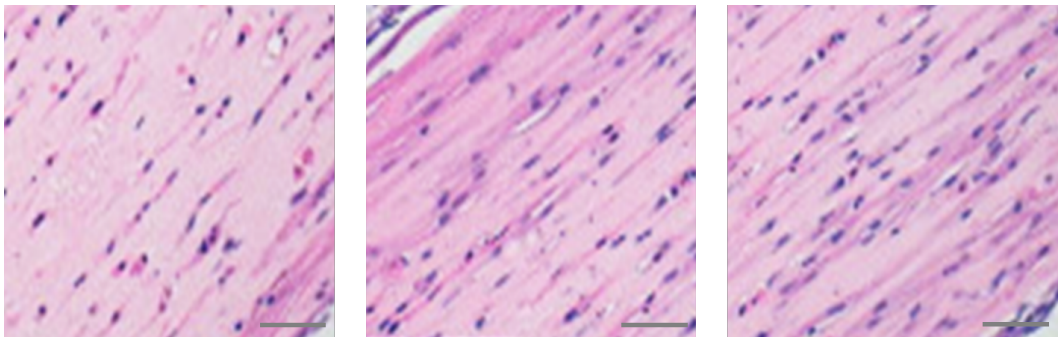


Figure 7- 12: H&E staining images of rEHT with non-stimulation, stimulation of 2V/cm and stimulation of 3V/cm. (scale bar represents to 50um)

It can be seen from figure 7-12 that the arrangement of neonatal rats cardiomyocytes with EHTs is more evenly while electrical pacing are applied. Higher amplitude of the voltage induced improved cell density within the tissue. Denser cell distribution corresponds to higher degree of cells maturation within the rEHTs. The cells align along the electrical filed. Hence we can conclude that the electrical stimulation is able to direct the development of engineered cardiac tissue and induces higher cells maturation and better cell networks within the tissue.

To further evaluate the functional and maturation change of rEHTs with electrical stimulations compared with control samples, confocal imaging was used to study fluorescent labelled samples. Figure 7-13 shows the confocal images of neonatal rats engineered cardiac tissues with sarcomeric alpha actinin to identify myocytes, CX43 to identify gap junctions, and (4', 6-diamidino-2-phenylindole) DAPI to identify nuclei.

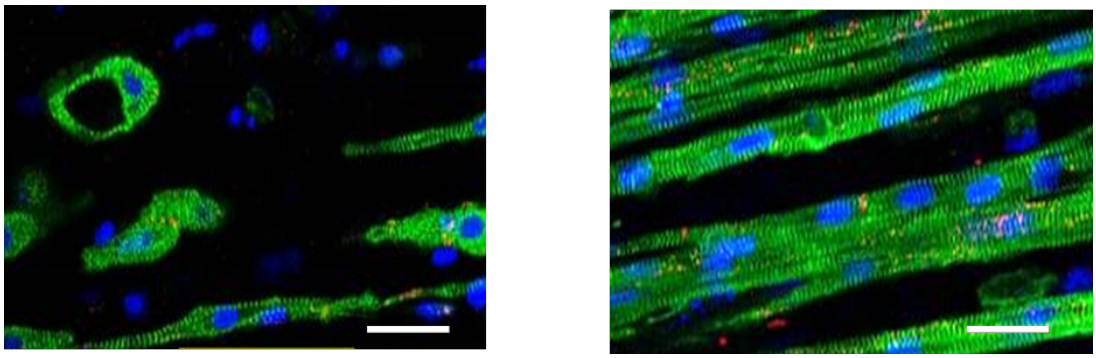


Figure 7- 13: Typical images of confocal microscopy of rEHTs (without and with 3V/cm electrical stimulation) to identify myocytes, gap junction and nuclei.

From the figure, it can be easily observed that cells in non-stimulated samples still exhibited round in shape and the cell density is relatively low. By contrast, in

chronic pacing rEHTs, the cells show elongated size with higher length to width and height ratio. Electrical stimulation also increased the cell density within the tissue as the size of the constructs condensed. Also it is observed that cell remodel the matrix and myocytes align along the electrical field. Cx43 displayed there show the better-developed intercalated disks and gap junctions of stimulated cardiac tissue compared with those within control samples.

Hence, according to the study above, a conclusion can be made that the presence of appropriate electrical stimulations is able to direct the development and growth of cardiomyocytes cultured in 3D constructs. With electrical field used here, denser and better-aligned cell distribution is achieved. Electrical stimulations also enhance function and improve maturation of cardiomyocytes within engineered cardiac tissue. Due to these outstanding effects, it is desirable to apply such system for culturing engineering cardiac tissue generated with human iPSC-CMs.

7.3.2. Development of Human Engineered Heart Tissues with Electrical Stimulations

Previous experiments of applying electrical stimulation onto rEHTs have shown its success in improving cellular maturation and tissue functions of bioengineered cardiac tissue. Thus, same parameters and conditions are directly used onto hEHTs. Briefly, monophasic electrical signals with 3V/cm in amplitude, 2Hz in frequency and 100ms in duration were initialled at day 5. Different from immediate response of rEHTs, hEHTs did not response to electrical pulses and start to beat until 3 days (day 8) after introducing electrical stimulations.

The contractile force variation of EHT generated with human iPSC-derived cardiomyocytes is also recorded from day 8 and measured every three days. Typical contraction pace at day 14 is shown in figure 7-14. It can be seen that electrical stimulation also induces better performance of cellular mechanical behaviour after two-week culture for human EHTs.

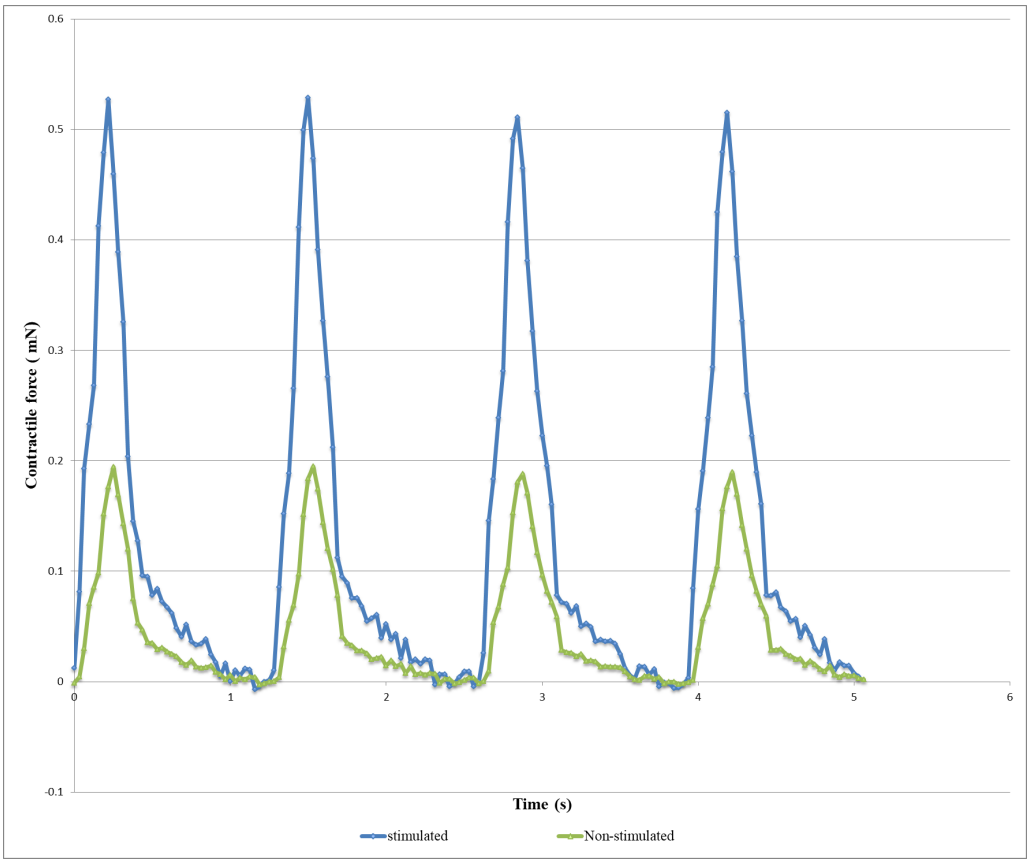


Figure 7- 14: Contractile force amplitude of human EHT increasing against time while electrical stimulation applied (data acquired from Day 14).

Compared with the force generated from rEHT, hEHTs show more active beating behaviour in terms of contractile force magnitude (about 0.52mN against 0.46mN of neonatal rEHT). Yet, the frequency of hEHTs is much lower than that of rEHTs.

Considering the heartbeat of rats is markedly faster than human, such difference is reasonable.

The contractile activities of hEHTs were tracked as well and the data were captured at the same periods. The maximum contraction force of samples in day 8, day 11, day 14, day 17 and day 20 are shown in figure 7-15.

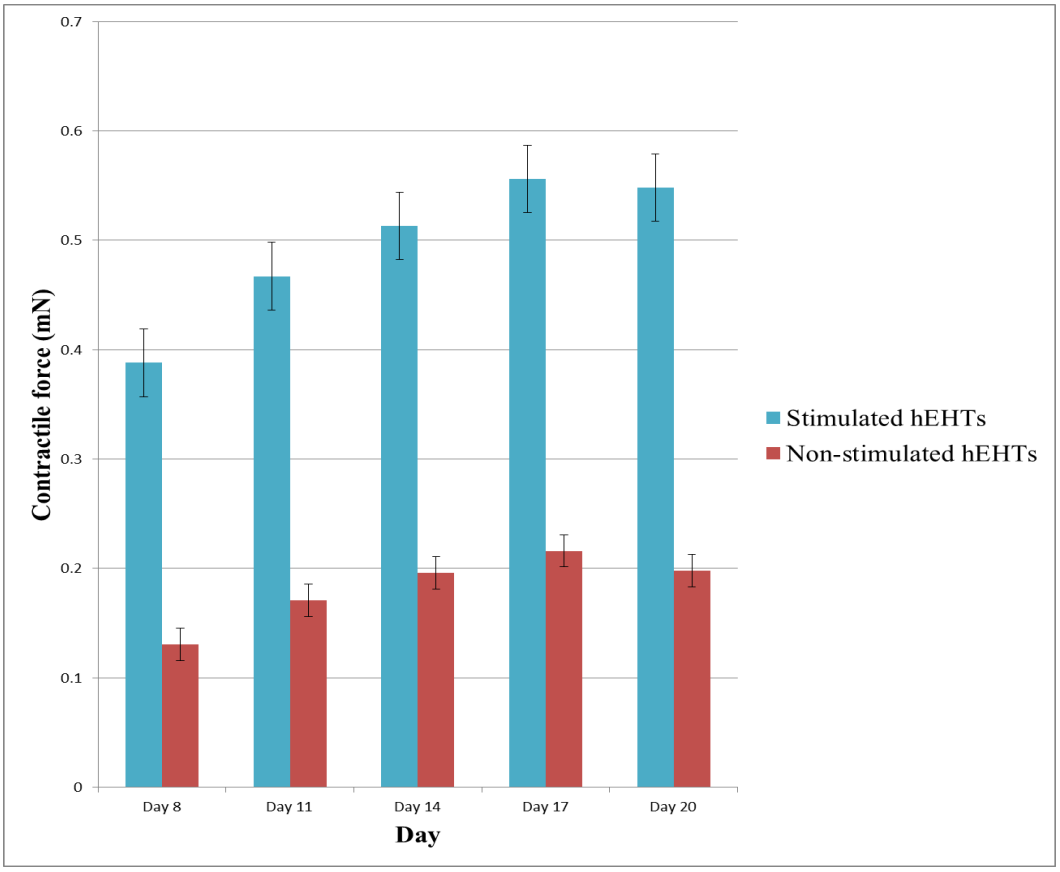


Figure 7- 15: Maximum amplitude of hEHT contractile force variation under different electrical stimulation condition. Data are represented as mean±SE. The analysis statistic is processed with one-way ANOVA test ($p < 0.05$) N =3 each group.

The figure shows the difference in cellular contractile behaviour between stimulated and non-stimulated samples of hEHTs. The non-stimulated engineered heart tissues

exhibit relatively stable contraction amplitudes over time. The force generated from hEHTs is around 0.2mN. This is close to rEHTs contractility. That means the samples of rats and human show similar contractile ability without electrical signals. A clear enhancement is shown of contractile force in terms of stimulated hEHTs (0.55mN at day 20). It took more time for hEHTs to stay stable at a constant level of contraction (at day 17). Hence, to further analyse or make other application, the pre-culture time for hEHTs should be at least 18 days week for hEHTs. According to this, we applied 20-day cultured hEHTs in the following drug testing.

The variations of electrical threshold and maximum capture rate were also detected with same methods to evaluation the performance of hEHTs under 3V/cm electrical stimulations. The excitation thresholds decreased from day 8 to day 20 for both stimulation and non-stimulation of hEHTs. The value of stimulated hEHTs drop from 2.95V/cm at day 8 to 1.32V/cm at day 20, while it halved for control group from around 2V/ cm to 1V/cm. It is obvious that ETs of stimulated samples are lower than control groups at same period. And the ETs of hEHTs are relatively smaller than those of rEHTs.

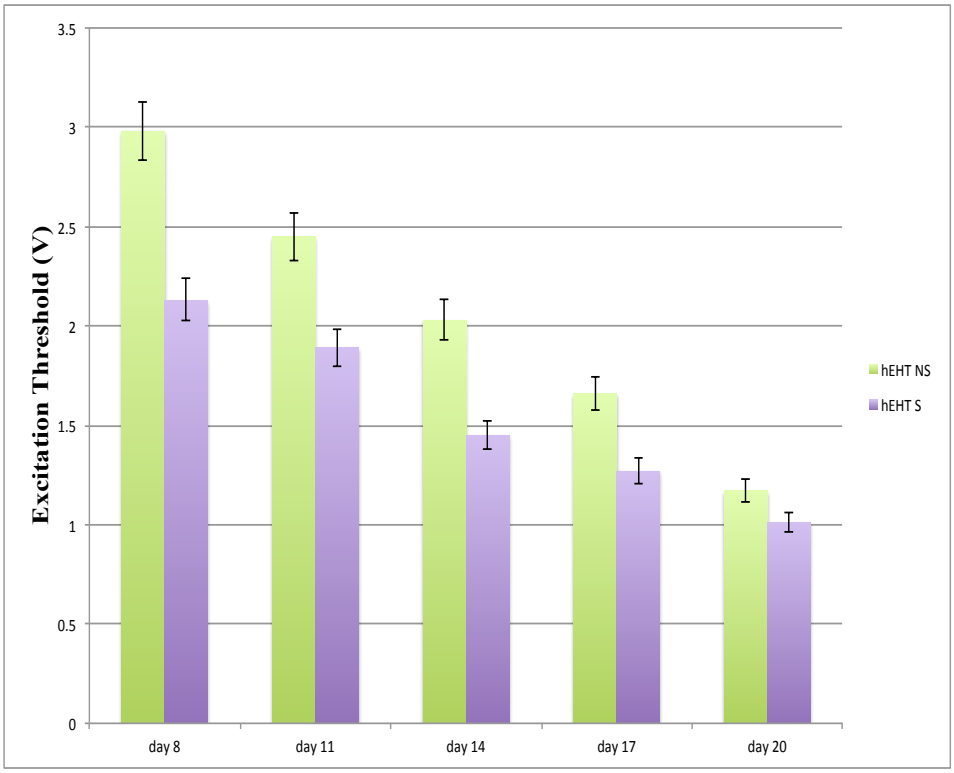


Figure 7- 16: Excitation thresholds of hEHTs from day 8 to day 20. They all decrease against culture time. Data are represented as mean ±SE. The analysis statistic is processed with one-way ANOVA test ($p < 0.05$) N =3 each group.

From the figure 7-17, it can be found that the MCR increased over cultured period. The rise of non-stimulated samples is just between from day 8 to day 14 and became stable after 2-week culture. But MCR of samples with stimulation keeps on increase until day 17 and not change between day 17 and day 20. Compared with rEHT, hEHT have much lower maximum capture rates.

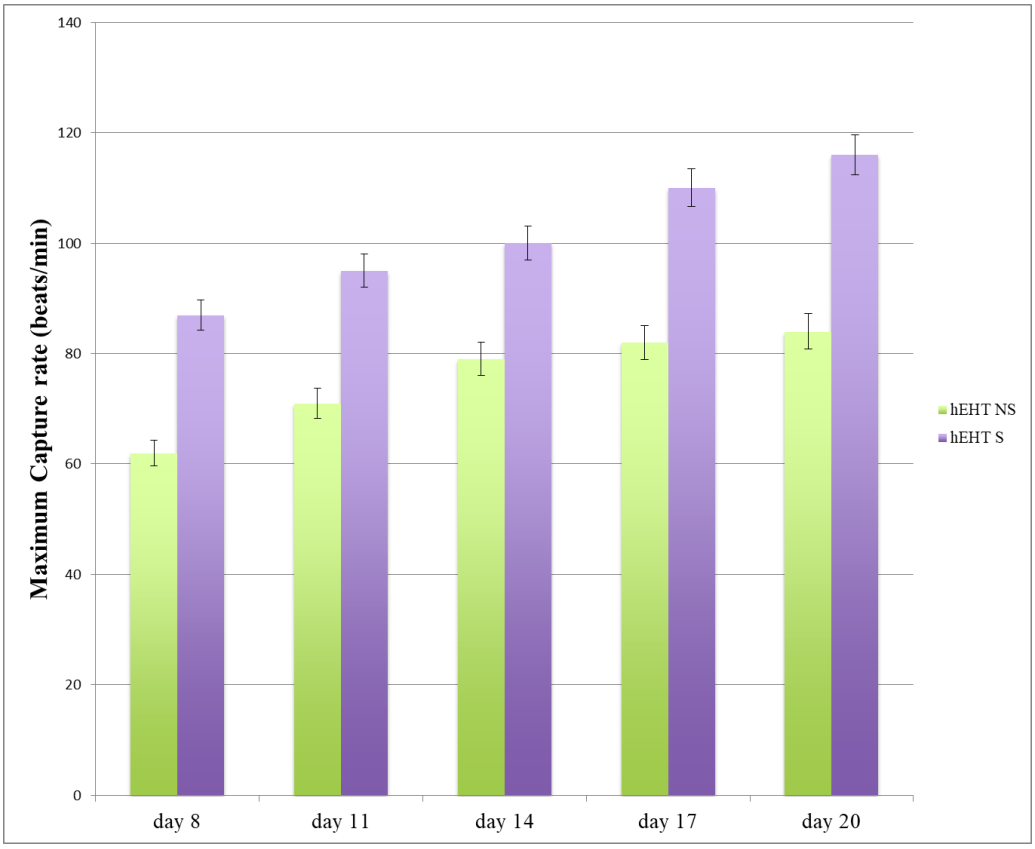


Figure 7- 17: Maximum capture rates of hEHT from day 8 to day 20. They all show an increase trend against culture time. Data are represented as mean±SE. The analysis statistic is processed with one-way ANOVA test ($p < 0.05$) N =3 each group.

In summary, same electrical fields were applied to culture hEHTs and we evaluated the functions of hEHTs with mechanical analysis of tissues' contraction activities. Cardiomyocytes in hEHTs exhibited spontaneous contraction from beginning, but coherent beating was not observed until day 8 (3 days after pacing). Spontaneous were reduced over culture time and largely decreased after electrical stimulation being introduced, so it means cells become more mature. The electrical threshold of hEHTs decreased as a function of culture time, while maximum capture rates exhibited an inverse trend. Contractile forces were significantly enhanced by

electrical stimulations. At day 20, average contractile forces generated from 3V/cm electrical stimulation are almost 3 times of control group, reaching 0.55mN. The performance of human engineered cardiac tissue in terms of contractile function is good enough for further application and tests.

The cellular morphology and viability study were also conducted at the same time. alamarBlue assay and live/dead staining assay were used as well for detecting cell viability within hEHTs over culture period. As it has been shown in rEHTs, the advantages of alamarBlue assay are non-toxic and do not affect cell functions. Hence it can be applied during cell culture process. The cell metabolic activities evaluation of hEHTs were made by alamarBlue and shown in figure 7-18.

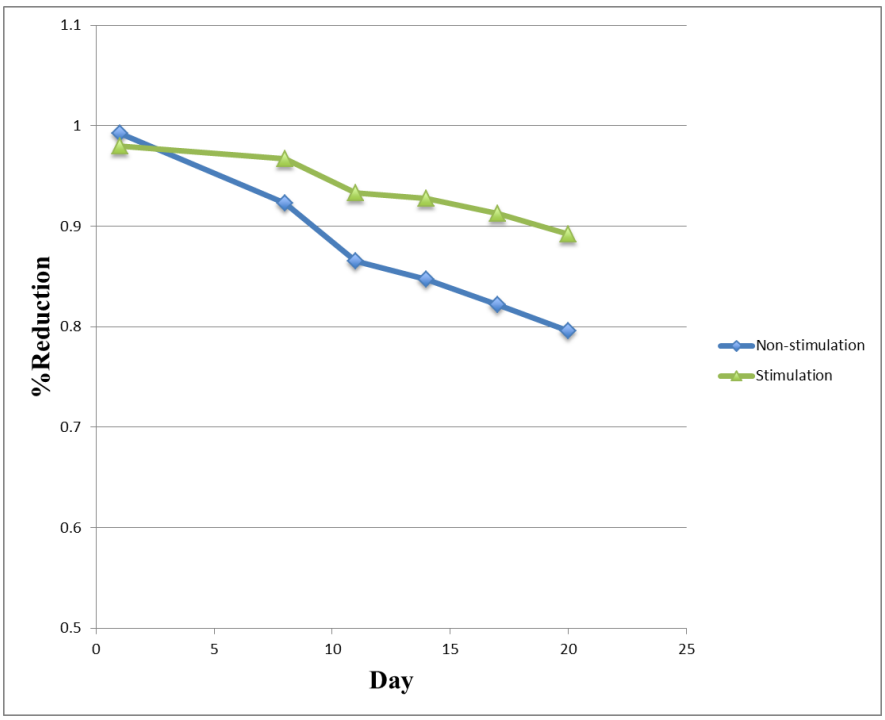


Figure 7- 18: The percentage reduction of AlamarBlue against time for hEHT treated with different electrical stimulations.

The cell viability of non-stimulation samples reduced to 80% of its original numbers. In contrast, the change of stimulated hEHTs in cell viability is not distinguished and they still kept at 90% level after 20 days culture.

Live/dead staining was process in the same method. We can observe an obvious difference between stimulated and non-stimulated hEHTs (figure 7-19). hEHTs with electrical stimulation have relatively higher number of live cells over culture time.

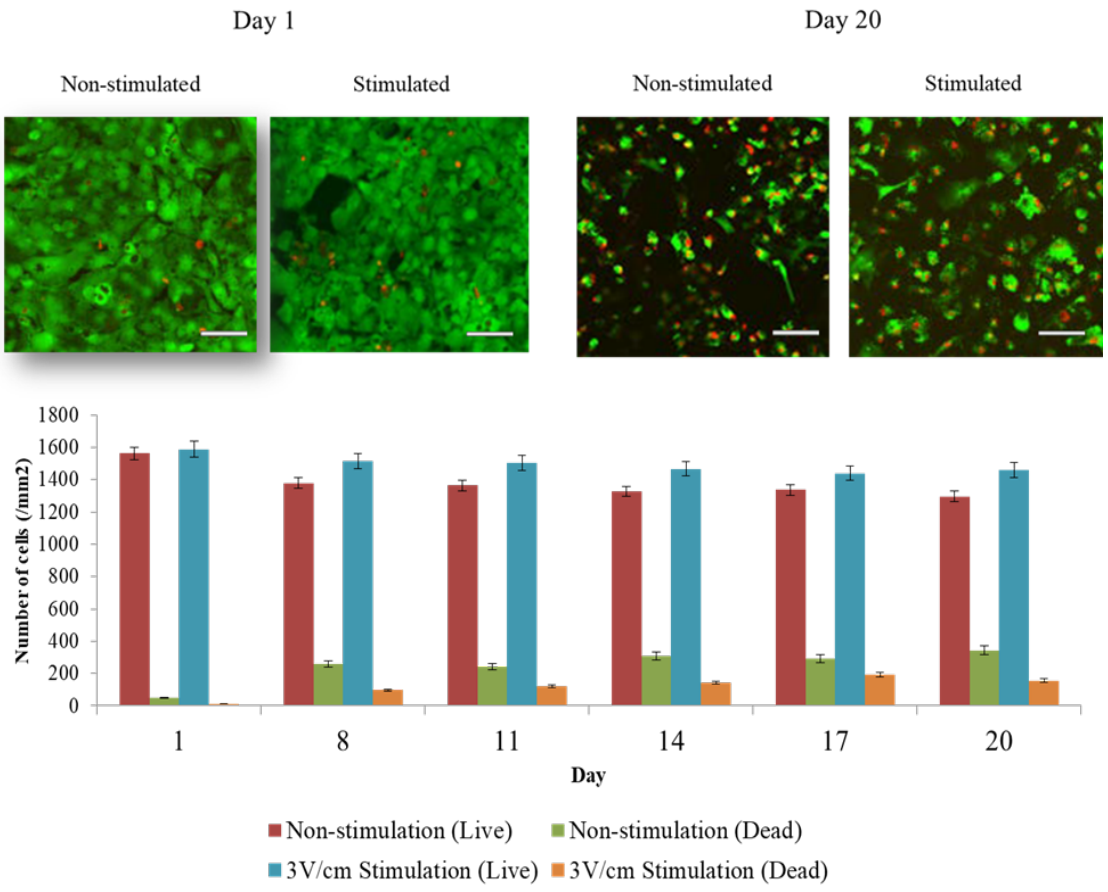


Figure 7- 19: (a) Live/dead staining image shows the cell viability, Green indicators indicate live cells and red dots correspond to dead cells. (Scale bar represents to 100um). (b) Quantitative analysis of the number of live/ dead cells for rEHTs with non-stimulation, 2V/cm and 3V/cm stimulations. Data are represented as mean±SE.

The analysis statistic is processed with one-way ANOVA test ($p < 0.05$) N=3 each group.

The distribution of human iPSC-CMs cultured in engineered heart tissue distribute within the matrix evenly after one-day culture. Interconnections between cells remodelled the matrix and it took 5 days for the hEHTs to generate contractions. The structures of hEHTs were observed with bright field microscope (shown in figure 7-20). The sizes of the hEHTs decreased over culture time at beginning and were unchanged after day 9.

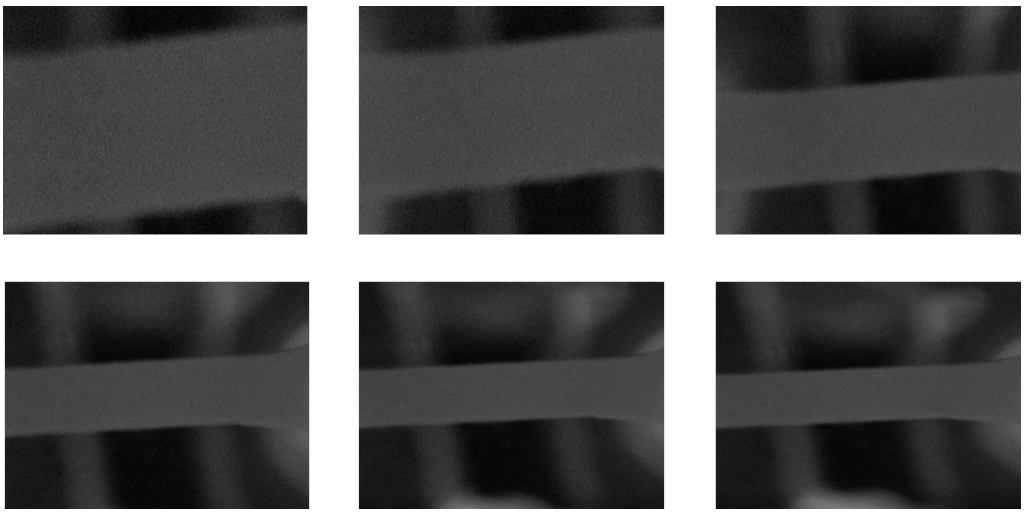


Figure 7- 20: The images show size variation of the human iPSCs engineered heart tissues stimulated with 3V/cm against time. (Day 1, day 3, day 6, day 9, day 12 and day 15).

The remodelling of the constructs for hEHTs is slower than that of rEHTs, but the effects of electrical stimulation on the change is also not significant. From figure 7-21, we can find that the reduction of hEHTs in size at day 3 is 15% from original

and it becomes 60% at day 6. This size of hEHTs eventually decreases to about 19% of that at day 1.

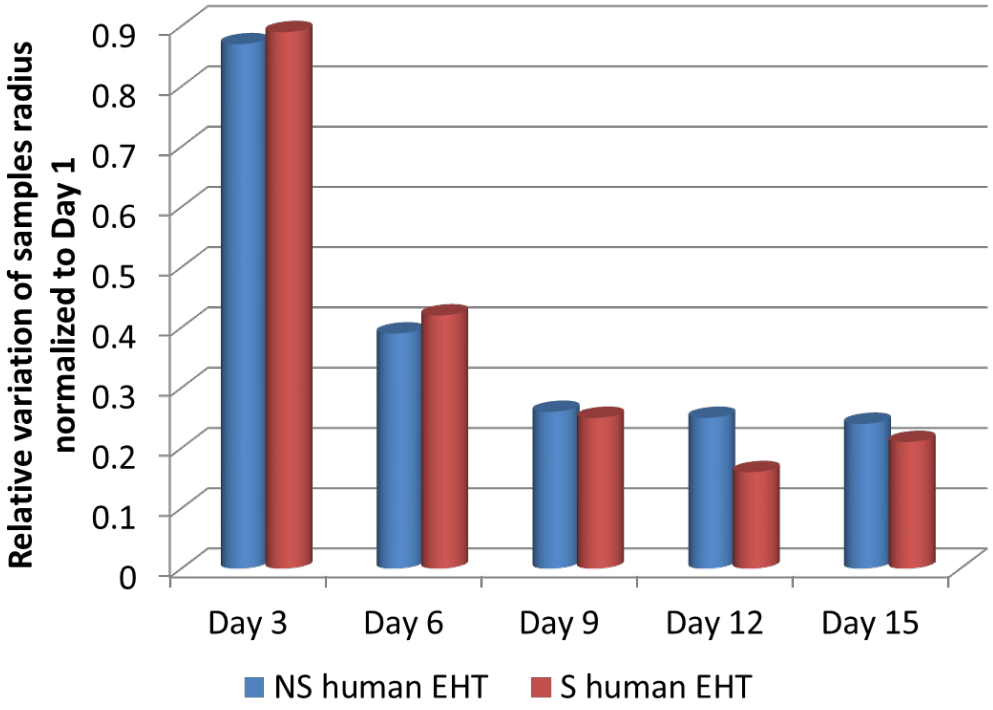


Figure 7- 21: The changes of cross-section radius normalized to Day 1 against culture time. (Day 3, day 6, day 9, day 12 and day 15).

H&E stained hEHTs at day 20 are observed with light microscope to learn their performances. Although the cardiomyocytes still show a round in shape and the maturation for single cells is well-established, it can be seen from figure 6-33 that the cardiomyocytes within human EHTs exhibit a higher cell density and the cells are relatively larger than neonatal rats' cardiomycoytes. The presence of electrical signals resulted in higher density of cell distribution and cardiomyocytes network with hEHTs is more uniform compared with non-stimulated EHTs. Alignment of

cardiac myocytes were formed due to guidance from the electrical filed. Higher degree of cellular maturation was achieved, and better cell networks appeared within the tissue.

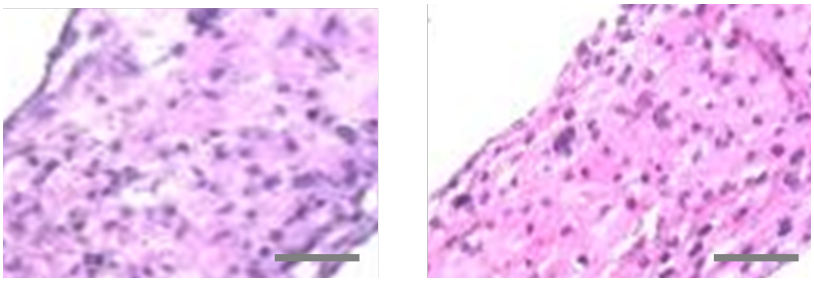


Figure 7- 22: H&E staining images of stimulated and non-stimulated hEHT at day 20. (Scale bar represents to 50um)

Figure 7-23 shows the confocal images of hEHTs fluorescence labelled with sarcomeric alpha actinin to identify myocytes, CX43 to identify gap junctions, and DAPI to identify nuclei. Paced tissues show a more densely packed cardiomyocytes and cell distributions within the tissue are more uniform throughout the whole tissue. Larger number and higher intensity of connexion-43 indicates firm interconnections between cells are formed and cell network is better-developed. Electrical field directly guided the development of cells within the tissues and enhanced coupling thereby inducing higher contractile force.

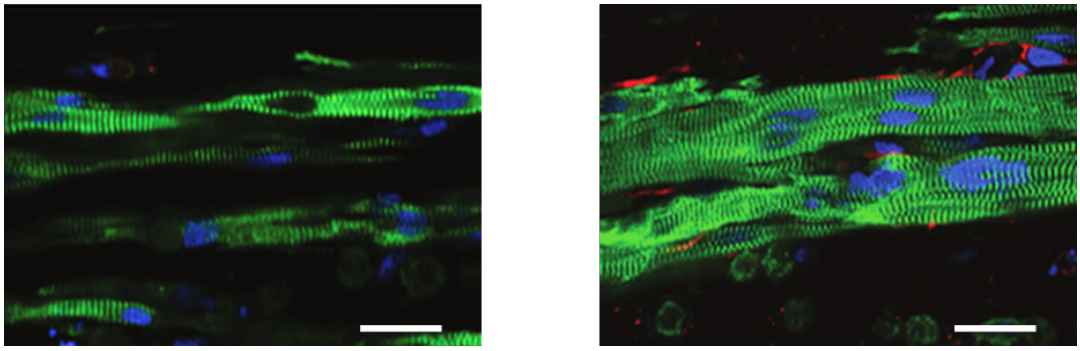


Figure 7- 23: Typical images of confocal microscopy of rEHTs (without and with 3V/cm electrical stimulation) to identify myocytes, gap junction and nuclei.

By staining the sarcomeric alpha-actinin with red and nuclei with blue, markedly difference of sarcomeres structure within the tissues between stimulated and control samples can be further clearly seen in detail. Well-aligned distribution of sarcomeres in paced tissues showed a higher degree of maturation of cardiomyocytes in hEHTs.

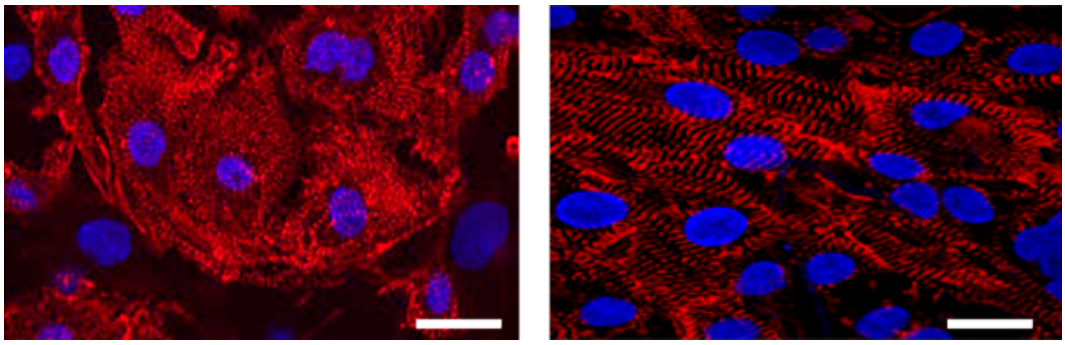


Figure 7- 24: Histological construct of sarcomeres within pacing and non-pacing engineered cardiac tissues.

So far the effects of field stimulation onto cardiomyocytes cultured in engineered cardiac tissue were investigated and hypothesis about its ability to improve cellular

maturation have been proved. Thus, we can conclude that our system is feasible to develop functional human engineered cardiac tissue for further application. With mechanical and electrical stimulations, more cells in such tissues were recruited to form interconnection and formed coordinated contractions. Also, these stimuli also advance the degree of maturation of human iPSC-CMs and improve contractile ability of single cell.

After generation and long-term culture of engineered heart tissue with human iPSC-CMs, these constructs were applied into pharmacological study. Primary drug testing was conducted to verify the tissues performance under drugs involvement.

7.3.3. Drug Testing with Human Engineered Heart Tissue

By exposing the 3D human engineered cardiac tissues to increasing concentration of inotropic modulator drugs, several groups of clinical drugs with known functions were tested in our system.

The first drug tested is Ouabain and it is a cardiac glycoside. The pacing track of the hEHT responding to this drug with 5uM is displayed in figure 6-35. It can be seen from the figure that this drug improved the force development but did not make any change to the kinetics of contraction.

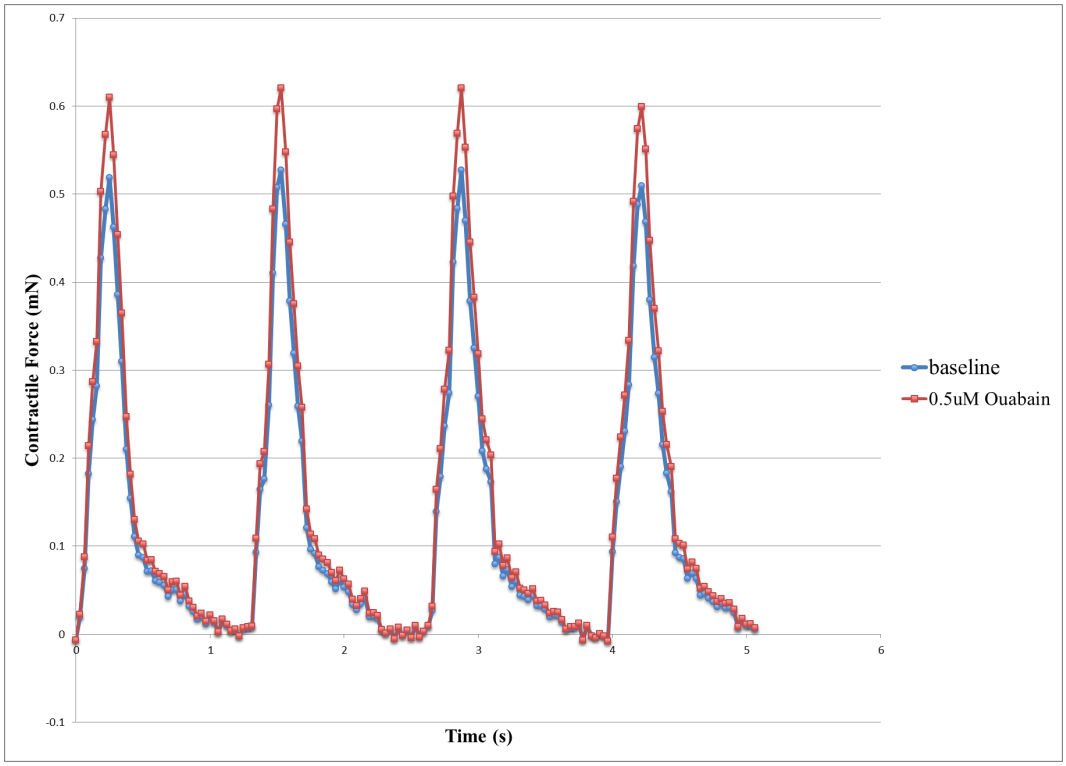


Figure 7- 25: hEHT contraction response curves before and after application of 0.5uM Ouabain.

To further investigate the performance of hEHT under effects of various concentrations of Ouabain, the results are displayed in figure 7-26. From the figure, we can find that with higher concentration of Ouabain applied, larger contractile forces were generated. Yet, this increase stops at 5uM concentration. By contrast, the increasing amount of the drug did not have great effects on contraction and relaxation time.

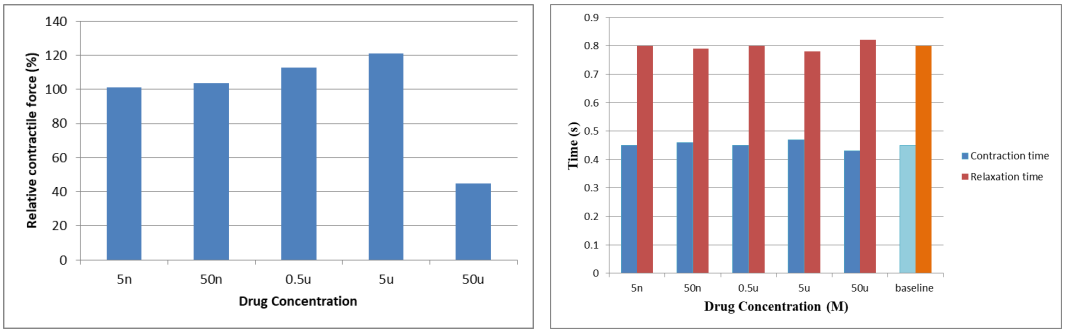


Figure 7- 26: The relationship of average maximum contractile forces, contraction time and relaxation time against increasing concentrations of Ouabain. Data are represented as mean±SE. The analysis statistic is processed with one-way ANOVA test ($p < 0.05$) N=3 each group.

Bay K8644 is a positive inotropic agent. From Figure, it can be observed that this drug not only enhances contraction but also prolongs relaxation time of hEHT. And higher concentration of drugs applied induces larger relaxation time.

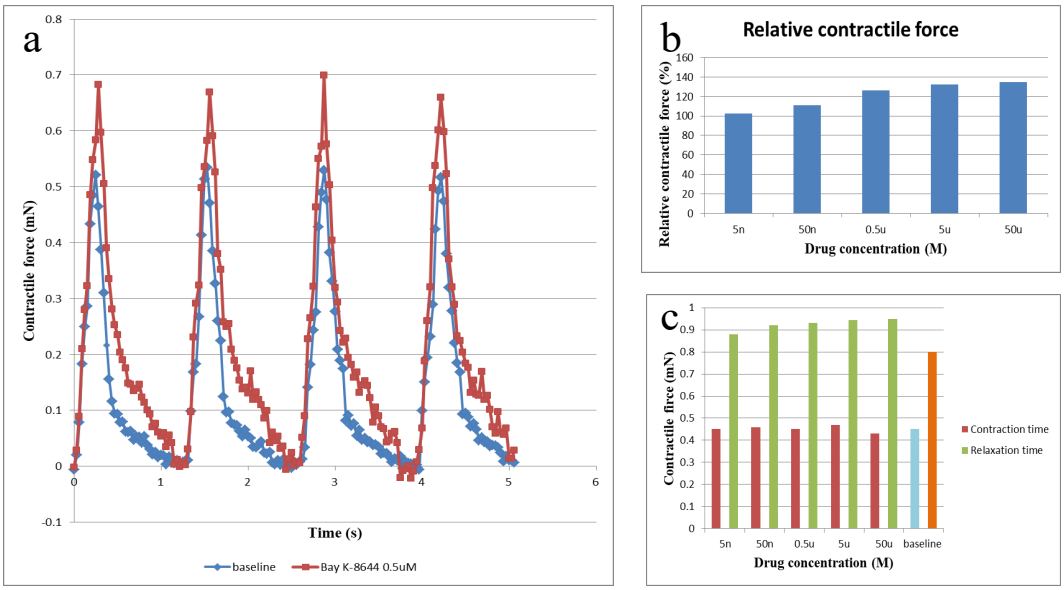


Figure 7- 27: Test of Bay K-8644 onto hEHT. (a) Contraction response curves before and after application of 0.5uM Bay K-8644. (b) The relationship of average maximum contractile forces and various concentration of Bay -8644. (c) Contraction time and relaxation time against increasing concentrations of Bay K-8644. Data are represented as mean±SE. The analysis statistic is processed with one-way ANOVA test ($p < 0.05$) N =3 each group.

In terms of Milrinone, it helps enhance contractile ability of heart by preventing degradation of cAMP. From the figure below, we can find force is enlarged while 5uM Milrinone is introduced onto tissues. And both contraction and relaxation period are prolonged. Also, we find that force and contraction time are enlarged against increasing concentration of drugs applied.

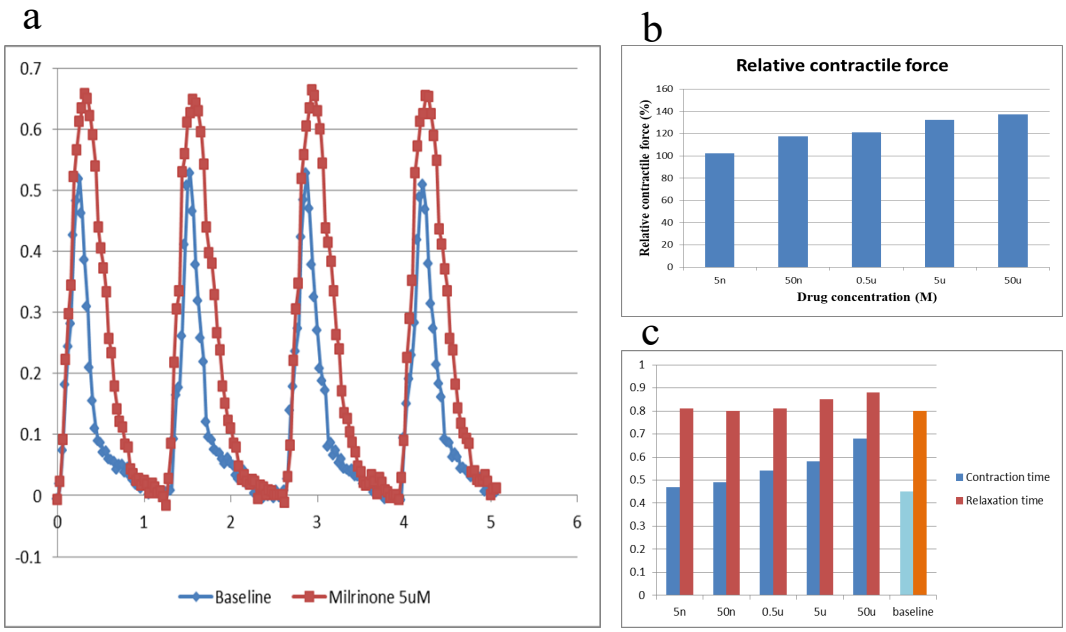


Figure 7- 28: Test of Milrinone onto hEHT. (a) Contraction response curves before and after application of 5uM Bay K-8644. (b) The relationship of average maximum contractile forces and various concentration of Milrinone. (c) Contraction time and relaxation time against increasing concentrations of Milrinon. Data are represented as mean±SE. The analysis statistic is processed with one-way ANOVA test ($p < 0.05$) N =3 each group.

As a calcium channel blocker, Amlodipine is used for limiting cardiac contractions. From figure 7-29, it is observed that maximum contraction amplitude is lowered after drugs applied without changing contraction kinetics.

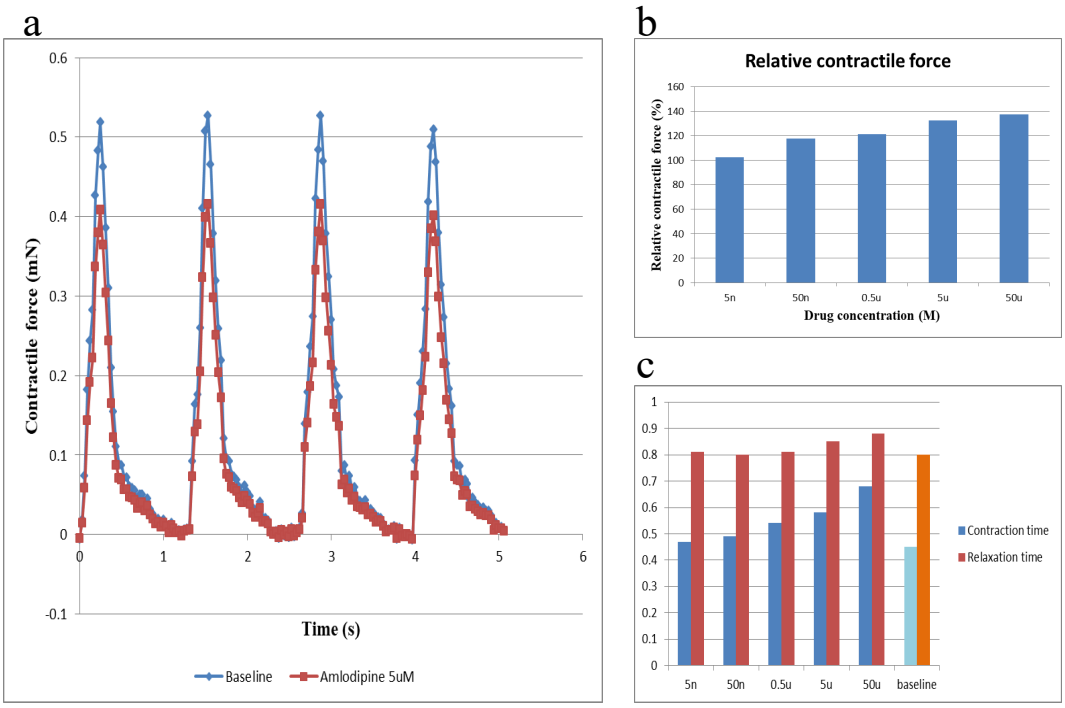


Figure 7- 29: Test of Amlodipine onto hEHT. (a) Contraction response curves before and after application of 5uM Amlodipine. (b) The relationship of average maximum contractile forces and various concentration of Amlodipine. (c) Contraction time and relaxation time against increasing concentrations of Amlodipine. Data are represented as mean±SE. The analysis statistic is processed with one-way ANOVA test ($p < 0.05$) N=3 each group.

Ryanodine shows a typical biphasic response. From the data obtained, it lowered the contractile force generated from EHT while low concentration (0.5uM) of drugs applied, but slightly increased it at high concentration (50uM). At the same time, this drug also increases the contraction time while does not make too much change of relaxation time.

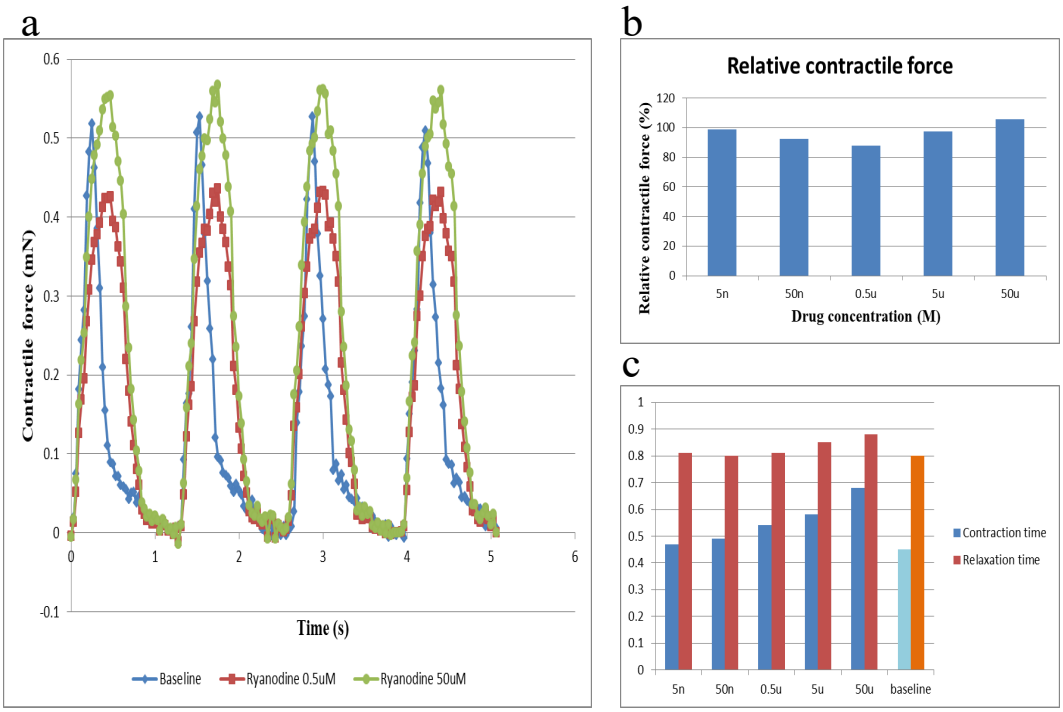


Figure 7- 30: Test of Ryanodine onto hEHT. (a) Contraction response curves before and after application of 5uM Ryanodine. (b) The relationship of average maximum contractile forces and various concentration of Ryanodine. (c) Contraction time and relaxation time against increasing concentrations of Ryanodine. Data are represented as mean±SE. The analysis statistic is processed with one-way ANOVA test ($p < 0.05$) N=3 each group.

The contracile force generated by cardomyocytes is resulted from interactions of bioelectrical activities, calcium ions transient, and myofilament movement. After analysing the effects of these drugs, a primary view of drug testing using human engineered cardiac tissue with iPSC-CMs. Five clinical drugs were applied to regulate the contractile functions of hEHTs from contractile force and kinectics. According to the results shown above, it can be found that the reactions of inotropic

modulation induced by these drugs meet their medical effects. From this view, our system could serve as a valuable tool for screening drugs before clinical trials.

7.4. Summary

In summary, a functional 3D human engineered heart tissues were developed according to protocol stated before. With the aim of creating a model for disease modelling and cardiotoxicity studies, we initialled the generation of EHTs with cardiac muscle cells isolated from neonatal rats. The tissues generated a 3D construct and were able to restore coherent contractile functions presenting in native. Perfusion system provides EHTs with even distribution of medium flow and this improves culture efficiency and cell viability.

The feasibility of our system is verified by applying such electrical signals onto rEHTs and for long-term culture. Stimulated samples show great advance in functions, cellular interconnects and tissue maturation.

Although the iPSC-CMs hold great potential applications in regeneration of cardiac tissue, the maturation of culturing these cells in engineered cardiac tissue is always a main problem. As the cellular maturation and tissue constructs are improved with electrical stimulations, it is meaningful to culture the human iPSC-EHTs in our system. Over a period time for tissue culture, cells within EHTs exhibit higher degree of maturation and better-developed cellular organization. The electrical fields help guide the development of engineered heart tissue and cells can form alignment

networks with such stimulations. The hiPSC-EHTs generated and cultured in our system are thus regarded as a stable and functional model for further analysis.

Several clinical inotropic modulators are introduced according to their specification to verify the practicability of using our *in vitro* model for drug testing. The reactions of the tissues to the drugs are in high agreement with their actual clinical effects. Therefore, we conclude that it is a reliable and functional system for primary drug screening by using our engineered heart tissues generated with human induced pluripotent stem cells derived cardiomyocytes.

Chapter 8 Conclusion and Future Work

In conclusion, we described here a model of setting up functional human engineered cardiac tissues in my DPhil project. The aims of building such bioengineered tissue are mimicking the structure of native cardiac tissue and restore parts of its functions. The engineered heart tissue is fabricated by seeding cardiomyocytes (Neonatal rats' cardiomyocytes and human iPSC derived cardiomyocytes) into fibrinogen-based hydrogel scaffold to form 3D construct. With a Polydimethylsiloxane (PDMS) platform used as support, the size of EHTs is minimized thereby lowering the requirements of cell number and cost. After accurate mechanical properties study of PDMS and mechanical modelling, this tensile platform can also work as a force transducer to preciously convert the relationship between silicon tubes deformation and the mechanical response from EHTs.

A perfused micro-bioreactor based on glass slide is manufactured with 3D printing to improve nutrient and small molecule delivery. Optimized dynamic culture system helps enhance cells viability and offer more flexible solutions for 3D cardiomyocytes culture, especially its potential application in drug screening. High-throughput and parallel testing can be realized benefit from automatic and non-invasive measurements of mechanical response of samples. It enables the integration of functional stimulations for the samples and study performance of different engineered cardiac tissue while various stimulations applied.

Two carbon electrodes were embedded within the culture chamber to provide electrical stimulation with amplitude less than 8V/cm. To achieve the optimal electrical field for EHTs, simulations and experiments were carried out under

different conditions. With application of electrical stimulation, more mature rats and human engineered cardiac tissues are formed. Especially, the maturation of cells in hEHTs is significant. These tissues present important functions of cardiac tissue with obvious contractile forces variation and regular heartbeat rhythm.

The purpose of our project is designing such platform and using it as a model for drug testing and cardiotoxicity studies. While system is set up and tissues are generated and culture over time, the EHT samples exhibit 3D cellular structure and their synchronous contractile forces can be observed. Relying on real-time video capture and quantitative imaging processing, the contractile force can be measured at tissue level. To evaluate the feasibility and robust of using this system for *in vitro* model of drug testing, several drugs including positive, negative and biphasic inotropic modulators were tested with our human EHT model with electrical stimulations in the micro-bioreactor. The results show a great agreement with the data of clinical trials. Therefore, it is workable to apply such 3D engineered heart tissue into large-scale drug testing including development, efficiency and toxicity evaluation.

In summary, it can be concluded that this micro-perfused platform would be an effective and efficient 3D *in vitro* model for human engineered heart tissue development for drug screening.

8.1. Conclusion of Findings

8.1.1. PDMS Material Characterization

A platform made from PDMS is used for engineered cardiac tissue attached. The platform is not just to be utilised for supporting the tissue, but also to work as a force transducer. The configuration of bioreactor plays a key role in this system, so it is worthwhile to carry out the mechanical model optimization studies to achieve accurate force transducer modelling. According to the literature, the contraction force from such a number of cells varies from 0.15mN to 0.2mN. Apart from the geometry (diameter and length), other conditions have been confirmed (PDMS mechanical properties). Following the beam deflection model, it was desirable to make the posts deformation within an easy-measure range. It was thus found that the diameter could not exceed 1mm and that the length needed to be from 10mm to 15mm. Hence, we decided to use 12mm length with 1mm diameter as the final design.

It is concluded that the micro-bioreactor with a silicon platform is effective for qualifying the contractile force of 3D cultured cardiomyocytes. Theoretical analysis on the displacement and force relationship proved to be correct as it was calibrated by the experimental data. To optimize the force transducer function, different geometries of the PDMS platform were investigated and the best design was a silicon post 1mm in diameter and 12mm in length. Using a controlled camera or microscope, the cellular force could be measured via an optical method with such a transfer model as has been proven correct before.

8.1.2. Bioreactor Configuration Design and Optimization

To provide a better culture environment compared with static culture, a dynamic perfused system is required. With commercial software, the configuration design of such bioreactor is determined via simulation for an optimized dynamic fluidic situation. It aims to realize laminar flow and avoid turbulent flow within the chamber, and it is easier to control the media flow to guarantee uniform distribution of nutrients and tissue can access to media evenly.

After making the stimulation of flow situation within three different configurations of chambers, the one with narrow shape channel (NSC) is chosen as the final design. The flow rate from the inlet is limited by 0.05rmp to lower the shear stress and higher value may lead to cells damage. In the experimental work, the inlet flow rate we used is 0.03rmp, but its practical velocity can range from 0.01rmp to 0.05rmp.

8.1.3. Electrical Stimulation System Design and Optimization

Two carbon electrodes are integrated in the bioreactor to provide a controllable electrical filed for generated 3D engineered cardiac tissues. The system of electrical stimulation is simulated with commercial software to achieve an optimized electrical environment. It is widely known that presence of electrical stimulation helps enhance cellular functions and maturation during tissue development and generation. Most previous work is made by qualitative rather than quantitative analysis. Hence, the purpose of this project is to develop a stable electrical stimulation system so that it can be used to investigae the cardiomyocytes and engineered heart tissue under different electrical conditions. In this system, carbon electrode is selected as the best

electrical source due to its high efficiency for electrical delivery and chemical inertness. A small integrated circuit plat called Raspberry Pi is used for introducing electrical signals. With a digital-analog-converter (DAC), the digital voltage can be transferred into dynamic waveforms and an especially precise voltage level can be achieved. In this situation, the output voltage from Raspberry Pi can be controlled by programming to achieve different levels with 3.22mV as the step.

The initial time of electrical stimulation is set to day 5 to avoid any side effects on protein formation due to too early electrical signals applied or weak stimulation effects resulting from late application. The electrodes used here are 12mm in length, 1mm in radius with 4mm spacing and EHTs are placed between two electrodes with 0.2mm gap above the surface of glass slide so that the tissues can experience even distribution of electrical signals in the chamber.

The maximum amplitude of electrical signals cannot be over 8V/cm and monophasic analogue pulses are selected as the electrical source with 100ms pulse duration. After all these conditions being confirmed and set up, the electrical system can be further applied in investigating the effects of electrical stimulation on culture and formation of engineered heart tissue.

8.1.4. Culture of Engineered Cardiac tissue and Application into Drug Test Platform

A functional 3D engineered cardiac tissue is developed and can be cultured *in vitro*. We found that the best electrical stimulation condition for such EHT is 3V/cm in

amplitude, 2Hz in frequency and 100ms in duration. This electrical field leads to low excitation threshold, high maximum capture rate and high maximum amplitude of contraction. Over period electrical stimulation, it is observed that the fibrinogen-based EHT profits from electrical signals. Compared with those control samples, electrical stimulations enhance contractile forces and induces high density of cell network including higher cell density, improved gap junctions, well-developed structure of sarcomere and better cell alignment.

The engineered cardiac tissue generated with human iPSC-derived cardiomyocytes is culture with our system for 20 days, while they are mature enough for further analysis. Five clinically approved drugs are used for initial drug testing to evaluate feasibility of our system. This system is able to monitor the change of contractile force and contraction kinetics. From the results, it can be found that this system is suitable for screening of drug effects. Hence, we can conclude that our model is a feasible method for application of primary *in vitro* drug testing.

8.2. Future Work

8.2.1. Study of PDMS Mechanical Properties Under Dynamic Condition in Different Frequency Domain

In the study of PDMS mechanical properties characterization, the effects of mixing ratio of base and regent and manufacturing processs have been investigated. All these experiments were undertaken in the condition of static analysis. However, the PDMS platform works as a force transducer to measure or transfer the displacement into contractile force. It is thus meaningful to determine the behaviour of PDMS

pillar under dynamic conditions. After taking into consideration of frequency, the mechanical model of estimating the ending force and bending situation can therefore be estimated more accurately. Furthermore, as we have found the network of various mixing ratio has great impact on the PDMS young's modulus, we can choose deserved mixing ratio for our platform design. Yet, the relationship between these two values is unknown and I think some further steps of mechanical test with more mixing ratio and determine suitable mathematic modelling to estimate this relationship can be done in the future. If the model is confirmed, the design of PDMS pillars will be more flexible with any network of mixing ratio to achieve special requirements.

8.2.2. Integrated Temperature and Gas Monitoring Control System for This Micro-bioreactor

Currently, the micro-bioreactor is designed and manufactured based on glass slides. After manufacturing the chamber of bioreactor with 3D printer, the perfusion system is introduced to the chamber via a pump to pump the media flow in and out.

8.2.3. Further Optimization of Electrical Stimulation

In this project, we have found that engineered cardiac tissues are highly dependent on parameters of electric stimulation, including electrode material, stimulation amplitude and frequency. Yet, for the purpose of simplify and convenient, the voltage source used here is monophasic pulses. To have better understanding of electrophysiology of engineered heart tissue, it is desirable to apply various

electrical signals, such as biphasic pulses, biphasic pulses with slow reversal and direct current.

8.2.4. Automatic Image Processing and Data Acquisition System

The force transducer process heavily relies on the video captured from microscope. The displacement of the silicon posts' ends is recorded by imaging and software can be used to measure it. According to equation stated in chapter 2, force can be therefore obtained from deformation of PDMS pillars. We are looking forward to designing software can accurately and automatically control imaging capture and process the data in a real-time analysis system while doing the observation under microscope.

8.2.5. Other Disease Modelling and Drug Testing Work

Now that we have proved the feasibility of using the engineered cardiac tissue for classic drug testing. Hence, this 3D cardiac tissue model can be applied to large-scale drug side-effect assessment for preclinical and clinical drug development and drug efficiency evaluation. In the future, more drugs can be evaluated with our bioengineered cardiac tissue system.

8.2.6. Future application of the system

The system can be further improved more functional and used for other purpose of investigation. Currently, the main function of the micro-bioreactor is force

measurement of engineered heart tissue. With some further modification, force can be measured more accurately. The system is generated based on 24-well culture dish. To make it smaller in size, the tissue can be generated in 64-well culture dish. In this case, the system can be integrated into conventional high-throughput drug discover machine.

This system can also be applied into investigating other cells and tissues like muscle cells or guiding growth of nervous tissue. The integrated mechanical and electrical stimulation system make it possible to directly apply desirable stimulations onto cells and tissues.

References

1. Benjamin, E. J. et al. Heart disease and stroke statistics - 2018 update: A report from the American Heart Association. Circulation 137, E67–E492 (2018).
2. British Heart Foundation. Heart Failure - Heart Conditions - British Heart Foundation. *British Heart Foundation* (2017).
3. Mozaffarian, D. *et al.* Heart Disease and Stroke Statistics—2016 Update. *Circulation* (2015).
4. Misra, A. Tissue engineering. in *Biotechnology: Recent Trends and Emerging Dimensions* (2017).
5. Tzatzalos, E., Abilez, O. J., Shukla, P. & Wu, J. C. Engineered heart tissues and induced pluripotent stem cells: Macro- and microstructures for disease modeling, drug screening, and translational studies. *Advanced Drug Delivery Reviews* 96, 233-244 (2016).
6. Grosberg, A., Alford, P. W., McCain, M. L. & Parker, K. K. Ensembles of engineered cardiac tissues for physiological and pharmacological study: Heart on a chip. *Lab Chip* 11, 4165-4173 (2011).
7. Coulombe, K. L. K., Bajpai, V. K., Andreadis, S. T. & Murry, C. E. Heart Regeneration with Engineered Myocardial Tissue. *Annu. Rev. Biomed. Eng.* 16, 1-28 (2014).
8. Chang, W. G. & Niklason, L. E. A short discourse on vascular tissue engineering. *npj Regen. Med.* (2017).
9. Anderson, R. H. Clinical anatomy of the aortic root. *Heart* 84, 670-673 (2000).
10. Duvernoy, H. M., Delon, S. & Vannson, J. L. Cortical blood vessels of the human brain. *Brain Res. Bull.* 7, 517-579 (1981).
11. Postma, A. V., Christoffels, V. M. & Moorman, A. F. M. Developmental aspects of the electrophysiology of the heart: Function follows form. *Electrical Diseases of the Heart: Volume 1: Basic Foundations and Primary Electrical Diseases* 1, 24-36 (2013).
12. Fessler, H. E. Heart-lung interactions: Applications in the critically ill. *European Respiratory Journal* 10, 226-237 (1997).
13. Kromhout, D., Menotti, A., Kesteloot, H. & Sans, S. Prevention of coronary heart disease by diet and lifestyle evidence from prospective cross-cultural, cohort, and intervention studies. *Circulation* 105, 893-898 (2002).

14. Kohl, P., Bollensdorff, C. & Morad, M. Progress in Biophysics and Molecular Biology of the Beating Heart. *Progress in Biophysics and Molecular Biology* 110, 151-153 (2012).

15. Anderson, R. H. Development of the heart: (2) Septation of the atriums and ventricles. *Heart* 89, 949-958 (2003).

16. Antolini, R. Seeing the heartbeat from matteucci's rheoscopic frog to image-guided arrhythmia ablation. *Il Nuovo Saggiatore* 2, 142-148 (2010).

17. Chen, G. H., Xia, J. & Liu, H. Bin. Application of stem cell transplantation in treating cardiovascular diseases. *Journal of Clinical Rehabilitative Tissue Engineering Research* 48, 2607-2655 (2007).

18. Bouten, C. V. C. *et al.* Substrates for cardiovascular tissue engineering. *Adv. Drug Deliv. Rev.* 63, 221-241 (2011).

19. Chiu, R. C. J., Zibaitis, A. & Kao, R. L. Cellular cardiomyoplasty: Myocardial regeneration with satellite cell implantation. *Ann. Thorac. Surg.* 60, 12-18 (1995).

20. Rhee, D., Sanger, J. M. & Sanger, J. W. The premyofibril: Evidence for its role in myofibrillogenesis. *Cell Motil. Cytoskeleton* 28, 1-24 (1994).

21. Hinken, A. C. & Solaro, R. J. A Dominant Role of Cardiac Molecular Motors in the Intrinsic Regulation of Ventricular Ejection and Relaxation. *Physiology* 22, 73-80 (2007).

22. Fuller, W. & Shattock, M. J. Phospholemman and the cardiac sodium pump: Protein kinase C, take a bow. *Circulation Research* 99, 1290-1292 (2006).

23. Krans, J. L. The Sliding Filament Theory of Muscle Contraction. *Nat. Educ.* 3, 66 (2010).

24. Fromm, J. & Lautner, S. Electrical signals and their physiological significance in plants. *Plant, Cell and Environment* 30, 249-257 (2007).

25. Limongelli, G. & Fratta, F. Cardiovascular involvement in Pompe disease. *Acta Myol.* 30, 202-203 (2011).

26. Richardson, P. *et al.* Report of the 1995 World Health Organization/International Society and Federation of Cardiology Task Force on the definition and classification of cardiomyopathies. *Circulation* 93, 841-842 (1996).

27. Morimoto, S. Editorial: Expanded spectrum of gene causing both hypertrophic cardiomyopathy and dilated cardiomyopathy. *Circulation Research* 105, 313-315 (2009).

28. Hou, L., Coller, J., Natu, V., Hastie, T. J. & Huang, N. F. Combinatorial extracellular matrix microenvironments promote survival and phenotype of human induced pluripotent stem cell-derived endothelial cells in hypoxia. *Acta Biomater.* 44, 188-199 (2016).

29. Yusuf, I., Arzai, A., Yushau, M. & Garba, L. Comparing Ebola virus disease and antimicrobial resistance outbreaks in Nigeria- a cross sectional survey of awareness level of health care workers and members of community. *Antimicrob. Resist. Infect. Control* 4, 1 (2015).

30. Balaji, G. N., Subashini, T. S. & Chidambaram, N. Detection and diagnosis of dilated cardiomyopathy and hypertrophic cardiomyopathy using image processing techniques. *Eng. Sci. Technol. an Int. J.* 19, 1871-1880(2016).

31. Int Task Force Prevent Coron Heart, D. Coronary heart disease: Reducing the risk. *Nutr. Metab. Cardiovasc. Dis.* 19, 1819-1824 (1998).

32. Abrams, J. Beneficial actions of nitrates in cardiovascular disease. *Am. J. Cardiol.* 77, C31-C37 (1996).

33. Johnson, W., Onuma, O., Owolabi, M. & Sachdev, S. Stroke: A global response is needed. *Bulletin of the World Health Organization* 94, 634-634A (2016).

34. Libby, P. & Theroux, P. Pathophysiology of coronary artery disease. *Circulation* 7, 08 (2005).

35. Levine, J. C. & Alexander, M. E. Overview of the general approach to diagnosis and treatment of fetal arrhythmias. *UpToDate* 20, 522-531 (2015).

36. Park, J. B. & Fung, Y. C. Biomaterials, an Introduction. *J. Biomech. Eng.* (1980).

37. Liu, S. Q. & Fung, Y. C. Zero-stress states of arteries. *J. Biomech. Eng.* 110, 82-84 (1988).

38. Shapira, A., Kim, D. H. & Dvir, T. Advanced micro- and nanofabrication technologies for tissue engineering. *Biofabrication* 6, 1-7 (2014).

39. Merrill, J. P., Murray, J. E., Harrison, J. H. & Guild, W. R. Successful homotransplantation of the human kidney between identical twins. *J. Am. Med. Assoc.* 160, 277-282 (1956).

40. Merrill, J. P. *et al.* Successful Homotransplantation of the Kidney between Nonidentical Twins. *N. Engl. J. Med.* 262, 1251-1260 (1960).

41. O'Brien, F. J. Biomaterials & scaffolds for tissue engineering. *Mater. Today* 14, 88-95 (2011).

42. Hutmacher, D. Scaffold design and fabrication technologies for engineering tissues—state of the art and future perspectives. *J. Biomater. Sci. Polym. Ed.* 12, 107-124 (2001).

43. Park, J. Y. *et al.* Differentiation of neural progenitor cells in a microfluidic chip-generated cytokine gradient. *Stem Cells* 27, 2646-2654 (2009).

44. Evans, M. J. & Kaufman, M. H. Establishment in culture of pluripotential cells from mouse embryos. *Nature* 292, 154-156 (1981).

45. Ullah, I., Baregundi Subbarao, R. & Rho, G.-J. Human Mesenchymal Stem Cells - Current trends and future prospective. *Biosci. Rep.* 35, e00191 (2015).

46. Takahashi, K. & Yamanaka, S. Induction of Pluripotent Stem Cells from Mouse Embryonic and Adult Fibroblast Cultures by Defined Factors. *Cell* 126, 663-676 (2006).

47. Chung, Y. *et al.* Embryonic and extraembryonic stem cell lines derived from single mouse blastomeres. *Nature* 439, 216-219 (2006).

48. Martin, G. R. Isolation of a pluripotent cell line from early mouse embryos cultured in medium conditioned by teratocarcinoma stem cells. *Proc. Natl. Acad. Sci.* 78, 7634-7638 (1981).

49. Thomson, J. A. Embryonic Stem Cell Lines Derived from Human Blastocysts. *Science* 282, 1145–1147 (1998).

50. Niwa, H. Mouse ES cell culture system as a model of development. *Dev. Growth Differ.* 52, 275-283 (2010).

51. Deans, R. J. & Moseley, A. B. Mesenchymal stem cells. *Exp. Hematol.* 28, 875-884 (2000).

52. Odorico, J. S., Kaufman, D. S. & Thomson, J. a. Multilineage differentiation from human embryonic stem cell lines. *Stem Cells* 19, 193-204 (2001).

53. Akter, F. Principles of Tissue Engineering. in *Tissue Engineering Made Easy* (2016).

54. Bártolo, P. J., Almeida, H. A., Rezende, R. A., Laoui, T. & Bidanda, B. Advanced processes to fabricate scaffolds for tissue engineering. in *Virtual Prototyping and Bio Manufacturing in Medical Applications* 149-170 (2008).

55. Griffith, L. G. & Swartz, M. A. Capturing complex 3D tissue physiology *in vitro. Nature Reviews Molecular Cell Biology* 7, 211-224 (2006).

56. Huh, D., Hamilton, G. A. & Ingber, D. E. From 3D cell culture to organs-on-chips. *Trends in Cell Biology* 21, 745-754 (2011).

57. Daley, W. P., Peters, S. B. & Larsen, M. Extracellular matrix dynamics in development and regenerative medicine. *J. Cell Sci.* 121, 255-264 (2008).

58. Charras, G. & Sahai, E. Physical influences of the extracellular environment on cell migration. *Nat. Rev. Mol. Cell Biol.* 15, 813-824 (2014).

59. Slack, J. M. W. Molecular Biology of the Cell. in *Principles of Tissue Engineering: Fourth Edition* (2013).

60. Ito, M. & Houkin, K. Cell culture. in *Cell Therapy against Cerebral Stroke: Comprehensive Reviews for Translational Researches and Clinical Trials* 49-72 (2017).

61. Ranga, A., Gjorevski, N. & Lutolf, M. P. Drug discovery through stem cell-based organoid models. *Advanced Drug Delivery Reviews* 69-70, 19-28 (2014).

62. Harrison, R. G. The outgrowth of the nerve fiber as a mode of protoplasmic movement. *J. Exp. Zool.* (1910).

63. Phelan, M. C. Techniques for mammalian cell tissue culture. *Current protocols in human genetics / editorial board, Jonathan L. Haines ... [et al.]* 36, A.3B.1-A.3B.18 (2006).

64. Sa, S., Wong, L. & McCloskey, K. E. Combinatorial Fibronectin and Laminin Signaling Promote Highly Efficient Cardiac Differentiation of Human Embryonic Stem Cells. *Biores. Open Access* 3, 150-161 (2014).

65. Anton, D., Burckel, H., Josset, E. & Noel, G. Three-dimensional cell culture: A breakthrough in vivo. *International Journal of Molecular Sciences* 16, 5517-5527 (2015).

66. Yu, F., Hunziker, W. & Choudhury, D. Engineering Microfluidic Organoid-on-a-Chip Platforms. *Micromachines* 10, 165 (2019).

67. Tanoue, T., Atarashi, K. & Honda, K. Development and maintenance of intestinal regulatory T cells. *Nature Reviews Immunology* 16, 295-309 (2016).

68. Mittler, F. *et al.* High-Content Monitoring of Drug Effects in a 3D Spheroid Model. *Front. Oncol.* 7, 293 (2017).

69. Meyskens, F. L. & Salmon, S. E. Inhibition of Human Melanoma Colony Formation by Retinoids. *Cancer Res.* 39, 4055-4057 (1979).

70. Tibbitt, M. W. & Anseth, K. S. Hydrogels as extracellular matrix mimics for 3D cell culture. *Biotechnology and Bioengineering* 103, 655-663 (2009).

71. Haraguchi, Y. *et al.* Fabrication of functional three-dimensional tissues by stacking cell sheets *in vitro. Nat. Protoc.* 7, 850-858 (2012).

72. Andersen, T., Auk-Emblem, P. & Dornish, M. 3D Cell Culture in Alginate Hydrogels. *Microarrays* 4, 133-161 (2015).

73. Ivascu, A. & Kubbies, M. Rapid generation of single-tumor spheroids for high-throughput cell function and toxicity analysis. *J. Biomol. Screen.* 11, 922-932 (2006).

74. Suri, S. & Schmidt, C. E. Cell-Laden Hydrogel Constructs of Hyaluronic Acid, Collagen, and Laminin for Neural Tissue Engineering. *Tissue Eng. Part A* 16, 1703-1716 (2010).

75. Zehnder, T., Freund, T., Demir, M., Detsch, R. & Boccaccini, A. R. Fabrication of cell-loaded two-phase 3D constructs for tissue engineering. *Materials (Basel).* 9, 887 (2016).

76. Wolf, K. *et al.* Collagen-based cell migration models *in vitro* and in vivo. *Seminars in Cell and Developmental Biology* 20, 931-941 (2009).

77. Edmondson, R., Broglie, J. J., Adcock, A. F. & Yang, L. Three-Dimensional Cell Culture Systems and Their Applications in Drug Discovery and Cell-Based Biosensors. *Assay Drug Dev. Technol.* 12, 207-218 (2014).

78. Eschenhagen, T. *et al.* Three-dimensional reconstitution of embryonic cardiomyocytes in a collagen matrix: a new heart muscle model system. *FASEB J.* 11, 683–694 (1997).

79. New, D. A. . A New Technique for the Cultivation of the Chick Embryo *in vitro*. *J. Embryol. Exp. Morphol.* 229, 125-128 (1955).

80. Harary, I. & Farley, B. *In vitro* studies on single beating rat heart cells. I. Growth and organization. *Exp. Cell Res.* 29, 451-465 (1963).

81. Chajek, T., Stein, O. & Stein, Y. Rat heart in culture as a tool to elucidate the cellular origin of lipoprotein lipase. *Biochim. Biophys. Acta (BBA)/Lipids Lipid Metab.* 488, 140-144 (1977).

82. Shimizu, T., Yamato, M., Kikuchi, A. & Okano, T. Cell sheet engineering for myocardial tissue reconstruction. *Biomaterials* 24, 2309-2316 (2003).

83. Sawa, Y. *et al.* Tissue engineered myoblast sheets improved cardiac function sufficiently to discontinue LVAS in a patient with DCM: Report of a case. *Surg. Today* 42, 181–184 (2012).

84. Guyette, J. P. *et al.* Bioengineering Human Myocardium on Native Extracellular Matrix. *Circ. Res.* 118, 56-72 (2016).

85. Linser, P. & Moscona, A. A. Induction of glutamine synthetase in embryonic neural retina: localization in Müller fibers and dependence on cell interactions. *Proc. Natl. Acad. Sci. U. S. A.* 76, 6476-6490 (1979).

86. Bian, W., Liau, B., Badie, N. & Bursac, N. Mesoscopic hydrogel molding to control the 3D geometry of bioartificial muscle tissues. *Nat. Protoc.* 4, 1522–1534 (2009).

87. Liau, B., Christoforou, N., Leong, K. W. & Bursac, N. Pluripotent stem cell-derived cardiac tissue patch with advanced structure and function. *Biomaterials* 32, 9180–9187 (2011).

88. Chang, S. S., Guo, W. H., Kim, Y. & Wang, Y. L. Guidance of cell migration by substrate dimension. *Biophys. J.* 104, 313-321 (2013).

89. Kanyal, N. The Science of Ischemic Stroke: Pathophysiology & Pharmacological Treatment. *Int. J. Pharma Res. Rev.* 4, 65-84 (2015).

90. Beaune, G. *et al.* How cells flow in the spreading of cellular aggregates. *Proc. Natl. Acad. Sci.* 111, 8055-8060 (2014).

91. Zheng, X. R. & Zhang, X. Microsystems for cellular force measurement: A review. *Journal of Micromechanics and Microengineering* 21, 13-17 (2011).

92. Metcalfe, A. D. & Ferguson, M. W. J. Tissue engineering of replacement skin: The crossroads of biomaterials, wound healing, embryonic development, stem cells and regeneration. *Journal of the Royal Society Interface* 4, 413-437 (2007).

93. Sorg, H., Tilkorn, D. J., Hager, S., Hauser, J. & Mirastschijski, U. Skin Wound Healing: An Update on the Current Knowledge and Concepts. *European Surgical Research* 58, 81-94 (2017).

94. Beltrami, A. P. *et al.* Adult cardiac stem cells are multipotent and support myocardial regeneration. *Cell* 114, 763-776 (2003).

95. Owens, G. K. Molecular Regulation of Vascular Smooth Muscle Cell Differentiation in Development and Disease. *Physiol. Rev.* 84, 767-801 (2004).

96. Brown, B. H. *Biological and Medical Physics , Biomedical Engineering*. *New York* (1999).

97. Daily, B., Elson, E. L. & Zahalak, G. I. Cell poking. Determination of the elastic area compressibility modulus of the erythrocyte membrane. *Biophys. J.* 45, 671–682 (1984).

98. Capitanio, M. Optical tweezers. in *An Introduction to Single Molecule Biophysics* (2017).

99. Parigger, C. Atomic force microscopy. in *Handbook of Physics in Medicine and Biology* (2010).

100. Gianola, D. S. *et al.* In situ nanomechanical testing in focused ion beam and scanning electron microscopes. *Rev. Sci. Instrum.* 82, 063901 (2011).

101. Hochmuth, R. M. Micropipette aspiration of living cells. *Journal of Biomechanics* 33, 15–22 (2000).

102. Du, P., Lin, I. K., Lu, H. & Zhang, X. Extension of the beam theory for polymer bio-transducers with low aspect ratios and viscoelastic characteristics. *J. Micromechanics Microengineering* 20, 095016 (2010).

103. Du, P., Cheng, C., Lu, H. & Zhang, X. Complex Modulus of Pdms and Its Application in Cellular Force Measuremes. *Rsc.Org* 674–676 (2012).

104. Stachiv, I., Vokoun, D. & Jeng, Y. R. Measurement of Young's modulus and volumetric mass density/thickness of ultrathin films utilizing resonant based mass sensors. *Appl. Phys. Lett.* 104, 083102 (2014).

105. Mannhardt, I. *et al.* Human Engineered Heart Tissue: Analysis of Contractile Force. *Stem Cell Reports* 7, 29-42 (2016).

106. Simmons, C. S., Petzold, B. C. & Pruitt, B. L. Microsystems for biomimetic stimulation of cardiac cells. *Lab on a Chip* 12, 3235-3248 (2012).

107. Kim, B. J. & Meng, E. Review of polymer MEMS micromachining. *Journal of Micromechanics and Microengineering* 26, 013001 (2015).

108. Bose, S., Robertson, S. F. & Bandyopadhyay, A. Surface modification of biomaterials and biomedical devices using additive manufacturing. *Acta Biomaterialia* 6, 6-22 (2018).

109. Zhang, H. & Chiao, M. Anti-fouling coatings of poly(dimethylsiloxane) devices for biological and biomedical applications. *Journal of Medical and Biological Engineering* 35, 143-155 (2015).

110. He, W. & Benson, R. Polymeric Biomaterials. in *Applied Plastics Engineering Handbook: Processing, Materials, and Applications: Second Edition* (2016).

111. McDonald, J. C. & Whitesides, G. M. Poly(dimethylsiloxane) as a material for fabricating microfluidic devices. *Acc. Chem. Res.* 35, 491-499 (2002).

112. Chang, T. P., Shih, J. Y., Yang, K. M. & Hsiao, T. C. Material properties of portland cement paste with nano-montmorillonite. *J. Mater. Sci.* 42, 7478-7487 (2007).

113. Granick, S., Lin, Z. & Bae, S. C. Molecules squeezed and stroked. *Nature* 425, 467-468 (2003).

114. Boudou, T. *et al.* A Microfabricated Platform to Measure and Manipulate the Mechanics of Engineered Cardiac Microtissues. *Tissue Eng. Part A* 18, 910-919 (2012).

115. Park, H., Larson, B. L., Kolewe, M. E., Vunjak-Novakovic, G. & Freed, L. E. Biomimetic scaffold combined with electrical stimulation and growth factor promotes tissue engineered cardiac development. *Exp. Cell Res.* 321, 297-306 (2014).

116. Radisic, M. *et al.* Functional assembly of engineered myocardium by electrical stimulation of cardiac myocytes cultured on scaffolds. *Proc. Natl. Acad. Sci.* 101, 18129-18134 (2004).

117. Zimmermann, W. H. *et al.* Three-dimensional engineered heart tissue from neonatal rat cardiac myocytes. *Biotechnol. Bioeng.* 68, 106-114 (2000).

118. Hirt, M. N. *et al.* Increased afterload induces pathological cardiac hypertrophy: a new *in vitro* model. *Basic Research in Cardiology* 107, 1–16 (2012).

119. FINK, C. *et al.* Chronic stretch of engineered heart tissue induces hypertrophy and functional improvement. *FASEB J.* 14, 669-679 (2018).

120. Vollert, I. *et al. In-vitro* perfusion of engineered heart tissue through endothelialized channels. *Tissue Eng. Part A* 20, 854-863 (2013).

121. Li, J., Han, A., Kim, S. & Park, J. Microfluidic systems for axonal growth and regeneration research. *Neural Regen. Res.* 9, 1703-1705 (2014).

122. Gutmann, E., Guttmann, L., Medawar, P. B. & Young, J. Z. The rate of regeneration of nerve. *J. Exp. Biol.* 19, 14-44 (1942).

123. Liaw, N. Y. & Zimmermann, W. H. Mechanical stimulation in the engineering of heart muscle. *Advanced Drug Delivery Reviews* 96, 156-160 (2016).

124. Tandon, N. *et al.* Electrical stimulation systems for cardiac tissue engineering. *Nat. Protoc.* 4, 155-173 (2009).

125. Wang, J. *et al.* Effect of engineered anisotropy on the susceptibility of human pluripotent stem cell-derived ventricular cardiomyocytes to arrhythmias. *Biomaterials* 34, 8878-8886 (2013).

126. Feiner, R. *et al.* Engineered hybrid cardiac patches with multifunctional electronics for online monitoring and regulation of tissue function. *Nat. Mater.* 15, 679-685 (2016).

127. Kim, L., Vahey, M. D., Lee, H. Y. & Voldman, J. Microfluidic arrays for logarithmically perfused embryonic stem cell culture. *Lab Chip* 6, 394-406 (2006).

128. Vickerman, V., Blundo, J., Chung, S. & Kamm, R. Design, fabrication and implementation of a novel multi-parameter control microfluidic platform for three-dimensional cell culture and real-time imaging. *Lab Chip* 8, 1468-1477 (2008).

129. Garcia-Ochoa, F. & Gomez, E. Bioreactor scale-up and oxygen transfer rate in microbial processes: An overview. *Biotechnology Advances* 27, 153-176 (2009).

130. Applications, T. & Al, B. E. T. Overview of Bioreactor Types. *Tissue Eng.* 1, 1-18(2003).

131. Vunjak-Novakovic, G. *et al.* Bioreactor cultivation conditions modulate the composition and mechanical properties of tissue-engineered cartilage. *J. Orthop. Res.* 17, 130-138 (1999).

132. Engelmayr, G. C., Hildebrand, D. K., Sutherland, F. W. H., Mayer, J. E. & Sacks, M. S. A novel bioreactor for the dynamic flexural stimulation of tissue engineered heart valve biomaterials. *Biomaterials* 24, 2523-2532 (2003).

133. Syedain, Z. H. & Tranquillo, R. T. Controlled cyclic stretch bioreactor for tissue-engineered heart valves. *Biomaterials* 30, 4078-4084 (2009).

134. König, F. *et al.* A Pulsatile Bioreactor for Conditioning of Tissue-Engineered Cardiovascular Constructs under Endoscopic Visualization. *J. Funct. Biomater.* 3, 480-496 (2012).

135. Robertson, M. J., Dries-Devlin, J. L., Kren, S. M., Burchfield, J. S. & Taylor, D. A. Optimizing recellularization of whole decellularized heart extracellular matrix. *PLoS One* 9, e90406 (2014).

136. Nugent, H. M. & Edelman, E. R. Tissue engineering therapy for cardiovascular disease. *Circulation Research* 92, 1068-1078 (2003).

137. Gupta, P. D. Pharmacogenetics, Pharmacogenomics and Ayurgenomics for Personalized Medicine: A Paradigm Shift. *Indian J. Pharm. Sci.* 77, 135-141 (2015).

138. Polio, S. R., Rothenberg, K. E., Stamenović, D. & Smith, M. L. A micropatterning and image processing approach to simplify measurement of cellular traction forces. *Acta Biomater.* 8, 82-88 (2012).

139. Ungefroren, H., Sebens, S., Seidl, D., Lehnert, H. & Hass, R. Interaction of tumor cells with the microenvironment. *Cell Communication and Signaling* 9,18 (2011).

140. Chiquet, M., Gelman, L., Lutz, R. & Maier, S. From mechanotransduction to extracellular matrix gene expression in fibroblasts. *Biochimica et Biophysica Acta - Molecular Cell Research* 1793, 911-920 (2009).

141. Balint, R., Cassidy, N. J. & Cartmell, S. H. Electrical Stimulation: A Novel Tool for Tissue Engineering. *Tissue Eng. Part B Rev.* 19, 48-57 (2013).

142. Wang, G., Zhang, L. & Zhang, J. A review of electrode materials for electrochemical supercapacitors. *Chemical Society Reviews* 41, 797-828 (2012).

143. Groothuis, J., Ramsey, N. F., Ramakers, G. M. J. & Van Der Plasse, G. Physiological challenges for intracortical electrodes. *Brain Stimulation* 7, 1-6 (2014).

144. Sreejit, P., Kumar, S. & Verma, R. S. An improved protocol for primary culture of cardiomyocyte from neonatal mice. *Vitr. Cell. Dev. Biol. - Anim.* 44, 45-50 (2008).

145. Ehler, E., Moore-Morris, T. & Lange, S. Isolation and Culture of Neonatal Mouse Cardiomyocytes. *J. Vis. Exp.* 50154 (2013).

146. Reinecke, H., Zhang, M., Bartosek, T. & Murry, C. E. Survival, integration, and differentiation of cardiomyocyte grafts: A study in normal and injured rat hearts. *Circulation* 100, 193-202 (1999).

147. Helgason, C. D., Miller, C., Schlüter, K.-D. & Schreiber, D. Adult Ventricular Cardiomyocytes: Isolation and Culture. in *Basic Cell Culture Protocols* 290, 305-314 (2004).

148. Duisit, J. *et al.* Perfusion-decellularization of human ear grafts enables ECM-based scaffolds for auricular vascularized composite tissue engineering. *Acta Biomater.* 73, 339-354 (2018).

149. Ceccarelli, J. & Putnam, A. J. Sculpting the blank slate: How fibrin's support of vascularization can inspire biomaterial design. *Acta Biomaterialia* 10, 1515-1523 (2014).

150. Belarbi, A. & Hsu, T. T. C. Constitutive laws of concrete in tension and reinforcing bars stiffened by concrete. *ACI Struct. J.* 91, 465-474 (1994).

151. Shi, Q. *et al.* Physical and degradation properties of binary or ternary blends composed of poly (lactic acid), thermoplastic starch and GMA grafted POE. *Polym. Degrad. Stab.* 96, 175-182 (2011).

152. Evans, U. R. & Simnad, M. T. The Mechanism of Corrosion Fatigue of Mild Steel. *Proc. R. Soc. A Math. Phys. Eng. Sci.* 188 (1947).

153. Rasmussen, K. J. R. Full-range stress-strain curves for stainless steel alloys. *J. Constr. Steel Res.* 59, 47-61 (2003).

154. Hu, C. & Li, Z. A review on the mechanical properties of cement-based materials measured by nanoindentation. *Construction and Building Materials* 90, 80-90 (2015).

155. Koelling, D. D. & Harmon, B. N. A technique for relativistic spin-polarised calculations. *J. Phys. C Solid State Phys.* 10, 3170 (1977).

156. Díez-Pascual, A. M., Gómez-Fatou, M. A., Ania, F. & Flores, A. Nanoindentation in polymer nanocomposites. *Prog. Mater. Sci.* 67, 1-94 (2015).

157. Pharr, G. M. & Oliver, W. C. Measurement of Thin Film Mechanical Properties Using Nanoindentation. *MRS Bull.* 17, 28-33 (1992).

158. Ferencz, R., Sanchez, J., Blümich, B. & Herrmann, W. AFM nanoindentation to determine Young's modulus for different EPDM elastomers. *Polym. Test.* 31, 425-432 (2012).

159. Mussert, K. M., Vellinga, W. P., Bakker, A. & Van Der Zwaag, S. A nano-indentation study on the mechanical behaviour of the matrix material in an AA6061 - Al2O3 MMC. *J. Mater. Sci.* 37, 789-794 (2002).

160. Li, X. & Bhushan, B. A review of nanoindentation continuous stiffness measurement technique and its applications. *Materials Characterization* 48, 11-36 (2002).

161. Choi, S. Independent component analysis. in *Handbook of Natural Computing* (2012).

162. Mata, A., Fleischman, A. J. & Roy, S. Characterization of polydimethylsiloxane (PDMS) properties for biomedical micro/nanosystems. *Biomed. Microdevices* 7, 281–293 (2005).

163. Armani, D., Liu, C., Aluru, N. & Deniz Armani, Chang Liu, N. A. Re-Configurable Fluid Circuits By Pdms Elastomer Micromachining. *Micro Electro Mech. Syst. 1999. MEMS '99; IEEE Int. Conf.* 222–227 (1999).

164. Béfahy, S. *et al.* Thickness and elastic modulus of plasma treated PDMS silica-like surface layer. *Langmuir* 26, 3372–3375 (2010).

165. Choi, N. W. *et al.* Microfluidic scaffolds for tissue engineering. *Nat. Mater.* 6, 908-915 (2007).

166. Novosel, E. C., Kleinhans, C. & Kluger, P. J. Vascularization is the key challenge in tissue engineering. *Advanced Drug Delivery Reviews* 63, 300-311 (2011).

167. Liu, H., Lin, J. & Roy, K. Effect of 3D scaffold and dynamic culture condition on the global gene expression profile of mouse embryonic stem cells. *Biomaterials* 27, 5978-5989 (2006).

168. van Duinen, V., Trietsch, S. J., Joore, J., Vulto, P. & Hankemeier, T. Microfluidic 3D cell culture: From tools to tissue models. *Current Opinion in Biotechnology* 35, 118-126 (2015).

169. Bhatia, S. N. & Ingber, D. E. Microfluidic organs-on-chips. *Nature Biotechnology* 32, 760-772 (2014).

170. Zuppinger, C. 3D culture for cardiac cells. *Biochim. Biophys. Acta - Mol. Cell Res.* 1863, 1873-1881 (2016).

171. Park, T. H. & Shuler, M. L. Integration of cell culture and microfabrication technology. *Biotechnology Progress* 19, 243–253 (2003).

172. Bhattacharjee, N., Urrios, A., Kang, S. & Folch, A. The upcoming 3D-printing revolution in microfluidics. *Lab on a Chip* 16, 1720-1742 (2016).

173. Casadevall I Solvas, X. & Demello, A. Droplet microfluidics: Recent developments and future applications. *Chem. Commun.* 47, 1936-1942 (2011).

174. Lee, K. W. *et al.* Three-dimensional hybrid integration technology of CMOS, MEMS, and photonics circuits for optoelectronic heterogeneous integrated systems. *IEEE Trans. Electron Devices* 58, 748-757 (2011).

175. Au, S. H., Shih, S. C. C. & Wheeler, A. R. Integrated microbioreactor for culture and analysis of bacteria, algae and yeast. *Biomed. Microdevices* 13, 41-50 (2011).

176. Gernaey, K. V. *et al.* Monitoring and control of microbioreactors: An expert opinion on development needs. *Biotechnol. J.* 7, 1308-1314 (2012).

177. Hemmerich, J., Noack, S., Wiechert, W. & Oldiges, M. Microbioreactor Systems for Accelerated Bioprocess Development. *Biotechnology Journal* 13, e1700141 (2018).

178. Zhu, X., Bersano-Begey, T., Kamotani, Y. & Takayama, S. Encylopedia of medical devices and instrumentations. *Microbioreactor* (Wiley & Sons, 2006).

179. Zanzotto, A. *et al.* Membrane-aerated microbioreactor for high-throughput bioprocessing. *Biotechnol. Bioeng.* 87, 243–254 (2004).

180. Taylor, R. J. *et al.* Dynamic analysis of MAPK signaling using a high-throughput microfluidic single-cell imaging platform. *Proc. Natl. Acad. Sci. U. S. A.* 106, 3758–3763 (2009).

181. Smith, G. D., Swain, J. E. & Bormann, C. L. Microfluidics for gametes, embryos, and embryonic stem cells. *Semin. Reprod. Med.* 29, 5–14 (2011).

182. Sharpe, M., Leoni, G. & Hyllner, J. Stem Cells. in *Comprehensive Toxicology: Third Edition* (2017).

183. Laposa, R. R. Stem cells for drug screening. *J. Cardiovasc. Pharmacol.* 58, 240–245 (2011).

184. Ma, G. Microencapsulation of protein drugs for drug delivery: Strategy, preparation, and applications. *J. Control. Release* 193, 324-340 (2014).

185. Zhao, K., Dalton, P., Yang, G. C. & Scherer, P. W. Numerical modeling of turbulent and laminar airflow and odorant transport during sniffing in the human and rat nose. *Openchannel flow* 31, 107-118 (2002).

186. Sano, M. & Tamai, K. A universal transition to turbulence in channel flow. *Nat. Phys.* 12, 249-253 (2016).

187. Schlichting, H., Gersten, K., Schlichting, H. & Gersten, K. Fundamentals of Turbulent Flows. *in Boundary-Layer Theory,* 205-228 (2016).

188. Celik, I. B. Wester. V. U. Introductory turbulence modeling. *Fluid Mechanics Books* (1999).

189. Savli, M. Turbulence kinetic energy - TKE. Turbulence Kinetic Energy (2012)

190. Thomson, J., Polagye, B., Durgesh, V. & Richmond, M. C. Measurements of turbulence at two tidal energy sites in puget sound, WA. *IEEE J. Ocean. Eng.* 37, 363-374 (2012).

191. Shoaib, M. S. R., Haque, M. A. & Asaduzzaman, M. Mathematical modeling of the heart. in *ICECE 2010 - 6th International Conference on Electrical and Computer Engineering* (2010).

192. Achten, J. & Jeukendrup, A. E. Heart rate monitoring: Applications and limitations. *Sports Medicine* 33, 517-538 (2003).

193. Severs, N. J. The cardiac muscle cell. *BioEssays* 22, 188-199 (2000).

194. DiFrancesco, D. Pacemaker Mechanisms in Cardiac Tissue. *Annu. Rev. Physiol.* 55, 455-472 (2002).

195. HOUTZ, S. J. & FISCHER, F. J. An analysis of muscle action and joint excursion during exercise on a stationary bicycle. *J. Bone Joint Surg. Am.* 41, 123-131 (1959).

196. Rohr, S. Role of gap junctions in the propagation of the cardiac action potential. *Cardiovascular Research* 62, 309-322 (2004).

197. Zaza, A. & Rosen, M. The Cardiac Action Potential. in *An Introduction to Cardiac Electrophysiology* 54, 607-634 (2016).

198. Pinnell, J., Turner, S. & Howell, S. Cardiac muscle physiology. *Contin. Educ. Anaesthesia, Crit. Care Pain* 475, 77-89 (2007).

199. Logothetis, N. K. *et al.* The effects of electrical microstimulation on cortical signal propagation. *Nat. Neurosci.* 13, 1283-1291 (2010).

200. McCaig, C. D., Song, B. & Rajnicek, A. M. Electrical dimensions in cell science. *J. Cell Sci.* 122, 4267-4276 (2009).

201. Chappell, M. & Payne, S. The action potential. in *Biosystems and Biorobotics* (2016).

202. Brevet, A., Pinto, E., Peacock, J. & Stockdale, F. E. Myosin synthesis increased by electrical stimulation of skeletal muscle cell cultures. *Science.* 193, 1152-1159 (1976).

203. Zhang, D. *et al.* Tissue-engineered cardiac patch for advanced functional maturation of human ESC-derived cardiomyocytes. *Biomaterials* 34, 5813-5820 (2013).

204. Scuderi, G. J. & Butcher, J. Naturally Engineered Maturation of Cardiomyocytes. *Front. Cell Dev. Biol.* 5, 50-63 (2017).

205. Collins, C. A. *et al.* Stem cell function, self-renewal, and behavioral heterogeneity of cells from the adult muscle satellite cell niche. *Cell* 122, 289-301 (2005).

206. Bian, W. & Tung, L. Structure-related initiation of reentry by rapid pacing in monolayers of cardiac cells. *Circ. Res.* 98, e29-38 (2006).

207. Li, S. C. *et al.* Stem cell engineering for treatment of heart diseases: Potentials and challenges. *Cell Biol. Int.* 33, 255-267 (2009).

208. Sauer, H., Rahimi, G., Hescheler, J. & Wartenberg, M. Effects of electrical fields on cardiomyocyte differentiation of embryonic stem cells. *J. Cell. Biochem.* 75, 710-723 (1999).

209. Blazeski, A. *et al.* Electrophysiological and contractile function of cardiomyocytes derived from human embryonic stem cells. *Progress in Biophysics and Molecular Biology* 110, 178-195 (2012).

210. Gobbo, M., Maffiuletti, N. A., Orizio, C. & Minetto, M. A. Muscle motor point identification is essential for optimizing neuromuscular electrical stimulation use. *Journal of NeuroEngineering and Rehabilitation* 11, 17-36 (2014).

211. Tripathy, S. & Tripathy, D. K. Multi-attribute optimization of machining process parameters in powder mixed electro-discharge machining using TOPSIS and grey relational analysis. *Eng. Sci. Technol. an Int. J.* 19, 62-70 (2016).

212. Newmarch, J. & Newmarch, J. Raspberry Pi. in *Linux Sound Programming* (2017).

213. John, A. et al. Automation of 11 kv substation using raspberry pi. *in Proceedings of IEEE International Conference on Circuit, Power and Computing Technologies, ICCPCT 2017* (2017).

214. Gay, W. W. Raspberry Pi Hardware Reference. *Raspberry Pi Hardware Reference* (2014).

215. Gabrielson, J. *et al.* Evaluation of redox indicators and the use of digital scanners and spectrophotometer for quantification of microbial growth in microplates. *J. Microbiol. Methods* 50, 63-73 (2002).

216. Pierce, B. the thermo Scientific alamarBlue Cell Viability Assay Reagent. *US Pat.* (2012).